Expanding the Repertoire of Chemical Modulators for Heat Shock Protein 70 (Hsp70): New Probes for Neurodegenerative Disease

by

Christopher G. Evans

A dissertation submitted in partial fulfillment
of the requirements for the degree of
Doctor of Philosophy
(Chemical Biology)
in The University of Michigan
2010

Doctoral Committee:

Assistant Professor Jason E. Gestwicki, Chair
Professor Richard R. Neubig
Professor David H. Sherman
Assistant Professor Matthew B. Soellner

2010

To My Family

Acknowledgements

I owe much gratitude to Dr. Jason Gestwicki, who has provided great mentorship over my five years in his lab. I could tell when I was rotating in your lab that your vision and guidance would provide an atmosphere where I could grow as a scientist. I have enjoyed working with everyone in lab. They have provided helpful feedback when I have been preparing for talks and interviews. By the nature of this project there was a lot of collaboration between myself and others in the lab. Lyra Chang and Srikanth Patury have provided much help in running ATPase assays for compounds that I have synthesized. Dr. Gladis Walter and Dr. Susanne Wisén were instrumental in obtaining yeast polyglutamine aggregation data for both the dihydropyrimidine and dihydropyrine classes of small molecules that I synthesized. Finally, Matt Smith has taken the 15-DSG analogs that I have synthesized and done stability testing. He has also conducted cellular protein aggregation assays with them.

I would also like to thank our collaborators Dr. Chad A. Dickey and Dr. Umesh K. Jinwal at the University of South Florida for conducting the tau stability assays.

My thesis committee has provided me with invaluable feedback as I have been progressing through these last five years. All of them have added to what I have accomplished through our discussions. Dr. Richard Neubig helped to reinforce the idea of really thinking about all aspects of my project in order to successfully answer the question at hand. Dr. David Sherman joined my committee when the 15-DSG project really took off and provided great insight into the biosynthesis of the natural product. I

want to thank Dr. Matthew Soellner for joining my committee recently after Dr. Kate Carroll unfortunately left the University of Michigan for Scripps Research Intitute in Florida.

During my time in graduate school I was fortunate to receive several sources of financial support. I would like to thank the Chemical Biology Doctoral Program for financial support. I was also fortunate to receive funding through the Cellular Biotechnology Training Program. During my time in the CBTP, I was fortunate to do an industrial internship at Cayman Chemical in Ann Arbor, MI under the direction of Dr. Nisha Palackal. This opportunity provided outstanding experience in what a career as a scientist in industry is like. I would also like to thank Rackham Graduate School for a Rackham Travel Grant.

Last but not least I would like to thank my family for their support and encouragement over the last five years. They have been there whenever I have needed them and I could not have been successful without them.

Preface

This dissertation is a compilation of both published and unpublished work on the synthesis of small molecule inhibitors of heat shock protein 70 (Hsp70) and their effect on neurodegenerative diseases. Chapter 1 largely came from a review article published in *J Med Chem*. The citation for this article is Evans, C.G., Chang, L., and Gestwicki, J.E., "Heat Shock Protein 70 (Hsp70) as an Emerging Drug Target", *J Med Chem*, **2010**, 53 (12), 4585-4602. Chapter 2 was largely a compilation of a paper where I contributed to the synthesis of dihydropyrimidines and a paper where we looked at the effect they had on Hsp70 in a model of neurodegeneration. The citation for the synthesis paper was Wisén, S., Androsavich, J., Evans, C.G., Chang, L., and Gestwicki, J.E., "Chemical modulators of heat shock protein 70 (Hsp70) by sequential, microwave-accelerated reactions on solid phase", *Bioorg Med Chem Lett*, **2008**, 18 (1), 60-5. The citation for the paper reporting their effect in the cellular model is Evans, C.G., Wisén, S., and Gestwicki, J.E., "Heat shock proteins 70 and 90 inhibit early stages of amyloid beta-(1-42) aggregation in vitro", *J Biol Chem*, **2006**, 281 (44), 33182-91. Chapter 3 is again a compilation of two papers. One involved the synthesis of a library of dihydropyridines and screening their effect on tau processing and a paper on the enantioselective synthesis of dihydropyridines using an organocatalyst. The citation for these enatioselective synthesis paper was Evans, C.G. and Gestwicki, J.E., "Enantioselective organocatalytic Hantzsch synthesis of polyhydroquinolines", Org Lett, **2009**, 11 (14), 2957-9. The other paper was recently submitted and the citation is Evans, C.G., Jinwal, U.K., Dickey, C.A.,

and Gestwicki, J.E., “Identification of Dihydropyridines That Reduce Cellular Tau Levels”, *Chem Comm*, **2010**, submitted. Finally Chapter 5 presents the conclusions and future direction.

Table of Contents

List of Figures

List of Schemes

List of Tables

List of Abbreviations

17-AAG	17-(Allylamino)-17-demethoxygeldanamycin
Aβ	β-amyloid
ACN	acetonitrile
AcOH	acetic acid
AD	Alzheimer's disease
Apaf-1	apoptotic peptidase activating factor 1
APIase	cis/trans aminopeptidyl isomerase
$ArB(OH)_2$	aryl boronate
BAG	Bcl-2-associated anthogene
Bax	Bcl-2-associated X protein
BBr_3	boron tribromide
BINAP	2,2'-bis(diphenylphosphino)-1,1'-binaphthyl
BINOL	1,1'-Bi-2-naphthol
Boc	*tert*-butoxycarbonyl
Br_2	bromine
CAN	ceric ammonium nitrate
CF	cystic fibrosis
CFTR	cystic fibrosis transmembrane receptor
CHIP	C-terminal of Hsc70 interacting protein
Cl_3CCN	trichloroacetonitrile

Cy_3P	tricyclohexylphosphine
1,4-DAB	1,4-diaminobutane
$(dba)_3Pd_2$	tris(dibenzylideneacetone)dipalladium (0)
DCE	1,2-dichloroethane
DCM	dichloromethane
DIBAL	diisobutylaluminum hydride
DIC	N,N'-diisopropylcarbodiimide
DMF	dimethylfomamide
DMSO	dimethylsulfoxide
DPE	(+)-1,2-Bis((2S,5S)-2,5-diphenylphospholano)ethane
DPPF	1,1'-Bis(diphenylphosphino)ferrocene
15-DSG	15-deoxyspergualin
%ee	percent enantiomeric excess
equiv	equivalent
ERAD	ER-associated degradation
Et_3N	triethylamine
EtOH	ethanol
Fmoc	9-fluorenylmethoxycarbonyl
g	gram
GI_{50}	concentration producing a half-maximal growth
h	hour
HCl	hydrochloric acid
HD	Huntington’s disease

H_2O	water
HOBt	N-hydroxybenzotriazole
HOP	Hsp70 organizing protein
HPLC	high pressure liquid chromatography
HSBP1	Hsp70 binding protein 1
Hsc70	Heat shock cognate 70
HSF1	Heat shock factor 1
Hsp70	Heat shock protein 70 family
htt	huntingtin protein
IC_{50}	concentration producing a half-maximal inhibition
IL-10	interleukin 10
ITC	isothermal titration calorimetry
K_d	dissociation constant at equilibrium
KF	potassium fluoride
MB	methylene blue
MeOH	methanol
$Mg(ClO_4)_2$	magnesium perchlorate
min	minute
µM	micromolar
mmol	millimoles
mtHsp70	mitochondrial HSP70
$NaBH_4$	sodium borohydride
$NaBH_3CN$	sodium cyanoborohydride

$NaBH(OAc)_3$	sodium triacetoxyborohydride
NBD	nucleotide binding domain
NEF	nucleotide exchange factor
NFT	neurofibrillary tangles
PD	Parkinson's disease
$Pd(OAc)_2$	palladium (II) acetate
PPAR	peroxisome proliferation-activated receptor
PES	phenylethynesulfonamide
$POCl_3$	phosphorus oxychloride
polyQ	polyglutamine
PPh_3	triphenylphosphine
SAR	structure-activity relationships
SBMA	spinal and bulbar muscular dystrophy
SBD	substrate binding domain
SCA	spinocerebellar ataxia
SBMA	spinal and bulbar muscular atrophy
Ssa1	stress seventy subfamily A
TEM	transmission electron microscopy
THF	tetrahydrofuran
TNFα	tumor necrosis factor α
TPR	tetratricopeptide repeat
$Yb(OTf)_3$	ytterbium triflate
Zn	zinc

$Zn(BH_4)_2$	zinc borohydride
$ZnCl_2$	zinc chloride

Abstract

Expanding the Repertoire of Chemical Modulators for Heat Shock Protein 70 (Hsp70): New Probes for Neurodegenerative Disease

by

Christopher G. Evans

Chair: Jason E. Gestwicki

Heat shock protein 70 (Hsp70) is a molecular chaperone that plays pivotal roles in protein homeostasis in nearly all organisms. In these roles, Hsp70 binds to newly synthesized or misfolded proteins and regulates their stability and turnover. Genetic and biochemical data have strongly implicated Hsp70 in many diseases, including cancer and neurodegeneration. However, there are few Hsp70 inhibitors available. This limitation has prevented detailed studies of Hsp70's roles in disease and has limited exploration of its potential as a drug target.

The purpose of this study is to synthesize new chemical probes that could be used to aid in our understanding of Hsp70's biology. Early Hsp70 inhibitors were assembled by the multi-component Biginelli reaction and they contained a dihydropyrimidine core. In my work, this reaction was further exploited to assemble a focused library of related compounds. This new series allowed for the identification of the putative binding site on Hsp70 and provided new insight into the relationship between Hsp70 and amyloid

formation. Based on this work, I generated a series of related dihydropyridines through the four-component, Hantzsch reaction. During the course of that work, an enantioselective route was developed using an organophosphorous catalyst. Some of these compounds showed promising activity in cellular models of neurodegeneration. Finally, derivatives of the natural product analog, 15-deoxyspergualin, were synthesized through the strategic use of the Ugi multi-component reaction. We found that this route provided for the rapid and efficient generation of derivatives, with increased opportunities for structural diversity. These compounds appeared to interrupt binding of Hsp70 to its co-chaperone, CHIP, and they blocked protein aggregation in cellular models.

Through utilizing different multi-component reactions, it has been possible to synthesize several new inhibitors of Hsp70. These probes have been used to better understand the relationships between Hsp70 and neurodegeneration. Thus, this series may aid in future efforts to understand Hsp70's biology.

Chapter 1

Introduction

1.1 Introduction to Hsp70 Structure and Function

Heat shock protein 70 (Hsp70) is a molecular chaperone that is expressed in response to stress, such as elevated temperature. In this role, Hsp70 is believed to bind to its protein substrates and stabilize them against denaturation or aggregation until conditions improve.[1] In addition to its functions during a stress response, Hsp70 has multiple responsibilities during normal growth; it assists in the folding of newly synthesized proteins,[2, 3] the subcellular transport of proteins and vesicles,[4] the formation and dissociation of complexes,[5] and the degradation of unwanted proteins.[6, 7] Thus, this chaperone broadly shapes protein homeostasis by controlling protein production, quality control and turnover during both normal and stress conditions.[8] Consistent with these diverse activities, genetic and biochemical studies have implicated this chaperone in a range of diseases, including cancer, neurodegeneration, allograft rejection and infection. This review provides a brief review of Hsp70 structure and function and then explores some of the emerging opportunities (and challenges) for drug discovery.

1.1.1 Hsp70 is Highly Conserved.

Members of the Hsp70 family are ubiquitously expressed and highly conserved; for example, the major Hsp70 from *Escherichia coli,* termed DnaK, is approximately

50% identical to human Hsp70s.[9] Eukaryotes often express multiple Hsp70 family members with major isoforms found in all the major cellular compartments: Hsp72 (HSPA1A) and heat shock cognate 70 (Hsc70/HSPA8) in the cytosol and nucleus, BiP (Grp78/HSPA5) in the endoplasmic reticulum and mtHsp70 (Grp75/mortalin/HSPA9) in mitochondria. Some of the functions of the cytosolic isoforms, Hsc70 and Hsp72, are thought to be redundant, but the transcription of Hsp72 is highly responsive to stress and Hsc70 is constitutively expressed. In the ER and mitochondria, the individual Hsp70 family members are thought to fulfill specific functions and have unique substrates, with BiP playing key roles in the folding and quality control of ER proteins and mtHsp70 being involved in the import and export of proteins from the mitochondria. For the purposes of this review, we will often use Hsp70 as a generic term to encompass the shared properties of the family members.

1.1.2 Domain Architecture of Hsp70.

All members of the Hsp70 family have an N-terminal nucleotide binding domain (NBD) (~40 kDa) and a C-terminal substrate-binding domain (SBD) (~25 kDa) connected by a short interdomain linker (Figure 1-1 A).[10] The NBD consists of two subdomains, I and II, which are further divided into regions a and b. The Ia and IIa subdomains interact with ATP through a nucleotide-binding cassette related to those of hexokinase, actin and glycerol kinase.[11, 12] The SBD consists of a 10-kDa α-helix subdomain and a 15-kDa β-sandwich. Crystal structures suggest that substrate peptides are bound in an extended conformation between loops of the β-sandwich and that the α-helix subdomain acts as a "lid".[13] The substrates of Hsp70 are thought to include both linear polypeptides, such as those found in newly synthesized proteins or folding

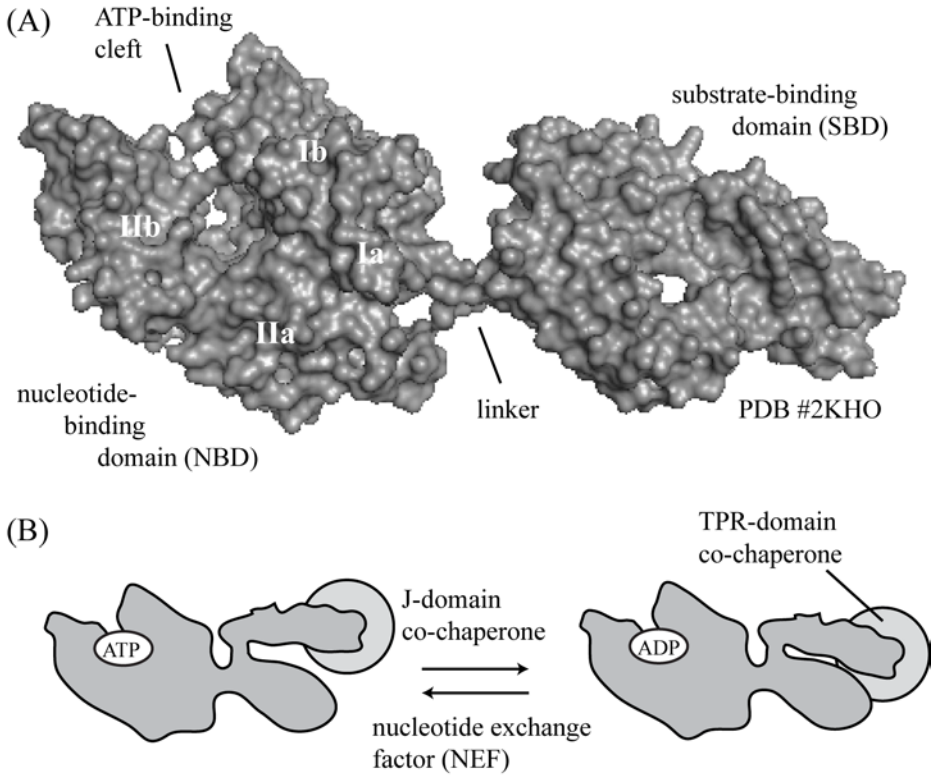

Figure 1-1. Structure and ATPase cycle of Hsp70. (A) Heat shock protein 70 is composed of a 45 kDa nucleotide-binding domain (NBD), connected to a 30kDa substrate-binding domain (SBD) by a short, hydrophobic linker. The SBD contains a beta-sandwich and a helical lid domain. The representative structure shown is of prokaryotic DnaK in complex with ADP and a peptide substrate (PDB # 2KHO). (B) Schematic of ATP hydrolysis and the role of co-chaperones (see text).

intermediates,[3] and exposed regions of fully or partially folded proteins. For example, Hsp70 is known to interact with clathrin, components of the transcriptional activation complex, nuclear hormone receptors and many others.[5, 14, 15] This diversity of substrates is allowed by the low sequence selectivity of the SBD, which binds to most peptides composed of non-polar amino acids.[16]

1.1.3 ATPase Activity of Hsp70.

Many of the functions of Hsp70 appear to revolve around crosstalk between ATPase activity in the NBD and substrate binding in the SBD. Hsp70 binds tightly to

ATP, with some reports of *E. coli* DnaK binding with a K_d of 1 nM.[17] Through an inter-domain, allosteric mechanism, ATP binding increases the on- and off-rate of peptide binding in the adjacent SBD. In turn, nucleotide hydrolysis to ADP closes the "lid" and enhances the affinity for substrate (Figure 1-1 B).[18] Likewise, interactions between the SBD and its substrates increase the rate of ATP hydrolysis in the NBD, suggesting that communication between the two domains is two-way.[18] The mechanisms of inter-domain communication have been studied extensively and appear to involve the conserved, hydrophobic linker.[19, 20] Thus, from a drug discovery viewpoint, this allostery in Hsp70 provides multiple opportunities for chemical intervention, including inhibition of ATP turnover, substrate binding or even blocking inter-domain allostery.

1.1.4 Hsp70 Co-Chaperones.

As isolated proteins, the ATP hydrolysis rates of Hsc70 and DnaK are extremely slow, 0.003 and 0.0003 s^{-1}, respectively.[17, 21] *In vivo*, this property provides the opportunity for regulation by co-chaperones, which associate with Hsp70s and control their nucleotide turnover. For example, the J proteins (or Hsp40s) are a large group of co-chaperones that stimulate ATP hydrolysis (Figure 1-1 B).[22] In the human genome, at least 40 different J protein genes have been identified[23] and each contains the conserved, ~70 amino acid J domain required for binding and stimulation of Hsp70s.[24] NMR, mutagenesis and crystallography studies indicate that at least one binding site of the J domain is on the NBD.[25, 26] Protein-protein interactions between the J domain and the surface of the NBD trigger an allosteric "hotwire" through the Hsp70 that enhances ATP turnover by approximately 7-fold. Thus, in the presence of a J-protein, the release of ADP becomes the rate-limiting step.[27] To complete the ATPase cycle, a distinct class of

co-chaperones, the nucleotide exchange factors (NEFs) catalyze ADP release. The major NEF families include, the GrpE-like family,[28] BAG family proteins,[29] HspBP1[30] and the atypical Hsp70 homologs (*e.g.* Hsp110).[31] All of these NEFs appear to bind the NBD and favor ADP release, but each class uses a different structural mechanism to achieve this effect.[32] Together, the J-domain proteins and NEFs regulate ATP cycling, and therefore substrate binding by the Hsp70s. In addition, some of the co-chaperones independently bind substrates and, through this activity, have the potential to influence substrate selection by the Hsp70 complex.[33, 34] Thus, although these co-chaperones do not have enzymatic activity, they are important regulatory factors and they are required for the many chaperone functions of Hsp70.

A final group of co-chaperones, the tetratricopeptide repeat (TPR)-containing proteins, bind to the EEVD sequence at the extreme C-terminus of Hsp72 and Hsc70. Interestingly, the evolutionarily unrelated molecular chaperone, Hsp90, also contains the EEVD motif, allowing it to interact with TPR domains. The TPR is characterized by a 34-amino acid motif that forms an antiparallel α-helical hairpin.[35] Most proteins that have TPR domains also have domains with additional activities and, thus, these co-chaperones are thought to recruit unique capabilities to the Hsp70 complex. For example, HOP has three domains (TPR1, TPR2A, and TPR2B) with three TPR motifs each.[36] HOP preferably binds to the ADP-bound form of Hsp70 family of proteins via TPR1 and TPR2B, while TPR2A specifically binds to Hsp90.[37-39] In this way, Hop bridges Hsp70s and Hsp90, assists substrate transfer between these chaperones and is believed to promote substrate folding.[40] Another TPR-domain protein, CHIP, contains a U-box domain and it supervises the triage of Hsp70- or Hsp90-bound proteins.[41, 42] Thus, although both HOP

and CHIP bind via TPR domains, the outcomes of these interactions are diametrically opposed: HOP favors folding, while CHIP favors degradation. Based on these observations and many others, it is thought that competition between co-chaperones might drive combinatorial assembly of chaperone complexes with specific functions.[5, 8, 43] Together, these features suggest that interfering with Hsp70's interactions with co-chaperones (*e.g.* J domains, NEFs and TPR domains) might be a viable mechanism for controlling chaperone function.

1.2 Roles of Hsp70 in Disease

1.2.1 Cancer and Apoptosis.

Hsp70 expression has been routinely associated with poor prognosis in multiple forms of cancer.[44] For example, high Hsp70 levels are associated with adverse outcomes in breast, endometrial, oral, colorectal, prostate cancers as well as certain leukemias.[45-48] Moreover, transgenic over-expression of Hsp70 is sufficient to induce T cell lymphoma in some models.[47] This observation is important because induction of Hsp70 can be misregulated in cancer, potentially mediated by the heat shock transcription factor 1 (HSF1).[44, 49, 50] In cancer cells, over-expression of Hsp70 is thought to provide a survival advantage because it is able to interact with multiple components of both the caspase-dependent and –independent apoptotic pathways (Figure 1-2 and Table 1-1).[44, 51, 52] For example, this chaperone was reported to down-regulate the important apoptotic mediator, Bcl-2.[53] Similarly, expression of Hsp72 blocks TNF-induced apoptosis, activation of caspase-3, translocation of Bax and cleavage of PPAR.[54-57] Some of these interactions are thought to be direct. For example, immunoprecipitation has shown an interaction between Hsp72 and Bax.[55] In this context, Hsp72 prevents Bax translocation by blocking

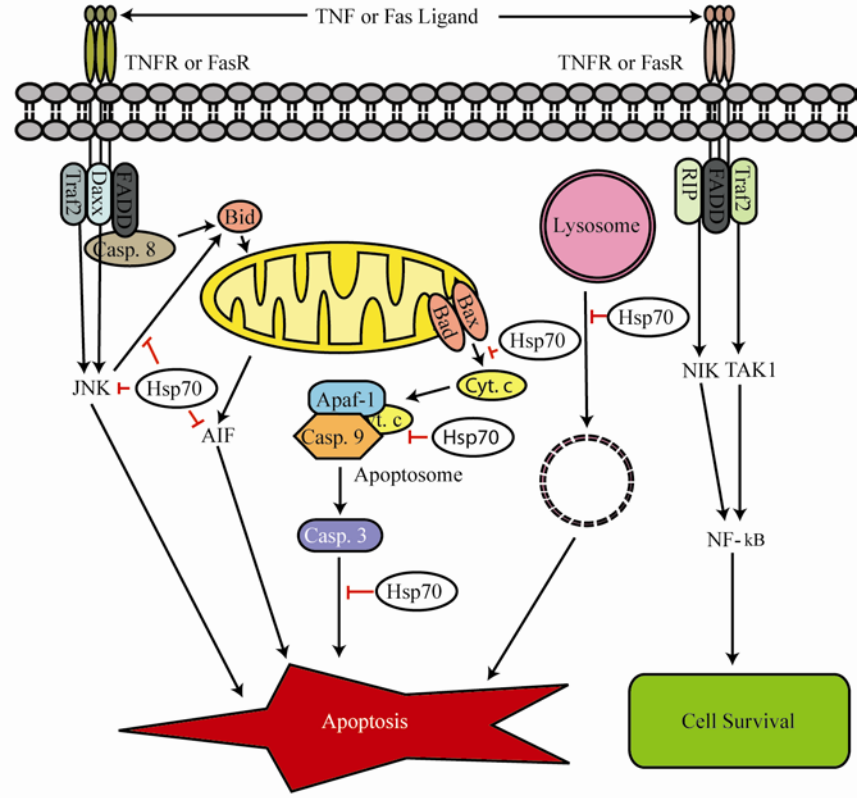

Figure 1-2. Roles of Hsp70 in anti-apoptotic signaling. Hsp70 is thought to promote survival and block apoptosis through interactions with multiple steps in the pathway. For some substrates, Hsp70's role appears to be stabilization of the substrate, while it appears to mediate the degradation of other substrates. The regulatory mechanisms that govern these activities are not known. See the main text and Table 1 for references.

its oligomerization, a step necessary for disruption of the mitochondrial membrane.[56, 57] By influencing multiple steps in the same cascade, Hsp70 is likely to exert even more potent anti-apoptotic activity than if it was acting at individual proteins. Similarly, Hsp70 has also been found to impact cell survival at multiple pathways by also blocking caspase-independent signaling through activity on cathepsins and Apaf-1.[58] For example, Hsp70 knockdown increases cathepsin B release and protects lysosomes from photo- and H_2O_2-mediated permeabilization.[59] In addition to these effects on the caspase-dependent

Table 1-1. Roles of Hsp70 in Apoptotic Signaling

process	role of Hsp70	ref.
	Caspase-Dependent Pathways	
Bid	Hsp72 inhibits TNF activation of the Bid pathway.	54
caspase -9	Hsp70 inhibits recruitment of procaspase-9 to the apoptosome.	58
	Hsp70 binds to Apaf-1, preventing formation of the active apoptosome.	194
BCL2	Hsp70 inhibits the proteasomal degradation of Bcl2 proteins.	53
	Hsp70 inhibits cytochrome c release from mitochondria by inhibiting Bad and Bax.	195
caspase -3	Hsp70 inhibits caspase-3 induced apoptosis.	195
	Caspse-Independent Pathways	
JNK	Hsp72 inhibits JNK induced apoptosis, but its ATPase activity is dispensable.	61, 196-200
AIF	Hsp70 prevents the release of AIF from mitochondria.	64, 201, 202
lysosome	Hsp70 stabilizes lysosomal membrane integrity.	59, 203, 204
p53	Hsp70 blocks p53-induced senescence through PI3K.	46, 60, 205-209

and –independent apoptotic pathways, Hsp72 also plays roles in senescence through effects on the p53-p21 pathway.[60] Together, these results suggest that Hsp70 proteins interacts with multiple partners in both the apoptosis and senescence pathways, a model that is consistent with Hsp70's known substrate promiscuity. Importantly, the ATPase activity of Hsp70 doesn't appear to be required for all of these activities, as the action of Hsp70 on JNK and AIF occurs independent of nucleotide hydrolysis.[61-63 64] This is an important observation, because many of the early Hsp70 inhibitors target its ATPase activity. While shRNA-mediated knockdown of Hsp70 induces apoptosis and slows cell proliferation in multiple cancer cell models,[46, 65, 66] it is unclear whether inhibitors of specific Hsp70 functions, such as nucleotide turnover, will mimic this cellular effect. Regardless, these studies suggest that cancer cells become "addicted" to Hsp70 through this chaperone's activity on multiple, parallel signaling pathways.[67]

Hsp70 over-expression has also been documented to provide resistance to chemotherapeutic agents, such as imatinib, etoposide, cisplatin and MG-132.[68, 69] Although the detailed mechanisms of resistance remain to be elucidated, recent evidence suggests that reduced activation of ERK, NF-κB, and JNK pathways may be responsible.[69] The protective effects of Hsp70 are particularly striking in response to treatment with Hsp90 inhibitors, such as geldanamycin and its derivatives.[67, 70] Like Hsp70, Hsp90 is an ATP-utilizing molecular chaperone with roles in protein turnover.[71] However, Hsp90 is often considered the more "specialized" chaperone, with a relatively restricted set of cellular substrates. Hsp90's substrates include Akt, Cdk4, Raf1, Her2 and other important anti-apoptotic targets, some of which appear to be shared with Hsp70 (see Figure 1-2).[71, 72] Inhibitors of Hsp90 lead to rapid, proteasomal degradation of these substrates and the promising anti-cancer potential of Hsp90 inhibitors has been reviewed extensively elsewhere.[50, 73, 74] In the context of our discussion, treatment with Hsp90 inhibitors has been found to induce expression of Hsp70, potentially through activation of HSF1.[70] As discussed above, this compensatory mechanism can cause resistance to apoptosis and stabilization of some shared protein substrates.[67, 70] Together, these observations suggest that dual therapy against both Hsp90 and Hsp70 might be beneficial. This hypothesis is strongly supported by observations that RNAi knockdown of Hsp70s enhances the efficacy of Hsp90 inhibitors.[75, 76]

1.2.2 Protein Misfolding and Neurodegenerative Disease.

One of the other important roles of Hsp70 is to assist protein folding and turnover. In normal cells, quality control systems prevent the accumulation of toxic misfolded protein species. However, in response to mutagenesis, aging or oxidative stress,

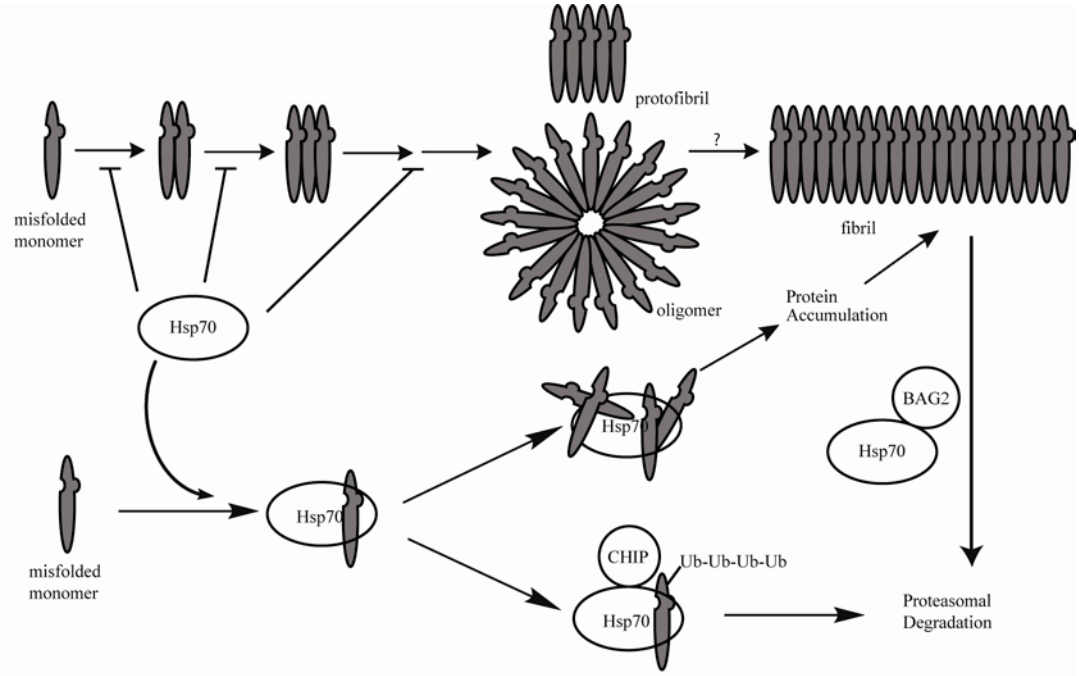

Figure 1-3. Potential roles for Hsp70 in protein misfolding and aggregation. Hsp70 has been linked to multiple steps of the protein misfolding and aggregation pathway, including in preventing misfolding, blocking early stages of aggregation and in mediating the degradation of misfolded intermediates through coupling to the ubiquitin-proteasome system. The Hsp70 co-chaperones BAG2 and CHIP have both been linked to clearance of misfolded substrates. In some systems (including yeast prions), Hsp70 activity is required for fibril formation. For simplicity, this schematic encompasses broad aspects of the misfolding pathway of amyloid beta, polyglutamines and tau, although important differences likely exist. See the main text and Table 2 for references.

misfolding can often occur.[77-79] As post-mitotic cells, neurons appear to be particularly sensitive to these effects and, consistent with this idea, many neurodegenerative diseases involve aberrant protein accumulation. Genetic studies have routinely linked Hsp70 and its co-chaperones to this process and, thus, it has emerged as a potential drug target for multiple neurodegenerative conditions (Table 1-2). One recent example has shown that Hsp70 directly stabilizes lysozomes and plays a key role in Niemann-Pick disease.[80] We will discuss two models here and further information can be found in recent reviews.[81, 82]

Table 1-2. Roles of Hsp70 Proteins in Protein Misfolding and Neurodegenerative Diseases

disease	role	ref.
HD	Hsp70 co-localizes with polyQ aggregates.	208
	Hsp70 and Hsp40 prevent aggregation of purified HD exon 1.	85
	Over-expression of Hsp70 and Hsp40 reduces polyQ aggregation and cytotoxicity.	88, 208
	Hsp70 inhibits polyQ-induced caspase 3 and 9 activation and M3/6 JNK phosphatase aggregation.	94, 209
	Over-expression of Hsp70 does not significantly ameliorate the disease symptoms of R6/2 HD model mice.	93
	HSF-1 activating compounds reduce polyQ aggregation and rescue neurodegeneration in cultured cells and HD model mice.	100, 102, 103
SCA1	Hsp70 over-expression suppresses neurodegeneration and improves motor function in *SCA1* mice.	91
SCA3	Hsp70 co-localizes with nuclear inclusions of ataxin-3.	89, 210
	Over-expression of Hsp70 suppresses polyQ-mediated neuropathy in a *Drosophila* model of *SCA3.*	89
SCA7	Hdj2 and Hsp70 prevent mutant ataxin-7 aggregation in cultured cells but not in a mouse model.	92
SBMA	Hsp70 co-localizes with nuclear inclusions of polyQ expanded androgen receptor (AR).	90, 211
	Hsp70 and Hsp40 increases the SDS-solubility and proteasomal degradation of mutated AR in cultured cells.	212
	Over-expression Hsp70 ameliorates disease phenotypes in a SBMA model	90
	Oral administration of GGA, an HSF1 inducer, ameliorates the SBMA phenotype in mouse models.	101
AD-Aβ	Hsp70 and Hsp40 block *in vitro* Aβ self assembly.	106
	Hsp70 reduces steady state Aβ levels and Aβ-induced cytoxicity in cultured cells	107
AD-Tau	Hsp70 interacts with sites in tau important for aggregation.	109
	Hsp70-Bag2 captures and delivers insoluble and phosphorylated tau to the proteasome for ubiquitin-independent degradation.	116
	Hsp70-Bag1 associates with tau and inhibits proteasomal degradation.	115
PD	Lewy bodies contain Hsp40 and Hsp70.	213
	Over-expression of Hsp70 reduces α-synuclein aggregation and cytotoxicity.	214
	Hsp70 over-expression prevents dopaminergic neuronal loss in PD models.	213, 215
CF	Immature CFTR and ΔF508 CFTR form complexes with Hdj-2 and Hsc70.	216
	Inactivation of Hsc70 and CHIP in cultured cell increase surface expression of ΔF508 CFTR.	217

Polyglutamine (polyQ) diseases are a family of at least nine inherited neurodegenerative disorders, including Huntington's disease (HD), spinocerebellar ataxia (SCA), and spinal and bulbar muscular atrophy (SBMA), caused by the expansion of trinucleotide CAG repeats in the disease genes.[83] This expansion leads to the formation

of an abnormally long glutamine tract in the synthesized protein.[84] PolyQ expansion renders disease proteins prone to aggregation, and the extent of aggregation is correlated with the length of the polyQ.[84] *In vitro*, Hsp70 family members (along with its J-domain co-chaperone Hdj1) can partially suppress the aggregation of the polyQ-expanded exon 1 of huntingtin (htt) in an ATP-dependent remodeling process.[85] Importantly, these chaperones are only active when added during the lag phase of the aggregation reaction, which suggests that Hsc70 and Hdj1 preferably act on early, prefibrillar states (Figure 1-3).[85] Similarly, in a yeast model, over-expression of the yeast Hsp70, Ssa1, decreases aggregation of htt and increases its SDS solubility[86] and over-expression of either full length Hsc70 or its SBD in mouse N2A neuroblastoma cells mildly decreases htt aggregation.[87] However, these relationships appear to be complex because, in O23, COS-7, PC12, SH-SY5Y, and HEK293 cells, Hsp70 over-expression showed little effect on htt aggregation.[88, 89] Similar themes are observed in animal models. For example, in fly models of SCA1 and mouse models of SCA1 and SBMA, Hsp70 family members suppresses the neurodegenerative phenotypes,[90-92] while no significant effect is observed in mouse models of HD or SCA7.[93, 94] It is worth noting that it is not clear whether polyQ aggregation is a good surrogate for toxicity. Moreover, it is not clear if Hsp70's effects on cell viability are always mediated by direct effects on polyQ assembly or through more general buffering of pro-survival signaling,[95, 96] as discussed above.

Despite these uncertainties, it is interesting to note that several co-chaperones, including J-domain proteins, CHIP and BAG, have dramatic effects on polyQ aggregate formation, either on their own or in concert with Hsp70. For example, over-expression of yeast Ydj1 (a J-domain co-chaperone) increases the solubility of htt,[85] whereas a related

J-domain co-chaperone, Sis1, splits large inclusions into smaller foci.[86] The TPR-domain co-chaperone, CHIP, ubiquitinates htt and facilitates its degradation in a U-box dependent manner (Figure 1-3).[97] The over-expression of CHIP significantly reduces neurodegenerative symptoms in animal models of SCA1, SCA3, SBMA, and HD. Similarly, CHIP -/- mice have exaggerated disease progression in models of HD and SCA3.[98-101] The role of Hsp70 in CHIP-mediated protection remains to be established, but current models suggest multiple roles for the Hsp70-CHIP complex.[97, 98] The observations that Hsp70 co-chaperones have effects on polyQ diseases suggest that the best protection against polyQ toxicity might require interplay between multiple components of the chaperone complex. Indeed, it has been shown that chemical stimulators of the heat shock response, such as geldanamycin, 17-(allylamino)-17-demethoxy geldanamycin, geranylgeranylacetone, and celastrol, upregulate multiple chaperone components and reduce neurodegenerative symptoms in cell culture, fly, and mouse models of SCA1, HD, and SBMA.[102-105]

Alzheimer's disease (AD) is the most common neurodegenerative disease and its patients are characterized by progressive memory loss and accumulation of senile plaques (SP) composed of β-amyloid (Aβ) and neurofibrillary tangles (NFT) assembled from tau.[106] Current models suggest that self-association of Aβ or tau into β-sheet rich oligomers leads to neuronal cell death (Figure 1-3).[106, 107] Hsp70 family members have been shown to play important roles in the aggregation and cytotoxicity of both Aβ and tau. Hsp72 blocks the early stages of Aβ aggregation *in vitro* at substoichiometric levels (Figure 1-3), and Hsp70 has been shown to alter processing of the amyloid precursor protein.[108, 109] Also, Hsp70 protects against Aβ-induced cytotoxicity via inhibiting

caspase-9 and accelerating the elimination of Aβ.[110] Tau directly binds to Hsp70 via two sites within its tubulin-binding repeats, which is the same region required for tau self-association.[111] This finding suggests that Hsc70 binding to tau might compete with self-aggregation and toxicity[111] and, consistent with this model, over-expression of Hsp70 reduces aggregated tau in mouse models.[112] Moreover, increasing Hsp70 levels promotes tau binding to microtubules and reduces the levels of hyperphosphorylated tau.[113] Similar to the polyQ examples listed above, co-chaperones of Hsp70 also play roles in tau processing. For example, CHIP ubiquitinates phosphorylated tau in an Hsc70-dependent manner[114, 115] and its over-expression accelerates tau degradation, reduces formation of insoluble tau and rescues tau-induced cell death (Figure 1-3).[115, 116] The TPR-domain co-chaperones, BAG-1 and BAG-2, also impact tau aggregation, but in opposing ways.[117, 118] An Hsc70-BAG-1 complex binds to tau and inhibits its turnover.[117] In contrast, BAG-2 and Hsc70 form a microtubule-tethered complex that can capture and deliver insoluble and phosphorylated tau to the proteasome for degradation (Figure 1-3), likely through a ubiquitin-independent mechanism.[118] Together, these results illuminate the complex relationships between Hsp70, its co-chaperones and their impact on AD and other tauopathies.

1.2.3 Infectious Disease and Immunity.

The prokaryotic Hsp70, DnaK, is required for survival of bacteria under stressful conditions, such as thermal stress and challenge with heavy metals or antibiotics (Table 1-3).[119-121] Consistent with this model, *Staphylococcus aureus dnaK* mutants have reduced viability and are susceptible to stress.[122] Most strikingly, these mutations increase sensitivity to oxacillin and methicillin in normally resistant *S. aureus* strains.

Table 1-3. Roles of Hsp70 in Infection and Immunity.

disease/process	role of Hsp70	ref.
	Bacterial Infection	
invasion	Mutations in DnaK make *S. aureus* less infective and inhibit biofilm formation in *S. mutans*.	118, 120, 218
	S. enterica DnaK is required for invasion of epithelial cells.	123
	Hsc70 enhances internalization of *Brucella* by trophoblasts.	219
	H. pylori Hsp70 allows for its attachment to the gastric epithelia.	220
survival	DnaK mutants are susceptible to stress.	
	S. enterica and *L. monocytogenes* DnaK are required for survival in macrophage.	117-120
	Overexpression of Hsp70 in *M. tuberculosis* reduces survival during the chronic phase of infection.	123, 124
replication	DnaK is necessary for replication of *Brucella suis* in macrophage.	221
immune system evansion	Hsp70 protects macrophages from cell death when infected with *Salmonella choleraesuis*.	125
	Immune Function	
antigen presentation	Hsp70s are involved in MHC class II antigen presentation and endocytic maturation.	223, 224
	Viral Infection	
cell entry and exit	Hsc70 is involved in rotavirus entry into cells.	225, 226
	Hsp70 is involved in the disassembly of polyomavirus and papillomaviruses in mouse cells.	227
replication	Hsp70 associates with RSV polymerase complex in lipid rafts.	228
	Interaction between Hsc70 and T-antigen is required for the replication of simian virus 40.	229-233
	Hsp72 is involved in Epstein-Barr virus replication.	234
	Hsp70 can replace viral protein R in the preintegration comples of HIV.	235
immune response	Hsp70 prevents cell cycle arrest and apoptosis in HIV infected cells.	236
viral assembly	Hsp70 is associated with capsid formation in polyomavirus and papillomaviruses.	237

Likewise, *dnaK* or *dnaJ* mutations in *Escherichia coli* make the cells susceptible to fluoroquinolones.[123, 124] These chaperones are also necessary for *Salmonella enterica* to invade epithelial cells and for *Listeria monocytogenes* to survive in macrophages.[125, 126] Thus, Hsp70 family proteins and their co-chaperones appear to be potential drug targets that would sensitize prokaryotes to stress, such as that provided by antibiotics or host responses.

In addition to its roles in bacterial physiology, Hsp70 is also important in host immunological responses and cell-cell interactions. For example, in mammalian cells infected with a virulent form of *Salmonella choleraesuis*, the levels of Hsp70 correlate with an increase in TNF-α induced cell death.[127] In another example, *Mycobacterium tuberculosis* leverages its own Hsp70 to activate inflammatory signals via NF-κB activation.[128] Hsc70 and other heat shock proteins also play important roles in IKK signaling, endocytic trafficking and possibly in antigen presentation, suggesting roles in activation and regulation of immune cells.[129-131]

1.3 Chemical Targeting of Hsp70s

Given these complex roles of Hsp70 in disease, it is not immediately apparent whether a good therapeutic strategy would be to stimulate, inhibit or otherwise re-direct the activity of this chaperone with chemical agents. For example, would stimulation of Hsp70's ATPase activity protect from neurodegeneration? Would inhibition sensitize cancer cells to apoptosis? Moreover, should the ATPase activity of Hsp70 be the ideal target or is another function (*e.g.* protein folding, protein trafficking *etc.*) more appropriate? Given the promiscuity of Hsp70's interactions with proteins, is it possible to influence the processing of individual substrates or will inhibitors have global effects? Although the answers to many of these important questions remain unknown, work over the last decade has provided first-generation, Hsp70-targeted compounds.[132, 133] Interestingly, these compounds belong to a broad range of structural classes and some have distinct, non-overlapping binding sites on the Hsp70 surface. These observations suggest that there are multiple ways to impact Hsp70's functions, such as through modulating its ATPase activity, its contacts with co-chaperones or binding to misfolded

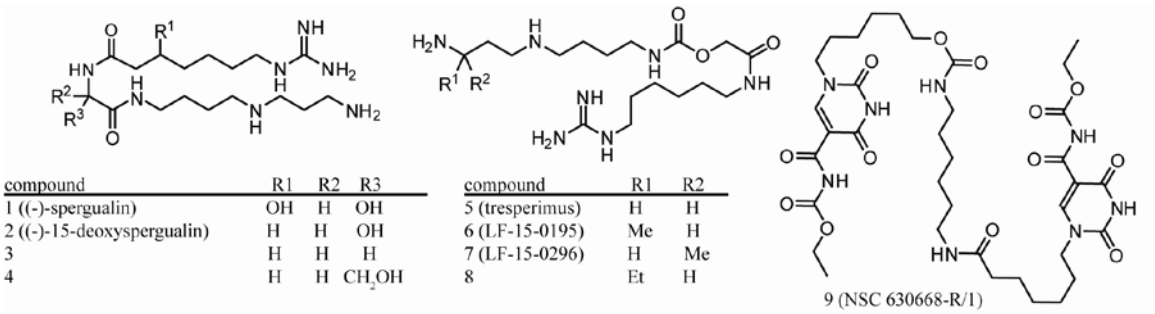

compound	R1	R2	R3
1 ((-)-spergualin)	OH	H	OH
2 ((-)-15-deoxyspergualin)	H	H	OH
3	H	H	H
4	H	H	CH_2OH

compound	R1	R2
5 (tresperimus)	H	H
6 (LF-15-0195)	Me	H
7 (LF-15-0296)	H	Me
8	Et	H

9 (NSC 630668-R/1)

Figure 1-4. Structures of spergualin and related polyamines. Select structrures from larger series shown for clarity. See the text for references.

substrates. Importantly, these early probes have also begun to reveal unexpected aspects of Hsp70's biology. Thus, even if these compounds do not directly lead to approved drugs, they have started to define Hsp70's roles in disease. In the following sections, we review the known chemical classes and briefly highlight the medicinal chemistry efforts and biological findings enabled by these probes.

1.3.1 Spergualin-like Compounds.

In 1981, Umezawa and colleagues reported the identification of a compound with antibiotic and anti-tumor activity from a *Bacillus sp.*[134] They further characterized the active compound as the polyamine, (-)-spergualin **1** (Figure 1-4).[135] Kondo and colleagues carried out the total synthesis of this compound in 14% overall yield.[136] However, the natural compound was found to have poor stability *in vitro* and *in vivo*, which led to the synthesis of analogues, including 15-deoxyspergualin (15-DSG; **2**).[137, 138] In an aqueous environment at pH 7, removal of the labile 15-hydroxyl group was found to improve stability to 2 days.[139] The route to 15-DSG and its derivatives involves formaldehyde-mediated cyclization of spermidine, followed by coupling of the free amine to an amino acid and installation of the ω-guanidino fatty acid.[140] Thus, this approach allows ready variation of the amino acid. However, in antitumor assays against

L1210 leukemia cells, only the glycine (**3**) and L-serine (**4**) derivatives retained activity, whereas even conservative replacements with alanine or leucine abolished function.[140] Likewise, variations in the polyamine regions, such as the number of methyl groups or secondary amines, decreased efficacy.[138] Taken together, these results suggest that the structure-activity profile of spergualin analogues is surprisingly narrow.

Despite the improved stability of 15-DSG, this compound still retained relatively poor bioavailability.[141] In an attempt to circumvent some of these shortcomings, a series of derivatives was developed in which the amides are inverted and this change was found to greatly improve the molecule's stability and activity.[139] Following from these efforts, the hydroxyglycine moiety was substituted with a carbamoyl group, producing the promising derivatives tresperimus **5** and LF 15-0195 **6** (Figure 1-4). However, in this series, only minor methyl substitutions were tolerated in a few positions without a dramatic loss of activity.[142] For example, an *R* methyl group appended near the terminus (**6**) was tolerated, while the opposite stereochemistry (**7**) had no apparent Hsp70 binding and 3-fold reduced immunosuppressive activity.[143] Likewise, conservative replacement of this methyl with an ethyl (**8**) greatly reduced activity. Other portions of the molecule were equally sensitive to manipulation; for example, replacement of the guanidine with a pyridine reduced activity by approximately 4-fold.[143] Taken together, the structure-activity studies have revealed a surprisingly limited range of acceptable modifications.

Using immobilized compound, 15-DSG and its derivatives were found to bind to several proteins, including Hsc70 and Hsp90.[143 144, 145] Based on mass spectrometry and competition studies, it was further proposed that 15-DSG binds to the EEVD domain of these chaperones with an affinity ~ 5 μM.[146, 147] This interaction appears to impact some

of Hsp70's functions, because 15-DSG was able to increase Hsc70's ATPase rate by approximately 20 to 40%.[148] Although this change in turnover rate seems minor, the biological activities of these compounds suggest that either (a) even modest changes might impact chaperone function or (b) ATP turnover is not the most relevant *in vitro* assay to describe their activity on the chaperone. More recently, 15-DSG was found to sequester Hsc70 in cells and limit its transport, which is proposed to stall protein synthesis.[149] This effect could be reversed by the addition of EEVD peptide, consistent with its known binding site. Despite this evidence, other proteins, such as α1-acidglycoprotein, have been suggested as targets of spergualin analogs.[150] Based on these reports and the relatively modest affinity for Hsp70 and Hsp90, it seems likely that 15-DSG and its derivatives may have multiple cellular targets.

Although spergualin was first identified as an anti-infective and anti-tumor agent, 15-DSG was subsequently identified as a potent immunosuppressant. The molecular mechanisms of this activity are not entirely clear, but 15-DSG has been proposed to block NF-κB trafficking and antigen presentation, two known cellular roles of Hsc70.[131, 151] Regardless, 15-DSG decreases the incidence of acute rejection in combination with cyclosporin and tacrolimus[152] and it prolongs renal allograft survival.[153] These immunological activities arise from 15-DSG's effects on dendritic cells[154] and leukocyte[155] and monocyte[151] activation; for example, Birck and colleagues looked at T-cell activation in patients with Wegener's granulomatosis and found that patients treated with 15-DSG had lower levels of proliferation markers, such as INF-γ and IL-10.[153] Similarly, treatment with 15-DSG leads to decreased mucosal injury and reduced TNF-α in a mouse model of colitis.[156]

Based on these activities, 15-DSG has been explored in multiple clinical trials, with allograft rejection and malignant cancers being the most widely studied indications. For additional details an excellent review is available.[150] Briefly, 15-DSG is poorly bioavailable (5%), so it is typically delivered by *i.v.* infusion.[141] It displays a bi-exponential decay, with an alpha half-life ($t_{1/2}$) of 5 to 12 minutes and terminal half-life of approximately 2 hours.[157] Metabolism is believed to occur, in part, through amine oxidases with seven inactive metabolites known.[150] In rodents, infusion of 25 mg/kg/day for 9 days leads to a 4-6_{log} reduction in tumor burden in a L1210 leukemia model.[158] However, a Phase I clinical trial of 15-DSG as a monotherapy against advanced malignancies showed no efficacy at 75 mg/kg/day.[150] Similarly, a Phase II trial against metastatic breast cancer in 14 patients at 1800 or 2150 mg/m^2/day by *i.v.* infusion for 5 days also showed no efficacy. However, in both trials, 15-DSG was well tolerated and only low toxicity was observed (mild neuromuscular side effects as the only grade III toxicities).[159] The experiences with immunological indications have been more promising. Since 1994, 15-DSG has been used in Japan for acute kidney allograft rejection.[150] The advantage of 15-DSG is that, unlike FK506 or cyclosporin, it can be used up to 48 hrs after initiation of rejection and, therefore, can reverse ongoing rejection in animal models and humans. For example, 81% of patients undergoing acute renal allograft rejection in one study of 31 patients showed reversal of rejection with administration of 15-DSG, even as a monotherapy in some cases.[160] Importantly, 15-DSG is not a P450 substrate and it can be used with cyclosporin or steroids.[157] In fact, studies of kidney and liver allograft rejections in Western Europe revealed 65% reversion in combination with bolus steroids.[161] In addition to these examples, many other pilot

clinical studies in Japan and the U.S. have been reported, and these generally document good tolerability, low toxicity and efficacy in transplant models.[150] While 15-DSG has been used successfully in the clinic, the mechanism by which it exerts this effect is not fully understood. For example, how specific is this compound for Hsc70? If it is specific, how does binding to the EEVD control chaperone functions? Does the seemingly minor change in ATPase rate (20 to 40%) lead directly to the robust cellular effects? Is binding to both Hsp70 family members and Hsp90 important for activity? Clearly, additional structural and mechanistic experiments are needed.

Given the promising biological activity of spergualin-like compounds, Brodsky and colleagues searched the Developmental Therapeutics database at the National Cancer Institute for related compounds. This effort yielded, NSC 630668-R/1 (R/1), which inhibits Hsc70's ATPase activity and partially blocks chaperone-mediated protein translocation (Figure 1-4).[162] However, unlike 15-DSG, R/1 inhibits stimulation of Hsc70's ATPase activity by J-domain co-chaperones.[162] This result is interesting because, although R/1 was originally identified as a 15-DSG analogue, it appears to operate by a different mechanism.

1.3.2 Dihydropyrimidines.

Following the successful identification of R/1, Brodsky and colleagues searched for other scaffolds able to alter Hsp70's ATPase activity. Guided by structural similarity to 15-DSG and R/1, they focused on a series of functionalized dihydropyrimidines (Figure 1-5).[163] The synthetic route to these compounds leveraged consecutive, Biginelli and Ugi multi-component reactions to yield diversity. In an ATPase assay, several compounds from this series were shown to inhibit ATP hydrolysis (e.g. MAL3-101 (**9**)),

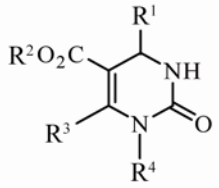

compound	R1	R2	R3	R4
10 (MAL3-101)	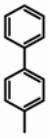	Bn	Me	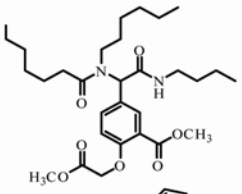
11 (MAL3-90)	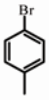	Et	Me	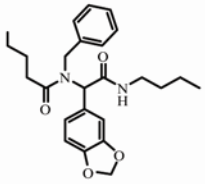
12		Et	Me	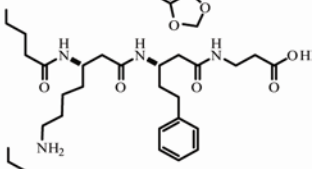
13		Et	Me	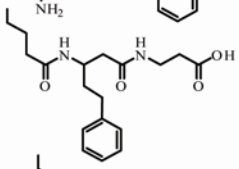
14 (SW02)		Et	Me	
15	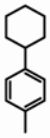	Bn	Me	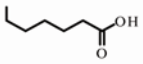
16		Me		H

Figure 1-5. Structures of dihydropyrimidines with activity against Hsp70 family members. Select compounds from larger series are shown for clarity. See the text for references.

while others enhanced this activity (e.g. MAL3-90 (**10**)).[163] Moreover, the activity of these compounds was dependent on the presence of a J-domain co-chaperone, similar to what had been seen with R/1.[162] For example, compound **9** had no effect on ATP hydrolysis by Hsc70 at up to 600 µM, but it gave a 4-fold reduction at 300 µM when

added to the combination of Hsc70 and the J-domain of T-antigen.[163] Approximately 30 compounds were tested in these experiments and, accordingly, quantitative SAR was not readily apparent. To further explore this series, seventeen additional dihydropyrimidines were synthesized in which the Ugi-derived peptoid portion was replaced with a protease-resistant, beta-peptide.[164] The activity of these derivatives was tested against the ATPase activity of two Hsp70s (either Hsc70 or DnaK) in complex with a J-domain co-chaperone. The results of that study suggest that hydrophobic substitutions near the dihydropyrimidine core (R4; Figure 1-5) may be important for activity. For example, compounds **11** and **12**, which have phenyl substitutions in this region, changed ATP turnover by between 20 and 45%.[164] Interestingly, **11** was an inhibitor of ATPase activity, while **12** was a stimulator, consistent with the general observations that compounds of this class can have either type of activity when J-domains are present. Also, **12** only stimulated bovine Hsc70 and not *E. coli* DnaK, suggesting that these highly homologous proteins might be independently targeted. Despite these efforts, the potency of these compounds is very weak (EC_{50} values ~ 75-300 μM), making it challenging to interpret the SAR and to confirm selectivity for Hsp70 in cells. Part of the challenge, until recently, was that compounds had to be tested in small numbers because a high throughput assay for Hsp70's ATPase activity had not been available. To improve this capacity, Chang *et al.* converted a malachite green assay into a high-throughput platform for DnaK. Importantly, this assay employs purified DnaK and its co-chaperones, DnaJ, and GrpE, to boost the signal and provide physiological turnover rates.[165] This advance allowed screening of a collection of more than 180 dihydropyrimidines and, from these efforts, several promising derivatives, such as **14**, which blocks more than 80% of

DnaK's activity at 150 μM, were identified. To complement this approach, a medium throughput luciferase-refolding assay was developed. In this assay, denatured firefly luciferase is diluted in the presence of the three-component chaperone complex and refolding is monitored by recovered luminescence. The ~180 member dihydropyrimidine collection was screened in 96-well format and the best of these compounds, such as **15**, had EC_{50} values around 4 μM.[166] Some compounds in this series inhibited chaperone-mediated luciferase folding, while others were stimulatory. Interestingly, there was not obvious structural similarity between the active compounds from the ATPase assay and the luciferase-folding assay.

Even though the dihydropyrimidines identified to date have relatively weak activity and their selectivity remains to be established, the first-generation compounds have been employed in a variety of biological systems. Importantly, these studies have provided surprising insights into Hsp70's functions in disease models. In one example, the stimulatory dihydropyrimidine, **13**, was found to enhance the Hsp70-mediated inhibition of amyloid-β aggregation.[108] Conversely, a weak inhibitor of ATPase activity led to suppression, suggesting that the ATP hydrolysis rate of the chaperone might impact its anti-aggregation activity *in vitro*. To test this model in cells, Jinwal *et al.* used both inhibitors and activators of Hsp70's ATPase activity in a model of tau aggregation.[167] Surprisingly, they found that stimulators, including **13**, led to dramatic accumulation of tau by Western blot analysis, while inhibitors had the opposite effect. The inhibitors reduced tau levels via rapid ubiquitination with EC_{50} values of ~5 to 10 μM. Importantly, over-expression of Hsp70 promoted the activity of the inhibitors and lowered their EC_{50} values, consistent with this chaperone as an important cellular target. Current models

suggest that this result could be achieved by the inhibitors keeping the Hsp70 family member in a specific conformation, such ATP-bound, which is conducive to interactions with components of the ubiquitin-proteasome system (Figure 1-1 B). Thus, the net result of ATPase inhibitors appears to be ubiquitination of the bound protein substrate. Finally, intracranial injection was found to reduce tau in tau transgenic mice, which suggests that inhibiting the ATPase activity of Hsp70 might be a viable strategy for reducing the accumulation of misfolded tau. In addition to these studies on protein misfolding and aggregation, dihydropyrimidines have also been employed to explore the potential of Hsp70 as a target in apoptotic signaling and cancer. For example, compound **9** was found to have good anti-cancer activity against SKBr3 cells by decreasing cell viability.[168] This activity appears to be mediated by the ability of the dihydropyrimidines to interrupt stimulation of Hsp70 by J-protein co-chaperones, because the GI_{50} values for a series of peptoid-modified dihydropyrimidines tend to correlate with their activity in a J-stimulated ATPase assay.[169] Moreover, the best compounds (of the nearly 50 derivatives tested) had promising GI_{50} values of approximately 6 to 10 μM against SKBR3 cells, suggesting the possibility that inhibition of Hsp70 alone is sufficient to induce apoptosis. To explore the potential mechanisms for anti-cancer activity, the effects of activators and inhibitors on stability of the pro-survival target, Akt, were explored.[170] In that study, it was found that activators promote Akt stabilization, while inhibitors promote dramatic Akt degradation and subsequent cell death in a panel of cancer cells.[170] This mechanism is similar to that proposed for Hsp90 inhibitors, which involves selective destabilization of key survival substrates, including Akt.[72] Because Hsp90 and Hsp70 often cooperate, it is not yet entirely clear what role Hsp90 might play in the response to Hsp70 inhibitors.

Together, these studies suggest that inhibition of Hsp70's ATPase activity leads to degradation of key apoptosis substrates in cancer cells. Further work is needed to understand the molecular mechanisms; however, these collective findings, across multiple models of protein misfolding and apoptosis, have begun to reveal potential avenues towards therapeutic intervention.

1.3.3 Fatty Acids.

Sulfogalactosyl ceramide and sulfogalactoglycerolipid are two sulfoglycolipids that have been found to bind Hsp70. Mamelak and Lingwood identified their putative binding site on the NBD through deletional analysis and site-directed mutagenesis; specifically, mutation of two residues in the NBD (Arg 342 and Phe 198) led to reduced binding of 3'sulfogalactolipid.[171] It was further shown that the aglycone portion determines whether the molecules bind to bacterial or eukaryotic Hsp70s. Eukaryotic Hsp70 bound $SG^{24}Cer$, $SG^{18}Cer$, and $SG^{20:OH}Cer$ while DnaK preferentially bound to $SG^{18:1}Cer$ and $SG^{20:OH}Cer$.[172] Other substitutions on the aglycone or manipulations of the sulfation (or phosphorylation) pattern on the sugar ablated binding, demonstrating the narrow tolerance in these regions.[173] A full SAR analysis of this class of molecules awaits expanded library synthesis and additional structural studies. However, early studies revealed that substituting the acyl chain with an adamantyl group improved

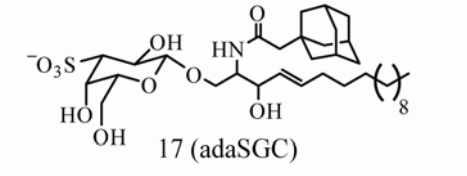

Figure 1-6. Chemical structures of a representative sulfoglycolipid (adaSGC).

affinity for Hsp70 (Figure 1-6). Compound adaSGC (**16**) was found to have an IC_{50} value of ~50 μM.[171] Interestingly, adaSGC is a noncompetitive inhibitor of ATPase activity, but the molecular mechanism of inhibition is not entirely clear.[174] In cells, **16** increases the protein levels of ΔF508CFTR,[174] a mutant of the cystic fibrosis transmembrane receptor (CFTR) that is prone to misfolding and degradation through ER-associated degradation (ERAD). Thus, this finding suggests that inhibition of Hsp70's ATPase activity might suppress the ERAD pathway that normally acts to reduce the levels of mutated CFTR, a result that would have implications on cystic fibrosis and other misfolding diseases. Moreover, the activity of **16** was found to be dependent on the actions of both Hsp70 and a J-domain containing co-chaperone, consistent with this complex as a cellular target. Despite these insights, the binding site for these glycolipids is only loosely defined and, further, their selectivity has yet to be firmly established.

Another example of a fatty acid-like derivative that inhibits Hsp70 function is the acyl benzamide family. This class of compounds arose from work by the Schiene-Fisher group in which they targeted the cis/trans aminopeptidyl isomerase (APIase) activity of DnaK, in an effort to identify potential antibiotics. DnaK has been shown to catalyze isomerase activity through a poorly understood mechanism. Efforts to target this activity with small molecules yielded acyl benzamides with IC_{50} values as low as 2.7 μM.[175] Further, they found that the length of the fatty acid chain is an important determinant of the molecule's activity (Figure 1-7). For example, short acyl chains, such as those in **17**, gave compounds with poor activity in both APIase and bacterial growth assays. Increasing the length of the chain tended to enhance potency: compound **18** had an IC_{50} in the APIase assay of 5 μM and an MIC against *E. coli* of 380 μg/mL, while **19** had an

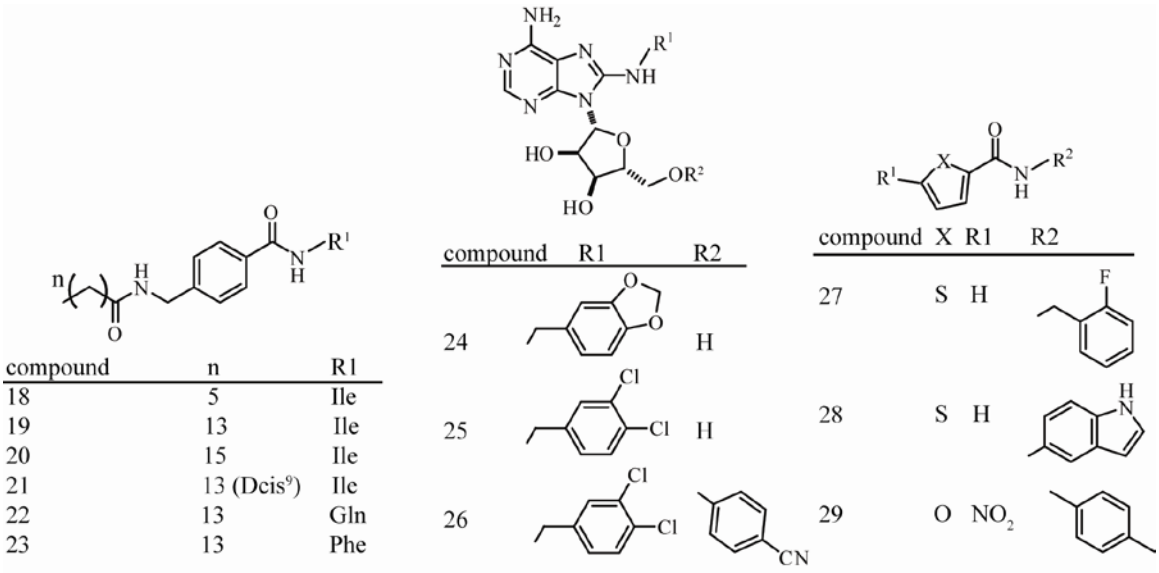

Figure 1-7. Chemical structures of Hsp70 inhibitors. Select compounds from larger series are shown for clarity. See the text for references.

IC_{50} of 1.2 µM and MIC of 180 µg/mL. However, increasing the fatty acid chain-length also enhanced undesirable erythrocyte hemolytic activity. Hemolytic activity could be partially avoided by installation of unsaturations in the fatty acid; for example, compound **20**, with a cis alkene at C9, had an EC_{50} >1500 µg/mL in the hemolytic assay, while it retained activity against APIase (36 µM) and bacterial growth (280 µg/mL). Substitutions in the amino acid portion (R1) altered the MIC values, with less predictable effects in the other *in vitro* assays.[175] For example, dramatic substitutions of the isoleucine for a glutamine (**21**) or phenylalanine (**22**) caused modest changes in APIase inhibition but they increased the MIC by approximately 3- to 7-fold. Together, these findings suggest that the *in vitro* activity assays ascribed to Hsp70 might not best reflect the key mechanistic roles played by this chaperone in bacteria. This is a re-occurring theme in the Hsp70 field because the roles of measurable Hsp70 functions (*e.g.* ATPase, APIase, refolding) in controlling its biology *in vivo* remain uncertain. Despite this discrepancy, the MIC of the best acyl benzylamide is approximately 7-fold lower than that of

ampicillin, which suggests that these compounds or their derivatives may be useful. However, it is important to note that their selectivity for Hsp70 has not been formally established and any off-target effects of these compounds remain unexplored.

1.3.4 Peptides.

As mentioned above, DnaK is considered a potential target for anti-bacterials, but this model has only recently been tested with pharmacological agents. For example, a series of 18-20 amino acid, proline-rich peptides, including drosocin, pyrrhocoricin, and apidaecin (Table 1-4), were described that bind DnaK (and another prokaryotic chaperone, GroEL) and kill susceptible bacteria without impacting mammalian cells.[176] Pyrrhocoricin inhibits the ATPase activity of *E. coli* DnaK and it binds in the SBD with a K_d of 50 μM.[177] This interaction is thought to keep the "lid" domain in the closed position, preventing substrate release, a model supported by computational simulations and mutagenesis studies, which identified the SBD residues Glu589, Gln595, and Met598 as the key targets in DnaK.[178] Interestingly, pyrrhocoricin does not bind to *S. aureus* DnaK,[177] suggesting a potential difference between gram-positive and –negative strains. In an effort to optimize the pharmacokinetics and antibacterial activity of these peptides, several analogues representing combinations of the consensus sequences were generated. Of these derivatives, GRPDKPRPYLPRPRPPRPVRL is the most active and it also has improved serum stability.[179] Importantly, this compound has activity against both *E. coli*

Table 1-4. Sequences of Antibacterial Peptides Targeting DnaK

peptide	sequence
drosocin	GKPRPYSPRPTSHPRPIRV
apidaecin	GNNRPVYIPQPRPPHPRI
pyrrhocoricin	VDKGSYLPRPTPPRPIYNRN

and a resistant strain of *Enterobactericeae sp.*, with an MIC approximately 4 times better than ciprofloxacin. Moreover, it was not toxic to eukaryotic cells at concentrations up to 1.5 mg/mL.[179] Cudic *et al.* recently generated dimers of pyrrhocoricin in an effort to further improve stability and potency. Some of these compounds have increased serum stability compared to pyrrhocoricin and activity against isolates normally resistant to β-lactams, tetracycline, or aminoglycosides.[180] While these compounds have not advanced to the clinic, they have shown that targeting DnaK may be a viable anti-bacterial strategy and further work will likely improve stability and potency.

1.3.5 ATP Mimics.

Given that Hsp70's ATPase activity appears to be one central determinant of chaperone function, compounds that are competitive for binding to ATP might be expected to have potent activity. This hypothesis arises, in part, from analogy with Hsp90, in which ATP competitive compounds, such as geldanamycin derivatives, induce degradation of Hsp90 substrates. Recently, Williamson *et al.* published the first adenosine analogues that can be used to test this important hypothesis in Hsp70. Using a fluorescence polarization assay, they screened adenosine derivatives and identified 8-amino adenosines with affinity for the ATP-binding site, with the most active (**23**) having an IC_{50} of 4.9 μM (Figure 1-7).[181] The intended binding orientation was confirmed by a co-crystal structure. Further, when the 8-amino group was substituted with 3,4-dichlorobenzyl (**24**), it retained activity (IC_{50} ~ 9.1 μM) and had an improved toxicity profile. Subsequent modifications optimized the π-stacking with residues in Hsc70 and the 5-substituent (R2) was further substituted with a 4-cyanophenyl group to yield a tight binding compound **25** (IC_{50} value of 0.5 μM). Importantly, **25** also had activity against

HCT 116 colon carcinoma cells (GI_{50} of 5 μM) and it reduced the levels of Her2, a substrate that is sensitive to Hsp70 knockdown.[181] Most recently, compounds from this class were also found to have synergy with an Hsp90 inhibitor in HCT116 cells,[182] which might be expected based on shared functions of these chaperones. Together, these studies represent an important step towards submicromolar affinities and structure-guided design of Hsp70 inhibitors.

1.3.6 Phenylethynesulfonamide.

Recently, Leu and colleagues reported the identification of 2-phenylethynesulfonamide (PES; **26**) as a compound that binds Hsp72.[183] PES (also known as Pfithrin-μ) has been shown to be selectively toxic to cancer cell lines and it was proposed to affect p53, but its mechanism of action had not been clear. Biotin-conjugated PES revealed Hsp72 (but not Hsc70, BiP or Hsp90) as a target and deletional analysis further restricted the binding site to the C-terminus.[183] Using immunoprecipitations, the authors characterized the effects of PES on assembly of the Hsp70 chaperone complex in different cell lines. They hypothesized that PES would alter co-chaperone associations with Hsp72 and, thereby, alter chaperone functions. These studies revealed that PES prevents the interaction between Hsp72 and some BAG proteins, depending on the cell type. Moreover, PES blocks association of Hsp72 with p53, consistent with the ability of PES to kill cancer cells and block caspase activation. Finally, PES appears to interrupt the interaction of Hsp72 and LAMP2, an important protein in chaperone-mediated autophagy. Consistent with this idea, long-lived proteins are degraded at a reduced rate in response to PES and this compound causes build up of procathespin L, indicating that autophagy and lysosomal enzyme processing are impaired.[183] Together, these studies

suggest that PES changes the interactions of Hsp70 with some of its co-chaperone partners and, through this activity, impacts substrate fate. Moreover, PES has a relatively simple structure and it seems likely that additional synthetic studies might improve its activity and, potentially, its selectivity. Those efforts will likely benefit from improved structural analysis and further biophysical studies on the mechanism for changes in Hsp70 complex assembly.

1.3.7 Thiophene-2-carboxamides.

Celliti *et al.* recently used NMR spectroscopy to identify compounds that bind to DnaK.[184] They specifically explored the protons in the aliphatic region of the 1D ^{1}H NMR spectra of *E. coli* DnaK SBD (residues 393-507) in an effort to find scaffolds that interact with that domain. These efforts yielded a pocket near Leu484 and Pro419, which forms a groove important for allosteric communication between the SBD and the NBD. The compounds that bound this site were principally thiophene-2-carboxamides, such as **26**, and their binding was confirmed by isothermal titration calorimetry (ITC), with K_d values around 70 μM. Based on these results, 15 derivatives with either a thiophene or furan core and a variety of hydrophobic groups appended to the 2-position were synthesized (Figure 1-7). Adding bulk to the R2 substituent seemed to improve affinity and these efforts yielded the indole-substituted **27**, which bound with a K_d of 12.7 μM. Finally, members of this series of compounds were found to inhibit growth of *E. coli* and *Yersinia pseudotuberculosis*, with MIC values of approximately 10 to 400 μM depending on the strain and growth temperature. The best compound was the 2-substituted furan **28**, which had an MIC of less than 12 μM against *Y. pseudotuberculosis* at 40 °C. Interestingly, the most potent inhibitor of microbial growth was not the compound with

the highest affinity to DnaK as determined by ITC, again suggesting a complex relationship between Hsp70 binding and *in vivo* potency.

1.3.8 Other Scaffolds.

Included in a comprehensive list of compounds with activity on Hsp70 are several molecules that have either recently been discovered or older ones that await further study. For instance, the rhodacyanine, MKT-077 (Figure 1-8), has been reported to bind to mtHsp70 for about a decade.[185] Because of its cationic character, this compound is thought to accumulate across the mitochondrial proton gradient in rapidly dividing cancer cells. In that subcellular compartment, it is proposed to bind the ATP binding site of mtHsp70, leading to mitochondrial disruption and anti-cancer activity.[186] In early experiments, MKT-077 was found to inhibit proliferation of multiple human cancer cell lines, including colon, bladder and breast carcinoma cells, with IC_{50} values ranging from 1 to 5 μM with no toxicity against normal kidney cells.[187] Based on these findings, pre-clinical evaluation in rats revealed low toxicity below 3 mg/kg/day and primarily renal impairment above that dose. In mouse xenograft studies, continuous infusion was required for anti-tumor activity.[188] Based on the preclinical findings, a Phase I clinical trial against solid tumors was performed using daily infusions carried out five times over three weeks at 30-50 $mg/m^2/day$.[189] In a subset of these patients, renal toxicity was again seen as the major toxicity. Importantly, pharmacokinetic measurements failed to detect MKT-077 above one micromolar in the serum, suggesting that therapeutic dose was not achieved. Consistent with this, little improvement in disease was seen (1 out of 10 patients achieved stable disease).[189] However, these studies suggest that targeting mitochondrial Hsp70 might be a viable strategy if the toxicity and pharmacokinetics of

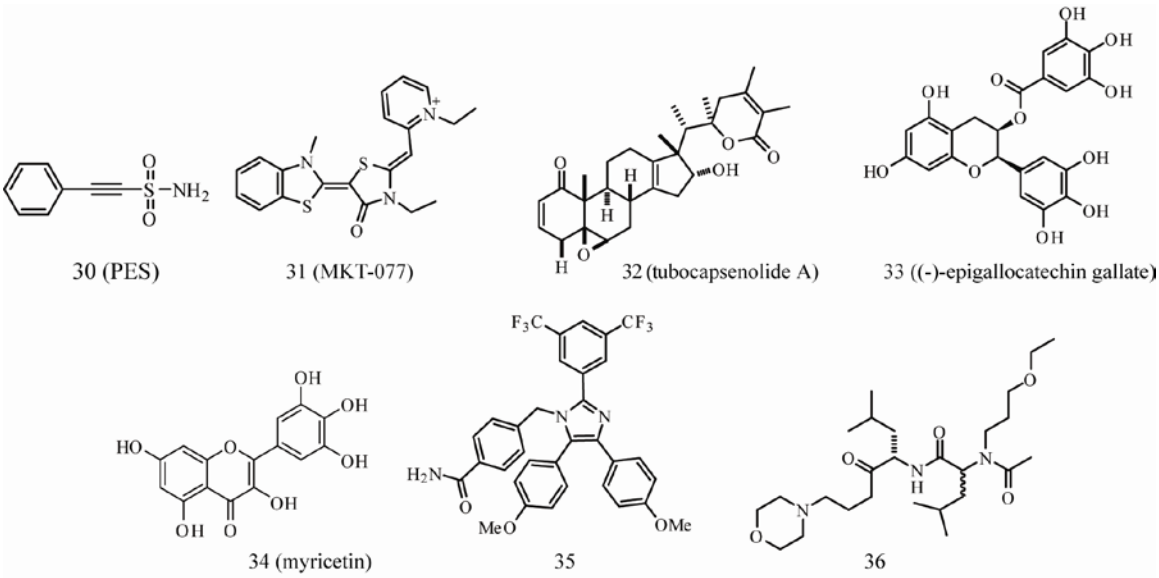

Figure 1-8. Chemical structures of miscellaneous Hsp70 inhibitors.

this scaffold could be improved. In addition, more detail about the selectivity and mtHsp70-binding activity of this compound might guide these efforts.

Other interesting scaffolds include, tubocapsenolide A, a steroid-like molecule, which was identified as an inhibitor of Hsp70. It was proposed to oxidize thiols on both Hsp70 and Hsp90, causing their inactivation.[190] Also, there are several reports suggesting that (-)-epigallocatechin gallate can inhibit Hsp70s, including BiP, allowing initiation of apoptotic pathways.[191-193] Likewise, the flavonoid, myricetin, inhibits the ATPase activity of Hsp70s, reduces tau levels and has anti-cancer activity in multiple models.[167, 170] It should be clearly noted that polyphenols, such as epigallocatechin gallate and myricetin, are notoriously promiscuous. However, uncovering their binding site(s) and mechanism(s) on Hsp70 might reveal new "druggable" sites and opportunities for structure-guided design. Recently, an imidazole was reported by Williams *et al.* to induce apoptosis through interactions with Hsp70 and Hsc70[194] and Haney *et al.* reported that Ugi-derived peptoids modulate Hsp70's ATPase activity by up to 40% through binding to

the SBD.[195] Finally, peptides derived from BAG1 were shown to inhibit the BAG1-Hsc70 interaction and inhibit proliferation of breast cancer cells.[196] These last results further emphasize the important contribution of co-chaperones in guiding the activity of the Hsp70 complex. While much work remains to optimize these compounds and establish their selectivity for Hsp70, they provide an illustration of the wide diversity of structures found to interact with this chaperone.

1.4 Analysis and Prospectus

Hsp70 is a critical molecular chaperone in cell survival signaling and protein homeostasis. As such, it has gathered significant attention as a potential, emerging drug target.[44, 67, 132, 133] Genetic studies (e.g. knockdown and over-expression) have clearly demonstrate that Hsp70 and its co-chaperones are involved in cancer, neurodegeneration and other diseases. The next steps are to determine if the various functions of Hsp70 can be pharmacologically manipulated and, further, whether the outcomes of this intervention will be well tolerated. On first glance, targeting of a core mediator of protein homeostasis might be considered challenging, given its widespread cellular roles and ample opportunities for toxicity. In part, enthusiasm for Hsp70 as a drug target is based on the success of programs targeting other core molecular chaperones, such as Hsp90.[67] As mentioned above, Hsp90 inhibitors specifically destabilize pro-survival signaling proteins in cancer cells and the results of early anti-cancer trials appear promising. However, the field of Hsp70 inhibitors is less mature and many, important questions remain before Hsp70 can be considered an equally good drug target.

In this review, we have discussed some of the early efforts to identify inhibitors of Hsp70 and highlighted some of the biological findings enabled by these reagents.

However, many questions remain before Hsp70 can be considered a fully validated drug target. For example, there are multiple assays used to measure Hsp70 activity *in vitro* (*e.g.* ATPase activity, APIase activity, substrate folding, anti-apoptotic signaling, *etc*) and the relationships between any of these measurable functions and the chaperone roles of Hsp70 *in vivo* remain unclear. Additionally, there is a general lack of selectivity information for the first-generation, Hsp70-targeted compounds. Thus, it seems likely that at least some of these compounds are enacting their cellular activities through multiple pathways, which precludes definitive statements on Hsp70 as a drug target.

Clearly, one of the major problems in the field is that consensus assays for studying Hsp70 are lacking. By analogy, Hsp90 inhibitors are often tested against a battery of standard assays, including those that measure chaperone binding *in vitro* and the ability to reduce the levels of Hsp90 substrates, such as Akt, Cdk4, Raf and Her2, in cells.[74] Future efforts on Hsp70 will benefit from similar, routine utilization of (a) *in vitro* binding assays, (b) examination of cellular effects on putative Hsp70 substrates, such as tau, and (c) studying the effects of Hsp70 over-expression on compound efficacy. This last point is particularly important because, in our opinion, the interpretation of pull-down studies (which are often used to document Hsp70 binding in cells) are complicated by both the hydrophobic promiscuity of this chaperone and its abundance. Thus, over-expression studies may provide a more readily interpretable alternative. Another interesting approach is transcriptional profiling, which was previously used to identify a novel Hsp90 inhibitor.[197] Finally, a greater emphasis on structural studies seems warranted, to permit insights into the binding sites of putative Hsp70 inhibitors. In the Hsp90 field, extensive crystallography studies have yielded important molecular details

into the binding sites. As the field of Hsp70 inhibitors matures, increasing utilization of structural analysis and broader assay profiling will ultimately accelerate discovery.

It is interesting to note that a wide variety of chemical scaffolds (e.g. polyamines, fatty acids, sulfoglycolipids, peptides, nucleosides, *etc.*) have been identified with affinity for Hsp70. Although some of these scaffolds are likely promiscuous, this observation still suggests that Hsp70 harbors an unusual number of potential drug-binding sites that can accommodate a variety of chemical scaffolds. These sites might include deep pockets, such as those found in the ATP-binding cleft and substrate-binding region, and more shallow surfaces, such as those involved in allostery and protein-protein interactions with co-chaperones. Although not all of the compounds discussed herein have been explored in sufficient molecular detail, the early findings suggest that there are multiple ways to impact Hsp70's functions. For example, PES, BAG1-related peptides and dihydropyrimidines seem to interrupt Hsp70's contacts with co-chaperones, while **25** directly competes for nucleotide binding. However, the suitability of each binding site for further development remains uncertain in most cases because direct relationships between the binding event and chaperone functions *in vivo* are not known.

One interesting aspect of Hsp70 biology that remains to be more fully leveraged is the ability of this chaperone to form multi-protein complexes. As discussed above, Hsp70 interacts with multiple classes of co-chaperones and these partners are known to shape its activities. Thus, specifically targeting the interactions between Hsp70 and its regulatory partners would be expected to control chaperone activity. This approach might be expected to have reduced toxicity because it might reduce global impairment of protein homeostasis. One challenge is that the activity of the various chaperone

complexes is not currently known.[8] Thus, one cannot readily choose the right Hsp70 / co-chaperone pair to target. Moving forward, we propose that an emphasis on the structural biology of co-chaperones, combined with a deeper insight into how these factors shape the proteome, will be required to rationally leverage Hsp70 as an effective drug target.

In summary, genetic and biochemical studies support Hsp70 as an interesting, potential drug target in a remarkably wide range of diseases. Early studies on Hsp70 inhibitors support this general conclusion. However, the field of Hsp70 inhibitors is clearly in its infancy and extensive work remains before it is clear how this chaperone can be best exploited.

The goal of my thesis work, described in the following Chapters, is to explore the use multicomponent reactions to generate libraries of compounds that target Hsp70 family members. My hypothesis is that multicomponent reactions might be a particularly powerful way to overcome the major challenges in the field. In Chapter 2, I use the Biginelli reaction to generate dihydropyrimidines that control ATP turnover by Hsp70. In Chapter 3, I focus on the Hantzsch reaction to approach this goal and develop the first enantio-selective, four-component route to dihydropyridines. In Chapter 4, I describe my work on the Ugi reaction to create analogs of the Hsp70-targeting compound, spergualin. The ultimate goal of this work is to identify compounds that can be used to understand how chaperones (i.e. Hsp70 proteins) are involved in neurodegenerative diseases.

Notes

This work has been published as “Heat Shock Protein 70 (Hsp70) as an Emerging Drug Target,” Evans, C.G., Chang, L., and Gestwicki, J.E., *J Med Chem*, 2010, 53(12), 4585-4602.

1.5 References

1. Mayer, M. P.; Bukau, B. Hsp70 chaperones: cellular functions and molecular mechanism. *Cell Mol Life Sci* **2005,** *62*, 670-684.

2. Schaffitzel, E.; Rudiger, S.; Bukau, B.; Deuerling, E. Functional dissection of trigger factor and DnaK: interactions with nascent polypeptides and thermally denatured proteins. *Biol Chem* **2001,** *382*, 1235-1243.

3. Frydman, J. Folding of newly translated proteins in vivo: the role of molecular chaperones. *Annu Rev Biochem* **2001,** *70*, 603-647.

4. Pratt, W. B.; Toft, D. O. Regulation of signaling protein function and trafficking by the hsp90/hsp70-based chaperone machinery. *Exp Biol Med (Maywood)* **2003,** *228*, 111-133.

5. Young, J. C.; Barral, J. M.; Ulrich Hartl, F. More than folding: localized functions of cytosolic chaperones. *Trends Biochem Sci* **2003,** *28*, 541-547.

6. Chiang, H. L.; Terlecky, S. R.; Plant, C. P.; Dice, J. F. A role for a 70-kilodalton heat shock protein in lysosomal degradation of intracellular proteins. *Science* **1989,** *246*, 382-385.

7. Bercovich, B.; Stancovski, I.; Mayer, A.; Blumenfeld, N.; Laszlo, A.; Schwartz, A. L.; Ciechanover, A. Ubiquitin-dependent degradation of certain protein substrates in vitro requires the molecular chaperone Hsc70. *J Biol Chem* **1997,** *272*, 9002-9010.

8. Meimaridou, E.; Gooljar, S. B.; Chapple, J. P. From hatching to dispatching: the multiple cellular roles of the Hsp70 molecular chaperone machinery. *J Mol Endocrinol* **2009,** *42*, 1-9.

9. Daugaard, M.; Rohde, M.; Jaattela, M. The heat shock protein 70 family: Highly homologous proteins with overlapping and distinct functions. *FEBS Lett* **2007,** *581*, 3702-3710.

10. Bertelsen, E. B.; Chang, L.; Gestwicki, J. E.; Zuiderweg, E. R. Solution conformation of wild-type E. coli Hsp70 (DnaK) chaperone complexed with ADP and substrate. *Proc Natl Acad Sci U S A* **2009,** *106*, 8471-8476.

11. Flaherty, K. M.; DeLuca-Flaherty, C.; McKay, D. B. Three-dimensional structure of the ATPase fragment of a 70K heat-shock cognate protein. *Nature* **1990,** *346*, 623-628.

12. Bork, P.; Sander, C.; Valencia, A. An ATPase domain common to prokaryotic cell cycle proteins, sugar kinases, actin, and hsp70 heat shock proteins. *Proc Natl Acad Sci U S A* **1992,** *89*, 7290-7294.

13. Zhu, X.; Zhao, X.; Burkholder, W. F.; Gragerov, A.; Ogata, C. M.; Gottesman, M. E.; Hendrickson, W. A. Structural analysis of substrate binding by the molecular chaperone DnaK. *Science* **1996,** *272*, 1606-1614.

14. Erbse, A.; Mayer, M. P.; Bukau, B. Mechanism of substrate recognition by Hsp70 chaperones. *Biochem Soc Trans* **2004,** *32*, 617-621.

15. Xing, Y.; Bocking, T.; Wolf, M.; Grigorieff, N.; Kirchhausen, T.; Harrison, S. C. Structure of clathrin coat with bound Hsc70 and auxilin: mechanism of Hsc70-facilitated disassembly. *EMBO J* **2010,** *29*, 655-665.

16. Flynn, G. C.; Pohl, J.; Flocco, M. T.; Rothman, J. E. Peptide-binding specificity of the molecular chaperone BiP. *Nature* **1991,** *353*, 726-730.

17. Russell, R.; Jordan, R.; McMacken, R. Kinetic characterization of the ATPase cycle of the DnaK molecular chaperone. *Biochemistry* **1998,** *37*, 596-607.

18. Mayer, M. P.; Schroder, H.; Rudiger, S.; Paal, K.; Laufen, T.; Bukau, B. Multistep mechanism of substrate binding determines chaperone activity of Hsp70. *Nat Struct Biol* **2000,** *7*, 586-593.

19. Vogel, M.; Mayer, M. P.; Bukau, B. Allosteric regulation of Hsp70 chaperones involves a conserved interdomain linker. *J Biol Chem* **2006,** *281*, 38705-38711.

20. Han, W.; Christen, P. Mutations in the interdomain linker region of DnaK abolish the chaperone action of the DnaK/DnaJ/GrpE system. *FEBS Lett* **2001,** *497*, 55-58.

21. Ha, J. H.; McKay, D. B. ATPase kinetics of recombinant bovine 70 kDa heat shock cognate protein and its amino-terminal ATPase domain. *Biochemistry* **1994,** *33*, 14625-14635.

22. Laufen, T.; Mayer, M. P.; Beisel, C.; Klostermeier, D.; Mogk, A.; Reinstein, J.; Bukau, B. Mechanism of regulation of hsp70 chaperones by DnaJ cochaperones. *Proc Natl Acad Sci U S A* **1999,** *96*, 5452-5457.

23. Qiu, X. B.; Shao, Y. M.; Miao, S.; Wang, L. The diversity of the DnaJ/Hsp40 family, the crucial partners for Hsp70 chaperones. *Cell Mol Life Sci* **2006,** *63*, 2560-2570.

24. Wall, D.; Zylicz, M.; Georgopoulos, C. The NH2-terminal 108 amino acids of the Escherichia coli DnaJ protein stimulate the ATPase activity of DnaK and are sufficient for lambda replication. *J Biol Chem* **1994,** *269*, 5446-5451.

25. Greene, M. K.; Maskos, K.; Landry, S. J. Role of the J-domain in the cooperation of Hsp40 with Hsp70. *Proc Natl Acad Sci U S A* **1998,** *95*, 6108-6113.

26. Jiang, J.; Maes, E. G.; Taylor, A. B.; Wang, L.; Hinck, A. P.; Lafer, E. M.; Sousa, R. Structural basis of J cochaperone binding and regulation of Hsp70. *Mol Cell* **2007,** *28*, 422-433.

27. Pierpaoli, E. V.; Sandmeier, E.; Baici, A.; Schonfeld, H. J.; Gisler, S.; Christen, P. The power stroke of the DnaK/DnaJ/GrpE molecular chaperone system. *J Mol Biol* **1997,** *269*, 757-768.

28. Harrison, C. GrpE, a nucleotide exchange factor for DnaK. *Cell Stress Chaperones* **2003,** *8*, 218-224.

29. Kabbage, M.; Dickman, M. B. The BAG proteins: a ubiquitous family of chaperone regulators. *Cell Mol Life Sci* **2008,** *65*, 1390-1402.

30. Kabani, M.; McLellan, C.; Raynes, D. A.; Guerriero, V.; Brodsky, J. L. HspBP1, a homologue of the yeast Fes1 and Sls1 proteins, is an Hsc70 nucleotide exchange factor. *FEBS Lett* **2002,** *531*, 339-342.

31. Shaner, L.; Morano, K. A. All in the family: atypical Hsp70 chaperones are conserved modulators of Hsp70 activity. *Cell Stress Chaperones* **2007,** *12*, 1-8.

32. Bukau, B.; Weissman, J.; Horwich, A. Molecular chaperones and protein quality control. *Cell* **2006,** *125*, 443-451.

33. Vos, M. J.; Hageman, J.; Carra, S.; Kampinga, H. H. Structural and functional diversities between members of the human HSPB, HSPH, HSPA, and DNAJ chaperone families. *Biochemistry* **2008,** *47*, 7001-7011.

34. Kota, P.; Summers, D. W.; Ren, H. Y.; Cyr, D. M.; Dokholyan, N. V. Identification of a consensus motif in substrates bound by a Type I Hsp40. *Proc Natl Acad Sci U S A* **2009,** *106*, 11073-11078.

35. Blatch, G. L.; Lassle, M. The tetratricopeptide repeat: a structural motif mediating protein-protein interactions. *Bioessays* **1999,** *21*, 932-939.

36. Scheufler, C.; Brinker, A.; Bourenkov, G.; Pegoraro, S.; Moroder, L.; Bartunik, H.; Hartl, F. U.; Moarefi, I. Structure of TPR domain-peptide complexes: critical elements in the assembly of the Hsp70-Hsp90 multichaperone machine. *Cell* **2000,** *101*, 199-210.

37. Carrigan, P. E.; Nelson, G. M.; Roberts, P. J.; Stoffer, J.; Riggs, D. L.; Smith, D. F. Multiple domains of the co-chaperone Hop are important for Hsp70 binding. *J Biol Chem* **2004,** *279*, 16185-16193.

38. Flom, G.; Behal, R. H.; Rosen, L.; Cole, D. G.; Johnson, J. L. Definition of the minimal fragments of Sti1 required for dimerization, interaction with Hsp70 and Hsp90 and in vivo functions. *Biochem J* **2007,** *404*, 159-167.

39. Hernandez, M. P.; Sullivan, W. P.; Toft, D. O. The assembly and intermolecular properties of the hsp70-Hop-hsp90 molecular chaperone complex. *J Biol Chem* **2002,** *277*, 38294-38304.

40. Onuoha, S. C.; Coulstock, E. T.; Grossmann, J. G.; Jackson, S. E. Structural studies on the co-chaperone Hop and its complexes with Hsp90. *J Mol Biol* **2008,** *379*, 732-744.

41. Connell, P.; Ballinger, C. A.; Jiang, J.; Wu, Y.; Thompson, L. J.; Hohfeld, J.; Patterson, C. The co-chaperone CHIP regulates protein triage decisions mediated by heat-shock proteins. *Nat Cell Biol* **2001,** *3*, 93-96.

42. Ballinger, C. A.; Connell, P.; Wu, Y.; Hu, Z.; Thompson, L. J.; Yin, L. Y.; Patterson, C. Identification of CHIP, a novel tetratricopeptide repeat-containing protein that interacts with heat shock proteins and negatively regulates chaperone functions. *Mol Cell Biol* **1999,** *19*, 4535-4545.

43. Hohfeld, J.; Cyr, D. M.; Patterson, C. From the cradle to the grave: molecular chaperones that may choose between folding and degradation. *EMBO Rep* **2001,** *2*, 885-890.

44. Mosser, D. D.; Morimoto, R. I. Molecular chaperones and the stress of oncogenesis. *Oncogene* **2004,** *23*, 2907-2918.

45. Ciocca, D. R.; Calderwood, S. K. Heat shock proteins in cancer: diagnostic, prognostic, predictive, and treatment implications. *Cell Stress Chaperones* **2005,** *10*, 86-103.

46. Rohde, M.; Daugaard, M.; Jensen, M. H.; Helin, K.; Nylandsted, J.; Jaattela, M. Members of the heat-shock protein 70 family promote cancer cell growth by distinct mechanisms. *Genes Dev* **2005,** *19*, 570-582.

47. Seo, J. S.; Park, Y. M.; Kim, J. I.; Shim, E. H.; Kim, C. W.; Jang, J. J.; Kim, S. H.; Lee, W. H. T cell lymphoma in transgenic mice expressing the human Hsp70 gene. *Biochem Biophys Res Commun* **1996,** *218*, 582-587.

48. Sliutz, G.; Karlseder, J.; Tempfer, C.; Orel, L.; Holzer, G.; Simon, M. M. Drug resistance against gemcitabine and topotecan mediated by constitutive hsp70 overexpression in vitro: implication of quercetin as sensitiser in chemotherapy. *Br J Cancer* **1996,** *74*, 172-177.

49. Whitesell, L.; Lindquist, S. Inhibiting the transcription factor HSF1 as an anticancer strategy. *Expert Opin Ther Targets* **2009,** *13*, 469-478.

50. Powers, M. V.; Workman, P. Inhibitors of the heat shock response: biology and pharmacology. *FEBS Lett* **2007,** *581*, 3758-3769.

51. Buzzard, K. A.; Giaccia, A. J.; Killender, M.; Anderson, R. L. Heat shock protein 72 modulates pathways of stress-induced apoptosis. *J Biol Chem* **1998,** *273*, 17147-17153.

52. Garrido, C.; Gurbuxani, S.; Ravagnan, L.; Kroemer, G. Heat shock proteins: endogenous modulators of apoptotic cell death. *Biochem Biophys Res Commun* **2001,** *286*, 433-442.

53. Yang, J.; Hong, Y.; Wang, W.; Wu, W.; Chi, Y.; Zong, H.; Kong, X.; Wei, Y.; Yun, X.; Cheng, C.; Chen, K.; Gu, J. HSP70 protects BCL2L12 and BCL2L12A from N-terminal ubiquitination-mediated proteasomal degradation. *FEBS Lett* **2009,** *583*, 1409-1414.

54. Gabai, V. L.; Mabuchi, K.; Mosser, D. D.; Sherman, M. Y. Hsp72 and stress kinase c-jun N-terminal kinase regulate the bid-dependent pathway in tumor necrosis factor-induced apoptosis. *Mol Cell Biol* **2002,** *22*, 3415-3424.

55. Gotoh, T.; Terada, K.; Oyadomari, S.; Mori, M. hsp70-DnaJ chaperone pair prevents nitric oxide- and CHOP-induced apoptosis by inhibiting translocation of Bax to mitochondria. *Cell Death Differ* **2004,** *11*, 390-402.

56. Stankiewicz, A. R.; Lachapelle, G.; Foo, C. P.; Radicioni, S. M.; Mosser, D. D. Hsp70 inhibits heat-induced apoptosis upstream of mitochondria by preventing Bax translocation. *J Biol Chem* **2005,** *280*, 38729-38739.

57. Li, B.; Dou, Q. P. Bax degradation by the ubiquitin/proteasome-dependent pathway: involvement in tumor survival and progression. *Proc Natl Acad Sci U S A* **2000,** *97*, 3850-3855.

58. Beere, H. M.; Wolf, B. B.; Cain, K.; Mosser, D. D.; Mahboubi, A.; Kuwana, T.; Tailor, P.; Morimoto, R. I.; Cohen, G. M.; Green, D. R. Heat-shock protein 70 inhibits apoptosis by preventing recruitment of procaspase-9 to the Apaf-1 apoptosome. *Nat Cell Biol* **2000,** *2*, 469-475.

59. Nylandsted, J.; Gyrd-Hansen, M.; Danielewicz, A.; Fehrenbacher, N.; Lademann, U.; Hoyer-Hansen, M.; Weber, E.; Multhoff, G.; Rohde, M.; Jaattela, M. Heat shock protein 70 promotes cell survival by inhibiting lysosomal membrane permeabilization. *J Exp Med* **2004,** *200*, 425-435.

60. Yaglom, J. A.; Gabai, V. L.; Sherman, M. Y. High levels of heat shock protein Hsp72 in cancer cells suppress default senescence pathways. *Cancer Res* **2007,** *67*, 2373-2381.

61. Volloch, V.; Gabai, V. L.; Rits, S.; Sherman, M. Y. ATPase activity of the heat shock protein hsp72 is dispensable for its effects on dephosphorylation of stress kinase JNK and on heat-induced apoptosis. *FEBS Lett* **1999,** *461*, 73-76.

62. Meriin, A. B.; Yaglom, J. A.; Gabai, V. L.; Zon, L.; Ganiatsas, S.; Mosser, D. D.; Sherman, M. Y. Protein-damaging stresses activate c-Jun N-terminal kinase via inhibition of its dephosphorylation: a novel pathway controlled by HSP72. *Mol Cell Biol* **1999,** *19*, 2547-2555.

63. Yaglom, J. A.; Gabai, V. L.; Meriin, A. B.; Mosser, D. D.; Sherman, M. Y. The function of HSP72 in suppression of c-Jun N-terminal kinase activation can be dissociated from its role in prevention of protein damage. *J Biol Chem* **1999,** *274*, 20223-20228.

64. Ravagnan, L.; Gurbuxani, S.; Susin, S. A.; Maisse, C.; Daugas, E.; Zamzami, N.; Mak, T.; Jaattela, M.; Penninger, J. M.; Garrido, C.; Kroemer, G. Heat-shock protein 70 antagonizes apoptosis-inducing factor. *Nat Cell Biol* **2001,** *3*, 839-843.

65. Nylandsted, J.; Brand, K.; Jaattela, M. Heat shock protein 70 is required for the survival of cancer cells. *Ann N Y Acad Sci* **2000,** *926*, 122-125.

66. Nylandsted, J.; Rohde, M.; Brand, K.; Bastholm, L.; Elling, F.; Jaattela, M. Selective depletion of heat shock protein 70 (Hsp70) activates a tumor-specific death program that is independent of caspases and bypasses Bcl-2. *Proc Natl Acad Sci U S A* **2000,** *97*, 7871-7876.

67. Powers, M. V.; Clarke, P. A.; Workman, P. Death by chaperone: HSP90, HSP70 or both? *Cell Cycle* **2009,** *8*, 518-526.

68. Pocaly, M.; Lagarde, V.; Etienne, G.; Ribeil, J. A.; Claverol, S.; Bonneu, M.; Moreau-Gaudry, F.; Guyonnet-Duperat, V.; Hermine, O.; Melo, J. V.; Dupouy, M.; Turcq, B.; Mahon, F. X.; Pasquet, J. M. Overexpression of the heat-shock protein 70 is associated to imatinib resistance in chronic myeloid leukemia. *Leukemia* **2007,** *21*, 93-101.

69. Gabai, V. L.; Budagova, K. R.; Sherman, M. Y. Increased expression of the major heat shock protein Hsp72 in human prostate carcinoma cells is dispensable for their viability but confers resistance to a variety of anticancer agents. *Oncogene* **2005,** *24*, 3328-3338.

70. Bagatell, R.; Paine-Murrieta, G. D.; Taylor, C. W.; Pulcini, E. J.; Akinaga, S.; Benjamin, I. J.; Whitesell, L. Induction of a heat shock factor 1-dependent stress response alters the cytotoxic activity of hsp90-binding agents. *Clin Cancer Res* **2000,** *6*, 3312-3318.

71. Wegele, H.; Muller, L.; Buchner, J. Hsp70 and Hsp90--a relay team for protein folding. *Rev Physiol Biochem Pharmacol* **2004,** *151*, 1-44.

72. Richter, K.; Buchner, J. Hsp90: chaperoning signal transduction. *J Cell Physiol* **2001,** *188*, 281-290.

73. Chaudhury, S.; Welch, T. R.; Blagg, B. S. Hsp90 as a target for drug development. *ChemMedChem* **2006,** *1*, 1331-1340.

74. Taldone, T.; Chiosis, G. Purine-scaffold Hsp90 inhibitors. *Curr Top Med Chem* **2009,** *9*, 1436-1446.

75. Powers, M. V.; Clarke, P. A.; Workman, P. Dual targeting of HSC70 and HSP72 inhibits HSP90 function and induces tumor-specific apoptosis. *Cancer Cell* **2008,** *14*, 250-262.

76. Zaarur, N.; Gabai, V. L.; Porco, J. A., Jr.; Calderwood, S.; Sherman, M. Y. Targeting heat shock response to sensitize cancer cells to proteasome and Hsp90 inhibitors. *Cancer Res* **2006,** *66*, 1783-1791.

77. Soskic, V.; Groebe, K.; Schrattenholz, A. Nonenzymatic posttranslational protein modifications in ageing. *Exp Gerontol* **2008,** *43*, 247-257.

78. Zeng, B. Y.; Medhurst, A. D.; Jackson, M.; Rose, S.; Jenner, P. Proteasomal activity in brain differs between species and brain regions and changes with age. *Mech Ageing Dev* **2005,** *126*, 760-766.

79. Shpund, S.; Gershon, D. Alterations in the chaperone activity of HSP70 in aging organisms. *Arch Gerontol Geriatr* **1997,** *24*, 125-131.

80. Kirkegaard, T.; Roth, A. G.; Petersen, N. H.; Mahalka, A. K.; Olsen, O. D.; Moilanen, I.; Zylicz, A.; Knudsen, J.; Sandhoff, K.; Arenz, C.; Kinnunen, P. K.; Nylandsted, J.; Jaattela, M. Hsp70 stabilizes lysosomes and reverts Niemann-Pick disease-associated lysosomal pathology. *Nature* **2010,** *463*, 549-553.

81. Witt, S. N. Hsp70 molecular chaperones and Parkinson's disease. *Biopolymers* **2010,** *93*, 218-228.

82. Liberek, K.; Lewandowska, A.; Zietkiewicz, S. Chaperones in control of protein disaggregation. *EMBO J* **2008,** *27*, 328-335.

83. Bauer, P. O.; Nukina, N. The pathogenic mechanisms of polyglutamine diseases and current therapeutic strategies. *J Neurochem* **2009,** *110*, 1737-1765.

84. Williams, A. J.; Paulson, H. L. Polyglutamine neurodegeneration: protein misfolding revisited. *Trends Neurosci* **2008,** *31*, 521-528.

85. Muchowski, P. J.; Schaffar, G.; Sittler, A.; Wanker, E. E.; Hayer-Hartl, M. K.; Hartl, F. U. Hsp70 and hsp40 chaperones can inhibit self-assembly of polyglutamine proteins into amyloid-like fibrils. *Proc Natl Acad Sci U S A* **2000,** *97*, 7841-7846.

86. Krobitsch, S.; Lindquist, S. Aggregation of huntingtin in yeast varies with the length of the polyglutamine expansion and the expression of chaperone proteins. *Proc Natl Acad Sci U S A* **2000,** *97*, 1589-1594.

87. Jana, N. R.; Tanaka, M.; Wang, G.; Nukina, N. Polyglutamine length-dependent interaction of Hsp40 and Hsp70 family chaperones with truncated N-terminal huntingtin: their role in suppression of aggregation and cellular toxicity. *Hum Mol Genet* **2000,** *9*, 2009-2018.

88. Wyttenbach, A.; Carmichael, J.; Swartz, J.; Furlong, R. A.; Narain, Y.; Rankin, J.; Rubinsztein, D. C. Effects of heat shock, heat shock protein 40 (HDJ-2), and proteasome inhibition on protein aggregation in cellular models of Huntington's disease. *Proc Natl Acad Sci U S A* **2000,** *97*, 2898-2903.

89. Rujano, M. A.; Kampinga, H. H.; Salomons, F. A. Modulation of polyglutamine inclusion formation by the Hsp70 chaperone machine. *Exp Cell Res* **2007,** *313*, 3568-3578.

90. Warrick, J. M.; Chan, H. Y.; Gray-Board, G. L.; Chai, Y.; Paulson, H. L.; Bonini, N. M. Suppression of polyglutamine-mediated neurodegeneration in Drosophila by the molecular chaperone HSP70. *Nat Genet* **1999,** *23*, 425-428.

91. Adachi, H.; Katsuno, M.; Minamiyama, M.; Sang, C.; Pagoulatos, G.; Angelidis, C.; Kusakabe, M.; Yoshiki, A.; Kobayashi, Y.; Doyu, M.; Sobue, G. Heat shock protein 70 chaperone overexpression ameliorates phenotypes of the spinal and bulbar muscular atrophy transgenic mouse model by reducing nuclear-localized mutant androgen receptor protein. *J Neurosci* **2003,** *23*, 2203-2211.

92. Cummings, C. J.; Sun, Y.; Opal, P.; Antalffy, B.; Mestril, R.; Orr, H. T.; Dillmann, W. H.; Zoghbi, H. Y. Over-expression of inducible HSP70 chaperone suppresses neuropathology and improves motor function in SCA1 mice. *Hum Mol Genet* **2001,** *10*, 1511-1518.

93. Helmlinger, D.; Bonnet, J.; Mandel, J. L.; Trottier, Y.; Devys, D. Hsp70 and Hsp40 chaperones do not modulate retinal phenotype in SCA7 mice. *J Biol Chem* **2004,** *279*, 55969-55977.

94. Hansson, O.; Nylandsted, J.; Castilho, R. F.; Leist, M.; Jaattela, M.; Brundin, P. Overexpression of heat shock protein 70 in R6/2 Huntington's disease mice has only modest effects on disease progression. *Brain Res* **2003,** *970*, 47-57.

95. Merienne, K.; Helmlinger, D.; Perkin, G. R.; Devys, D.; Trottier, Y. Polyglutamine expansion induces a protein-damaging stress connecting heat shock protein 70 to the JNK pathway. *J Biol Chem* **2003,** *278*, 16957-16967.

96. Zhou, H.; Li, S. H.; Li, X. J. Chaperone suppression of cellular toxicity of huntingtin is independent of polyglutamine aggregation. *J Biol Chem* **2001,** *276*, 48417-48424.

97. Jana, N. R.; Dikshit, P.; Goswami, A.; Kotliarova, S.; Murata, S.; Tanaka, K.; Nukina, N. Co-chaperone CHIP associates with expanded polyglutamine protein and promotes their degradation by proteasomes. *J Biol Chem* **2005,** *280*, 11635-11640.

98. Miller, V. M.; Nelson, R. F.; Gouvion, C. M.; Williams, A.; Rodriguez-Lebron, E.; Harper, S. Q.; Davidson, B. L.; Rebagliati, M. R.; Paulson, H. L. CHIP suppresses polyglutamine aggregation and toxicity in vitro and in vivo. *J Neurosci* **2005,** *25*, 9152-9161.

99. Williams, A. J.; Knutson, T. M.; Colomer Gould, V. F.; Paulson, H. L. In vivo suppression of polyglutamine neurotoxicity by C-terminus of Hsp70-interacting protein (CHIP) supports an aggregation model of pathogenesis. *Neurobiol Dis* **2009,** *33*, 342-353.

100. Al-Ramahi, I.; Lam, Y. C.; Chen, H. K.; de Gouyon, B.; Zhang, M.; Perez, A. M.; Branco, J.; de Haro, M.; Patterson, C.; Zoghbi, H. Y.; Botas, J. CHIP protects from the neurotoxicity of expanded and wild-type ataxin-1 and promotes their ubiquitination and degradation. *J Biol Chem* **2006,** *281*, 26714-26724.

101. Adachi, H.; Waza, M.; Tokui, K.; Katsuno, M.; Minamiyama, M.; Tanaka, F.; Doyu, M.; Sobue, G. CHIP overexpression reduces mutant androgen receptor protein and ameliorates phenotypes of the spinal and bulbar muscular atrophy transgenic mouse model. *J Neurosci* **2007,** *27*, 5115-5126.

102. Sittler, A.; Lurz, R.; Lueder, G.; Priller, J.; Lehrach, H.; Hayer-Hartl, M. K.; Hartl, F. U.; Wanker, E. E. Geldanamycin activates a heat shock response and inhibits huntingtin aggregation in a cell culture model of Huntington's disease. *Hum Mol Genet* **2001,** *10*, 1307-1315.

103. Katsuno, M.; Sang, C.; Adachi, H.; Minamiyama, M.; Waza, M.; Tanaka, F.; Doyu, M.; Sobue, G. Pharmacological induction of heat-shock proteins alleviates polyglutamine-mediated motor neuron disease. *Proc Natl Acad Sci U S A* **2005,** *102*, 16801-16806.

104. Zhang, Y. Q.; Sarge, K. D. Celastrol inhibits polyglutamine aggregation and toxicity though induction of the heat shock response. *J Mol Med* **2007,** *85*, 1421-1428.

105. Fujikake, N.; Nagai, Y.; Popiel, H. A.; Okamoto, Y.; Yamaguchi, M.; Toda, T. Heat shock transcription factor 1-activating compounds suppress polyglutamine-induced neurodegeneration through induction of multiple molecular chaperones. *J Biol Chem* **2008,** *283*, 26188-26197.

106. Findeis, M. A. The role of amyloid beta peptide 42 in Alzheimer's disease. *Pharmacol Ther* **2007,** *116*, 266-286.

107. Ballatore, C.; Lee, V. M.; Trojanowski, J. Q. Tau-mediated neurodegeneration in Alzheimer's disease and related disorders. *Nat Rev Neurosci* **2007,** *8*, 663-672.

108. Evans, C. G.; Wisen, S.; Gestwicki, J. E. Heat shock proteins 70 and 90 inhibit early stages of amyloid beta-(1-42) aggregation in vitro. *J Biol Chem* **2006,** *281*, 33182-33191.

109. Kumar, P.; Ambasta, R. K.; Veereshwarayya, V.; Rosen, K. M.; Kosik, K. S.; Band, H.; Mestril, R.; Patterson, C.; Querfurth, H. W. CHIP and HSPs interact with beta-APP in a proteasome-dependent manner and influence Abeta metabolism. *Hum Mol Genet* **2007,** *16*, 848-864.

110. Veereshwarayya, V.; Kumar, P.; Rosen, K. M.; Mestril, R.; Querfurth, H. W. Differential effects of mitochondrial heat shock protein 60 and related molecular chaperones to prevent intracellular beta-amyloid-induced inhibition of complex IV and limit apoptosis. *J Biol Chem* **2006,** *281*, 29468-29478.

111. Sarkar, M.; Kuret, J.; Lee, G. Two motifs within the tau microtubule-binding domain mediate its association with the hsc70 molecular chaperone. *J Neurosci Res* **2008,** *86*, 2763-2773.

112. Petrucelli, L.; Dickson, D.; Kehoe, K.; Taylor, J.; Snyder, H.; Grover, A.; De Lucia, M.; McGowan, E.; Lewis, J.; Prihar, G.; Kim, J.; Dillmann, W. H.; Browne, S. E.; Hall, A.; Voellmy, R.; Tsuboi, Y.; Dawson, T. M.; Wolozin, B.; Hardy, J.; Hutton, M. CHIP and Hsp70 regulate tau ubiquitination, degradation and aggregation. *Hum Mol Genet* **2004,** *13*, 703-714.

113. Dou, F.; Netzer, W. J.; Tanemura, K.; Li, F.; Hartl, F. U.; Takashima, A.; Gouras, G. K.; Greengard, P.; Xu, H. Chaperones increase association of tau protein with microtubules. *Proc Natl Acad Sci U S A* **2003,** *100*, 721-726.

114. Shimura, H.; Schwartz, D.; Gygi, S. P.; Kosik, K. S. CHIP-Hsc70 complex ubiquitinates phosphorylated tau and enhances cell survival. *J Biol Chem* **2004,** *279*, 4869-4876.

115. Hatakeyama, S.; Matsumoto, M.; Kamura, T.; Murayama, M.; Chui, D. H.; Planel, E.; Takahashi, R.; Nakayama, K. I.; Takashima, A. U-box protein carboxyl terminus of Hsc70-interacting protein (CHIP) mediates poly-ubiquitylation preferentially on four-repeat Tau and is involved in neurodegeneration of tauopathy. *J Neurochem* **2004,** *91*, 299-307.

116. Dickey, C. A.; Kamal, A.; Lundgren, K.; Klosak, N.; Bailey, R. M.; Dunmore, J.; Ash, P.; Shoraka, S.; Zlatkovic, J.; Eckman, C. B.; Patterson, C.; Dickson, D. W.; Nahman, N. S., Jr.; Hutton, M.; Burrows, F.; Petrucelli, L. The high-affinity HSP90-CHIP complex recognizes and selectively degrades phosphorylated tau client proteins. *J Clin Invest* **2007,** *117*, 648-658.

117. Elliott, E.; Tsvetkov, P.; Ginzburg, I. BAG-1 associates with Hsc70.Tau complex and regulates the proteasomal degradation of Tau protein. *J Biol Chem* **2007,** *282*, 37276-37284.

118. Carrettiero, D. C.; Hernandez, I.; Neveu, P.; Papagiannakopoulos, T.; Kosik, K. S. The cochaperone BAG2 sweeps paired helical filament- insoluble tau from the microtubule. *J Neurosci* **2009,** *29*, 2151-2161.

119. Henderson, B.; Allan, E.; Coates, A. R. Stress wars: the direct role of host and bacterial molecular chaperones in bacterial infection. *Infect Immun* **2006,** *74*, 3693-3706.

120. Lemos, J. A.; Luzardo, Y.; Burne, R. A. Physiologic effects of forced down-regulation of dnaK and groEL expression in Streptococcus mutans. *J Bacteriol* **2007,** *189*, 1582-1588.

121. Wolska, K. I.; Bugajska, E.; Jurkiewicz, D.; Kuc, M.; Jozwik, A. Antibiotic susceptibility of Escherichia coli dnaK and dnaJ mutants. *Microb Drug Resist* **2000,** *6*, 119-126.

122. Singh, V. K.; Utaida, S.; Jackson, L. S.; Jayaswal, R. K.; Wilkinson, B. J.; Chamberlain, N. R. Role for dnaK locus in tolerance of multiple stresses in Staphylococcus aureus. *Microbiology* **2007,** *153*, 3162-3173.

123. Yamaguchi, Y.; Tomoyasu, T.; Takaya, A.; Morioka, M.; Yamamoto, T. Effects of disruption of heat shock genes on susceptibility of Escherichia coli to fluoroquinolones. *BMC Microbiol* **2003,** *3*, 16.

124. Sell, S. M.; Eisen, C.; Ang, D.; Zylicz, M.; Georgopoulos, C. Isolation and characterization of dnaJ null mutants of Escherichia coli. *J Bacteriol* **1990,** *172*, 4827-4835.

125. Takaya, A.; Tomoyasu, T.; Matsui, H.; Yamamoto, T. The DnaK/DnaJ chaperone machinery of Salmonella enterica serovar Typhimurium is essential for invasion of epithelial cells and survival within macrophages, leading to systemic infection. *Infect Immun* **2004,** *72*, 1364-1373.

126. Hanawa, T.; Fukuda, M.; Kawakami, H.; Hirano, H.; Kamiya, S.; Yamamoto, T. The Listeria monocytogenes DnaK chaperone is required for stress tolerance and efficient phagocytosis with macrophages. *Cell Stress Chaperones* **1999,** *4*, 118-128.

127. Nishimura, H.; Emoto, M.; Kimura, K.; Yoshikai, Y. Hsp70 protects macrophages infected with Salmonella choleraesuis against TNF-alpha-induced cell death. *Cell Stress Chaperones* **1997,** *2*, 50-59.

128. Bulut, Y.; Michelsen, K. S.; Hayrapetian, L.; Naiki, Y.; Spallek, R.; Singh, M.; Arditi, M. Mycobacterium tuberculosis heat shock proteins use diverse Toll-like receptor pathways to activate pro-inflammatory signals. *J Biol Chem* **2005,** *280*, 20961-20967.

129. Salminen, A.; Paimela, T.; Suuronen, T.; Kaarniranta, K. Innate immunity meets with cellular stress at the IKK complex: regulation of the IKK complex by HSP70 and HSP90. *Immunol Lett* **2008,** *117*, 9-15.

130. Todryk, S. M.; Gough, M. J.; Pockley, A. G. Facets of heat shock protein 70 show immunotherapeutic potential. *Immunology* **2003,** *110*, 1-9.

131. Li, Z.; Menoret, A.; Srivastava, P. Roles of heat-shock proteins in antigen presentation and cross-presentation. *Curr Opin Immunol* **2002,** *14*, 45-51.

132. Brodsky, J. L.; Chiosis, G. Hsp70 molecular chaperones: emerging roles in human disease and identification of small molecule modulators. *Curr Top Med Chem* **2006,** *6*, 1215-1225.

133. Patury, S.; Miyata, Y.; Gestwicki, J. E. Pharmacological targeting of the Hsp70 chaperone. *Curr Top Med Chem* **2009,** *9*, 1337-1351.

134. Takeuchi, T.; Iinuma, H.; Kunimoto, S.; Masuda, T.; Ishizuka, M.; Takeuchi, M.; Hamada, M.; Naganawa, H.; Kondo, S.; Umezawa, H. A new antitumor antibiotic, spergualin: isolation and antitumor activity. *J Antibiot (Tokyo)* **1981,** *34*, 1619-1621.

135. Umezawa, H.; Kondo, S.; Iinuma, H.; Kunimoto, S.; Ikeda, Y.; Iwasawa, H.; Ikeda, D.; Takeuchi, T. Structure of an antitumor antibiotic, spergualin. *J Antibiot (Tokyo)* **1981,** *34*, 1622-1624.

136. Kondo, S.; Iwasawa, H.; Ikeda, D.; Umeda, Y.; Ikeda, Y.; Iinuma, H.; Umezawa, H. The total synthesis of spergualin, an antitumor antibiotic. *J Antibiot (Tokyo)* **1981,** *34*, 1625-1627.

137. Umeda, Y.; Moriguchi, M.; Kuroda, H.; Nakamura, T.; Iinuma, H.; Takeuchi, T.; Umezawa, H. Synthesis and antitumor activity of spergualin analogues. I. Chemical modification of 7-guanidino-3-hydroxyacyl moiety. *J Antibiot (Tokyo)* **1985,** *38*, 886-898.

138. Umeda, Y.; Moriguchi, M.; Ikai, K.; Kuroda, H.; Nakamura, T.; Fujii, A.; Takeuchi, T.; Umezawa, H. Synthesis and antitumor activity of spergualin analogues. III. Novel method for synthesis of optically active 15-deoxyspergualin and 15-deoxy-11-O-methylspergualin. *J Antibiot (Tokyo)* **1987,** *40*, 1316-1324.

139. Lebreton, L.; Annat, J.; Derrepas, P.; Dutartre, P.; Renaut, P. Structure-immunosuppressive activity relationships of new analogues of 15-deoxyspergualin. 1. Structural modifications of the hydroxyglycine moiety. *J Med Chem* **1999,** *42*, 277-290.

140. Nishizawa, R.; Takei, Y.; Yoshida, M.; Tomiyoshi, T.; Saino, T.; Nishikawa, K.; Nemoto, K.; Takahashi, K.; Fujii, A.; Nakamura, T. Synthesis and biological activity of spergualin analogues. I. *J Antibiot (Tokyo)* **1988,** *41*, 1629-1643.

141. Thomas, F. T.; Tepper, M. A.; Thomas, J. M.; Haisch, C. E. 15-Deoxyspergualin: a novel immunosuppressive drug with clinical potential. *Ann N Y Acad Sci* **1993,** *685*, 175-192.

142. Lebreton, L.; Jost, E.; Carboni, B.; Annat, J.; Vaultier, M.; Dutartre, P.; Renaut, P. Structure-immunosuppressive activity relationships of new analogues of 15-deoxyspergualin. 2. Structural modifications of the spermidine moiety. *J Med Chem* **1999,** *42*, 4749-4763.

143. Komesli, S.; Dumas, C.; Dutartre, P. Analysis of in vivo immunosuppressive and in vitro interaction with constitutive heat shock protein 70 activity of LF08-0299 (Tresperimus) and analogues. *Int J Immunopharmacol* **1999,** *21*, 349-358.

144. Nadler, S. G.; Tepper, M. A.; Schacter, B.; Mazzucco, C. E. Interaction of the immunosuppressant deoxyspergualin with a member of the Hsp70 family of heat shock proteins. *Science* **1992,** *258*, 484-486.

145. Mazzucco, C. E.; Nadler, S. G. A member of the Hsp70 family of heat-shock proteins is a putative target for the immunosuppressant 15-deoxyspergualin. *Ann N Y Acad Sci* **1993,** *685*, 202-204.

146. Nadler, S. G.; Dischino, D. D.; Malacko, A. R.; Cleaveland, J. S.; Fujihara, S. M.; Marquardt, H. Identification of a binding site on Hsc70 for the immunosuppressant 15-deoxyspergualin. *Biochem Biophys Res Commun* **1998,** *253*, 176-180.

147. Nadeau, K.; Nadler, S. G.; Saulnier, M.; Tepper, M. A.; Walsh, C. T. Quantitation of the interaction of the immunosuppressant deoxyspergualin and analogs with Hsc70 and Hsp90. *Biochemistry* **1994,** *33*, 2561-2567.

148. Brodsky, J. L. Selectivity of the molecular chaperone-specific immunosuppressive agent 15-deoxyspergualin: modulation of Hsc70 ATPase activity without compromising DnaJ chaperone interactions. *Biochem Pharmacol* **1999,** *57*, 877-880.

149. Ramya, T. N.; Karmodiya, K.; Surolia, A.; Surolia, N. 15-deoxyspergualin primarily targets the trafficking of apicoplast proteins in Plasmodium falciparum. *J Biol Chem* **2007,** *282*, 6388-6397.

150. Kaufman, D. B.; Gores, P. F.; Kelley, S.; M., G. D.; Nadler, S. G.; Ramos, E. 15-Deoxyspergualin: Immunotheray in solid organ and cellular transplantation. *Transplant. Rev.* **1996,** *10*, 160-174.

151. Hoeger, P. H.; Tepper, M. A.; Faith, A.; Higgins, J. A.; Lamb, J. R.; Geha, R. S. Immunosuppressant deoxyspergualin inhibits antigen processing in monocytes. *J Immunol* **1994,** *153*, 3908-3916.

152. Amada, N.; Okazaki, H.; Sato, T.; Ohashi, Y.; Kikuchi, H. Deoxyspergualin prophylaxis with tacrolimus further improves long-term graft survival in living-related renal-transplant recipients transfused with donor-specific blood. *Transplant Proc* **2005,** *37*, 927-929.

153. Birck, R.; Warnatz, K.; Lorenz, H. M.; Choi, M.; Haubitz, M.; Grunke, M.; Peter, H. H.; Kalden, J. R.; Gobel, U.; Drexler, J. M.; Hotta, O.; Nowack, R.; Van Der Woude, F. J. 15-Deoxyspergualin in patients with refractory ANCA-associated systemic vasculitis: a six-month open-label trial to evaluate safety and efficacy. *J Am Soc Nephrol* **2003,** *14*, 440-447.

154. Sugawara, A.; Torigoe, T.; Tamura, Y.; Kamiguchi, K.; Nemoto, K.; Oguro, H.; Sato, N. Polyamine compound deoxyspergualin inhibits heat shock protein-induced activation of immature dendritic cells. *Cell Stress Chaperones* **2009,** *14*, 133-139.

155. Kalsch, A. I.; Schmitt, W. H.; Breedijk, A.; Marinaki, S.; Weigerding, S.; Nebe, T. C.; Nemoto, K.; van der Woude, F. J.; Yard, B. A.; Birck, R. In vivo effects of cyclic administration of 15-

deoxyspergualin on leucocyte function in patients with Wegener's granulomatosis. *Clin Exp Immunol* **2006,** *146*, 455-462.

156. Lee, J.; Kim, M. S.; Kim, E. Y.; Park, H. J.; Chang, C. Y.; Jung, D. Y.; Kwon, C. H.; Joh, J. W.; Kim, S. J. 15-deoxyspergualin prevents mucosal injury by inhibiting production of TNF-alpha and down-regulating expression of MD-1 in a murine model of TNBS-induced colitis. *Int Immunopharmacol* **2007,** *7*, 1003-1012.

157. Ohlman, S.; Zilg, H.; Schindel, F.; Lindholm, A. Pharmacokinetics of 15-deoxyspergualin studied in renal transplant patients receiving the drug during graft rejection. *Transpl Int* **1994,** *7*, 5-10.

158. Plowman, J.; Harrison, S. D., Jr.; Trader, M. W.; Griswold, D. P., Jr.; Chadwick, M.; McComish, M. F.; Silveira, D. M.; Zaharko, D. Preclinical antitumor activity and pharmacological properties of deoxyspergualin. *Cancer Res* **1987,** *47*, 685-689.

159. Dhingra, K.; Valero, V.; Gutierrez, L.; Theriault, R.; Booser, D.; Holmes, F.; Buzdar, A.; Fraschini, G.; Hortobagyi, G. Phase II study of deoxyspergualin in metastatic breast cancer. *Invest New Drugs* **1994,** *12*, 235-241.

160. Okubo, M.; Tamura, K.; Kamata, K.; Tsukamoto, Y.; Nakayama, Y.; Osakabe, T.; Sato, K.; Go, M.; Kumano, K.; Endo, T. 15-Deoxyspergualin "rescue therapy" for methylprednisolone-resistant rejection of renal transplants as compared with anti-T cell monoclonal antibody (OKT3). *Transplantation* **1993,** *55*, 505-508.

161. Ohlman, S.; Gannedahl, G.; Tyden, G.; Tufveson, G.; Groth, C. G. Treatment of renal transplant rejection with 15-deoxyspergualin--a dose-finding study in man. *Transplant Proc* **1992,** *24*, 318-320.

162. Fewell, S. W.; Day, B. W.; Brodsky, J. L. Identification of an inhibitor of hsc70-mediated protein translocation and ATP hydrolysis. *J Biol Chem* **2001,** *276*, 910-914.

163. Fewell, S. W.; Smith, C. M.; Lyon, M. A.; Dumitrescu, T. P.; Wipf, P.; Day, B. W.; Brodsky, J. L. Small molecule modulators of endogenous and co-chaperone-stimulated Hsp70 ATPase activity. *J Biol Chem* **2004,** *279*, 51131-51140.

164. Wisen, S.; Androsavich, J.; Evans, C. G.; Chang, L.; Gestwicki, J. E. Chemical modulators of heat shock protein 70 (Hsp70) by sequential, microwave-accelerated reactions on solid phase. *Bioorg Med Chem Lett* **2008,** *18*, 60-65.

165. Chang, L.; Bertelsen, E. B.; Wisen, S.; Larsen, E. M.; Zuiderweg, E. R.; Gestwicki, J. E. High-throughput screen for small molecules that modulate the ATPase activity of the molecular chaperone DnaK. *Anal Biochem* **2008,** *372*, 167-176.

166. Wisen, S.; Gestwicki, J. E. Identification of small molecules that modify the protein folding activity of heat shock protein 70. *Anal Biochem* **2008,** *374*, 371-377.

167. Jinwal, U. K.; Miyata, Y.; Koren, J., 3rd; Jones, J. R.; Trotter, J. H.; Chang, L.; O'Leary, J.; Morgan, D.; Lee, D. C.; Shults, C. L.; Rousaki, A.; Weeber, E. J.; Zuiderweg, E. R.; Gestwicki, J. E.; Dickey, C. A. Chemical manipulation of hsp70 ATPase activity regulates tau stability. *J Neurosci* **2009,** *29*, 12079-12088.

168. Rodina, A.; Vilenchik, M.; Moulick, K.; Aguirre, J.; Kim, J.; Chiang, A.; Litz, J.; Clement, C. C.; Kang, Y.; She, Y.; Wu, N.; Felts, S.; Wipf, P.; Massague, J.; Jiang, X.; Brodsky, J. L.; Krystal, G. W.; Chiosis, G. Selective compounds define Hsp90 as a major inhibitor of apoptosis in small-cell lung cancer. *Nat Chem Biol* **2007,** *3*, 498-507.

169. Wright, C. M.; Chovatiya, R. J.; Jameson, N. E.; Turner, D. M.; Zhu, G.; Werner, S.; Huryn, D. M.; Pipas, J. M.; Day, B. W.; Wipf, P.; Brodsky, J. L. Pyrimidinone-peptoid hybrid molecules with distinct effects on molecular chaperone function and cell proliferation. *Bioorg Med Chem* **2008,** *16*, 3291-3301.

170. Koren, J.; Jinwal, U. K.; Jin, Y.; O'Leary, J.; Jones, J. R.; Johnson, A. G.; Blair, L. J.; Abisambra, J. F.; Chang, L.; Miyata, Y.; Cheng, A. M.; Guo, J.; Cheng, J. Q.; Gestwicki, J. E.; Dickey, C. A. Facilitating Akt clearance via manipulation of Hsp70 activity and levels. *J Biol Chem* **2009**.

171. Mamelak, D.; Lingwood, C. The ATPase domain of hsp70 possesses a unique binding specificity for 3'-sulfogalactolipids. *J Biol Chem* **2001,** *276*, 449-456.

172. Mamelak, D.; Mylvaganam, M.; Whetstone, H.; Hartmann, E.; Lennarz, W.; Wyrick, P. B.; Raulston, J.; Han, H.; Hoffman, P.; Lingwood, C. A. Hsp70s contain a specific sulfogalactolipid binding site. Differential aglycone influence on sulfogalactosyl ceramide binding by recombinant prokaryotic and eukaryotic hsp70 family members. *Biochemistry* **2001,** *40*, 3572-3582.

173. Mamelak, D.; Mylvaganam, M.; Tanahashi, E.; Ito, H.; Ishida, H.; Kiso, M.; Lingwood, C. The aglycone of sulfogalactolipids can alter the sulfate ester substitution position required for hsc70 recognition. *Carbohydr Res* **2001,** *335*, 91-100.

174. Park, H. J.; Mylvaganum, M.; McPherson, A.; Fewell, S. W.; Brodsky, J. L.; Lingwood, C. A. A soluble sulfogalactosyl ceramide mimic promotes Delta F508 CFTR escape from endoplasmic reticulum associated degradation. *Chem Biol* **2009,** *16*, 461-470.

175. Liebscher, M.; Jahreis, G.; Lucke, C.; Grabley, S.; Raina, S.; Schiene-Fischer, C. Fatty acyl benzamido antibacterials based on inhibition of DnaK-catalyzed protein folding. *J Biol Chem* **2007,** *282*, 4437-4446.

176. Otvos, L., Jr.; O, I.; Rogers, M. E.; Consolvo, P. J.; Condie, B. A.; Lovas, S.; Bulet, P.; Blaszczyk-Thurin, M. Interaction between heat shock proteins and antimicrobial peptides. *Biochemistry* **2000,** *39*, 14150-14159.

177. Kragol, G.; Lovas, S.; Varadi, G.; Condie, B. A.; Hoffmann, R.; Otvos, L., Jr. The antibacterial peptide pyrrhocoricin inhibits the ATPase actions of DnaK and prevents chaperone-assisted protein folding. *Biochemistry* **2001,** *40*, 3016-3026.

178. Kragol, G.; Hoffmann, R.; Chattergoon, M. A.; Lovas, S.; Cudic, M.; Bulet, P.; Condie, B. A.; Rosengren, K. J.; Montaner, L. J.; Otvos, L., Jr. Identification of crucial residues for the antibacterial activity of the proline-rich peptide, pyrrhocoricin. *Eur J Biochem* **2002,** *269*, 4226-4237.

179. Otvos, L., Jr.; Wade, J. D.; Lin, F.; Condie, B. A.; Hanrieder, J.; Hoffmann, R. Designer antibacterial peptides kill fluoroquinolone-resistant clinical isolates. *J Med Chem* **2005,** *48*, 5349-5359.

180. Cudic, M.; Condie, B. A.; Weiner, D. J.; Lysenko, E. S.; Xiang, Z. Q.; Insug, O.; Bulet, P.; Otvos, L., Jr. Development of novel antibacterial peptides that kill resistant isolates. *Peptides* **2002,** *23*, 2071-2083.

181. Williamson, D. S.; Borgognoni, J.; Clay, A.; Daniels, Z.; Dokurno, P.; Drysdale, M. J.; Foloppe, N.; Francis, G. L.; Graham, C. J.; Howes, R.; Macias, A. T.; Murray, J. B.; Parsons, R.; Shaw, T.; Surgenor, A. E.; Terry, L.; Wang, Y.; Wood, M.; Massey, A. J. Novel adenosine-derived inhibitors of 70 kDa heat shock protein, discovered through structure-based design. *J Med Chem* **2009,** *52*, 1510-1513.

182. Massey, A. J.; Williamson, D. S.; Browne, H.; Murray, J. B.; Dokurno, P.; Shaw, T.; Macias, A. T.; Daniels, Z.; Geoffroy, S.; Dopson, M.; Lavan, P.; Matassova, N.; Francis, G. L.; Graham, C. J.; Parsons, R.; Wang, Y.; Padfield, A.; Comer, M.; Drysdale, M. J.; Wood, M. A novel, small molecule inhibitor of

Hsc70/Hsp70 potentiates Hsp90 inhibitor induced apoptosis in HCT116 colon carcinoma cells. *Cancer Chemother Pharmacol* **2009**.

183. Leu, J. I.; Pimkina, J.; Frank, A.; Murphy, M. E.; George, D. L. A small molecule inhibitor of inducible heat shock protein 70. *Mol Cell* **2009,** *36*, 15-27.

184. Cellitti, J.; Zhang, Z.; Wang, S.; Wu, B.; Yuan, H.; Hasegawa, P.; Guiney, D. G.; Pellecchia, M. Small molecule DnaK modulators targeting the beta-domain. *Chem Biol Drug Des* **2009,** *74*, 349-357.

185. Wadhwa, R.; Sugihara, T.; Yoshida, A.; Nomura, H.; Reddel, R. R.; Simpson, R.; Maruta, H.; Kaul, S. C. Selective toxicity of MKT-077 to cancer cells is mediated by its binding to the hsp70 family protein mot-2 and reactivation of p53 function. *Cancer Res* **2000,** *60*, 6818-6821.

186. Deocaris, C. C.; Widodo, N.; Shrestha, B. G.; Kaur, K.; Ohtaka, M.; Yamasaki, K.; Kaul, S. C.; Wadhwa, R. Mortalin sensitizes human cancer cells to MKT-077-induced senescence. *Cancer Lett* **2007,** *252*, 259-269.

187. Koya, K.; Li, Y.; Wang, H.; Ukai, T.; Tatsuta, N.; Kawakami, M.; Shishido; Chen, L. B. MKT-077, a novel rhodacyanine dye in clinical trials, exhibits anticarcinoma activity in preclinical studies based on selective mitochondrial accumulation. *Cancer Res* **1996,** *56*, 538-543.

188. Chiba, Y.; Kubota, T.; Watanabe, M.; Matsuzaki, S. W.; Otani, Y.; Teramoto, T.; Matsumoto, Y.; Koya, K.; Kitajima, M. MKT-077, localized lipophilic cation: antitumor activity against human tumor xenografts serially transplanted into nude mice. *Anticancer Res* **1998,** *18*, 1047-1052.

189. Propper, D. J.; Braybrooke, J. P.; Taylor, D. J.; Lodi, R.; Styles, P.; Cramer, J. A.; Collins, W. C.; Levitt, N. C.; Talbot, D. C.; Ganesan, T. S.; Harris, A. L. Phase I trial of the selective mitochondrial toxin MKT077 in chemo-resistant solid tumours. *Ann Oncol* **1999,** *10*, 923-927.

190. Chen, W. Y.; Chang, F. R.; Huang, Z. Y.; Chen, J. H.; Wu, Y. C.; Wu, C. C. Tubocapsenolide A, a novel withanolide, inhibits proliferation and induces apoptosis in MDA-MB-231 cells by thiol oxidation of heat shock proteins. *J Biol Chem* **2008,** *283*, 17184-17193.

191. Ermakova, S. P.; Kang, B. S.; Choi, B. Y.; Choi, H. S.; Schuster, T. F.; Ma, W. Y.; Bode, A. M.; Dong, Z. (-)-Epigallocatechin gallate overcomes resistance to etoposide-induced cell death by targeting the molecular chaperone glucose-regulated protein 78. *Cancer Res* **2006,** *66*, 9260-9269.

192. Tang, X. Y.; Zhu, Y. Q. Epigallocatechin-3-gallate suppressed the over-expression of HSP 70 and MDR1 induced by heat shock in SGC 7901. *J Chemother* **2008,** *20*, 355-360.

193. Li, M.; Wang, J.; Jin, J.; Hua, H.; Luo, T.; Xu, L.; Wang, R.; Liu, D.; Jiang, Y. Synergistic promotion of breast cancer cells death by targeting molecular chaperone GRP78 and heat shock protein 70. *J Cell Mol Med* **2008**.

194. Williams, D. R.; Ko, S. K.; Park, S.; Lee, M. R.; Shin, I. An apoptosis-inducing small molecule that binds to heat shock protein 70. *Angew Chem Int Ed Engl* **2008,** *47*, 7466-7469.

195. Haney, C. M.; Schneider, C.; Beck, B.; Brodsky, J. L.; Domling, A. Identification of Hsp70 modulators through modeling of the substrate binding domain. *Bioorg Med Chem Lett* **2009,** *19*, 3828-3831.

196. Sharp, A.; Cutress, R. I.; Johnson, P. W.; Packham, G.; Townsend, P. A. Short peptides derived from the BAG-1 C-terminus inhibit the interaction between BAG-1 and HSC70 and decrease breast cancer cell growth. *FEBS Lett* **2009,** *583*, 3405-3411.

197. Lamb, J.; Crawford, E. D.; Peck, D.; Modell, J. W.; Blat, I. C.; Wrobel, M. J.; Lerner, J.; Brunet, J. P.; Subramanian, A.; Ross, K. N.; Reich, M.; Hieronymus, H.; Wei, G.; Armstrong, S. A.; Haggarty, S. J.; Clemons, P. A.; Wei, R.; Carr, S. A.; Lander, E. S.; Golub, T. R. The Connectivity Map: using gene-expression signatures to connect small molecules, genes, and disease. *Science* **2006,** *313*, 1929-1935.

198. Saleh, A.; Srinivasula, S. M.; Balkir, L.; Robbins, P. D.; Alnemri, E. S. Negative regulation of the Apaf-1 apoptosome by Hsp70. *Nat Cell Biol* **2000,** *2*, 476-483.

199. Schmitt, E.; Gehrmann, M.; Brunet, M.; Multhoff, G.; Garrido, C. Intracellular and extracellular functions of heat shock proteins: repercussions in cancer therapy. *J Leukoc Biol* **2007,** *81*, 15-27.

200. Volloch, V.; Gabai, V. L.; Rits, S.; Force, T.; Sherman, M. Y. HSP72 can protect cells from heat-induced apoptosis by accelerating the inactivation of stress kinase JNK. *Cell Stress Chaperones* **2000,** *5*, 139-147.

201. Meriin, A. B.; Gabai, V. L.; Yaglom, J.; Shifrin, V. I.; Sherman, M. Y. Proteasome inhibitors activate stress kinases and induce Hsp72. Diverse effects on apoptosis. *J Biol Chem* **1998,** *273*, 6373-6379.

202. Gabai, V. L.; Meriin, A. B.; Yaglom, J. A.; Volloch, V. Z.; Sherman, M. Y. Role of Hsp70 in regulation of stress-kinase JNK: implications in apoptosis and aging. *FEBS Lett* **1998,** *438*, 1-4.

203. Gabai, V. L.; Meriin, A. B.; Yaglom, J. A.; Wei, J. Y.; Mosser, D. D.; Sherman, M. Y. Suppression of stress kinase JNK is involved in HSP72-mediated protection of myogenic cells from transient energy deprivation. HSP72 alleviates the stress-induced inhibition of JNK dephosphorylation. *J Biol Chem* **2000,** *275*, 38088-38094.

204. Gabai, V. L.; Yaglom, J. A.; Volloch, V.; Meriin, A. B.; Force, T.; Koutroumanis, M.; Massie, B.; Mosser, D. D.; Sherman, M. Y. Hsp72-mediated suppression of c-Jun N-terminal kinase is implicated in development of tolerance to caspase-independent cell death. *Mol Cell Biol* **2000,** *20*, 6826-6836.

205. Ruchalski, K.; Mao, H.; Li, Z.; Wang, Z.; Gillers, S.; Wang, Y.; Mosser, D. D.; Gabai, V.; Schwartz, J. H.; Borkan, S. C. Distinct hsp70 domains mediate apoptosis-inducing factor release and nuclear accumulation. *J Biol Chem* **2006,** *281*, 7873-7880.

206. Ruchalski, K.; Mao, H.; Singh, S. K.; Wang, Y.; Mosser, D. D.; Li, F.; Schwartz, J. H.; Borkan, S. C. HSP72 inhibits apoptosis-inducing factor release in ATP-depleted renal epithelial cells. *Am J Physiol Cell Physiol* **2003,** *285*, C1483-1493.

207. Dudeja, V.; Mujumdar, N.; Phillips, P.; Chugh, R.; Borja-Cacho, D.; Dawra, R. K.; Vickers, S. M.; Saluja, A. K. Heat shock protein 70 inhibits apoptosis in cancer cells through simultaneous and independent mechanisms. *Gastroenterology* **2009,** *136*, 1772-1782.

208. Gyrd-Hansen, M.; Nylandsted, J.; Jaattela, M. Heat shock protein 70 promotes cancer cell viability by safeguarding lysosomal integrity. *Cell Cycle* **2004,** *3*, 1484-1485.

209. Gabai, V. L.; Yaglom, J. A.; Waldman, T.; Sherman, M. Y. Heat shock protein Hsp72 controls oncogene-induced senescence pathways in cancer cells. *Mol Cell Biol* **2009,** *29*, 559-569.

210. Sherman, M. Y.; Gabai, V.; O'Callaghan, C.; Yaglom, J. Molecular chaperones regulate p53 and suppress senescence programs. *FEBS Lett* **2007,** *581*, 3711-3715.

211. Park, M. A., Yacoub, A., Rahmani, M., Zhang, G., Hart, L., Hagan, M., Calderwood, S. K., Sherman, M. Y., Koumenis, C., Spiegel, S., Chen, C., Graf, M., Curiel, D. T., Fisher, P. B., Grant, S., Dent, P. OSU-03012 stimulates PRK-like endoplasmic reticulum-dependent increases in 70-kDa heat shock protein expression, attenuating its lethal actions in transformed cells. *Mol Pharmacol* **2008,** *73*, 1168-1184.

212. Chai, Y.; Koppenhafer, S. L.; Bonini, N. M.; Paulson, H. L. Analysis of the role of heat shock protein (Hsp) molecular chaperones in polyglutamine disease. *J Neurosci* **1999,** *19*, 10338-10347.

213. Kobayashi, Y.; Kume, A.; Li, M.; Doyu, M.; Hata, M.; Ohtsuka, K.; Sobue, G. Chaperones Hsp70 and Hsp40 suppress aggregate formation and apoptosis in cultured neuronal cells expressing truncated androgen receptor protein with expanded polyglutamine tract. *J Biol Chem* **2000,** *275*, 8772-8778.

214. Bailey, C. K.; Andriola, I. F.; Kampinga, H. H.; Merry, D. E. Molecular chaperones enhance the degradation of expanded polyglutamine repeat androgen receptor in a cellular model of spinal and bulbar muscular atrophy. *Hum Mol Genet* **2002,** *11*, 515-523.

215. Auluck, P. K.; Chan, H. Y.; Trojanowski, J. Q.; Lee, V. M.; Bonini, N. M. Chaperone suppression of alpha-synuclein toxicity in a Drosophila model for Parkinson's disease. *Science* **2002,** *295*, 865-868.

216. Klucken, J.; Shin, Y.; Hyman, B. T.; McLean, P. J. A single amino acid substitution differentiates Hsp70-dependent effects on alpha-synuclein degradation and toxicity. *Biochem Biophys Res Commun* **2004,** *325*, 367-373.

217. Dong, Z.; Wolfer, D. P.; Lipp, H. P.; Bueler, H. Hsp70 gene transfer by adeno-associated virus inhibits MPTP-induced nigrostriatal degeneration in the mouse model of Parkinson disease. *Mol Ther* **2005,** *11*, 80-88.

218. Meacham, G. C.; Lu, Z.; King, S.; Sorscher, E.; Tousson, A.; Cyr, D. M. The Hdj-2/Hsc70 chaperone pair facilitates early steps in CFTR biogenesis. *Embo J* **1999,** *18*, 1492-1505.

219. Younger, J. M.; Ren, H. Y.; Chen, L.; Fan, C. Y.; Fields, A.; Patterson, C.; Cyr, D. M. A foldable CFTR{Delta}F508 biogenic intermediate accumulates upon inhibition of the Hsc70-CHIP E3 ubiquitin ligase. *J Cell Biol* **2004,** *167*, 1075-1085.

220. Wild, J.; Kamath-Loeb, A.; Ziegelhoffer, E.; Lonetto, M.; Kawasaki, Y.; Gross, C. A. Partial loss of function mutations in DnaK, the Escherichia coli homologue of the 70-kDa heat shock proteins, affect highly conserved amino acids implicated in ATP binding and hydrolysis. *Proc Natl Acad Sci U S A* **1992,** *89*, 7139-7143.

221. Watanabe, K.; Tachibana, M.; Tanaka, S.; Furuoka, H.; Horiuchi, M.; Suzuki, H.; Watarai, M. Heat shock cognate protein 70 contributes to Brucella invasion into trophoblast giant cells that cause infectious abortion. *BMC Microbiol* **2008,** *8*, 212.

222. Hoffman, P. S.; Garduno, R. A. Surface-associated heat shock proteins of Legionella pneumophila and Helicobacter pylori: roles in pathogenesis and immunity. *Infect Dis Obstet Gynecol* **1999,** *7*, 58-63.

223. Stewart, G. R.; Snewin, V. A.; Walzl, G.; Hussell, T.; Tormay, P.; O'Gaora, P.; Goyal, M.; Betts, J.; Brown, I. N.; Young, D. B. Overexpression of heat-shock proteins reduces survival of Mycobacterium tuberculosis in the chronic phase of infection. *Nat Med* **2001,** *7*, 732-737.

224. Kohler, S.; Ekaza, E.; Paquet, J. Y.; Walravens, K.; Teyssier, J.; Godfroid, J.; Liautard, J. P. Induction of dnaK through its native heat shock promoter is necessary for intramacrophagic replication of Brucella suis. *Infect Immun* **2002,** *70*, 1631-1634.

225. Tobian, A. A.; Canaday, D. H.; Harding, C. V. Bacterial heat shock proteins enhance class II MHC antigen processing and presentation of chaperoned peptides to CD4+ T cells. *J Immunol* **2004,** *173*, 5130-5137.

226. Lagaudriere-Gesbert, C.; Newmyer, S. L.; Gregers, T. F.; Bakke, O.; Ploegh, H. L. Uncoating ATPase Hsc70 is recruited by invariant chain and controls the size of endocytic compartments. *Proc Natl Acad Sci U S A* **2002,** *99*, 1515-1520.

227. Guerrero, C. A.; Bouyssounade, D.; Zarate, S.; Isa, P.; Lopez, T.; Espinosa, R.; Romero, P.; Mendez, E.; Lopez, S.; Arias, C. F. Heat shock cognate protein 70 is involved in rotavirus cell entry. *J Virol* **2002,** *76*, 4096-4102.

228. Zarate, S.; Cuadras, M. A.; Espinosa, R.; Romero, P.; Juarez, K. O.; Camacho-Nuez, M.; Arias, C. F.; Lopez, S. Interaction of rotaviruses with Hsc70 during cell entry is mediated by VP5. *J Virol* **2003,** *77*, 7254-7260.

229. Chromy, L. R.; Oltman, A.; Estes, P. A.; Garcea, R. L. Chaperone-mediated in vitro disassembly of polyoma- and papillomaviruses. *J Virol* **2006,** *80*, 5086-5091.

230. Brown, G.; Rixon, H. W.; Steel, J.; McDonald, T. P.; Pitt, A. R.; Graham, S.; Sugrue, R. J. Evidence for an association between heat shock protein 70 and the respiratory syncytial virus polymerase complex within lipid-raft membranes during virus infection. *Virology* **2005,** *338*, 69-80.

231. May, E.; Breugnot, C.; Duthu, A.; May, P. Immunological evidence for the association between simian virus 40 115-kDa super T antigen and hsp70 proteins in rat, monkey, and human cells. *Virology* **1991,** *180*, 285-293.

232. Campbell, K. S.; Mullane, K. P.; Aksoy, I. A.; Stubdal, H.; Zalvide, J.; Pipas, J. M.; Silver, P. A.; Roberts, T. M.; Schaffhausen, B. S.; DeCaprio, J. A. DnaJ/hsp40 chaperone domain of SV40 large T antigen promotes efficient viral DNA replication. *Genes Dev* **1997,** *11*, 1098-1110.

233. Sullivan, C. S.; Tremblay, J. D.; Fewell, S. W.; Lewis, J. A.; Brodsky, J. L.; Pipas, J. M. Species-specific elements in the large T-antigen J domain are required for cellular transformation and DNA replication by simian virus 40. *Mol Cell Biol* **2000,** *20*, 5749-5757.

234. Sainis, L.; Angelidis, C.; Pagoulatos, G. N.; Lazaridis, L. HSC70 interactions with SV40 viral proteins differ between permissive and nonpermissive mammalian cells. *Cell Stress Chaperones* **2000,** *5*, 132-138.

235. Salma, A.; Tsiapos, A.; Lazaridis, I. The viral SV40 T antigen cooperates with dj2 to enhance hsc70 chaperone function. *Febs J* **2007,** *274*, 5021-5027.

236. Peng, C.-W., Zhoa, B., Chen, H.-C., Chou, M.-L., Lai, C.-Y., Lin, S.-Z., Hsu, H.-Y., Kieff, E. Hsp72 up-regulates Epstein-Barr virus EBNALP coactivation with EBNA2. *Blood* **2007,** *109*, 5447-5454.

237. Agostini, I.; Popov, S.; Li, J.; Dubrovsky, L.; Hao, T.; Bukrinsky, M. Heat-shock protein 70 can replace viral protein R of HIV-1 during nuclear import of the viral preintegration complex. *Exp Cell Res* **2000,** *259*, 398-403.

238. Iordanskiy, S.; Zhao, Y.; DiMarzio, P.; Agostini, I.; Dubrovsky, L.; Bukrinsky, M. Heat-shock protein 70 exerts opposing effects on Vpr-dependent and Vpr-independent HIV-1 replication in macrophages. *Blood* **2004,** *104*, 1867-1872.

239. Chromy, L. R.; Pipas, J. M.; Garcea, R. L. Chaperone-mediated in vitro assembly of Polyomavirus capsids. *Proc Natl Acad Sci U S A* **2003,** *100*, 10477-10482.

Chapter 2

Dihydropyrimidines Modulate Hsp70's Ability to Prevent Protein-Protein Interactions

2.1 Abstract

Alzheimer's disease (AD) is a neurological disorder that is characterized by the accumulation of plaques composed of aggregated amyloid beta (Aβ) peptide and neurofibrillary tangles composed of microtubule-binding protein tau. These structures are assembled by the ordered self-association of the component peptides, producing small soluble aggregates, intermediate oligomers and, eventually, the mature fibrils that deposit in the AD brain. As discussed in Chapter 1, over-expression of Hsp90, Hsp70 proteins and certain co-chaperones have been found to reduce AD-related pathology in models of AD. However, little is known about how Hsp70 might physically interact with these amyloid-forming proteins, which proteins are bound to the amyloid-forming protein and how this interaction might alter the course of disease. To better understand this relationship, we undertook a systematic analysis of how purified molecular chaperones impact Aβ aggregation *in vitro*. We found that Hsp70, in combination with Hsp40 and ATP, could specifically block formation of the pre-fibrillar Aβ structures. Interestingly, these chaperones were not able to reverse fibril formation. Finally, we used new chemical probes and hydrolysis-resistant nucleotide mimetics to demonstrate a key role for ATP turnover in the ability of Hsp70 to block Aβ aggregation.

2.1.1 Amyloid diseases

The amyloid diseases are a collection of protein misfolding disorders associated with the formation of distinctive fibrils.[1-5] Alzheimer's disease is one of the most common amyloid diseases and it is characterized by fibrils composed of Aβ, a 39-43 amino acid proteolytic fragment of the amyloid precursor protein (APP).[6] Upon release from APP, Aβ becomes enriched in β-sheet structure and acquires the propensity to self-assemble.[7] Initial theories to explain the pathology of AD focused on the involvement of the visually striking fibrils, but more recent evidence has strongly supported a role for soluble oligomers.[3, 8-10] Aβ oligomers can be prepared *in vitro*[11, 12], biosynthesized by cultured cells[13, 14], or collected from AD tissues[15] and, in all cases, these structures are highly neurotoxic. Despite these important observations, numerous questions about the basis of disease are unanswered. For example, although there is active research in this area[8, 11, 16], the number of Aβ monomers present in an oligomer hasn't been fully described. Moreover, the subcellular site(s) of oligomer production and the conditions that lead to their assembly is still debated; fibrils are found in extracellular space but there is growing evidence that oligomers may be produced in intracellular compartments.[8, 13, 17-19] Additional insights into the molecular mechanisms that contribute to AD are needed.

One of the important consequences of the oligomer hypothesis is that it implies that therapeutic benefits could arise from preventing early (i.e. pre-oligomeric) stages of amyloid formation. Accordingly, small molecules that directly block Aβ aggregation[20-22], reduce its production from APP[23-25], decrease soluble amyloid load[26, 27] and enhance progression to fibrils[28, 29] are being actively explored.[30] The goal of most of these

approaches is to intervene at a stage prior to oligomerization and prevent accumulation. Consistent with this idea, it has been suggested that stimulating natural cellular mechanisms that combat protein aggregation, including proteases that digest Aβ and chaperones that inhibit misfolding, might have therapeutic benefit.[31-33]

2.1.2 Genetic evidence for the role of chaperones in Alzheimer's disease

Molecular chaperones are involved in many important aspects of protein homeostasis, including folding, degradation and subcellular trafficking.[34-36] These tasks typically involve the heat shock proteins, such as Hsp70 and Hsp90, which (as discussed in Chapter 1) are chaperones that recognize misfolded polypeptides and use energy-driven cycles of substrate binding and release to favor productive folding.[37, 38] One of the important consequences of chaperone binding is that deleterious protein aggregation is prevented. Consistent with this activity, numerous studies have suggested that heat shock proteins are important for the prevention of amyloid formation.[39-41,31, 42, 43] For example, genetic overexpression of Hsp70 has been shown to reduce amyloid-related phenotypes in mouse models of spinocerebellar ataxia type 1[44] and Parkinson's disease[45]. Similar results are seen in *Drosophila melanogaster*[46], *Saccharomyces cerevisae*[47, 48], and *Caenorhabditis elegans*[49] models of neurodegeneration. These experiments suggest that chaperones, particularly Hsp70, may bind amyloidogenic peptides and help prevent disease by restoring the balance between aggregation and folding. This hypothesis is supported by biochemical evidence in some systems. In models of AD, overexpression of molecular chaperones, specifically heat shock protein 70 (Hsp70) family of proteins, suppresses phenotypes related to Aβ aggregation. These observations led to the hypothesis that chaperones might interact with Aβ and block self-association.

2.1.3 Hsp70's involvement in the aggregation of amyloid beta

Purified Hsp70 proteins blocks aggregation of α-synuclein, a protein implicated in Parkinson's disease, *in vitro*.[50] Similarly, addition of Hsp70 and its co-chaperone partner, Hsp40, to huntingtin, an aggregation-prone protein that causes Huntington's disease, blocks oligomer formation.[43, 51] In addition to these findings, other chaperones, such as Hsp20[52] and Hsp104[53], have been shown to limit amyloid formation *in vitro*. Together, the combination of genetic and biochemical evidence provides compelling support for a direct role of chaperones in these diseases. In Alzheimer's disease, genetic evidence to suggest a role for chaperones has been reported[54], but corresponding biochemical analysis is lacking. Similar to what occurs in other disease models, Hsp70 protein family overexpression improves the viability of cells that express excess Aβ.[54] Additionally, abundant chaperone levels block formation of Aβ aggregates in *C. elegans*.[49] Biochemical evidence would help elucidate the mechanism(s) responsible for these favorable effects. For example, the type of Aβ structure (e.g. monomers, oligomers and/or fibrils) bound by chaperone is not known. Moreover, it isn't clear how much chaperone is required or if this process is ATP-driven. A more detailed understanding of this system would be beneficial in both (a) understanding chaperone function and (b) designing potential therapeutics to enhance favorable chaperone functions.

2.1.4 Synthesis of Hsp70 modulators by the Biginelli reaction

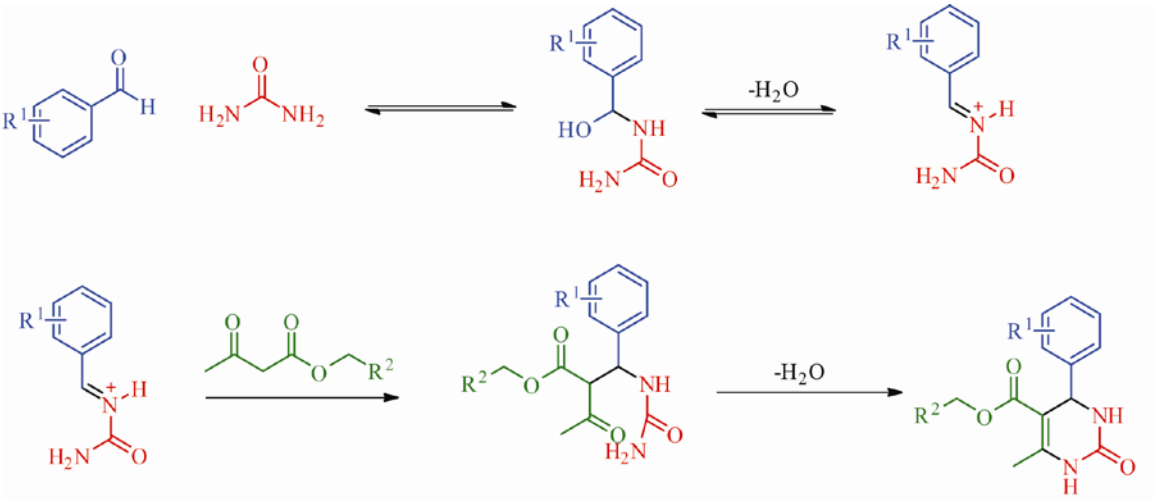

Scheme 2-1. Reaction Mechanism Proposed by Kappe for the Biginelli Reaction. First urea acts as a nucleophile and attackes the carbonyl of the aldehyde. This ultimately results in the formation of the imminium ion. The β-ketoester then adds to the imminium ion, which leads to the a structure which upon the loss of water yields the dihydropyrimidine core.

As discussed in Chapter 1, early Hsp70 modulators, such as MAL3-101, were generated by the Bignelli reaction. For these compounds the Biginelli-derived dihydropyrimidines were subsequently subjected to the Ugi reaction to yield the final active compound.[55] The Biginelli portion of the sequence of reaction employs three components. An aldehyde, urea, and β-keto ester are combined to form a dihydropyrimidine under conditions catalyzed by a Lewis or Brønsted acid. The most recent mechanism for this reaction was proposed by Kappe in 1997 (Scheme 2-1).[56] The dihydropyrimidine scaffold has yielded a multitude of biologically active compounds some of which have been shown to have activity on Hsp70.[57-62] Using these studies as a guide, we sought to generate Hsp70-targeted probes using this multi-component reaction. In turn, these reagents could be used to understand the relationships between Hsp70 and amyloids, leading towards potential drug-like molecules.

2.2 Results

2.2.1 Recombinant Hsp70/40 blocks aggregation of freshly prepared amyloid beta (1-42)

Results from overexpression experiments have suggested a role for Hsp70 family of proteins in the aggregation of amyloid beta[54], but evidence for this interaction *in vitro* is lacking. To explore this question, freshly prepared amyloid beta (1-42) was treated with recombinant Hsp70 and its co-chaperone Hsp40 in the presence of excess ATP. Hsp40 stimulates Hsp70's ATPase activity[63, 64] at a low molar ratio (100:1 Hsp70:40). Thus, the goal of these experiments was to establish if an activated Hsp70/40 combination could inhibit amyloid formation. In our initial experiments, we monitored turbidity to discern the extent of Aβ self-assembly.[7] Strikingly, the results of these experiments revealed that Hsp70/40 is a potent sub-stoichiometric inhibitor (Figure 2-1A). At a molar ratio of ~1:50 (overall chaperone:Aβ), Hsp70/40 significantly slowed the rate of aggregation and delayed the onset time. This effect was dependent on chaperone concentration; lowering the levels to less than ~ 1:200 abolished inhibition. To confirm these results under different conditions, we employed the well-known thioflavin T assay. Thioflavin T is an indicator dye that becomes strongly fluorescent in the presence of amyloid.[65] Confirming the turbidity results, there was a strong dose-dependent decrease in fluorescence after 80 minutes of treatment with chaperones (Figure 2-1B). Finally, we used transmission electron microscopy (TEM) to examine the ultrastructure of the chaperone-treated samples. These experiments revealed that, rather than forming fibrils, Aβ was redirected into roughly circular structures by Hsp70/40 (Figure 2-1C). Although these spheres were prevalent, short fibrils were occasionally observed, which suggests

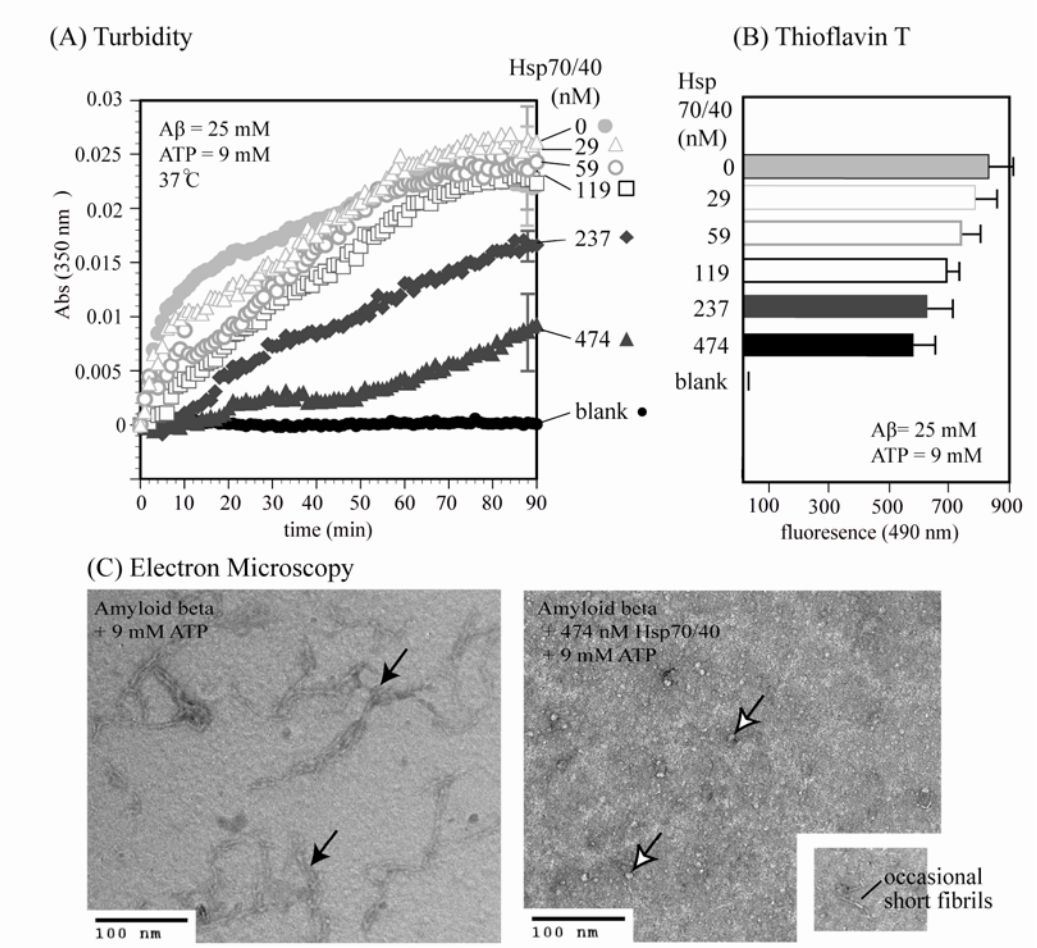

Figure 2-1. Heat Shock Proteins 70/40 Counteract Aggregation of Amyloid Beta (1-42) In Vitro. (A) Turbidity measurements reveal that sub-stoichiometric chaperone levels can block aggregation. The concentration of amyloid, Hsp70/40 (molar ratio 100:1), and ATP are indicated. The blank control is buffer alone (i.e. no amyloid beta). Results are the average of triplicate wells and are representative of other experiments. Error (standard deviation of the mean) is represented by the bars on the penultimate time points. (B) Thioflavin T fluorescence assays were performed on samples at the conclusion of the turbidity assay (90 min). Results are the average of 2-4 experiments in triplicate each. In each case, the fluoresence was normalized by substracting the blank sample (20-50 fluorescence units). (C) Analysis of samples by transmission electron microscopy at the conclusion of the turbidity experiments (90 min). The inset (right panel) shows occasional (approximately 1%) short fibrils observed in the Hsp70/40-treated samples. The dark arrows point to fibrils and the light arrows to small, roughly spherical structures.

that some Aβ escapes the block. Further, the barrier to aggregation wasn't complete; over the time course studied, the initial rate of assembly was slowed but not entirely stopped.

2.2.2 The combination of Hsp70/40 is more effective than Hsp70 alone

Hsp40 is a known co-chaperone and stimulator of Hsp70's ATPase activity.[66] Thus, we were interested in understanding if the combination of Hsp70/40 is more effective than Hsp70 alone. This result would suggest that ATPase activity is important for Hsp70's anti-aggregation function. To test this idea, we treated Aβ with Hsp70 or the combination (100:1 Hsp70:40) and monitored aggregation by the thioflavin T assay. Consistent with reports in other systems[50], Hsp70 alone blocks aggregation (Figure 2-2).

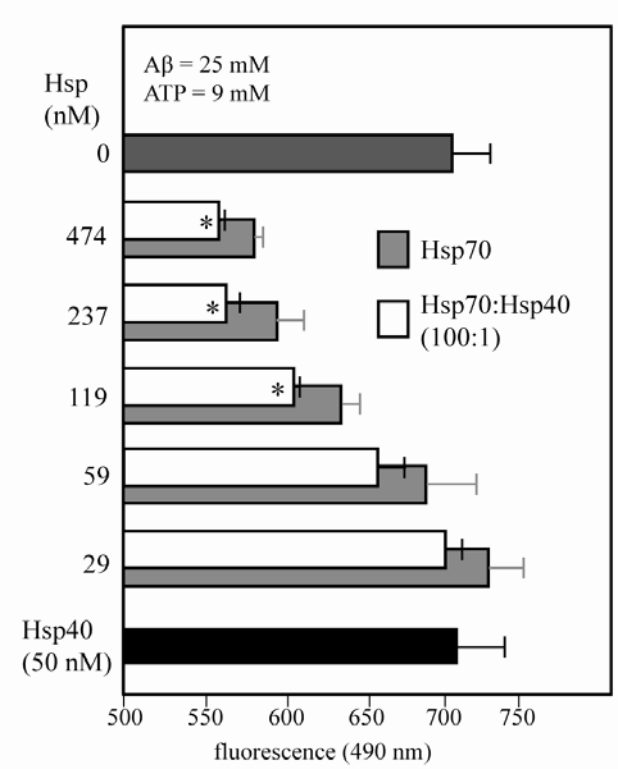

Figure 2-2. Hsp70's anti-aggregation activity is enhanced by co-chaperone. Thioflavin T measurements of freshly prepared samples treated with Hsp70 or the Hsp70/40 combination, which has a constant molar ratio of 100:1 (Hsp70:40). Errors are standard deviation from the mean for experiments performed in triplicate. The asterisks indicate P values of < 0.1.

However, when we added low levels of Hsp40 to Hsp70, we found an enhancement over

the chaperone alone. As a control, we tested whether Hsp40 could inhibit aggregation in the absence of its partner. We found that Hsp40 failed to block Aβ self-assembly, even at 10-fold higher concentrations (50 nM) than those used in the previous experiments. Therefore, we conclude that, although both Hsp70 and Hsp70/40 prevent amyloid formation *in vitro*, the combination is most effective.

2.2.3 Recombinant Hsp90 blocks aggregation of freshly prepared amyloid beta (1-42)

Although Hsp70 and Hsp40 have both been implicated in counteracting amyloid formation in certain neurodegenerative systems, Hsp90 has attracted less attention. In one *in vitro* model, Hsp90 has been shown to be insufficient to prevent amyloid formation.[43] However, Hsp90 is an important and highly abundant component of the chaperone machinery that shares some pro-folding tasks with other heat shock proteins.[36, 37] To explore potential roles of this chaperone in Aβ aggregation, we performed similar experiments to those described in the preceding section. Similar to what we observed with Hsp70/40, Hsp90 provided a strong dose-dependent block to amyloid formation when added to freshly prepared Aβ samples (Figure 2-3). The peak of Hsp90's anti-aggregation activity was also observed at sub-stoichiometric concentrations (between 1:50 and 1:200). TEM images revealed that Aβ in the Hsp90-treated samples was again re-directed into small, roughly circular structures instead of fibrils. Thus, both Hsp70/40 and Hsp90 could partially prevent assembly of freshly prepared Aβ *in vitro*.

2.2.4 ATPase activity is required for chaperones to block aggregation

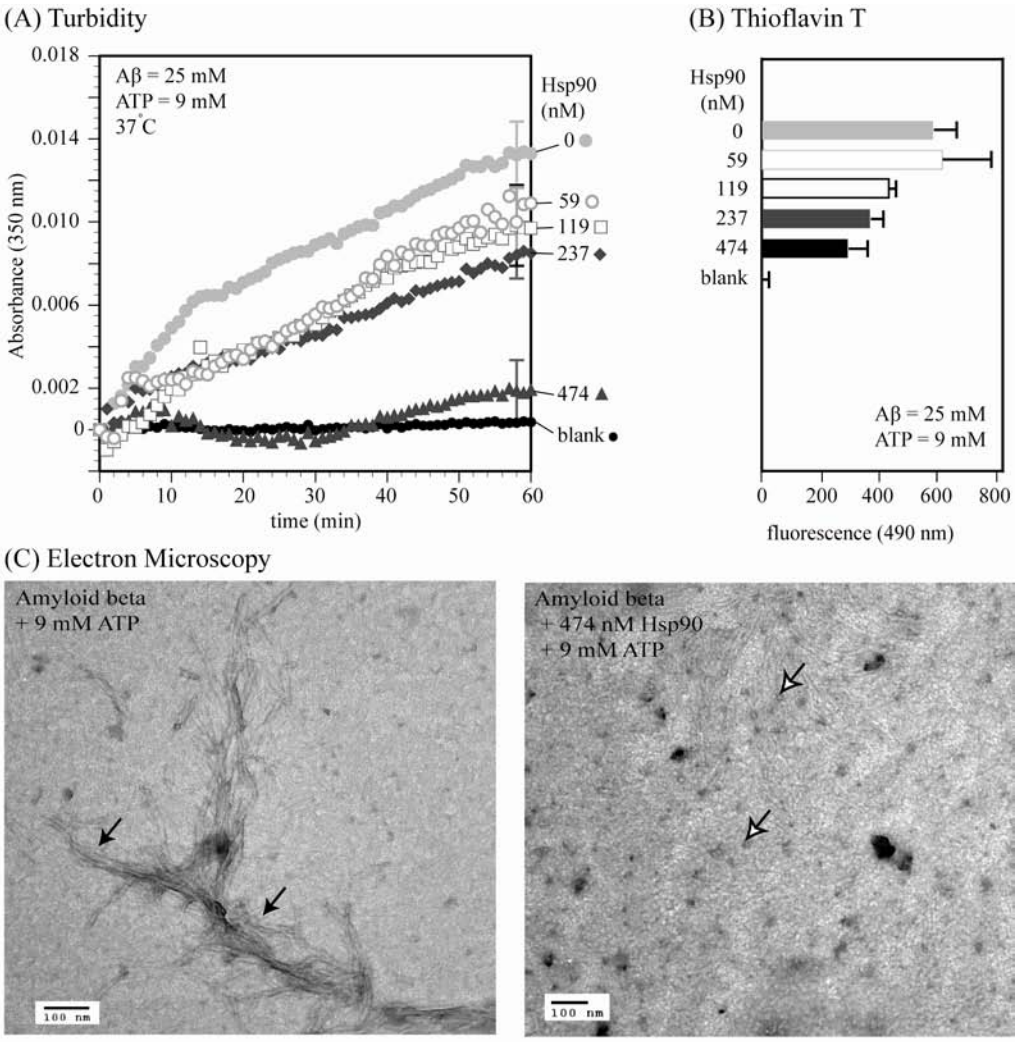

FIGURE 2-3. Heat Shock Protein 90 Blocks Aggregation of Amyloid Beta (1-42) in Vitro. (A) Turbidity measurement reveal that substoichiometric chaperone levels can prevent fibrilligenesis. The experimental conditions used are identical to those used to collect the data shown in Figure 1. Results are the average of triplicate wells. Representative standard deviations are shown. (B) Thioflavin T fluorescence results show dose-dependent reduction in fibril formation after treatment with Hsp90. Measurements were taken at the conclusion of the turbidity experiment (60 min). Results are the average (with standard deviations) of at least two experiments in triplicate each. Fluorescence is normalized to a buffer alone control (signal was approximately 12-15 units). (C) Analysis of samples by TEM at the conclusion of the turbidity experiment (60 min).

Because the ATP- and ADP-bound forms of Hsp70 have different affinities for peptide substrate,[63] we sought to study the role of ATPase activity in preventing Aβ aggregation. Our results (see Figure 2-2) suggest that Hsp40-enhanced ATP turnover may

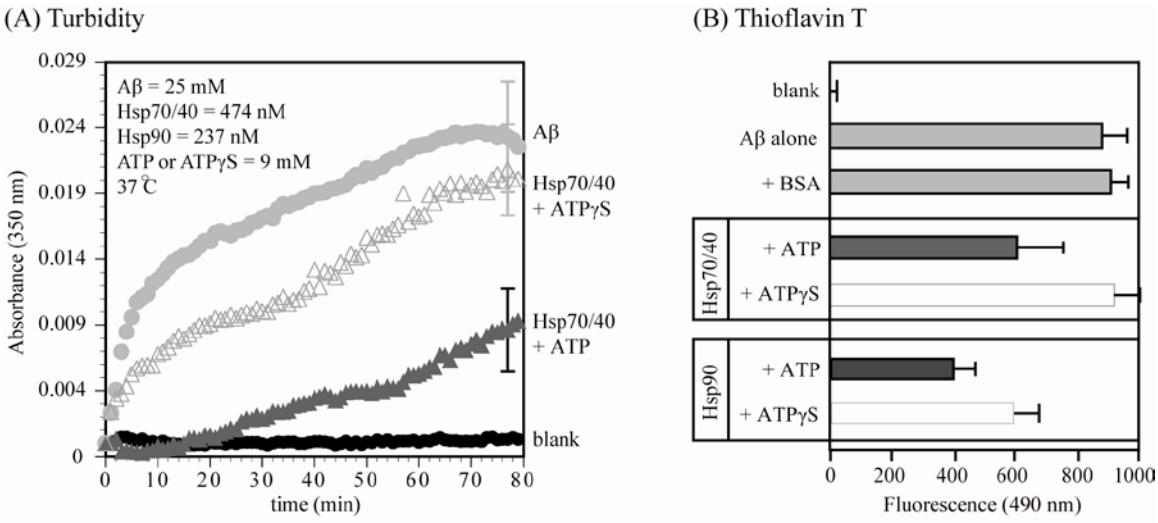

FIGURE 2-4. ATPase Activity Is Required to Fully Inhibit Amyloid Beta (1-42) Aggregation. (A) Turbidity measurements performed on amyloid samples treated with Hsp70/40 and either ATP or non-hydrolyzable ATPγS (9 mM). Similar results were observed with Hsp90 treatments. Results are the average of a representative experiment performed in triplicate and error bars are standard deviations. Error is shown on single time points for clarity but are representative of overall error. Note that some of the curves from Figure 2-1 are replicated here for comparison. (B) Thioflavin T fluorescence of samples treated for 60-90 minutes. Results are the average of 3-4 experiments performed in triplicate each. Hsp70/40 or BSA were added to 474 nM, Hsp90 to 237 nM, and ATP or ATPγS to 9 mM. Results are normalized to the buffer control (intensity between 20-50 fluorescence units).

be important, but we sought additional evidence using a complementary approach. Therefore, the non-hydrolyzable ATP analog, ATPγS, was employed. Freshly prepared Aβ was treated with Hsp70/40 or Hsp90 in the presence of either ATP or ATPγS. Turbidity and thioflavin T measurements revealed that these chaperone's inhibitory effects are partially disrupted by ATPγS (Figure 2-4). However, we found that Hsp70 had a stronger requirement for ATPase activity than Hsp90; ATPγS disrupted nearly all of Hsp70's anti-aggregation activity, but over 50% of Hsp90's function remained. Thus, these results suggest that the catalytic cycle of ATP hydrolysis is required for Hsp70's anti-aggregation activity but that Hsp90 only partly depends on its enzymatic function.

As part of these studies, we also were interested in determining if any protein might substitute for the chaperones. To explore this possibility, we attempted to block

amyloid formation with bovine serum albumin (BSA). At the highest concentrations used (474 nM, equivalent to the top chaperone levels employed), no effect on Aβ aggregation was observed (Figure 2-4). These results are consistent with previous reports using non-chaperone proteins,[43] and demonstrate that the chaperone interaction cannot be replaced by contacts with the BSA interface.

2.2.5 An Hsp70 agonist promotes anti-aggregation activity

Because our results indicate that ATPase activity is required for chaperones to fully block aggregation, we hypothesized that agonists (particularly those that promote turnover by Hsp70) might stimulate this function. The natural product analog, 15-deoxyspergualin, is an agonist of Hsp70 that binds outside the nucelotide binding site [67-69]. Recent work by the Wipf, Day and Brodsky laboratories has shown that certain synthetically-accessible dihydropyrimidines, which structurally mimic 15-deoxyspergualin, can likewise enhance ATPase activity and regulate protein translocation.[55, 70] Based on these studies, we have recently developed a route to the modular synthesis of additional dihydropyrimidines and shown that some of these molecules modify Hsp70's ATPase activity and it ability to refold denatured luciferase.[71, 72] During the course of those studies, we found that one of these compounds, SW02, enhanced ATPase activity and folding ability by at least 20% *in vitro*. Conversely, a related compound, SW08, blocked luciferase refolding by ~50%. More recently, we also identified the binding site of a dihydropyrimidine on Hsp70 and showed that these compounds alter interactions between Hsp70 and Hsp40.[62] Importantly, these studies revealed how compounds with a similar core chemical structure can operate as either promoters or inhibitors of Hsp70 functions.

Based on these studies and the apparent importance of nucleotides, we hypothesized that SW02 (Figure 2-5A) might stimulate Hsp70's ability to block Aβ aggregation and SW08 might be inhibitory. To test this theory, we started with an Hsp70 concentration, 119 nM, that was insufficient to block aggregation. Under these conditions, we propose that aggregation could only be inhibited if the chaperone activity were artificially enhanced. When SW02 was added to this suboptimal chaperone pool, significant anti-aggregation activity was gained (Figure 2-5B). In control experiments, SW02 had no effect in the presence of Hsp40 or Hsp90. Moreover, in the absence of any chaperone, SW02 did not alter Aβ aggregation. Thus, these results suggest that SW02 is

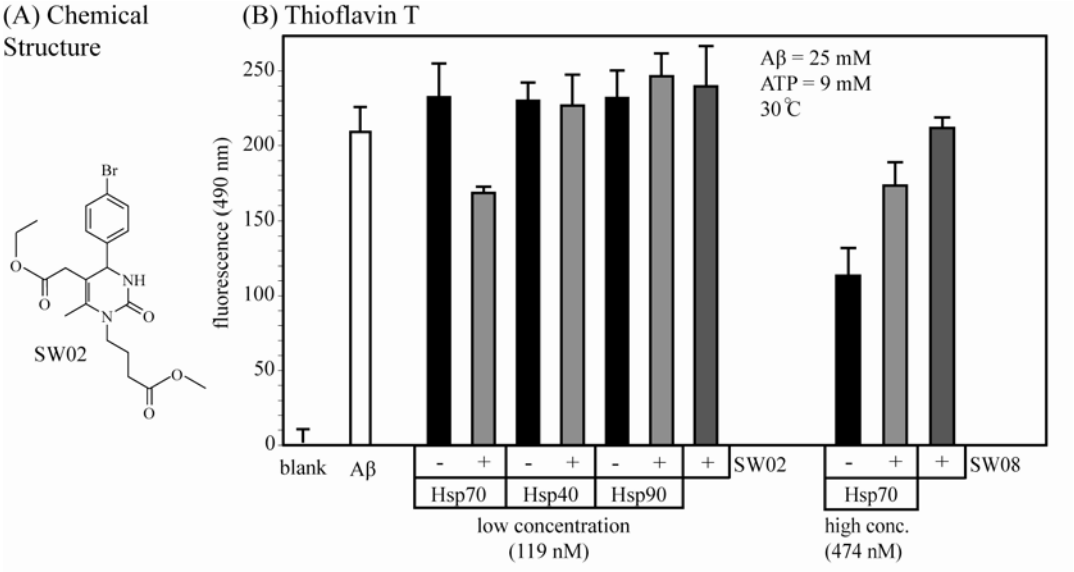

Figure 2-5. A small molecule specifically promotes Hsp70's anti-aggregation activity. (A) Chemical structure of SW02, the agonist used in these studies. (B) Thioflavin T measurements suggest that SW02 activates Hsp70's anti-aggregation activity, but doesn't assist function of Hsp40 or Hsp90 at 119 nM. This chaperone concentration was chosen to minimize inherent activity. Conversely, an antagonist (SW08) modestly inhibits Hsp70 at higher chaperone levels. In the absence of chaperone, neither SW02 nor SW08 has any effect. Experiments were performed in triplicate and error is standard deviation from the mean.

relatively specific for Hsp70 and that it indirectly promotes anti-aggregation activity. To

gain further evidence in support of this idea, we used a higher concentration of Hsp70 (474 nM) and added the antagonist SW08. This treatment partially blocked Hsp70's function and restored aggregation (Figure 2-5B). Thus, agonists and antagonists could be used to adjust or "tune" chaperone activity.

2.2.6 The potency of SW02 is modest, but it enhances Hsp70/40 function

To determine SW02's efficacy, we varied the concentration of the agonist at a constant

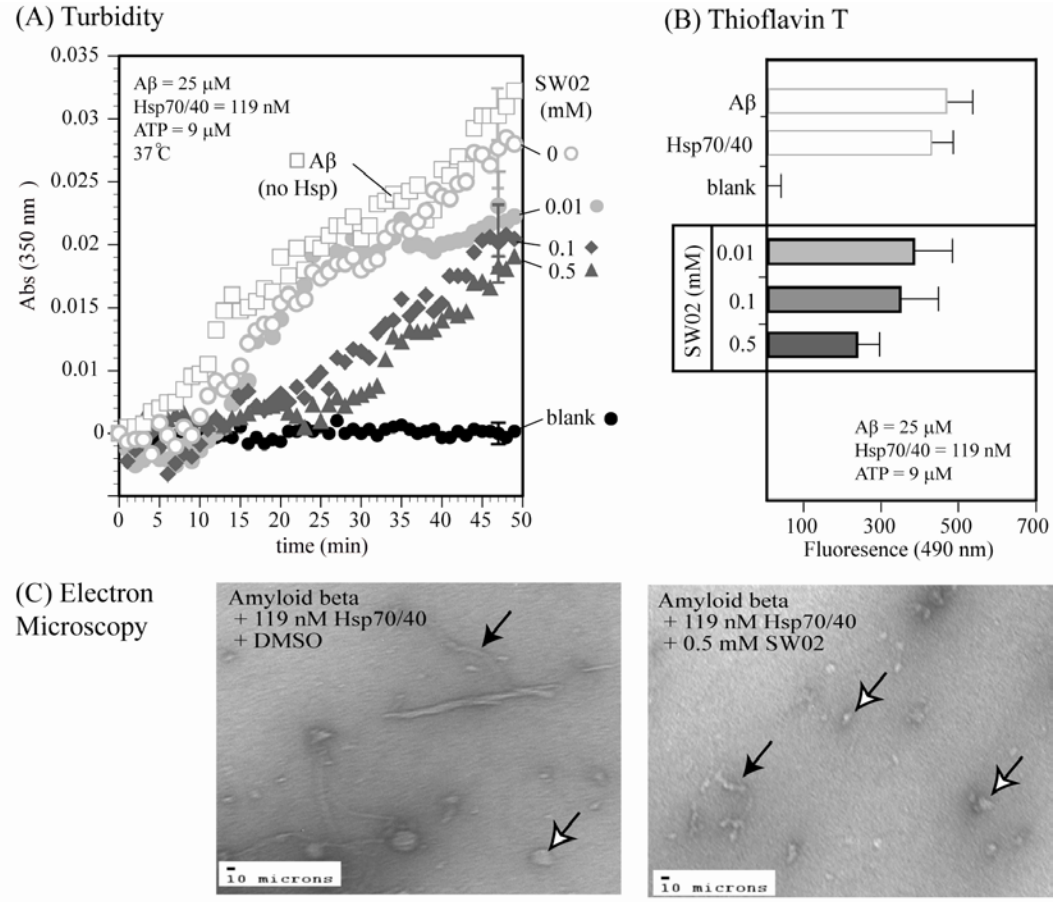

Figure 2-6. SW02 is a modest agonist of Hsp70/40 anti-aggregation activity. (A) Turbidity reveals enhanced anti-aggregation activity of Hsp70/40 in the presence of SW02. Error bars represent standard deviation of experiments performed in triplicate. SW02 was added from 100 x stocks in DMSO, so all samples were normalized to 1% DMSO. (B) Thioflavin T fluoresence of samples after turbidity measurements (50 min). The results are the average of at least 3 experiments done in triplicate and the errors are standard deviations. The results are normalized to the buffer control (fluorescence between 20-50). (E) TEM analysis of amyloid structures after the indicated treatments for 50 minutes. Dark arrows indicate fibrils and light arrows point to other structures.

level of Hsp70/40 (119 nM) and measured Aβ aggregation by turbidity and thioflavin T assays (Figure 2-6). In both platforms, we found that high concentrations of SW02 (between 100 and 500 μM) were required to activate the chaperone. By TEM, treatment with Hsp70/40 and 500 μM compound yielded similar Aβ structures to those produced by treatment with higher concentrations of unstimulated chaperone (Figure 2-6C). Together, these results suggest that, although the potency of SW02 is modest, promoting Hsp70/40's anti-aggregation activity can enhance inhibition *in vitro*.

2.2.7 Chaperones recognize amyloid oligomers but have little effect on mature fibrils

Despite the characteristic presence of Aβ fibrils in the brains of AD patients, recent evidence suggests that oligomers are critical in the development of disease. Therefore, we sought to determine if chaperones would have any effects on preformed oligomers or mature fibrils. The impetus for these experiments was to understand (in an *in vitro* system), the types of amyloid forms that can be recognized by chaperones. The answer to this question might provide insight into how chaperones counteract Aβ toxicity *in vivo*. Moreover, we (and others) have an interest in pharmacological stimulators of chaperone activity. These efforts would benefit from additional mechanistic knowledge about the types of amyloid structures that can be modified by chaperones. For example, if mature fibrils were dissolved by chaperones and processed into toxic oligomers, this could have a strongly negative effect on the organism. Moreover, if chaperones only act on freshly prepared Aβ samples (as used in Figures 2-1,-2, and -3 above), this suggests that pre-existing oligomers might be safe from chaperone intervention. Because of these questions, we decided to supplement our studies with experiments that explore the effects of chaperones on pre-formed oligomers and fibrils *in vitro*.

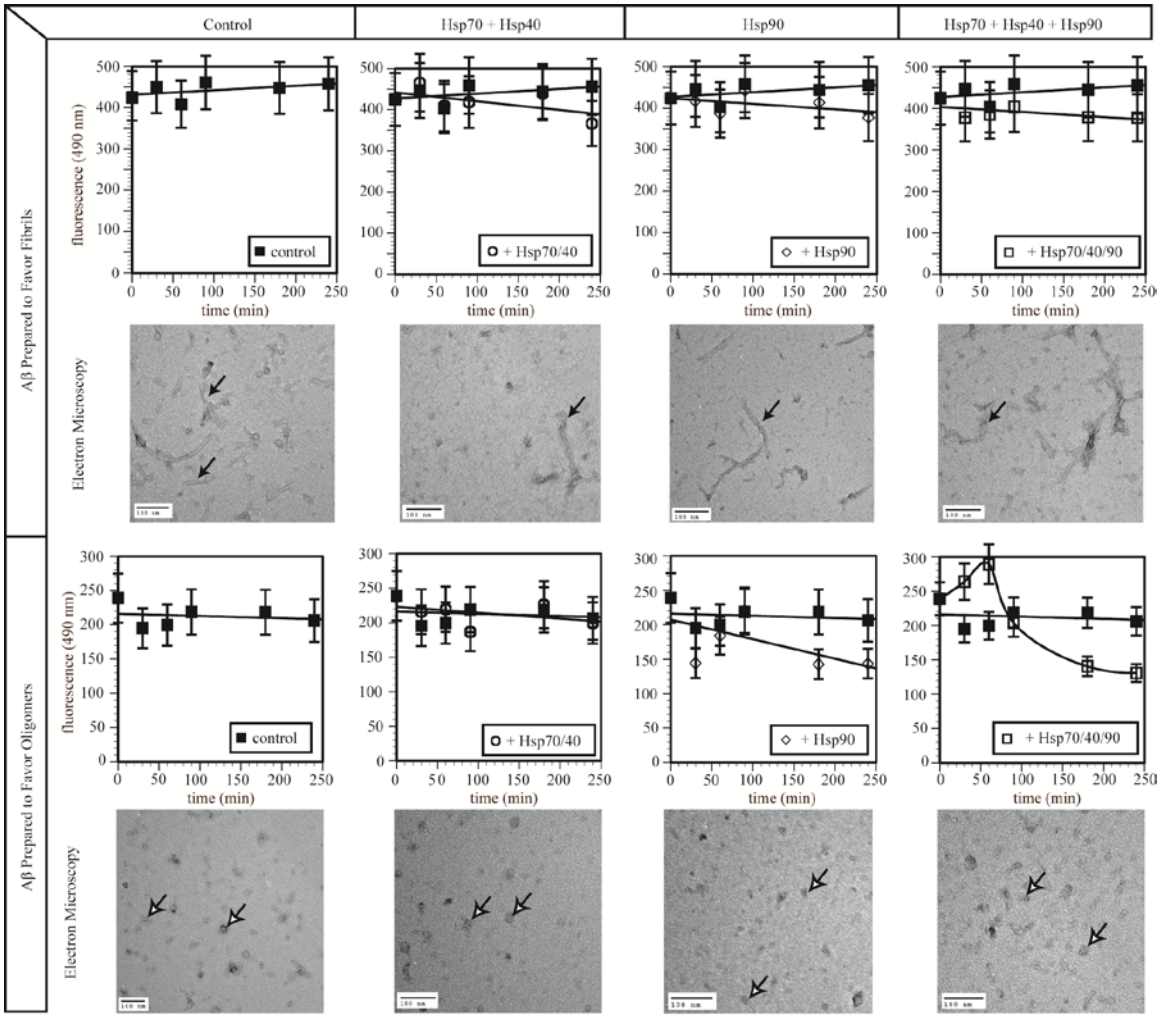

Figure 2-7. Effects of Heat Shock Proteins 70/40 and 90 on Pre-formed Oligomers and Fibrils. Thioflavin T experiments were used to monitor the effects of Hsp co-incubation on pre-formed fibrils (top) or oligomers (bottom). Results are the average of at least two experiments performed in triplicate each. Ultrastructure was examined using TEM at the conclusion of the thioflavin experiments (240 min).

By varying the temperature and buffer conditions used to prepare Aβ, we were able to produce solutions of soluble oligomers or fibrils, consistent with previous reports.[73, 74] After formation of these structures, chaperones and ATP were added and any effects measured by thioflavin T fluorescence and TEM. Treatment of preformed fibrils with Hsp70/40 or Hsp90 had little effect on the thioflavin T fluorescence (Figure 2-7). Because the native cellular environment might posses both of these chaperone systems, we also combined them. In samples treated with the Hsp70/40/90 mixture, there was a

small, but not statistically significant drop in fluorescence. TEM results supported this observation; very little change in fibril structure was observed. However, in analyzing the samples, we noticed that the fibril length tended to be shorter in the Hsp70/40/90-treated samples (Figure 2-8). To further investigate this observation, we used image analysis to quantify average fibril length. Although this result is not striking, there was a slight tendency for chaperone-treated samples to contain fewer long fibrils. However, because this effect is subtle we conclude that these chaperones have very little impact on fibrils.

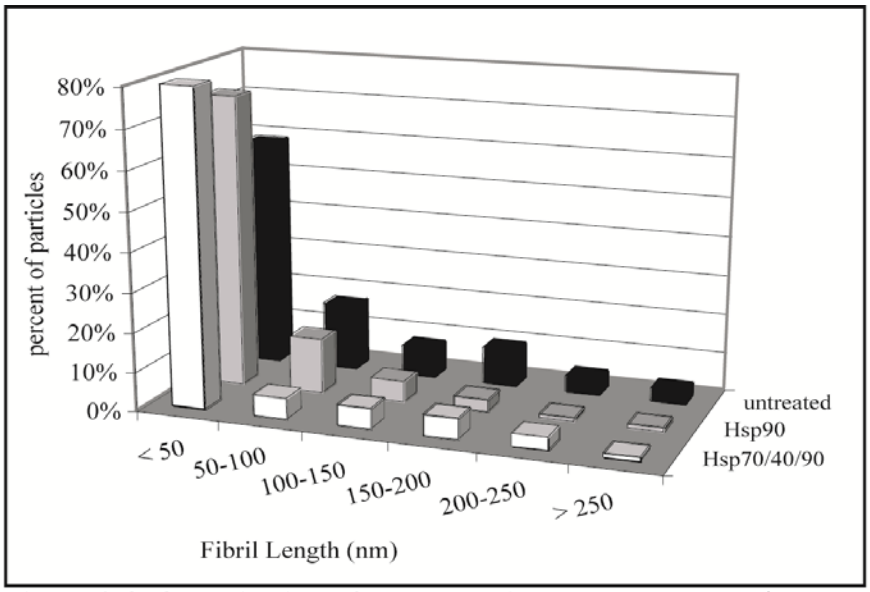

Figure 2-8. Quantitation of electron microscopy results. Ultra-structure was examined using TEM at the conclusion of the thioflavin experiments (240 min).The distribution of approximate fibril lengths after the 240 min chaperone treatment was obtained using NIH Image software (n = 90 to 125). The quantification results mirror what is seen upon gross examination of the images, fibril length tended to be shorter in chaperone treated samples.

Preformed oligomers were treated with chaperones and studied by thioflavin T fluorescence and TEM. Under these conditions, Hsp70/40 did not measurably change the thioflavin T reactivity or structure of oligomers (Figure 2-9). The combination of Hsp70/40/90, however, caused an initial increase in fluorescence followed by steady

drop. Hsp90 alone could produce similar effects, but these changes were more pronounced in the triple chaperone-treated samples. To study the ultrastructure of the treated oligomers, we studied the resulting solutions by TEM. The oligomers in the samples treated for 240 minutes with Hsp70/40/90 become noticeably less defined and more diffuse (Figure 2-9). This effect was most obvious during attempts to focus the images; it wasn't possible to capture images in which the oligomer boundaries were well defined. Additional experiments will be required to further characterize this effect, but these results suggest that Hsp70/40/90 can alter the structure of pre-formed oligomers.

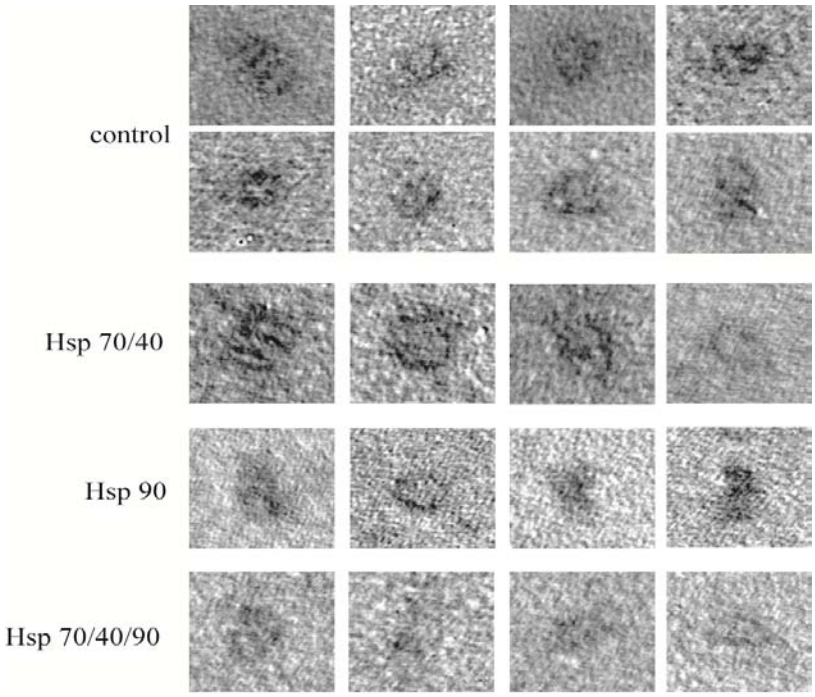

Figure 2-9. Oligomers Treated with Hsp70/40/90 Are Diffuse. The panel depicts a number of representative structures observed in the oligomer preparations. Note that when Hsp's 70/40/90 are all added to the oligomer preperations the resulting images are more diffuse than when they are added to the preperations individually.

2.3 Discussion

2.3.1 Model for Hsp70's potential roles in neurodegenerative disease

Self-assembly of Aβ produces a number of distinctive structures, such as dimers, oligomers, unstructured aggregates and characteristic amyloid fibrils. Of these structures, oligomers are believed to be the most neurotoxic and important in the development of disease.[3, 8, 9] Thus, any strategies to reduce amyloid-related phenotypes must avoid producing toxic oligomers from relatively benign structures, such as fibrils. In genetic models of AD, Hsp70/40 overexpression reduces cell death, which is a result that is consistent with decreased oligomer load. Moreover, in a *D. melanogaster* model of Huntington's disease, Hsp70 overexpression inhibits neurodegeneration without preventing the formation of large inclusions.[46] These results provide indirect evidence that chaperones specifically inhibit early stages of aggregation. However, we reasoned that biochemical support for this conclusion would enhance our understanding of the types of amyloid structures recognized by chaperones. These considerations led us to explore the interaction of chaperones with various types of Aβ structures *in vitro*. Specifically, we have studied the effects of Hsp70/40 and Hsp90 on three types of amyloid structures: freshly prepared Aβ, oligomers, and fibrils. Although the exact temporal and causal relationships between these structures are unclear, we use the freshly prepared samples and oligomers as representative of earlier stages in self-assembly. This distinction is partially based on the observation that aged Aβ preparations and terminal AD patient's brains often contain elongated fibrils.[75] Using this paradigm, we conclude that Hsp70/40 and Hsp90 specifically influence aggregation at "early" stages in the process; freshly prepared Aβ (Figures 2-1, -2, and -3) and oligomers (Figure 2-7) were

most susceptible, while fibrils were less affected (Figure 2-7). This result is consistent with findings in other systems that suggest an early role for chaperones in blocking protein aggregation.[43, 50, 51] One interesting question related to this observation is whether samples treated with chaperones *in vitro* are neurotoxic. We have not characterized toxicity in this system, but chaperones are protective in other systems[3, 8-10] and we predict that treated Aβ will also be less toxic.

What is the molecular mechanism used by chaperones to inhibit Aβ self-assembly? Although the details of this process remain unclear, we will discuss our results in the context of two specific models (Figure 2-10). In the "holding" model, the chaperone binds misfolded amyloid (likely via its substrate-binding domain). We propose that this interaction decreases free monomer concentration and, thereby, slow the rate of self-assembly, which is known to be dependent on monomer availability.[75-77] This model predicts that inhibition would be independent of ADP-ATP exchange because cycles of substrate release do not contribute to the inhibitory mechanism. Some of our results are consistent with this prediction. Specifically, we report that Hsp90 is only partially inhibited by ATPγS. Thus, for this chaperone, we speculate that a "holding" or partitioning model describes some of the observations. However, Hsp90 was effective at substoichiometric concentrations (Figure 2-3). This result seems at odds with the "holding" model because one might presume that a 1:1 (or greater) stoichiometry should be optimal. The dependence of Aβ aggregation on monomer concentration might partly resolve this apparent conflict; decrease in available monomer is expected to directly influence rate. Thus, removal of monomer might be effective even if only a portion of the total pool is deactivated. Similar arguments have been made for other homo-

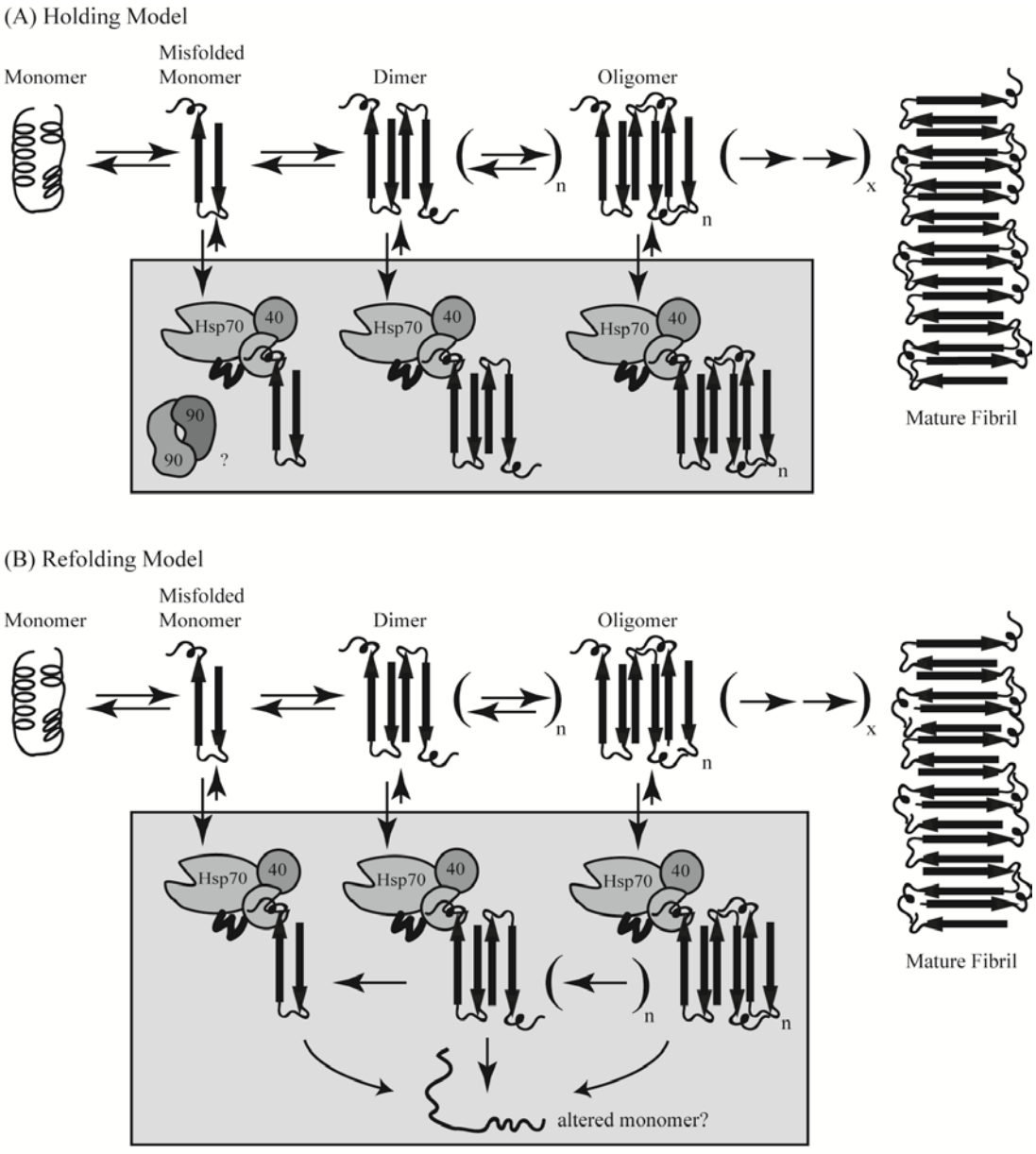

Figure 2-10. Models for chaperone-mediated inhibition of amyloid aggregation. (A) The "holding" mechanism involves removal of aggregation-competent structures by direct binding to chaperone. (B) The "refolding" model invokes an active reorganization of amyloids by the chaperone machine. Note that the number of steps involved in formation of oligomer (n) and the completion of fibril formaton (x) are currently unclear. Additionally, no specific path to fibril formation is implied and a linear path is only used for clarity. Importantly, our results suggest that chaperones (Hsp70/40, Hsp90) do not effectively alter fibril structure, but these proteins might still bind. Finally, our results with Hsp90 seem somewhat consistent with a "holding" model, while the importance of ATPase activity suggest that Hsp70 might operate by a "refolding" mechanism. More experiments will be required to explore these possibilities and it seems likely that, in a cellular environment, both mechanisms would be viable and effective.

polymerization reactions, such as actin filament assembly, that are dependent on the level

of competent monomer.[78] Further analysis of this model awaits, but we cannot dismiss the possibility that Hsp70/40 partly accesses a "holding" mode and we consider it likely that Hsp90's behavior is consistent with this mechanism.

A more active role for chaperones is proposed in the "refolding" model (Figure 2-10B). In this model, chaperones not only bind Aβ but they also change its structure; release from chaperone is coupled to conversion of Aβ to an altered state. The altered structure is defined as being less competent for progression through the aggregation pathway (or, alternatively, better able to travel a non-productive route[51]). How would this structural modification occur? Some clues might be gleaned by studying Hsp70's function during normal *de novo* protein biosynthesis. Current models suggest that Hsp70 acts by "entropic pulling";[79] chaperone binding to extended polypeptides precludes certain entropically accessible conformations. Thus, the presence of Hsp70 forces the peptide to sample other conformations, which likely have fewer exposed hydrophobic regions. Therefore, under this model, chaperone would bind Aβ in an aggregation-prone state (i.e. exposed hydrophobic regions and primed for self-association) and release it in a modified conformation. We propose that this model is consistent with our data on Hsp70. For example, we found that Hsp70's ATPase activity was required to inhibit aggregation (Figure 2-4) and that its potency could be stimulated by co-chaperone (Figure 2-2) or an agonist (Figure 2-5). These results suggest that ATP-driven cycles of substrate binding-and-release are important. Further, the "refolding" model predicts that a low molar ratio of chaperone could be effective if a single enzyme acts on multiple substrates. We found this to be true for both Hsp70/40 and Hsp90 (Figures 2-1 and -3). Thus, although more data is certainly required, we speculate that Hsp70/40 might actively

process Aβ in a "refolding" model. Whether this conclusion describes the behavior of other combinations of chaperones and misfolded peptides is unclear.

An important aspect of both models (Figure 2-10) is that neither Hsp70/40 nor Hsp90 are effective at dealing with fibrils. Based on our results (Figure 2-7) and observations from other systems,[50, 51] we suggest that chaperones may have difficulty recognizing hydrophobic regions embedded in fibrils. Alternatively, the interaction energy supplied by extensive monomer-monomer contacts may be an insurmountable barrier to chaperone-mediated reorganization (at least by the chaperones tested). Regardless, our results suggest that fibrils are not readily reversible by the action of Hsp70/40 or Hsp90. Oligomers, on the other hand, seem susceptible to manipulation by the tri-chaperone system (Figures 2-7 and 2-9). This suggests that these structures contain sufficiently exposed hydrophobic "flags" to trigger chaperone recognition and subsequent reorganization.

Recently, an interesting hypothesis was developed by Morimoto and colleagues to explain the favorable effects of chaperone overexpression.[80, 81] This "sink hypothesis" states that cellular toxicity might develop because chaperones and other proteins are being sequestered onto amyloid fibrils and re-directed from their normal tasks. Under this model, depleted cellular levels of these factors may trigger apoptosis by decreasing the levels below a threshold needed to maintain necessary processes.[82] Thus, chaperone over-expression might circumvent the problem by supplying a less exhaustible supply. Moreover, higher chaperone levels might block other proteins from becoming trapped by the "sink". This intriguing hypothesis has been developed around work with Huntington's disease, but it might be more generally applicable to other amyloid disorders. For

example, we have shown that Hsp70/40 and Hsp90 can influence early stages of Aβ aggregation but that fibrils are not significantly changed. Although direct evidence is still needed, these results suggest that chaperones might accumulate on fibrils because they are unable to process these structures.

An interesting component of these discussions is whether oligomers and pre-oligomeric Aβ are normally present in the same subcellular space as chaperones. Chaperones are expressed in all intracellular regions, including the nucleus, secretory pathway, and cytoplasm. Aβ fibrils are found in extracellular regions, but the exact location of oligomer production is unclear. Recent reports have examined extracellular[83-86] and intracellular[18, 49, 54, 87-92] models. Thus, the exact mechanism by which the protective effect of chaperones is manifested awaits definition. For example, it isn't clear if chaperones simply provide a general cytoprotection or if direct physical interaction is required. Regardless, our results strongly suggest that, if early Aβ structures are formed in the presence of Hsp70/40 or Hsp90, these proteins prevent further self-assembly.

Our results support a hypothesis in which stimulation of chaperone activity may be a viable means of therapy for neurodegenerative diseases. Previous studies to test this idea were conducted in mouse[93, 94] and tissue culture[95, 96] models of neurodegenerative disease. For example, an analog of the natural product, geldanamycin, was shown to promote the clearance of huntingtin in a mouse model of Huntington's disease. This drug is proposed to be anti-neurodegenerative by virtue of its ability to activate the transcription factor, heat shock factor-1 (HSF-1).[93, 94] HSF-1 controls transcription of proteins involved in the stress response, including Hsp70. Thus, geldanamycin may alleviate amyloid-related phenotypes via mimicking the effects of Hsp70 overexpression.

In another approach, Morimoto and colleagues screened a chemical library for compounds that could modify amyloid formation in a yeast model of Huntington's disease.[97] They reported the discovery of celastrols that, like geldanamycin, stimulate HSF-1 and inhibit amyloid formation. Both these strategies take advantage of cellular mechanisms for coping with stress. Here, we suggest a complementary approach that involves direct stimulation of Hsp70. Based on pioneering work,[55, 70] we have synthesized an agonist of Hsp70 and tested its activity *in vitro*. This molecule, SW02, was able to compensate for insufficient chaperone levels and promote anti-aggregation activity. Compounds that have this effect *in vivo* might activate endogenous Hsp70 and combat neurodegenerative diseases without concomitant involvement of a stress response, a result that is supported by more recent studies of SW02 and related dihydropyrimidines in mammalian models of tau deposition.[97] One compelling aspect of this approach is that it relies on boosting a physiological mechanism that normally protects asymptomatic individuals.

2.4 Experimental Procedures

2.4.1 Preparation of Amyloid Beta

Synthetic amyloid beta 1-42 (AnaSpec, San Jose, CA) was prepared for aggregation according to previously developed methods.[73, 74] Briefly, lyophilized Aβ was resuspended in hexafluoroisopropanol (HFIP), dried under a nitrogen stream, and stored as a film at -20 °C. Immediately prior to use, Aβ was resuspended in DMSO to 10 mM and sonicated for 10 minutes. For experiments in which early stages of aggregation were studied, these aliquots were rapidly brought to 25 μM in phosphate buffered saline (PBS) pH 7.2 and used immediately. Oligomers were prepared by diluting the Aβ to 25 μM with phenol red-free DMEM-F12 and incubating for 24 hours at 4 °C without shaking. Fibrils were similarly prepared by incubating 25 μM Aβ in PBS at 37 °C for 24 hours with vigorous shaking.

2.4.2 Turbidity Measurements

Human Hsp70, Hsp40, and Hsp90 were provided by Assay Designs (Ann Arbor, MI). Hsp70 (catalog number ESP-555) is endotoxin-free, recombinant, human protein expressed and purified from bacteria; Hsp40 (SPP-400) is also recombinant, human protein and from bacteria; Hsp90 (SPP-770) is human and purified from HeLa cells. Concentrated stocks (100x) of these proteins or buffer control were dispensed into the wells of 96-well, half-volume, clear bottom plates (Corning, NY). To these solutions, Aβ in either PBS or DMEM-F12 was added. In the final volume (75 μL), Aβ was present at approximately 25 μM, ATP or ATPγS at 9 mM, and the heat shock proteins at the indicated concentrations. Plates were immediately placed in a pre-warmed SpectraMax M5 multimode plate reader and the turbidity measurements initiated. The turbidity

program began with a 20 sec mixing shake and was followed by absorbance readings at 330 or 350 nm every 60 sec. A 20 sec shaking step immediately followed each reading, followed by 40 seconds of settling time. The temperature was set at 30 or 37 °C (see Figure legends). For Hsp70/40 treated samples, the listed concentration is the concentration of Hsp70 and the Hsp40 was held at 100-fold lower value. For example, treatment with 474 nM Hsp70/40 involved final concentrations of 474 nM Hsp70 and 4.7 nM Hsp40.

2.4.3 Electron Microscopy

At the conclusion of the turbidity measurements, 25 µL aliquots were removed from each well and immediately frozen at -80 °C. Thawed samples were placed on glow-discharged Formvar-coated 300-mesh copper grids (Electron Microscopy Sciences) for 1 minute, washed twice with distilled water, and treated with 3% uranyl acetate for 1 minute. Images were taken at 80 kV at magnifications between 46,000x and 130,000x. Image quantitation was performed with NIH Image using at least 10 random fields.

2.4.4 Thioflavin T Experiments

Immediately following removal of samples for electron microscopy, the remaining volume from the turbidity experiments (50 µL) was treated with 75 µL of freshly prepared 50 mM glycine pH 8.0 containing 25 µM thioflavin T. After 10 min at room temperature, the fluorescence was measured on a SpectraMax M5 multimode plate reader using an excitation of 440 nm and emission of 490 nm (475 nm cut-off). The reported values have been corrected by subtracting the background fluorescence of thioflavin T in the absence of amyloid.

2.4.5 Synthesis

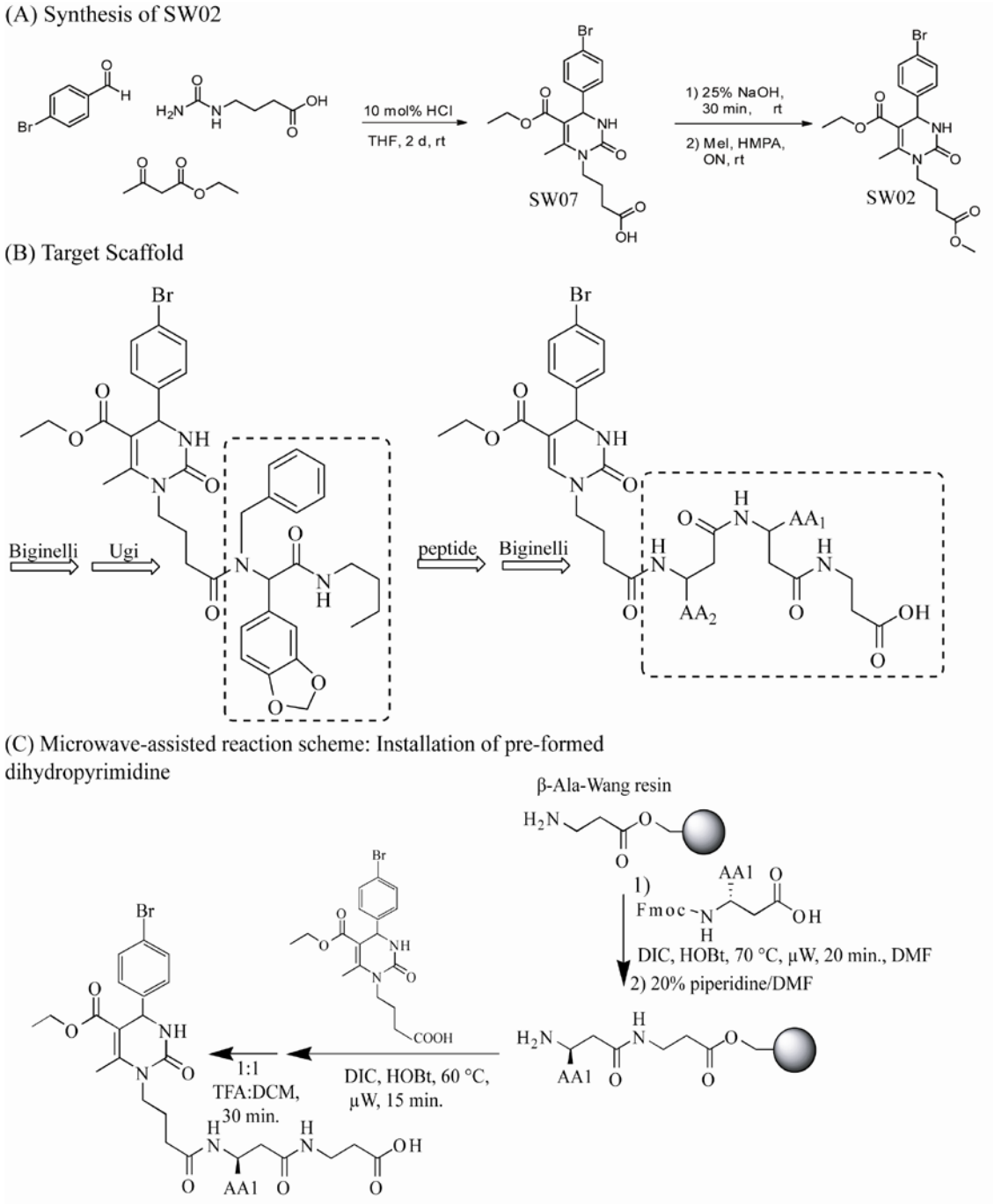

Scheme 2-2. Dihydropyrimidine Synthesis. (A) Synthesis of SW02. (B) Target structure identified by the Brodsky group and the target structure identified by the Gestwicki group. (C) Microwave assisted synthesis of peptide-dihydropyrimidine structures.

The synthesis route selected for the production of the dihydropyrimidine core was based upon that identified by the Brodsky group.[55] Two classes of ligands were synthesized.

First compounds such as SW02 were synthesized using the Biginelli reaction to yield the dihydropyrimidine THF. Two equivalents of the β-keto ester ethylacetoacetate (4mmol) were added to one equivalent (2 mmol) each of 4-bromobenzaldehyde and the urea of γ-aminobutryric acid. Following five minutes of stirring, HCl (10 mol%) was added. The reaction is allowed to stir for 48 hours and is then poured into ice water. After stirring in water for 1 hour, the precipitate is filtered and the solid is re-crystallized from ethanol to afford pure product in 85-92% yield. This intermediate (1 mmol) was then diluted into HMPA and an equal amount of 25% NaOH was added and it was allowed to stir at room temperature for 30 minutes. Methyliodide (1.5 equiv, 1.5 mmol) was added and allowed to stir overnight (Scheme 2-2A).[61] It gives about a 90% yield. The other class of dihydropyrimidines was directly inspired from previously reported examples of Hsp70 ligands. Rather than utilizing the Ugi reaction to produce a peptoid, the dihydropyrmidine was attached to small peptides (Scheme 2-2B). In this case β-amino acids (3eq, 0.75 mmol), which are resistant to hydrolysis, were coupled to Wang resin (0.25 g, 0.25 mmol) under microwave conditions. Through iterative couplings with HOBt/DIC (5 eq, 1.25 mmol) in DMF at 60 °C with microwave irradiation, di- and tripeptides were synthesized. Following deprotection of the last Fmoc protected amino acid with 20% piperidine, the dihydropyrmidine (3 eq, 0.75 mmol) was coupled using HOBt/DIC (5 eq, 1.25 mmol) in DMF at 80 °C in the microwave.[61] The product was then cleaved off Wang resin using 50% TFA and purified on reverse phase HPLC to afford compounds such as SW08 (Scheme 2-2C). The overall yield ranged from 1%-30%.

2.4.6 Characterization of Dihydropyrimidines

Ethyl 4-(4-bromophenyl)-1-(4-methoxy-4-oxobutyl)-6-methyl-2-oxo-1,2,3,4-tetrahydropyrimidine-5-carboxylate (**SW02**) : ^{1}H δ ($CDCl_3$) 7.43-7.41 (2H, d), 7.13-7.11 (2H, d), 5.73 (1H, s), 5.33 (1H, s), 4.09 (2H, m), 3.89-3.63 (2H, d), 3.69 (3H, s), 2.55 (3H, s), 2.27 (2H, m), 1.90-1.80 (2H, d), 1.20-1.16 (3H, t). ^{13}C δ ($CDCl_3$) 173.24, 165.82, 153.29, 148.29, 142.28, 121.73, 104.32, 60.35, 53.44, 51.72, 41.89, 30.77, 24.71, 16.03, 14.14. [M+H] e: 439.08, o: 439.1. Yield 82% overall.

4-(5-((benzyloxy)carbonyl)-4-(2,4-dichlorophenyl)-6-methyl-2-oxo-3,4-dihydropyrimidin-1(2H)-yl)butanoic acid (**115-7c**): ^{1}H δ (d-DMSO) 12.16 (1H, bs), 8.02 (1H, s), 7.57 (1H, s), 7.29 (1H, d), 7.27 (4H, m), 7.06 (2H, d), 5.64 (1H, s), 5.09-4.96 (2H, dd), 3.85-3.60 (2H, d), 2.68 (3H, s), 2.21 (2H, m), 1.85-1.66 (2H, m). ^{13}C δ (d-DMSO) 174.36, 165.22, 152.16, 151.97, 140.15, 136.63, 133.40, 129.43, 128.55, 128.23, 128.11, 127.81, 100.76, 65.41, 50.35, 31.17, 25.00, 16.03. [M+H] e: 477.09, o: 477.1. Yield 94% overall.

Notes

This work has been published as “Heat shock protein 70 and 90 inhibit early stages of amyloid beta-(1-42) aggregation in vitro,” Evans, C.E., Wisén, S., and Gestwicki, J.E., 2006, 281(44), 33182-91.

Author contributions

Christopher G. Evans, Dr. Susanne Wisén, and Dr. Jason E. Gestwicki designed the experiments;
Christopher G. Evans conducted tubidity and thioflavin T assays as well as synthesis of dihydropyrimidines;
Dr. Susanne Wisén conducted synthesis of dihydropyrimidines;
Dr. Jason E. Gestwicki conducted turbidity and thioflavin T assays as well as doing the TEM.

2.5 Appendix of Selected ^{1}H NMR and ^{13}C Spectra

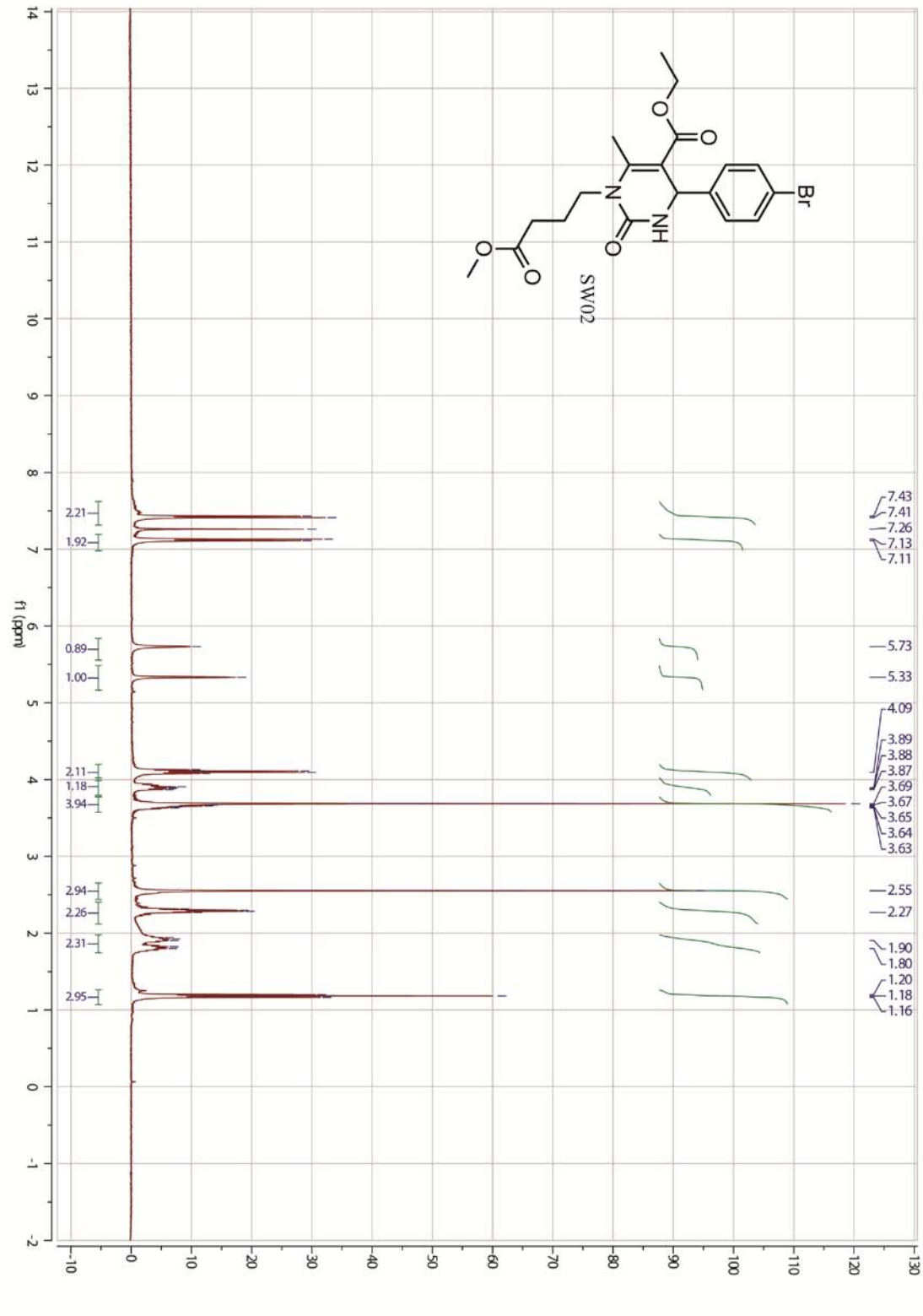

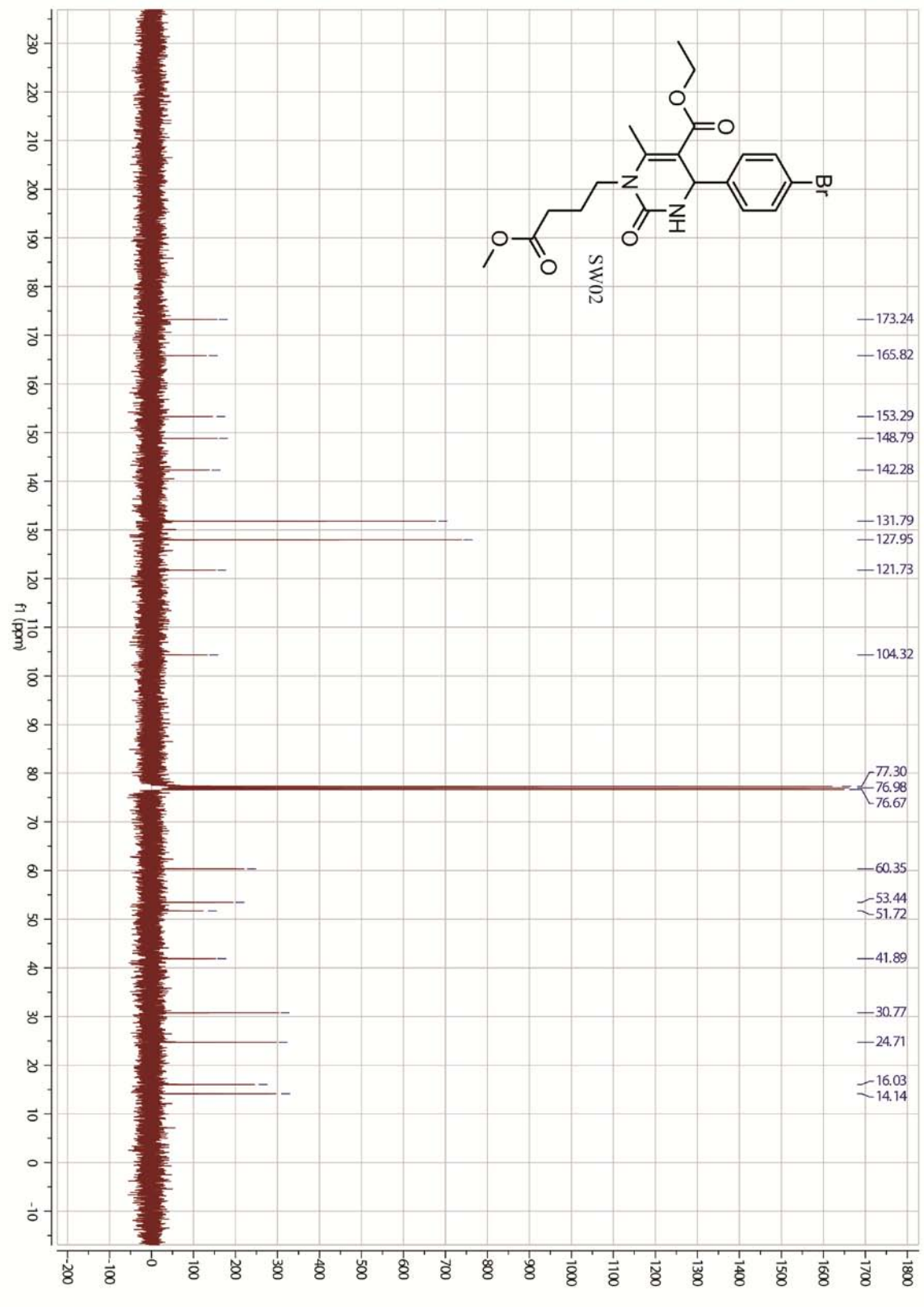
SW02
Br
NH
173.24
165.82
153.29
148.79
142.28
131.79
127.95
121.73
104.32
77.30
76.98
76.67
60.35
53.44
51.72
41.89
30.77
24.71
16.03
14.14
f1 (ppm)

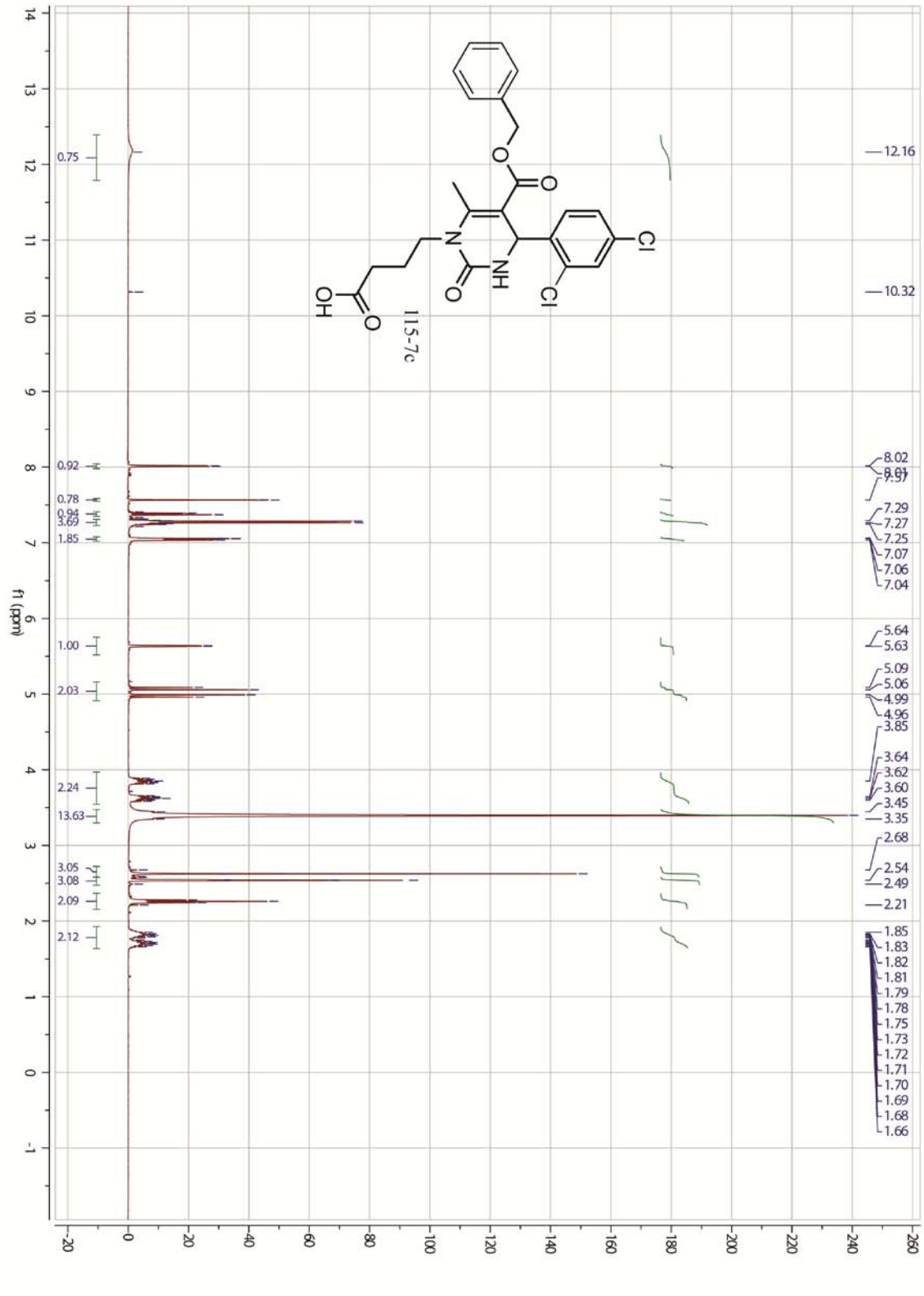
115-7c
f1 (ppm)

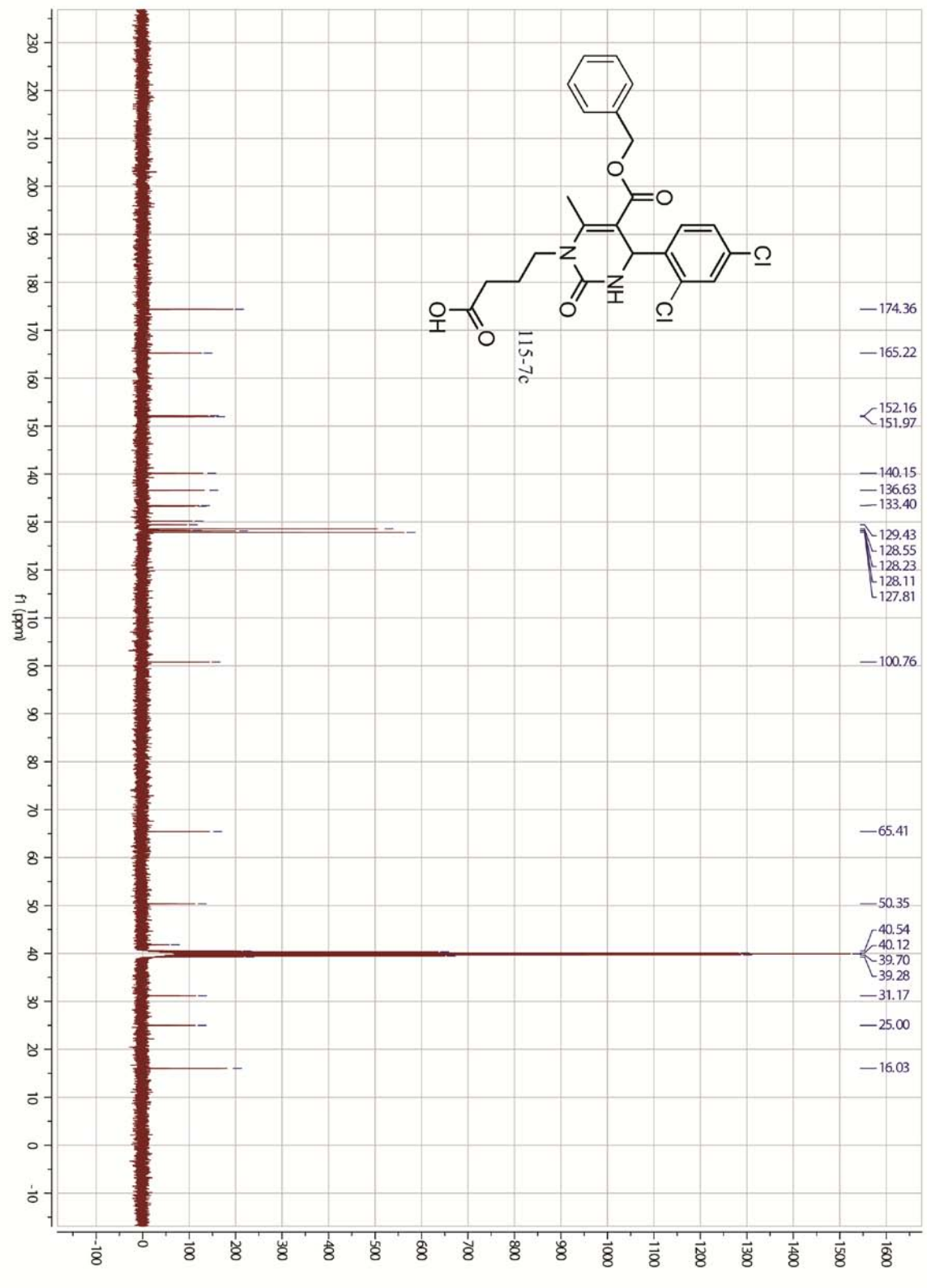
115-7c
174.36
165.22
152.16
151.97
140.15
136.63
133.40
129.43
128.55
128.23
128.11
127.81
100.76
65.41
50.35
40.54
40.12
39.70
39.28
31.17
25.00
16.03
f1 (ppm)

2.6 References

1. Selkoe, D. J., Folding proteins in fatal ways. *Nature* **2003,** *426* (6968), 900-4.

2. Koo, E. H.; Lansbury, P. T., Jr.; Kelly, J. W., Amyloid diseases: abnormal protein aggregation in neurodegeneration. *Proceedings of the National Academy of Sciences of the United States of America* **1999,** *96* (18), 9989-90.

3. Caughey, B.; Lansbury, P. T., Protofibrils, pores, fibrils, and neurodegeneration: separating the responsible protein aggregates from the innocent bystanders. *Annual review of neuroscience* **2003,** *26*, 267-98.

4. Tanzi, R. E.; Bertram, L., Twenty years of the Alzheimer's disease amyloid hypothesis: a genetic perspective. *Cell* **2005,** *120* (4), 545-55.

5. Aguzzi, A.; Heikenwalder, M.; Miele, G., Progress and problems in the biology, diagnostics, and therapeutics of prion diseases. *The Journal of clinical investigation* **2004,** *114* (2), 153-60.

6. Mattson, M. P., Pathways towards and away from Alzheimer's disease. *Nature* **2004,** *430* (7000), 631-9.

7. Soto, C.; Castano, E. M.; Frangione, B.; Inestrosa, N. C., The alpha-helical to beta-strand transition in the amino-terminal fragment of the amyloid beta-peptide modulates amyloid formation. *J Biol Chem* **1995,** *270* (7), 3063-7.

8. Walsh, D. M.; Selkoe, D. J., Oligomers on the brain: the emerging role of soluble protein aggregates in neurodegeneration. *Protein Pept Lett* **2004,** *11* (3), 213-28.

9. Catalano, S. M.; Dodson, E. C.; Henze, D. A.; Joyce, J. G.; Krafft, G. A.; Kinney, G. G., The role of amyloid-beta derived diffusible ligands (ADDLs) in Alzheimer's disease. *Curr Top Med Chem* **2006,** *6* (6), 597-608.

10. Glabe, C. G., Common mechanisms of amyloid oligomer pathogenesis in degenerative disease. *Neurobiol Aging* **2006,** *27* (4), 570-5.

11. Chromy, B. A.; Nowak, R. J.; Lambert, M. P.; Viola, K. L.; Chang, L.; Velasco, P. T.; Jones, B. W.; Fernandez, S. J.; Lacor, P. N.; Horowitz, P.; Finch, C. E.; Krafft, G. A.; Klein, W. L., Self-assembly of Abeta(1-42) into globular neurotoxins. *Biochemistry* **2003,** *42* (44), 12749-60.

12. Dahlgren, K. N.; Manelli, A. M.; Stine, W. B., Jr.; Baker, L. K.; Krafft, G. A.; LaDu, M. J., Oligomeric and fibrillar species of amyloid-beta peptides differentially affect neuronal viability. *J Biol Chem* **2002,** *277* (35), 32046-53.

13. Walsh, D. M.; Klyubin, I.; Fadeeva, J. V.; Cullen, W. K.; Anwyl, R.; Wolfe, M. S.; Rowan, M. J.; Selkoe, D. J., Naturally secreted oligomers of amyloid beta protein potently inhibit hippocampal long-term potentiation in vivo. *Nature* **2002,** *416* (6880), 535-9.

14. Townsend, M.; Shankar, G. M.; Mehta, T.; Walsh, D. M.; Selkoe, D. J., Effects of secreted oligomers of amyloid beta-protein on hippocampal synaptic plasticity: a potent role for trimers. *J Physiol* **2006,** *572* (Pt 2), 477-92.

15. Gong, Y.; Chang, L.; Viola, K. L.; Lacor, P. N.; Lambert, M. P.; Finch, C. E.; Krafft, G. A.; Klein, W. L., Alzheimer's disease-affected brain: presence of oligomeric A beta ligands (ADDLs) suggests a molecular basis for reversible memory loss. *Proc Natl Acad Sci U S A* **2003,** *100* (18), 10417-22.

16. Lesne, S.; Koh, M. T.; Kotilinek, L.; Kayed, R.; Glabe, C. G.; Yang, A.; Gallagher, M.; Ashe, K. H., A specific amyloid-beta protein assembly in the brain impairs memory. *Nature* **2006,** *440* (7082), 352-7.

17. Takahashi, R. H.; Almeida, C. G.; Kearney, P. F.; Yu, F.; Lin, M. T.; Milner, T. A.; Gouras, G. K., Oligomerization of Alzheimer's beta-amyloid within processes and synapses of cultured neurons and brain. *J Neurosci* **2004,** *24* (14), 3592-9.

18. Kienlen-Campard, P.; Miolet, S.; Tasiaux, B.; Octave, J. N., Intracellular amyloid-beta 1-42, but not extracellular soluble amyloid-beta peptides, induces neuronal apoptosis. *J Biol Chem* **2002,** *277* (18), 15666-70.

19. Magrane, J.; Rosen, K. M.; Smith, R. C.; Walsh, K.; Gouras, G. K.; Querfurth, H. W., Intraneuronal beta-amyloid expression downregulates the Akt survival pathway and blunts the stress response. *J Neurosci* **2005,** *25* (47), 10960-9.

20. Findeis, M. A., Peptide inhibitors of beta amyloid aggregation. *Curr Top Med Chem* **2002,** *2* (4), 417-23.

21. Gestwicki, J. E.; Crabtree, G. R.; Graef, I. A., Harnessing chaperones to generate small-molecule inhibitors of amyloid beta aggregation. *Science* **2004,** *306* (5697), 865-9.

22. Lowe, T. L.; Strzelec, A.; Kiessling, L. L.; Murphy, R. M., Structure-function relationships for inhibitors of beta-amyloid toxicity containing the recognition sequence KLVFF. *Biochemistry* **2001,** *40* (26), 7882-9.

23. John, V., Human beta-secretase (BACE) and BACE inhibitors: progress report. *Curr Top Med Chem* **2006,** *6* (6), 569-78.

24. Schmidt, B.; Baumann, S.; Braun, H. A.; Larbig, G., Inhibitors and Modulators of beta- and gamma-Secretase. *Curr Top Med Chem* **2006,** *6* (4), 377-92.

25. Aisen, P. S., The development of anti-amyloid therapy for Alzheimer's disease : from secretase modulators to polymerisation inhibitors. *CNS Drugs* **2005,** *19* (12), 989-96.

26. Pangalos, M. N.; Jacobsen, S. J.; Reinhart, P. H., Disease modifying strategies for the treatment of Alzheimer's disease targeted at modulating levels of the beta-amyloid peptide. *Biochem Soc Trans* **2005,** *33* (Pt 4), 553-8.

27. Brendza, R. P.; Bacskai, B. J.; Cirrito, J. R.; Simmons, K. A.; Skoch, J. M.; Klunk, W. E.; Mathis, C. A.; Bales, K. R.; Paul, S. M.; Hyman, B. T.; Holtzman, D. M., Anti-Abeta antibody treatment promotes the rapid recovery of amyloid-associated neuritic dystrophy in PDAPP transgenic mice. *J Clin Invest* **2005,** *115* (2), 428-33.

28. Ghanta, J.; Shen, C. L.; Kiessling, L. L.; Murphy, R. M., A strategy for designing inhibitors of beta-amyloid toxicity. *J Biol Chem* **1996,** *271* (47), 29525-8.

29. Bohrmann, B.; Adrian, M.; Dubochet, J.; Kuner, P.; Muller, F.; Huber, W.; Nordstedt, C.; Dobeli, H., Self-assembly of beta-amyloid 42 is retarded by small molecular ligands at the stage of structural intermediates. *J Struct Biol* **2000,** *130* (2-3), 232-46.

30. Selkoe, D. J., Alzheimer disease: mechanistic understanding predicts novel therapies. *Ann Intern Med* **2004,** *140* (8), 627-38.

31. Westerheide, S. D.; Morimoto, R. I., Heat shock response modulators as therapeutic tools for diseases of protein conformation. *J Biol Chem* **2005,** *280* (39), 33097-100.

32. Morelli, L.; Llovera, R.; Ibendahl, S.; Castano, E. M., The degradation of amyloid beta as a therapeutic strategy in Alzheimer's disease and cerebrovascular amyloidoses. *Neurochem Res* **2002,** *27* (11), 1387-99.

33. Leissring, M. A.; Farris, W.; Chang, A. Y.; Walsh, D. M.; Wu, X.; Sun, X.; Frosch, M. P.; Selkoe, D. J., Enhanced proteolysis of beta-amyloid in APP transgenic mice prevents plaque formation, secondary pathology, and premature death. *Neuron* **2003,** *40* (6), 1087-93.

34. Wegele, H.; Wandinger, S. K.; Schmid, A. B.; Reinstein, J.; Buchner, J., Substrate transfer from the chaperone Hsp70 to Hsp90. *J Mol Biol* **2006,** *356* (3), 802-11.

35. Pratt, W. B.; Toft, D. O., Regulation of signaling protein function and trafficking by the hsp90/hsp70-based chaperone machinery. *Exp Biol Med (Maywood)* **2003,** *228* (2), 111-33.

36. Bukau, B.; Weissman, J.; Horwich, A., Molecular chaperones and protein quality control. *Cell* **2006,** *125* (3), 443-51.

37. Pearl, L. H.; Prodromou, C., Structure and in vivo function of Hsp90. *Curr Opin Struct Biol* **2000,** *10* (1), 46-51.

38. Pellecchia, M.; Montgomery, D. L.; Stevens, S. Y.; Vander Kooi, C. W.; Feng, H. P.; Gierasch, L. M.; Zuiderweg, E. R., Structural insights into substrate binding by the molecular chaperone DnaK. *Nat Struct Biol* **2000,** *7* (4), 298-303.

39. Dul, J. L.; Davis, D. P.; Williamson, E. K.; Stevens, F. J.; Argon, Y., Hsp70 and antifibrillogenic peptides promote degradation and inhibit intracellular aggregation of amyloidogenic light chains. *J Cell Biol* **2001,** *152* (4), 705-16.

40. Diamant, S.; Ben-Zvi, A. P.; Bukau, B.; Goloubinoff, P., Size-dependent disaggregation of stable protein aggregates by the DnaK chaperone machinery. *J Biol Chem* **2000,** *275* (28), 21107-13.

41. Bakthisaran, R.; Ban, T.; Sakai, M.; Pasta, S. Y.; Tangirala, R.; Naiki, H.; Goto, Y.; Rao, M. C., alphaB-crystallin, a small heat shock protein, prevents the amyloid fibril growth of an amyloid beta-peptide and beta 2-microglobulin. *Biochem J* **2005**.

42. Barral, J. M.; Broadley, S. A.; Schaffar, G.; Hartl, F. U., Roles of molecular chaperones in protein misfolding diseases. *Semin Cell Dev Biol* **2004,** *15* (1), 17-29.

43. Muchowski, P. J.; Schaffar, G.; Sittler, A.; Wanker, E. E.; Hayer-Hartl, M. K.; Hartl, F. U., Hsp70 and hsp40 chaperones can inhibit self-assembly of polyglutamine proteins into amyloid-like fibrils. *Proc Natl Acad Sci U S A* **2000,** *97* (14), 7841-6.

44. Cummings, C. J.; Sun, Y.; Opal, P.; Antalffy, B.; Mestril, R.; Orr, H. T.; Dillmann, W. H.; Zoghbi, H. Y., Over-expression of inducible HSP70 chaperone suppresses neuropathology and improves motor function in SCA1 mice. *Hum Mol Genet* **2001,** *10* (14), 1511-8.

45. Klucken, J.; Shin, Y.; Masliah, E.; Hyman, B. T.; McLean, P. J., Hsp70 Reduces alpha-Synuclein Aggregation and Toxicity. *J Biol Chem* **2004,** *279* (24), 25497-502.

46. Warrick, J. M.; Chan, H. Y.; Gray-Board, G. L.; Chai, Y.; Paulson, H. L.; Bonini, N. M., Suppression of polyglutamine-mediated neurodegeneration in Drosophila by the molecular chaperone HSP70. *Nat Genet* **1999,** *23* (4), 425-8.

47. Willingham, S.; Outeiro, T. F.; DeVit, M. J.; Lindquist, S. L.; Muchowski, P. J., Yeast genes that enhance the toxicity of a mutant huntingtin fragment or alpha-synuclein. *Science* **2003,** *302* (5651), 1769-72.

48. Glover, J. R.; Lindquist, S., Hsp104, Hsp70, and Hsp40: a novel chaperone system that rescues previously aggregated proteins. *Cell* **1998,** *94* (1), 73-82.

49. Fonte, V.; Kapulkin, V.; Taft, A.; Fluet, A.; Friedman, D.; Link, C. D., Interaction of intracellular beta amyloid peptide with chaperone proteins. *Proc Natl Acad Sci U S A* **2002,** *99* (14), 9439-44.

50. Dedmon, M. M.; Christodoulou, J.; Wilson, M. R.; Dobson, C. M., Heat shock protein 70 inhibits alpha-synuclein fibril formation via preferential binding to prefibrillar species. *J Biol Chem* **2005,** *280* (15), 14733-40.

51. Wacker, J. L.; Zareie, M. H.; Fong, H.; Sarikaya, M.; Muchowski, P. J., Hsp70 and Hsp40 attenuate formation of spherical and annular polyglutamine oligomers by partitioning monomer. *Nat Struct Mol Biol* **2004,** *11* (12), 1215-22.

52. Lee, S.; Carson, K.; Rice-Ficht, A.; Good, T., Hsp20, a novel alpha-crystallin, prevents Abeta fibril formation and toxicity. *Protein Sci* **2005,** *14* (3), 593-601.

53. Shorter, J.; Lindquist, S., Hsp104 catalyzes formation and elimination of self-replicating Sup35 prion conformers. *Science* **2004,** *304* (5678), 1793-7.

54. Magrane, J.; Smith, R. C.; Walsh, K.; Querfurth, H. W., Heat shock protein 70 participates in the neuroprotective response to intracellularly expressed beta-amyloid in neurons. *J Neurosci* **2004,** *24* (7), 1700-6.

55. Fewell, S. W.; Smith, C. M.; Lyon, M. A.; Dumitrescu, T. P.; Wipf, P.; Day, B. W.; Brodsky, J. L., Small molecule modulators of endogenous and co-chaperone-stimulated Hsp70 ATPase activity. *J Biol Chem* **2004,** *279* (49), 51131-40.

56. Kappe, C. O., A Reexamination of the Mechanism of the Biginelli Dihydropyrimidine Synthesis. Support for an N-Acyliminium Ion Intermediate(1). *The Journal of organic chemistry* **1997,** *62* (21), 7201-7204.

57. Dondoni, A.; Massi, A., Decoration of dihydropyrimidine and dihydropyridine scaffolds with sugars via Biginelli and Hantzsch multicomponent reactions: an efficient entry to a collection of artificial nucleosides. *Molecular diversity* **2003,** *6* (3-4), 261-70.

58. Kappe, C. O., Biologically active dihydropyrimidones of the Biginelli-type--a literature survey. *European journal of medicinal chemistry* **2000,** *35* (12), 1043-52.

59. Kappe, C. O., Recent advances in the Biginelli dihydropyrimidine synthesis. New tricks from an old dog. *Accounts of chemical research* **2000,** *33* (12), 879-88.

60. Kappe, C. O.; Stadler, A., Building dihydropyrimidine libraries via microwave-assisted Biginelli multicomponent reactions. *Methods in enzymology* **2003,** *369*, 197-223.

61. Wisen, S.; Androsavich, J.; Evans, C. G.; Chang, L.; Gestwicki, J. E., Chemical modulators of heat shock protein 70 (Hsp70) by sequential, microwave-accelerated reactions on solid phase. *Bioorganic & medicinal chemistry letters* **2008,** *18* (1), 60-5.

62. Wisen, S.; Bertelsen, E. B.; Thompson, A. D.; Patury, S.; Ung, P.; Chang, L.; Evans, C. G.; Walter, G. M.; Wipf, P.; Carlson, H. A.; Brodsky, J. L.; Zuiderweg, E. R.; Gestwicki, J. E., Binding of a small molecule at a protein-protein interface regulates the chaperone activity of hsp70-hsp40. *ACS chemical biology 5* (6), 611-22.

63. Bukau, B.; Horwich, A. L., The Hsp70 and Hsp60 chaperone machines. *Cell* **1998,** *92* (3), 351-66.

64. Minami, Y.; Hohfeld, J.; Ohtsuka, K.; Hartl, F. U., Regulation of the heat-shock protein 70 reaction cycle by the mammalian DnaJ homolog, Hsp40. *J Biol Chem* **1996,** *271* (32), 19617-24.

65. LeVine, H., 3rd; Scholten, J. D., Screening for pharmacologic inhibitors of amyloid fibril formation. *Methods Enzymol* **1999,** *309*, 467-76.

66. Hartl, F. U., Molecular chaperones in cellular protein folding. *Nature* **1996,** *381* (6583), 571-9.

67. Umezawa, H.; Kondo, S.; Iinuma, H.; Kunimoto, S.; Ikeda, Y.; Iwasawa, H.; Ikeda, D.; Takeuchi, T., Structure of an antitumor antibiotic, spergualin. *J Antibiot (Tokyo)* **1981,** *34* (12), 1622-4.

68. Nadler, S. G.; Dischino, D. D.; Malacko, A. R.; Cleaveland, J. S.; Fujihara, S. M.; Marquardt, H., Identification of a binding site on Hsc70 for the immunosuppressant 15-deoxyspergualin. *Biochem Biophys Res Commun* **1998,** *253* (1), 176-80.

69. Brodsky, J. L., Selectivity of the molecular chaperone-specific immunosuppressive agent 15-deoxyspergualin: modulation of Hsc70 ATPase activity without compromising DnaJ chaperone interactions. *Biochem Pharmacol* **1999,** *57* (8), 877-80.

70. Fewell, S. W.; Day, B. W.; Brodsky, J. L., Identification of an inhibitor of hsc70-mediated protein translocation and ATP hydrolysis. *J Biol Chem* **2001,** *276* (2), 910-4.

71. Wisen, S.; Gestwicki, J. E., Identification of small molecules that modify the protein folding activity of heat shock protein 70. *Analytical biochemistry* **2008,** *374* (2), 371-7.

72. Chang, L.; Bertelsen, E.B.; Wisén, S.; Larsen, E.M.; Zuiderweg, E.R.; Gestwicki, J. E., High-throughput screen for small molecules that modulate the ATPase activity of the molecular chaperone DnaK. *Anal Biochem* **2008**, 372 (2), 167-76.

73. Fezoui, Y.; Hartley, D. M.; Harper, J. D.; Khurana, R.; Walsh, D. M.; Condron, M. M.; Selkoe, D. J.; Lansbury, P. T., Jr.; Fink, A. L.; Teplow, D. B., An improved method of preparing the amyloid beta-protein for fibrillogenesis and neurotoxicity experiments. *Amyloid* **2000,** *7* (3), 166-78.

74. Stine, W. B., Jr.; Dahlgren, K. N.; Krafft, G. A.; LaDu, M. J., In vitro characterization of conditions for amyloid-beta peptide oligomerization and fibrillogenesis. *J Biol Chem* **2003,** *278* (13), 11612-22.

75. Burdick, D.; Soreghan, B.; Kwon, M.; Kosmoski, J.; Knauer, M.; Henschen, A.; Yates, J.; Cotman, C.; Glabe, C., Assembly and aggregation properties of synthetic Alzheimer's A4/beta amyloid peptide analogs. *J Biol Chem* **1992,** *267* (1), 546-54.

76. Sengupta, P.; Garai, K.; Sahoo, B.; Shi, Y.; Callaway, D. J.; Maiti, S., The amyloid beta peptide (Abeta(1-40)) is thermodynamically soluble at physiological concentrations. *Biochemistry* **2003,** *42* (35), 10506-13.

77. Esler, W. P.; Stimson, E. R.; Ghilardi, J. R.; Vinters, H. V.; Lee, J. P.; Mantyh, P. W.; Maggio, J. E., In vitro growth of Alzheimer's disease beta-amyloid plaques displays first-order kinetics. *Biochemistry* **1996,** *35* (3), 749-57.

78. Pollard, T. D.; Mooseker, M. S., Direct measurement of actin polymerization rate constants by electron microscopy of actin filaments nucleated by isolated microvillus cores. *J Cell Biol* **1981,** *88* (3), 654-9.

79. De Los Rios, P.; Ben-Zvi, A.; Slutsky, O.; Azem, A.; Goloubinoff, P., Hsp70 chaperones accelerate protein translocation and the unfolding of stable protein aggregates by entropic pulling. *Proc Natl Acad Sci U S A* **2006,** *103* (16), 6166-71.

80. Gidalevitz, T.; Ben-Zvi, A.; Ho, K. H.; Brignull, H. R.; Morimoto, R. I., Progressive disruption of cellular protein folding in models of polyglutamine diseases. *Science* **2006,** *311* (5766), 1471-4.

81. Rieger, T. R.; Morimoto, R. I.; Hatzimanikatis, V., Bistability explains threshold phenomena in protein aggregation both in vitro and in vivo. *Biophys J* **2006,** *90* (3), 886-95.

82. Satyal, S. H.; Schmidt, E.; Kitagawa, K.; Sondheimer, N.; Lindquist, S.; Kramer, J. M.; Morimoto, R. I., Polyglutamine aggregates alter protein folding homeostasis in Caenorhabditis elegans. *Proc Natl Acad Sci U S A* **2000,** *97* (11), 5750-5.

83. Tienari, P. J.; Ida, N.; Ikonen, E.; Simons, M.; Weidemann, A.; Multhaup, G.; Masters, C. L.; Dotti, C. G.; Beyreuther, K., Intracellular and secreted Alzheimer beta-amyloid species are generated by distinct mechanisms in cultured hippocampal neurons. *Proc Natl Acad Sci U S A* **1997,** *94* (8), 4125-30.

84. Hama, E.; Shirotani, K.; Masumoto, H.; Sekine-Aizawa, Y.; Aizawa, H.; Saido, T. C., Clearance of extracellular and cell-associated amyloid beta peptide through viral expression of neprilysin in primary neurons. *J Biochem (Tokyo)* **2001,** *130* (6), 721-6.

85. Vekrellis, K.; Ye, Z.; Qiu, W. Q.; Walsh, D.; Hartley, D.; Chesneau, V.; Rosner, M. R.; Selkoe, D. J., Neurons regulate extracellular levels of amyloid beta-protein via proteolysis by insulin-degrading enzyme. *J Neurosci* **2000,** *20* (5), 1657-65.

86. Tabaton, M.; Cammarata, S.; Mancardi, G.; Manetto, V.; Autilio-Gambetti, L.; Perry, G.; Gambetti, P., Ultrastructural localization of beta-amyloid, tau, and ubiquitin epitopes in extracellular neurofibrillary tangles. *Proc Natl Acad Sci U S A* **1991,** *88* (6), 2098-102.

87. Vetrivel, K. S.; Thinakaran, G., Amyloidogenic processing of beta-amyloid precursor protein in intracellular compartments. *Neurology* **2006,** *66* (2 Suppl 1), S69-73.

88. Grant, S. M.; Ducatenzeiler, A.; Szyf, M.; Cuello, A. C., Abeta immunoreactive material is present in several intracellular compartments in transfected, neuronally differentiated, P19 cells expressing the human amyloid beta-protein precursor. *J Alzheimers Dis* **2000,** *2* (3-4), 207-22.

89. Yan, S. D.; Fu, J.; Soto, C.; Chen, X.; Zhu, H.; Al-Mohanna, F.; Collison, K.; Zhu, A.; Stern, E.; Saido, T.; Tohyama, M.; Ogawa, S.; Roher, A.; Stern, D., An intracellular protein that binds amyloid-beta peptide and mediates neurotoxicity in Alzheimer's disease. *Nature* **1997,** *389* (6652), 689-95.

90. Martin, B. L.; Schrader-Fischer, G.; Busciglio, J.; Duke, M.; Paganetti, P.; Yankner, B. A., Intracellular accumulation of beta-amyloid in cells expressing the Swedish mutant amyloid precursor protein. *J Biol Chem* **1995,** *270* (45), 26727-30.

91. Fuller, S. J.; Storey, E.; Li, Q. X.; Smith, A. I.; Beyreuther, K.; Masters, C. L., Intracellular production of beta A4 amyloid of Alzheimer's disease: modulation by phosphoramidon and lack of coupling to the secretion of the amyloid precursor protein. *Biochemistry* **1995,** *34* (25), 8091-8.

92. Matsumoto, A.; Matsumoto, R., Familial Alzheimer's disease cells abnormally accumulate beta-amyloid-harbouring peptides preferentially in cytosol but not in extracellular fluid. *Eur J Biochem* **1994,** *225* (3), 1055-62.

93. Hay, D. G.; Sathasivam, K.; Tobaben, S.; Stahl, B.; Marber, M.; Mestril, R.; Mahal, A.; Smith, D. L.; Woodman, B.; Bates, G. P., Progressive decrease in chaperone protein levels in a mouse model of Huntington's disease and induction of stress proteins as a therapeutic approach. *Hum Mol Genet* **2004,** *13* (13), 1389-405.

94. Waza, M.; Adachi, H.; Katsuno, M.; Minamiyama, M.; Sang, C.; Tanaka, F.; Inukai, A.; Doyu, M.; Sobue, G., 17-AAG, an Hsp90 inhibitor, ameliorates polyglutamine-mediated motor neuron degeneration. *Nat Med* **2005,** *11* (10), 1088-95.

95. McLean, P. J.; Klucken, J.; Shin, Y.; Hyman, B. T., Geldanamycin induces Hsp70 and prevents alpha-synuclein aggregation and toxicity in vitro. *Biochem Biophys Res Commun* **2004,** *321* (3), 665-9.

96. Katsuno, M.; Sang, C.; Adachi, H.; Minamiyama, M.; Waza, M.; Tanaka, F.; Doyu, M.; Sobue, G., Pharmacological induction of heat-shock proteins alleviates polyglutamine-mediated motor neuron disease. *Proc Natl Acad Sci U S A* **2005,** *102* (46), 16801-6.

97. Westerheide, S. D.; Bosman, J. D.; Mbadugha, B. N.; Kawahara, T. L.; Matsumoto, G.; Kim, S.; Gu, W.; Devlin, J. P.; Silverman, R. B.; Morimoto, R. I., Celastrols as inducers of the heat shock response and cytoprotection. *J Biol Chem* **2004,** *279* (53), 56053-60.

Chapter 3

Dihydropyridines Affect Tau Stability in Cellular Models of Neurodegeneration: Enantioselective Synthesis and Determination of Structure-Activity Relationships

3.1 Abstract

A series of dihydropyridines were identified that impact the accumulation of tau, an important target in Alzheimer's disease. Interestingly, these compounds appeared to operate in a manner similar to the dihydropyrimidines SW02 and 115-7c described in Chapter 2. Based on these findings, the dihydropyridine collection was expanded using the Hantzsch multicomponent reaction to develop preliminary structure-activity relationships (SAR). These studies revealed the SAR in cultured neuronal cells, providing a path towards creating more potent derivatives. Finally, because of shortcomings in the existing enantioselective routes, we developed the first enantioselective, organocatalytic route to these four-component Hantzsch products. Using this route, we found that only one of the enantiomers reduced aggregation of polyglutamine in a yeast model, validating the synthetic approach. In summary, this chemical series provides a new set of probes that can be used to explore tau and polyglutamine processing in models of neurodegeneration.

3.1.1 Introduction to Tau and Known Chemical Probes

Tau is a microtubule-binding protein that accumulates in a number of neurodegenerative disorders, including some forms of frontotemporal dementia and Alzheimer's disease (AD).[1-3] These diseases are collectively termed tauopathies and they

are characterized by aggregation of hyperphosphorylated tau. The presence of abnormal tau correlates with neuron loss and memory deficits in patients with AD and other tauopathies.[4] Therefore, selectively reducing its levels might be an effective therapeutic strategy.

Efforts towards that goal have largely focused on either inhibitors of tau aggregation,[5, 6] inhibitors of its phosphorylation[7] or compounds that stimulate chaperone-mediated degradation.[8-10] While each these strategies are potentially promising and well supported by genetic evidence, many of the compounds identified to date have relatively modest activity. For example, methylene blue (MB), which both inhibits tau aggregation[5, 6] and stimulates its degradation through heat shock protein 70 (Hsp70),[8-10] has an EC_{50} value of approximately 10 μM. Other promising compounds, such as the Hsp90 inhibitors 17-AAG and EC1012, reduce tau levels but they also produce a robust stress response, which is expected to diminish their long-term efficacy.[8-11] Thus, new compounds that counteract tau accumulation are needed.

During pilot screens for small molecules that impact cellular tau levels, we identified the 1,4-dihydropyridine **4a** (data not shown). Interestingly, this scaffold bears structural resemblance to the dihydropyrimidines, such as 115-7c and SW02, that we explored in Chapter 2. Based on this finding, we sought to synthesize a focused collection of compounds related to **4a** to facilitate characterization of structure-activity relationships (SAR). Towards that goal, we were attracted to the Hantzsch multicomponent reaction because of its high atom economy and suitability for combinatorial synthesis.

3.1.2 The Hantzsch Reaction

Scheme 3-1. Mechanism for the Hantzsch reaction. Formation of the enamine occurs via condensation of the amine with a 1,3-dicarbonyl. The other 1,3-dicarbonyl forms the α,β-unsaturated carbonyl via a Knovenagel-like condensation. Following a Michael addition of the enamine to the α,β-unsaturated carbonyl, there is a ring closure step and subsequent loss of water to afford the 1,4-dihydropyridine.

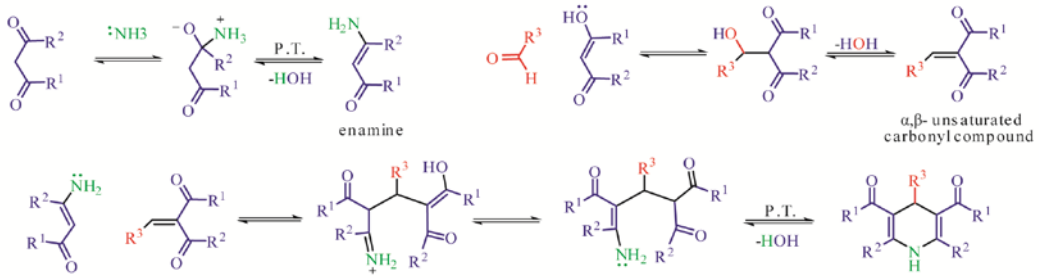

Multicomponent reactions, such as the Biginelli,[12-20] the Passerini,[21] the Ugi,[22] and the Hantzsch, provide a wide variety of pharmaceutically-important heterocycles.[14, 23-33] For example, the Hantzsch reaction provides products with a variety of biological activities, including calcium channel antagonists, modulators of multi-drug resistence (MDR) proteins, 5-hydroxytryptamine (5-HT) receptor inhibitors and anti-inflammatories.[34-40] Beyond their myriad biological activities, Hantzsch dihydropyridines are also useful as synthetic tools for reducing imines to amines.[41-44] The mechanism for the Hantzsch reaction is believed to consist of enamine formation due to the condensation between the amine and one of the 1,3-dicarbonyl components and the formation of an α,β-unsaturated carbonyl from the Knoevenagel-like condensation of the other 1,3-dicarbonyl and aldehyde components. The enamine and the α,β-unsaturated carbonyl then undergo a Michael addition followed by a ring closing step to afford the 1,4-dihydropyridine (Scheme 3-1).

3.1.3 Known Enantioselective Methodology to Synthesize 1,4-Dihydropyridines

While enantioselective Biginelli,[45, 46] Mannich,[47, 48] and Passerini[49] reactions are well known, parallel methodologies have not been developed for the four-component Hantzsch reaction. Historically, the harsh conditions required for this reaction, such as

Scheme 3-2. Current Enantioselective Methodology for 1,4-Dihydropyridines

(A) Asymmetric three-component Hantzsch reaction using C-glycosylated reagents[50]

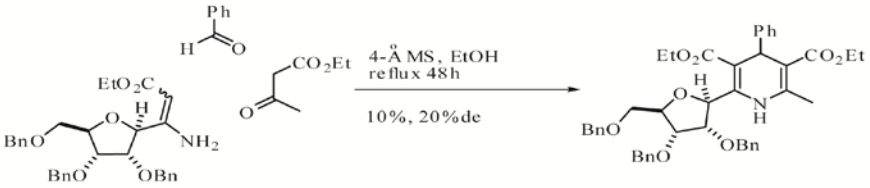

(B) Enantioselective Hantzsch variant employing a chiral auxiliary[51]

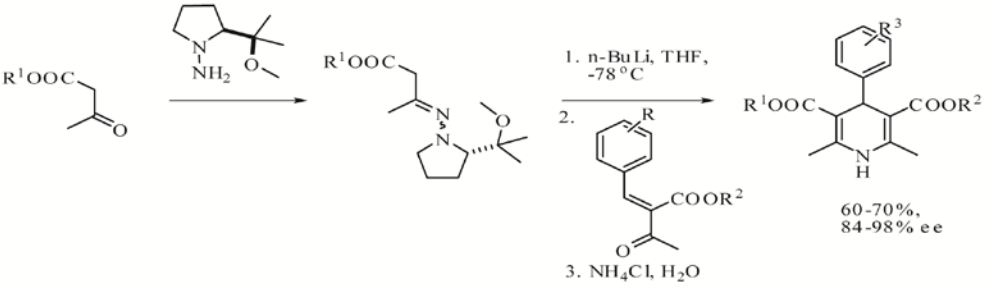

refluxing ethanol, have made development of an asymmetric route challenging. For example, attempts to develop diasterioselective products with glycosylated enamines have yielded only modest selectivity (Scheme 3-2).[50] With more recent advances in Lewis acid-catalyzed reactions,[51] one way to achieve enantio-enrichment is to use an enamine attached to a chiral auxillary in the presence of n-butyllithium (Scheme 3-2).[52] While the enrichment values for this method are good to excellent (~54 to 96%), this approach reduces the reaction to three components and limits the diversity of the products. Because of the shortcomings of these routes and in response to our need for an expanded collection of dihydropyrimidines, we have developed a relatively benign and efficient method to four-component Hantzsch products by employing an organocatalyst, which is described below.

3.2 Results and Discussion

3.2.1 Creation of a Dihydropyridine Library for SAR Studies

Based on the structure of the active compound **4a**, we first employed dimedone **1**, ethylacetoacetate **2**, ammonium acetate, and a series of functionalized aldehydes to create derivatives (Scheme 3-3). Our goal was to vary specific functional groups on the 1,4-

Scheme 3-3. Variation of the aldhyde in the Hantzsch reaction to expand the diversity of the dihydropyridine collection.

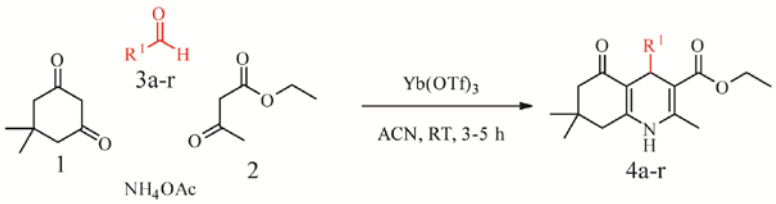

Entry	Compound	R^1	Yield
1	4a	2,4-Cl-C_6H_3-	89-94%
2	4b	C_6H_5-	82-85%
3	4c	4-Br-C_6H_4-	80-84%
4	4d	3,5-OMe-C_6H_3-	72-74%
5	4e	3-F-C_6H_4-	89-92%
6	4f	4-$(CH_3)_2$N-C_6H_4-	75-78%
7	4g	2-CF_3-C_6H_4-	79-84%
8	4h	2,5-F-C_6H_3-	90-94%
9	4i	4-tBu-C_6H_4-	84-88%
10	4j	2-Naphthyl	81-83%
11	4k	4-CN-C_6H_4-	72%
12	4l	3,4-OH-C_6H_3-	69%
13	4m	C_6H_5-CH_2CH_2-	92-94%
14	4n	2-Cl-C_6H_4-	89-94%
15	4o	4-C_6H_5-C_6H_4-	72-77%
16	4p	$CH_3CH_2(CH_3)CH$-	66%
17	4q	CH_3-	72%
18	4r	C_6H_7-$C_2H_3O_2$-	75%

dihydropyridine core to identify the key preliminary SAR for this series. We expected that these studies would facilitate identification of the target and, moreover, provide chemical probes for studying tau processing in cellular and animal models. Towards that

goal, a series of aldehydes were chosen to sample both bulky aromatics and smaller, alkyl functionalities. Briefly, dimedone (1.5 equiv), ethylacetoacetate (1 equiv), and $Yb(OTf)_3$ (10 mol%) were mixed in acetonitrile. After stirring for 10 minutes, the aldehyde (1.0 equiv) and ammonium acetate (1.0 equiv) were added. The reactions then proceeded for 3-5 hours, after which it was poured into saturated sodium chloride, washed with ethylacetate and the product was re-crystallized from 1:3 water:ethanol. Using this approach, compounds **4a-r** were obtained in moderate to good yields (ranging from 69-94%).

3.2.2 Further Modifications of the 1,4-Dihydropyridine Core

To expand diversity in this collection, we took advantage of published methods[53] to exchange the ester for a thioester on representative compounds **4a** and **4b**. Briefly, these examples were refluxed in toluene with 2.2 equivalents of Lawesson's reagent for 1 hr. The resulting products, **5a** and **5b**, were filtered through Celite and purified as above

Scheme 3-4. Introduction of a thioester into the dihydropyridines.

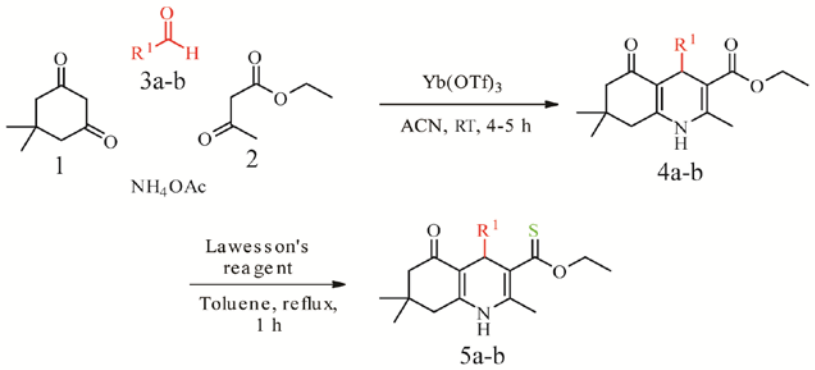

Entry	Compound	R^1	Yield
1	5a	2,4-Cl-C_6H_3-	89-94%
2	5b	C_6H_5-	82-85%

in good yield (Scheme 3-4).

Next, to test whether modifications to the heterocyclic amine could be tolerated, we combined dimedone with aryl or alkyl amines in acetonitrile to form the enamine.[54, 55] After 30 minutes, ethylacetoacetate (1.0 eq), 2,4-dicholoro benzaldehyde **3a** (1.0 eq) and 10% $Yb(OTf)_3$ were added and the reaction was allowed to proceed for an additional 4-5 hours. This procedure generated compounds **7a-d** with yields ranging from 71-82% (Scheme 3-5).

Scheme 3-5. Substitutions of the amine in the dihydropyridine.

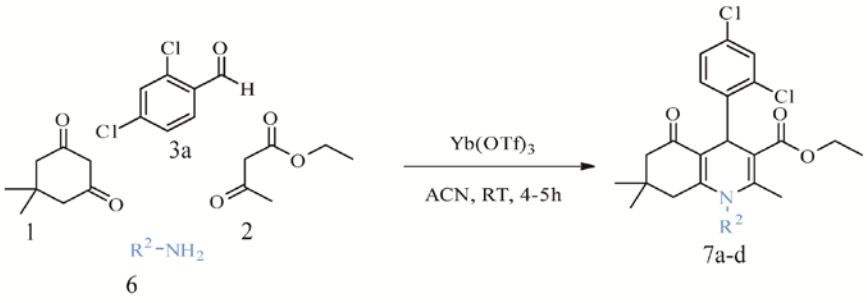

Entry	Compound	R^2	Yield
1	7a	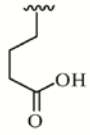	71%
2	7b		74%
3	7c	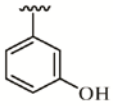	82%
4	7d	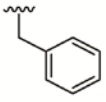	77%

To further diversify the scaffold, we next varied the identity of the 1,3-dicarbonyls (**8** and **9**; Scheme 3-6). Specifically, we used indanedione and 2,4-pentanedione in place of dimedone to produce derivatives **10a** and **10b** in good yields. On the other side of the molecule, we substituted either methylacetoacetate or benzylacetoacetate for ethylacetoacetate to produce **10c** and **10d** in 82 and 85% yield, respectively.

Scheme 3-6. Substitutions of 1,3-dicarbonyls to add diversity to the dihydropyridine scaffold.

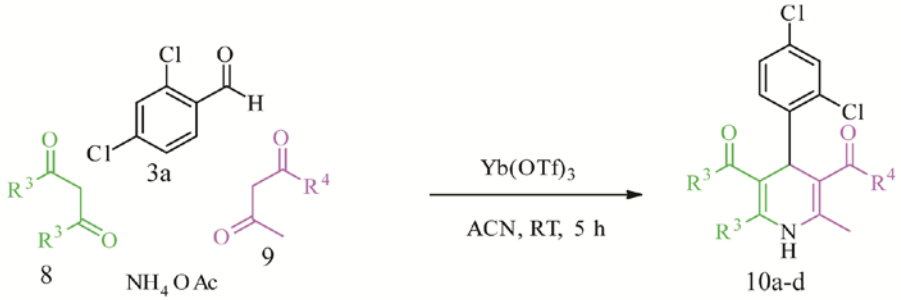

Entry	Compound	R^3	R^4	Yield
1	10a	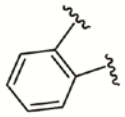	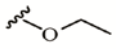	71%
2	10b		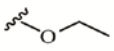	75%
3	10c	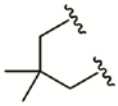		82%
4	10d	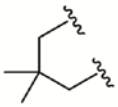	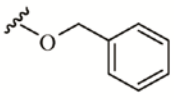	85%

Finally, to fully exploit the strengths of the Hantzsch reaction we varied multiple components simultaneously. Using the reaction conditions and starting materials

employed earlier, we made compounds **11a-11k** (Scheme 3-7). These compounds include examples, such as **11b** and **11c**, which included β-ketoamides. Together, these efforts produced a library of 39 functionalized dihydropyridines. No attempts were made to control stereochemistry in these specific studies, and thus the compounds were purified as racemic mixtures.

Scheme 3-7. Multiple components of the Hantzsch reaction were simultaneously exchanged to created dihydropyridines with increased diversity.

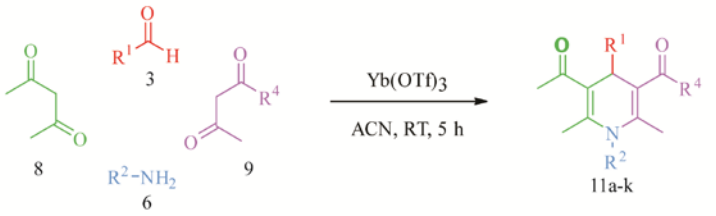

Entry	Compound	R^1	R^2	R^4	Yield
1	11a	2,4-Cl-C_6H_3-	H-	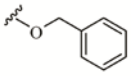	81%
2	11b	2,4-Cl-C_6H_5 -	H-	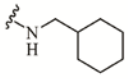	82%
3	11c	2,4-Cl-C_6H_3-	H-	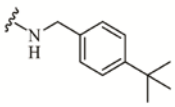	76%
4	11d	2,4-Cl-C_6H_3-			69%
5	11e	2,4-Cl-C_6H_3-			82%
6	11f	2-Naphthyl	H-		71%
7	11g	4-Br-C_6H_4-	H-		84%
8	11h	3-F-C_6H_4-	H-		82%
9	11i	4-(2-pyridyl)-Ph-	H-		79%
10	11j	CH_3-	H-		71%
11	11k	$CH_3CH_2(CH_3)CH$-	H-		74%

3.2.3 Organocatalytic Method for Enantioselective Synthesis of Dihydropyridines

To this point, our collection contained racemic mixtures. Because we were interested in whether one of the enantiomers might be more active than the other, we sought an enantio-enriched route to these products. As mentioned above, existing routes have significant drawbacks. Thus, we developed an enantioselective route to Hantzch dihydropyrimidines. As a model reaction, we selected a known polyhydroquinoline that would afford one stereocenter (Table 3-1). Consistent with previous reports, one equivalent dimedone (0.4 mmol), ethylacetoacetate, a benzaldehyde and ammonium acetate, in the presence of $Yb(OTf)_3$ (10 mol%), produced product 4a in both ethanol and acetonitrile (entries 2-3, Table 3-1). Work-up consisted of precipitating with 1 mL of ice/water, stirring for approximately one hour, filtration of the precipitate and recrystallization of the product from a ethanol:water system (3:1 vol). Using this procedure, we found good yields (68% in ethanol and 72% in acetonitrile), but the reaction also resulted in formation of the symmetrical side product. In an attempt to minimize this competing pathway, the equivalents of dimedone were increased (entries 4-6, Table 3-1). At 1.5 equivalents, the yield increased to 90% with concomitant reduction in the side product. Next, we explored the influence of catalyst concentration by screening at 0.1, 1.0 and 5.0 mol%. In each case, increasing the catalyst improved yield (52%, 65%, and 84%, respectively; entries 8-10 Table 3-1). Based on these observations, we selected reaction conditions of 1.5 equivalents (0.6 mmol) of dimedone, 1 equivalent (0.4 mmol) of ethylacetoacetate, ammonium acetate, and a substituted benzaldehyde with 10 mol% catalyst in 1 mL of acetonitrile for further studies.

Table 3-1. Reaction Optimization

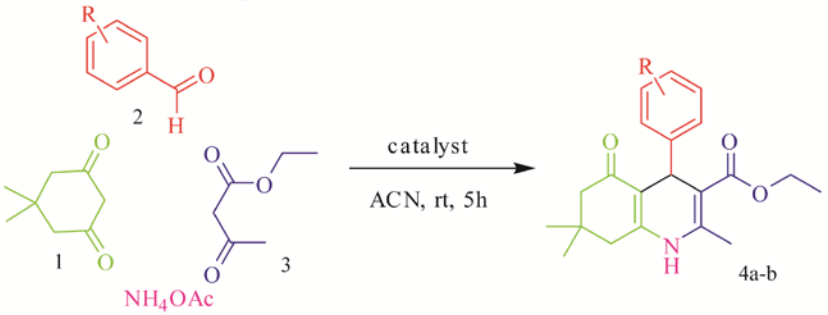

Entry	Catalyst	Solvent	1 (eq)	Aldehyde	Compound	Side Product	Yield
1	$FeCl_3$	ACN	1	2,4-Cl-Ph	4a	Yes	62%
2	$Yb(OTf)_3$	EtOH	1	2,4-Cl-Ph	4a	Yes	68%
3	$Yb(OTf)_3$	ACN	1	2,4-Cl-Ph	4a	Yes	72%
4	$Yb(OTf)_3$	ACN	0.9	2,4-Cl-Ph	4a	Yes	53%
5	$Yb(OTf)_3$	ACN	1.2	2,4-Cl-Ph	4a	Yes	79%
6	$Yb(OTf)_3$	ACN	1.5	2,4-Cl-Ph	4a	No	92%
7	$Yb(OTf)_3$	ACN	1.5	Ph	4b	No	90%
8	$Yb(OTf)_3$-O	ACN	1.5	Ph	4b	No	52%
9	$Yb(OTf)_3$-*	ACN	1.5	Ph	4b	No	65%
10	$Yb(OTf)_3$-#	ACN	1.5	Ph	4b	No	84%

Catalyst concentration 10 mol % except for 0.1 mol % (O), 1 mol % (*), and 5 mol % (#).

Using these conditions, our plan was to screen organocatalysts for those that would afford a high degree of enantioselectivity. Chiral Lewis acids[56-59] as well as proline and its derivatives[56] have been explored in this context, but these have produced poor stereoselectivity. Therefore, we sought to screen an expanded collection. In these studies, we used polarimetry to estimate enantio-enrichment and chiral HPLC to confirm these observations. Consistent with the previous reports, proline derivative (I) provided good yields (86%) but poor enrichment. Next, a series of phosphine based ligands (BINAP—II and III, DPPF—IV, and DPE—V) was explored. These catalysts were used at 10 mol% with 11 mol% of a co-catalyst, $Pd(OAc)_2$, which provided yields between 75-

84% but no enantio-enrichment. Finally, we synthesized[60-62] and explored chiral BINOL-phosphoric acid derivatives (VI and VII). Both catalysts provided good yields (84-85%) and 98% ee (Table 3-2). Thus, we were able to identify catalysts that supported a high yielding and enantioselective Hantzsch reaction.

Table 3-2. Catalyst Screening

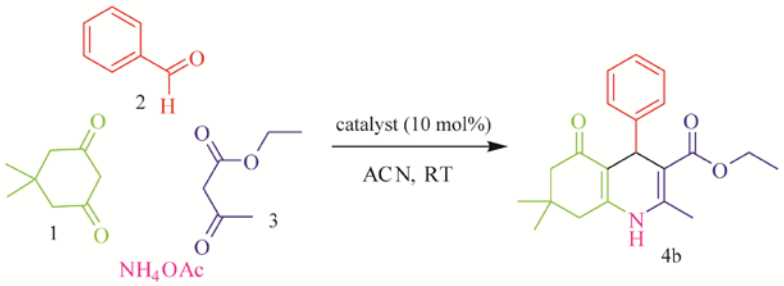

Entry	Catalyst	Time (h)	Yield (%)	$[\alpha]_D^{20}$ (deg)	%ee
1	$Yb(OTf)_3$	3	90	+0.17	
2	I	5	86	-0.20	
3	II	5	82	+0.06	
4	III	5	80	-0.41	
5	IV	5	84	+0.05	
6	V	5	75	+0.00	
7	VI	4	84	+15	98%
8	VII	4	85	+16	98%

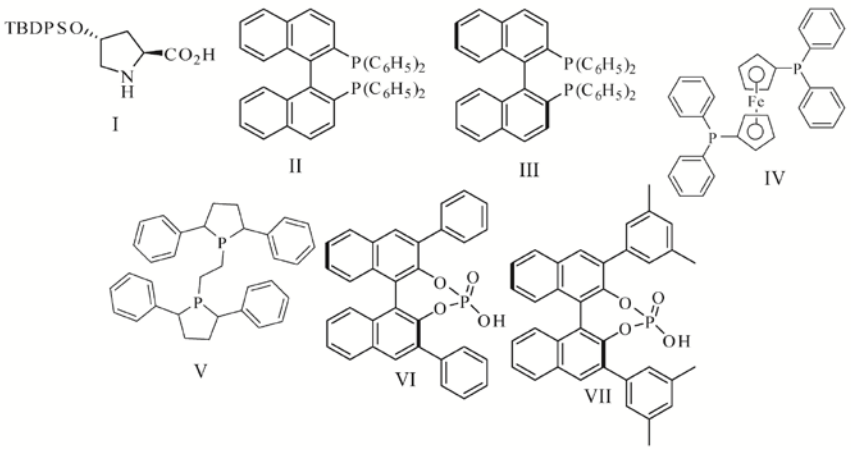

One of the expected advantages of an enantioselective four-component Hantzsch reaction is in the combinatorial synthesis of substituted dihydropyridines. To explore this possibility, we selected polar and non-polar substituted aldehydes with a range of electron withdrawing and donating groups and assembled a small collection of 16 polyhydroquinolines (4a-o Table 3-3). Several of the more polar products such as 4p,

Table 3-3. Investigation of Reaction Scope

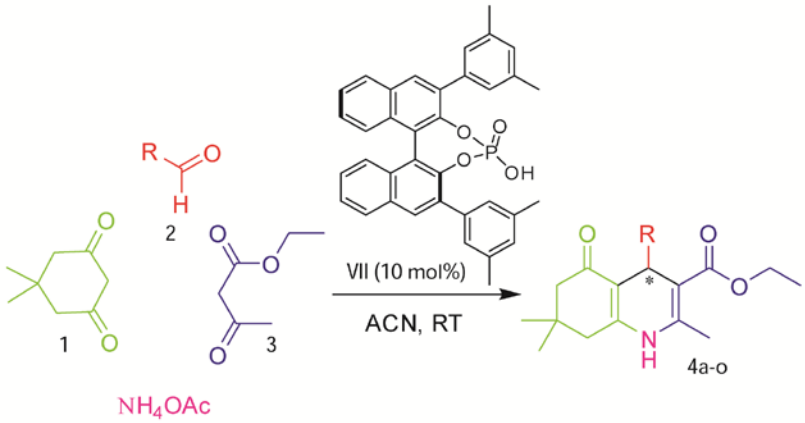

Entry	Time (h)	Aldehyde (R)	Compound	Yield (%)	$[\alpha]_D^{20}$ (deg)	%ee
1	3	2,4-Cl-Ph	4a	89-94	+3.8	>99%
2	4	Ph	4b	82-85	+16	98%
3	4	4-Br-Ph	4c	80-84	+4.1	96%
4	5	3,5-MeO-Ph	4d	72-74	+30	>99%
5	3	3-F-Ph	4e	89-92	+23	87%
6	5	4-$(CH_3)_2$N-Ph	4f	75-78	+29	93%
7	4	2-CF_3-Ph	4g	79-85	-4.4	>99%
8	3	2,5-F-Ph	4h	90-94	+5.5	>99%
9	4	4-tBu-Ph	4i	84-88	+12	97%
10	5	2-Naphthyl	4j	81-83	+8.5	>99%
11	5	4-CN-Ph	4k	72	+5.0	99%
12	5	3,4-OH-Ph	4l	69	+4.1 #	95%
13	4	Ph-CH_2CH_2	4m	92-94	+4.2	94%
14	3	2-Cl-Ph	4n	89-94	+8.6	>99%
15	5	4-C_6H_5-Ph	4o	72-77	+12	>99%
16	5	$C_2H_5CH(CH_3)$	4p	66	-0.3	
17	5	CH_3	4q	72	+0.7	

*-Determined by chiral HPLC on Astec Chirobiotic V2 column under normal phase conditions (isopropanol/hexanes).
#Determined in methanol unlike other compounds that were dissolved in chloroform due to insolubility in chloroform.

which employed 3,4-dihydroxybenzaldehyde, required modified work-up conditions; in these cases, the reactions were poured over brine and washed with ethylacetate prior to recrystallization. Otherwise, a uniform method involving 10 mol% catalyst VII was employed. These experiments revealed that most aromatic aldehydes proceed to the expected product in good yield (80-94%). Aromatic aldehydes with unprotected polar groups generally produced slightly lower yields (69-72%; compounds 4k and 4l). As determined by HPLC, excellent enantioselective-enrichment (87 to >99%) was observed for all compounds. Thus, from these studies, we identified a robust synthetic route for the four-component synthesis of 1,4-dihydropyrimidines. Next, we wanted to determine the SAR for the initial series to focus the enantioselective, synthetic efforts on more advanced derivatives.

3.2.4 Preliminary SAR Obtained from Screening

With this collection of compounds in hand, we treated cultured IMR32 neuroblastoma cells and measured endogenous tau levels by Western blot.[63] We had previously found that the example **4a** increased tau levels in these cells (data not shown) and sought to understand the SAR underlying these findings, to assist with target identification and biological studies. Although **4a** had a significant impact on tau levels, its potency was modest (EC_{50} ~ 50 μM), necessitating further medicinal chemistry.

Towards those goals, Dr. Umesh Jinwal in Chad Dickey's group at University of South Florida treated IMR32 cells with compounds at 100 μM and, after 24 hours, the tau levels were compared to those in a mock treated control (1% DMSO). Some of the compounds, such as **11b-f**, were found to be toxic under these conditions and they were excluded from further analysis. We compared the remaining examples to the benchmark

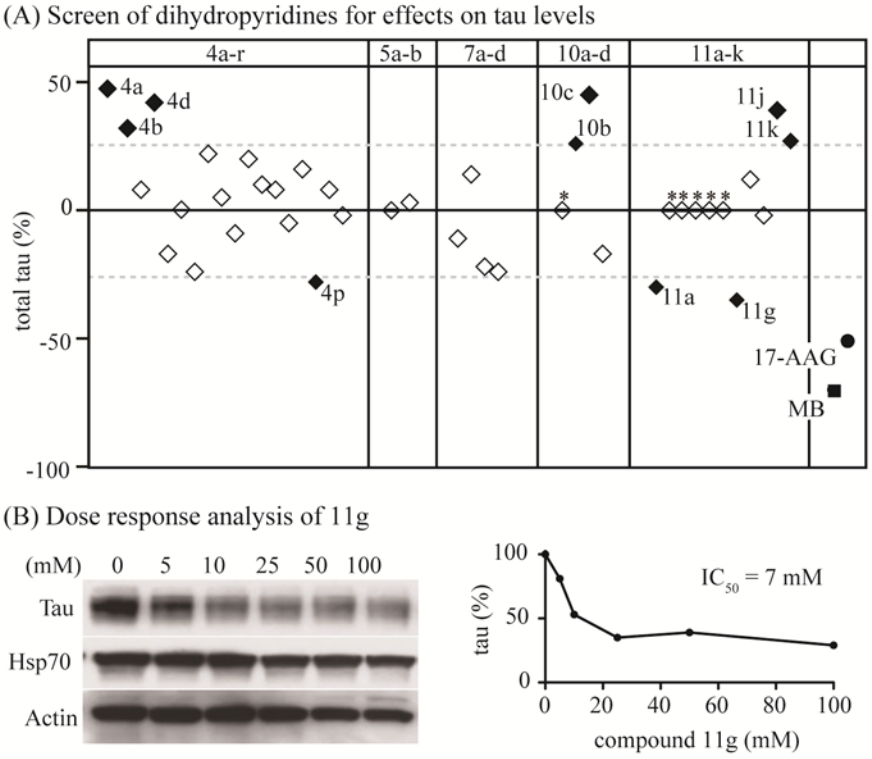

Figure 3-1. Screening results for the dihydropyridine collection against cellular tau. (A) IMR32 cells were treated for 24hrs with 100 mM compound, followed by Western blots for total tau. Quantification of these blots are shown versus a vehicle control (1% DMSO). Also shown are two positive controls, methylene blue (MB) and 17-AAG. Arbitrary activity cut-offs are shown at +/- 25% change in tau levels (dotted line). Inactive compounds are shown as open symbols. Active compounds are shown in solid symbols and are labeled. *Toxic compounds. (B) Dose response analysis of the promising compound 11g.

compounds MB and 17-AAG, which reduced tau levels by approximately 50 to 70% (Figure 3-1).[8-11] Based on those values, we imposed an arbitrary threshold of 25% to focus on the most active compounds in the dihydropyridine collection. This approach revealed that **4p**, **11a** and **11g** reduced tau levels by at least 25%. Interestingly, we also identified examples, such as **4a**-**b**, **4d**, **10b**-**c**, **11j** and **11k**, which *increased* tau levels by at least 25%. Previous efforts have also noted compounds that either increase or decrease tau levels and both sets of molecules have been useful probes of tau biology.[8-10]

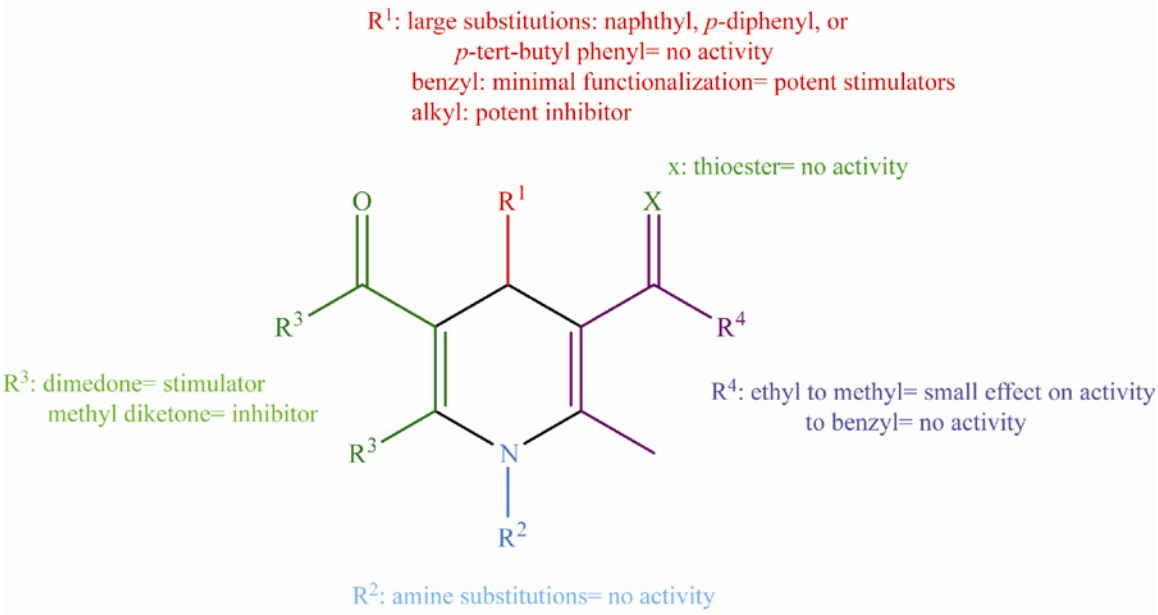

Figure 3-2. Initial SAR determined from tau stability data.

An analysis of these results suggested some preliminary SAR (Figure 3-2). Specifically, large substitutions on the aldehyde, such as napthyl (**4j**), *p*-diphenyl (**4o**) or *p*-tert-butyl phenyl (**4i**), were not tolerated. Likewise, conversion of the ester to a thioester in **5a** and **5b** reduced activity, as did any modification of the heterocyclic amine (compounds **7a-d**). Modest substitutions of an ethyl to methyl group (*e.g.* from **4a** to **10c**) had marginal effect on activity but larger groups, such as the benzyl ester in **10d**, abolished activity. Interestingly, minimally functionalized benzyls in the aldehyde position, such as **4a**, **4b** and **4d**, produced the most potent stimulators of tau accumulation, while smaller alkyl groups, such as in **4p**, tended to produce compounds that reduced tau levels. This finding suggests a way of converting a compound from one that causes tau accumulation to one that leads to tau reductions. However, the impact of modifications at the aldehyde position also seemed to be influenced by the identity of the 1,3-diketone. For example, if dimedone was used, compounds **4a** and **4b** promoted tau

accumulation, but replacing it for a methyl diketone, as in **11a** and **11g**, produced relatively strong inhibitors. Together, these findings reveal patterns of substitution that result in compounds that either promote tau degradation or accumulation.

Following this initial screening, we selected compound **11g** for dose response studies. We found that this compound reduced tau levels by ~75% with an IC_{50} of ~7 μM (Figure 3-1B). This activity is comparable to some of the most potent anti-tau compounds, such as MB.[8-10] As mentioned above, inhibitors of Hsp90, such as 17-AAG, have short-term effects on tau stability but they also induce a strong stress response.[11] To test whether **11g** shares this property, we examined the levels of stress-inducible Hsp70 in the IMR32 cells. By Western blots, Hsp72 levels were unchanged, suggesting that **11g** does not act through the Hsp90 pathway (Figure 3-1B). The cellular target of these dihydropyridines is currently unclear, but the relatively good activity of **11g** suggests that further studies are warranted. The follow-up studies should be facilitated by the SAR and enantioselective route established here.

Further cell-based studies were carried out following the synthesis of **11g** with both **R** and **S** enantiomers of the phosphoric acid BINOL catalysts, as described above. Comparable yields were obtained (82% and 85% with the **R** and **S** enantiomers, respectively) following flash column purification. A yeast polyglutamine assay was then used to screen which product was more active. In this model, longer repeats of glutamine (*e.g.* Q103), aggregate and the subcellular puncta can be visualized by the appended CFP tag. Cells were treated with the enantio-pure **11g** derivatives (10 μM), which revealed that only the **11g** synthesized from catalyst (**S)-VII** had anti-aggregation activity (Figure 3-2).

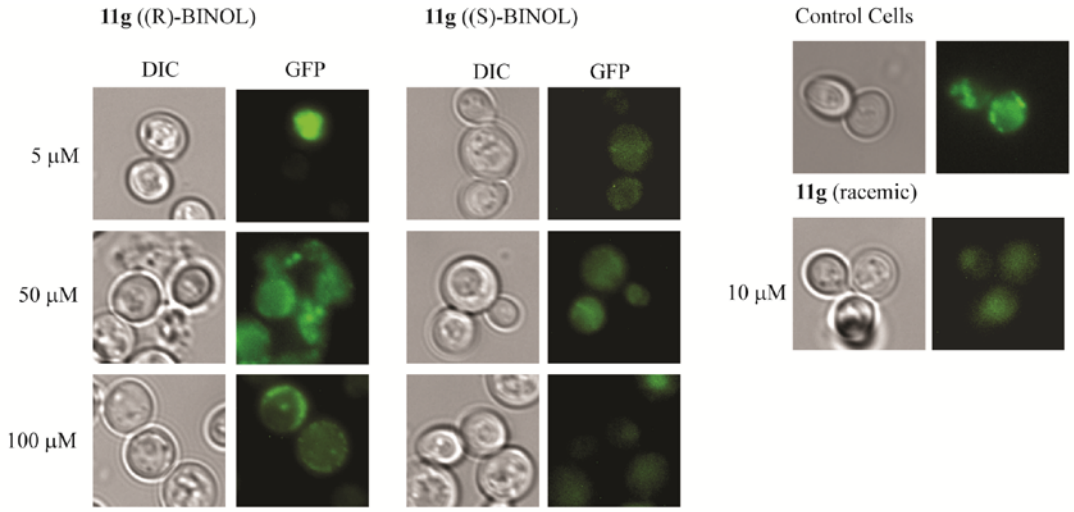

Figure 3-3. Yeast cells expressing Q103 are sensitive to compound 11g synthesized from chiral organophoshorus catalys (S)-BINOL. *S. cerevisiae* (YKO-pdr5Δ) were induced to express the N-terminus of the huntingtin protein with 103 repeats (polyQ103P). These cells were treated with compound **11g** and after 24 hours were fixed and examined under the microscope. **11g** synthesized with the (S) enantiomer of BINOL were active and lead to a more diffuse pattern of fluorscence. This indicated that there was less aggregation of the ployQ protein, which would normally localize into puncta.

3.3 Summary

In summary, we have developed an enantioselective route for the Hantzsch reaction using a chiral phosphoric acid organocatalyst under relatively mild conditions and suitable for a wide range of aldehydes that has enabled us to synthesize **11g**, a promising new compound that reduces tau levels by up to 70%. Recent studies indicate the one enantiomer of **11g** is more active than the other, thus validating the synthetic route. This syntheitc method may find use in the synthesis of other medically important dihydropyridines and, potentially, as reagents for enantioselective hydrogenation reactions. Moreover, the dihydropyridine SAR may lead to improved potency and the discovery of the compound's target in cells.

3.4 Experimental Procedures

3.4.1 Synthesis of Compounds 4a-4r (Scheme 3-3).

Component 1 dimedone (1.5eq, 0.6mmol) and component 3 ethylacetoacetate (1eq, 0.4mmol) were suspended along with 10mol% VII in 1mL of acetonitrile. After stirring under inert gas for 10min, component 2 (1eq, 0.4mmol) and ammonium acetate (1eq, 0.4mmol) were added. The reaction was allowed to stir for 3-5h. All reactions except for 4d, 4f, 4k, 4l, and 4o were precipitated by the addition of ice/water. Following precipitation the reactions were recrystallized with an ethanol/water system. For the other reactions (4d, 4f, 4k, 4l, and 4o), the reactions were added to brine and extracted with ethylacetate. Following concentration, these products were also recrystallized with an ethanol/water system.

3.4.2 Characterization of compounds 4a-4r.

All NMR collected and analyzed on Varian 400MHz system using VnmrJ™ version 2.2 revision C. Samples diluted in $CDCl_3$ immediately prior to data collection. Mass spectrometry data collected on and Micromass LCT time-of-flight mass spectrometer in the ES+ mode.

Ethyl 4-(2,4-dichlorophenyl)-2,7,7-trimethyl-5-oxo-1,4,5,6,7,8-hexahydroquinoline-3-carboxylate (**4a**): ^{1}H δ ($CDCl_3$) 7.33-7.31 (1H, d), 7.24 (1H, s), 7.11-7.08 (1H, d), 6.53 (1H, s), 5.33 (1H,s), 4.07-3.99 (2H, m), 2.30 (3H, s), 2.29-2.21 (2H, dd), 2.18-2.09 (2H, dd), 1.19-1.16 (3H, t), 1.06 (3H, s), 0.94 (3H, s). ^{13}C δ ($CDCl_3$) 195.38, 167.18, 149.44, 142.38, 133.63, 132.83, 131.94, 129.13, 126.89, 111.07, 104.65, 60.09, 50.54, 40.90, 32.78, 29.10, 27.41, 19.23, 14.42. [M+H] e: 408.11, o: 408.1. $[\alpha]_D$ = +3.8 (c 2.19, $CHCl_3$). Yield 89-94%.

Ethyl 2,7,7-trimethyl-5-oxo-4-phenyl-1,4,5,6,7,8-hexahydroquinoline-3-carboxylate (**4b**): ^{1}H δ ($CDCl_3$) 7.3-7.29 (2H, d), 7.21-7.17 (2H, t), 7.11-7.07 (1H, t),5.93 (1H, s), 5.05 (1H, s), 4.08-4.03 (2H, m), 2.37 (3H, s),2.34- 2.2.22 (2H, dd), 2.21-2.13 (2H, dd), 1.21-1.17 (3H, t), 1.07 (3H, s), 0.93 (3H, s). ^{13}C δ ($CDCl_3$) 195.36, 167.28, 147.72, 147.07, 143.43, 112.32, 106.06, 59.77, 50.69, 41.19, 36.52, 32.64, 29.38, 27.14, 19.34, 14.19. [M+H] e: 340.18, o: 340.2. $[\alpha]_D$ = +16 (c 2.5, $CHCl_3$). Yield 82-85%.

Ethyl 4-(4-bromophenyl)-2,7,7-trimethyl-5-oxo-1,4,5,6,7,8-hexahydroquinoline-3-carboxylate (**4c**): ^{1}H δ ($CDCl_3$) 7.32-7.30 (2H, d), 7.18-7.16 (2H, d), 6.29 (1H, s), 5.00 (1H, s), 4.08-4.03 (2H, m), 2.37 (3H, s), 2.35-2.23 (2H, dd), 2.21-2.12 (2H, dd), 1.20-1.17 (3H, t), 1.07 (3H, s), 0.92 (3H, s). ^{13}C δ ($CDCl_3$) 195.36, 166.87, 148.88, 145.75, 143.74, 131.07, 129.70, 111.38, 106.01, 59.85, 50.78, 40.90, 36.18, 32.47, 29.36, 26.85, 19.23, 14.17. [M+H] e: 418.09, o: 418.1. $[\alpha]_D$ = +4.1 (c 1.77, $CHCl_3$). Yield 80-84%.

Ethyl 4-(3,5-dimethoxyphenyl)-2,7,7-trimethyl-5-oxo-1,4,5,6,7,8-hexahydroquinoline-3-carboxylate (**4d**): ^{1}H δ ($CDCl_3$) 6.55 (1H, s), 6.47 (2H, s), 6.23-6.22 (1H, t), 5.01 (1H, s), 4.10-4.05 (2H, m), 3.72 (6H, s), 2.34 (3H, s), 2.31-2.25 (2H, dd), 2.22-2.15 (2H, dd), 1.24-1.20 (3H, t), 1.05 (3H, s), 0.96 (3H, s). ^{13}C δ ($CDCl_3$) 195.54, 167.36, 160.26, 149.35, 143.35, 111.63, 106.36, 105.83, 97.78, 59.78, 55.11, 50.61, 40.92, 36.57, 32.62, 29.32, 27.18, 19.27, 14.28. [M+H] e: 400.20, o: 400.2. $[\alpha]_D$ = +30 (c 1.96, $CHCl_3$). Yield 72-74%.

Ethyl 4-(3-fluorophenyl)-2,7,7-trimethyl-5-oxo-1,4,5,6,7,8-hexahydroquinoline-3-carboxylate (**4e**): ^{1}H δ ($CDCl_3$) 7.17-7.09 (2H, m), 6.99-6.95 (1H, d), 6.80-6.76 (2H, t), 6.28 (1H, s), 5.06 (1H, s), 4.09-4.04 (2H, m), 2.38 (3H, s), 2.33-2.26 (2H, d), 2.22-2.14

(2H, dd), 1.21-1.17 (3H, t), 1.07 (3H, s), 0.93 (3H, s). ^{13}C δ ($CDCl_3$) 195.37, 167.19, 164.05, 161.57, 149.13, 143.51, 129.15, 114.77, 114.62, 112.92, 112.64, 111.64, 105.89, 59.94, 50.38, 40.87, 36.49, 32.89, 29.37, 26.86, 19.42, 14.26. [M+H] e: 358.17, o: 358.2. $[\alpha]_D$ = +13 (c 2.53, $CHCl_3$). Yield 89-92%.

Ethyl 4-(4-(dimethylamino)phenyl)-2,7,7-trimethyl-5-oxo-1,4,5,6,7,8-hexahydroquinoline-3-carboxylate (**4f**): ^{1}H δ ($CDCl_3$)7.18-7.16 (2H, d), 6.64-6.62 (2H, d), 6.44 (1H, s), 4.95 (1H, s), 4.09-4.04 (2H, m), 2.86 (6H, s), 2.34 (3H, s), 2.28-2.23 (2H, dd), 2.19-2.11 (2H, dd), 1.24-1.20 (3H, t), 1.05 (3H, s), 0.94 (3H, s). ^{13}C δ ($CDCl_3$) 195.93, 167.44, 148.32, 143.19, 128.58, 112.19, 109.95, 106.03, 59.85, 50.77, 40.90, 35.29, 32.78, 29.65, 27.42, 19.23, 14.17. [M+H] e: 383.23, o: 383.2. $[\alpha]_D$ = +29 (c 1.48, $CHCl_3$). Yield 75-78%.

Ethyl 2,7,7-trimethyl-5-oxo-4-(2-(trifluoromethyl)phenyl)-1,4,5,6,7,8-hexahydroquinoline-3-carboxylate (**4g**): ^{1}H δ ($CDCl_3$) 7.50-7.48 (1H, d), 7.45-7.43 (1H, d), 7.39-7.35 (1H, t), 7.22-7.18 (1H, t), 6.48 (1H, s), 5.60 (1H, s), 4.15-3.93 (2H, m), 2.36-2.22 (2H, d), 2.28 (3H, t), 2.21-2.07 (2H, dd), 1.14-1.11 (3H, t), 1.05 (3H, s), 0.90 (3H, s). ^{13}C δ ($CDCl_3$) 195.21, 167.40, 148.20, 146.05, 142.61, 131.34, 130.90, 127.45, 126.64, 126.22, 112.35, 109.94, 107.30, 59.87, 50.39, 41.07, 33.50, 32.60, 29.16, 27.11, 19.17, 13.96. [M+H] e: 408.17, o: 408.2. $[\alpha]_D$ = -4.4 (c 1.94, $CHCl_3$). Yield 79-85%.

Ethyl 4-(2,5-difluorophenyl)-2,7,7-trimethyl-5-oxo-1,4,5,6,7,8-hexahydroquinoline-3-carboxylate (**4h**): ^{1}H δ ($CDCl_3$) 7.02 (1H, m), 6.84-6.74 (2H, m), 6.33 (1H, s), 5.19 (1H, s), 4.07-4.02 (2H, m), 2.38-2.26 (2H, dd), 2.34 (3H, s), 2.21-2.13 (2H, dd), 1.21-1.17 (3H, t), 1.08 (3H, s), 0.95 (3H, s). ^{13}C δ (d-DMSO) 194.40, 166.90, 157.22, 157.07,

154.80, 150.45, 146.22, 136.80, 116.91-116.73, 114.64-114.31, 108.90, 102.43, 59.49, 50.51, 32.53-32.16, 29.45, 26.69, 18.66, 14.34. [M+H] e: 376.16, o: 376.2. $[\alpha]_D$ = +5.5 (c 1.89, $CHCl_3$). Yield 90-94%.

Ethyl 4-(4-tert-butylphenyl)-2,7,7-trimethyl-5-oxo-1,4,5,6,7,8-hexahydroquinoline-3-carboxylate (**4i**): ^{1}H δ ($CDCl_3$) 7.18 (4H, s), 6.22, (1H, s), 5.02 (1H, s), 4.11-4.04 (2H, m), 2.37-2.26 (2H, dd), 2.34 (3H, s), 2.24-2.16 (2H, dd), 1.26 (9H, s), 1.21-1.19 (3H, t), 1.07 (3H, s), 0.97 (3H, s). ^{13}C δ (CDCl3) 195.92, 167.43, 148.32, 143.75, 143.19, 127.44, 124.87, 112.20, 106.33, 59.84, 50.77, 41.23, 35.86, 34.52, 32.90, 31.34, 29.35, 27.40, 19.23, 14.19. [M+H] e: 396.25, o: 396.3. $[\alpha]_D$ = +12 (c 1.95, $CHCl_3$). Yield 84-88%.

Ethyl 2,7,7-trimethyl-4-(naphthalen-2-yl)-5-oxo-1,4,5,6,7,8-hexahydroquinoline-3-carboxylate (**4j**): ^{1}H δ ($CDCl_3$) 7.74-7.67 (4H, m), 7.50 (1H, d), 7.38-7.35 (2H, t), 6.52 (1H, s), 5.22 (1H, s), 4.07-4.02 (2H, m), 2.41 (3H, s), 2.21-2.19 (2H, dd), 2.14-2.06 (2H, dd), 1.21-1.17 (3H, t), 1.10 (3H, s), 0.87 (3H, s). ^{13}C δ ($CDCl_3$) 195.53, 167.36, 148.88, 144.41, 143.55, 133.34, 132.21, 127.37, 126.28, 125.06, 111.81, 106.07, 59.82, 50.03, 40.91, 36.80, 32.57, 29.40, 27.01, 19.38, 14.20. [M+H] e: 390.20, o: 390.2. $[\alpha]_D$ = +8.5 (c 2.14, $CHCl_3$). Yield 81-83%.

Ethyl 4-(4-cyanophenyl)-2,7,7-trimethyl-5-oxo-1,4,5,6,7,8-hexahydroquinoline-3-carboxylate (**4k**): ^{1}H δ ($CDCl_3$) 7.51-7.49 (2H, d), 7.43-7.41 (2H, d), 6.29 (1H, s), 5.09 (1H, s), 4.07-4.01 (2H, m), 2.40 (3H, s), 2.34-2.25 (2H, d), 2.21-2.12 (2H, dd), 1.18-1.14 (3H, t), 1.07 (3H, s), 0.90 (3H, s). ^{13}C δ ($CDCl_3$) 195.28, 166.82, 152.21, 148.79, 144.23, 131.82, 128.88, 119.25, 111.15, 109.58, 105.06, 60.00, 50.46, 40.98, 37.25, 32.70, 29.31, 27.04, 19.39, 14.14. [M+H] e: 365.18, o:365.2. $[\alpha]_D$ = +5.0 (c 1.21, $CHCl_3$). Yield 72%.

Ethyl 4-(3,4-dihydroxyphenyl)-2,7,7-trimethyl-5-oxo-1,4,5,6,7,8-hexahydroquinoline-3-carboxylate (**4l**): ^{1}H δ (CD_3OD) 6.68 (1H, s), 6.54 (2H, s), 4.84 (2H, s), 4.81 (1H, s), 4.06-4.00 (2H, m), 3.28 (1H, s), 2.42-2.24 (2H, dd), 2.31 (3H, s), 2.19-2.06 (2H, dd), 1.20-1.17 (3H, t), 1.04 (3H, s), 0.91 (3H, s). ^{13}C δ (CD_3OD) 197.11, 168.20, 150.85, 144.09, 142.91, 139.29, 118.91, 114.87, 111.05, 105.53, 59.40, 50.00, 39.65, 35.49, 32.03, 28.17, 25.73, 17.12, 13.14. [M+H] e: 371.17, o: 372.2. $[\alpha]_D$ = +4.1 (c 1.56, MeOH). Yield 69%.

Ethyl 2,7,7-trimethyl-5-oxo-4-phenethyl-1,4,5,6,7,8-hexahydroquinoline-3-carboxylate (**4m**): ^{1}H δ ($CDCl_3$) 7.25-7.08 (5H, m), 6.33 (1H, s), 4.21-4.00 (3H, m), 2.57-2.48 (2H, m), 2.23 (3H, s), 2.30-2.25 (2H, d), 2.20-2.16 (2H, d), 1.59-1.82 (2H, m), 1.29-1.25 (3H, t), 1.10 (3H, s), 1.08 (3H, s). ^{13}C δ ($CDCl_3$) 195.96, 189.42, 167.77, 149.81, 144.48, 142.99, 128.21, 125.37, 116.31, 110.94, 105.04, 59.74, 50.86, 46.17, 37.96, 31.16, 27.18, 19.30, 14.38. [M+H] e: 368.21, o: 368.2. $[\alpha]_D$ = +4.2 (c 1.61, $CHCl_3$). Yield 92-94%.

Ethyl 4-(2-chlorophenyl)-2,7,7-trimethyl-5-oxo-1,4,5,6,7,8-hexahydroquinoline-3-carboxylate (**4n**): ^{1}H δ ($CDCl_3$) 7.39-7.37 (1H, d), 7.24-7.22 (1H, d), 7.13-7.09 (1H, t), 7.03-7.00 (1H, t), 6.76 (1H, s), 5.38 (1H, s), 4.07-4.00 (2H, m), 2.33-2.23 (2H, dd), 2.27 (3H, s), 2.18-2.08 (2H, dd), 1.19-1.15 (3H, t), 1.05 (3H, s), 0.93 (3H, s). ^{13}C δ ($CDCl_3$) 195.61, 167.44, 149.44, 143.73, 133.09, 129.68, 127.13, 126.34, 110.83, 110.27, 105.21, 59.29, 50.55, 40.89, 35.84, 32.48, 29.10, 27.10, 18.98, 14.17. [M+H] e: 374.14, o: 374.1. $[\alpha]_D$ = +8.6 (c 1.67, $CHCl_3$). Yield 89-94%.

Ethyl 4-(biphenyl-4-yl)-2,7,7-trimethyl-5-oxo-1,4,5,6,7,8-hexahydroquinoline-3-carboxylate (**4o**): ^{1}H δ ($CDCl_3$) 7.53-7.51 (2H, d), 7.44-7.36 (6H, m), 7.30-7.28 (1H, d),

6.50 (1H, s), 5.10 (1H, s), 4.10-4.05 (2H, m), 2.38 (3H, s), 2.36-2.26 (2H, dd), 2.22-2.14 (2H, dd), 1.23-1.20 (3H, t), 1.07 (3H, s), 0.95 (3H, s). ^{13}C δ ($CDCl_3$) 195.60, 167.40, 148.87, 146.12, 143.51, 141.13, 138.75, 128.57 126.91, 111.87, 106.11, 59.85, 50.63, 41.00, 36.30, 32.71, 29.39, 27.19, 19.35, 14.21. [M+H] e: 416.21, o: 416.2. $[\alpha]_D$ = +12 (c 1.75, $CHCl_3$). Yield 72-77%.

Ethyl 4-sec-butyl-2,7,7-trimethyl-5-oxo-1,4,5,6,7,8-hexahydroquinoline-3-carboxylate (**4p**): ^{1}H δ ($CDCl_3$) 6.11 (1H, s), 4.21-4.10 (2H, m), 4.08-4.07 (1H, d), 2.31-2.24 (4H, dd), 2.30 (3H, s), 2.22-2.18 (1H, dd), 1.37-1.30 (2H, m), 1.29-1.26 (3H, t), 1.08 (6H, d), 0.87-0.83 (3H, t), 0.73-0.71 (3H, t). ^{13}C δ ($CDCl_3$) 196.27, 168.36, 143.91, 110.37, 104.75, 59.66, 50.96, 43.23, 41.27, 32.38, 29.87, 27.00, 25.56, 19.08, 14.67, 12.29. [M+H] e: 320.21, o: 320.2. $[\alpha]_D$= -0.33 (c 2.4, $CHCl_3$). Yield 66%.

Ethyl 2,4,7,7-tetramethyl-5-oxo-1,4,5,6,7,8-hexahydroquinoline-3-carboxylate (**4q**): ^{1}H δ ($CDCl_3$) 6.19 (1H, s), 4.21-4.10 (2H, m), 3.93-3.88 (1H, dd), 2.31-2.14 (4H, dd), 2.28 (3H, t), 1.29-1.25 (3H, t), 1.07-1.06 (6H, d), 0.99-0.97 (3H,d). ^{13}C δ ($CDCl_3$) 195.83, 167.70, 149.08, 143.68, 112.63, 106.99, 59.64, 50.81, 41.00, 32.66, 29.47, 26.97, 25.44, 19.24, 14.38. [M+H] e: 278.17, o: 278.2. $[\alpha]_D$= +0.67 (c1.48, $CHCl_3$). Yield 72%.

Ethyl 2,7,7-trimethyl-5-oxo-4-(1,4-dioxaspiro[4.5]decan-2-yl)-1,4,5,6,7,8-hexahydroquinoline-3-carboxylate (**4r**): ^{1}H δ ($CDCl_3$) 5.83-5.66 (1H, d), 4.32-4.30 (1H, m), 4.26-4.11 (2H, m), 3.99-3.92 (1H, m), 3.84-3.79 (1H, m), 3.73-3.66 (1H, m), 2.44-2.16 (4H, t), 1.55-1.43 (6H, dd), 1.38-1.20 (4H, m), 1.15-1.05 (3H, t). [M+H] e: 404.24, o: 404.2. Yield 75%.

3.4.3 Synthesis of Compounds 5a-b (Scheme 3-4).

Component 1 dimedone (1.5eq, 0.6mmol) and component 3 ethylacetoacetate

(1eq, 0.4mmol) were suspended along with 10mol% $Yb(OTf)_3$ in 1mL of acetonitrile. After stirring under inert gas for 10min, component 2 (1eq, 0.4mmol) and ammonium acetate (1eq, 0.4mmol) were added. The reaction was allowed to stir for 3-5h. All reactions were precipitated by the addition of ice/water. Following precipitation the reactions were recrystallized with an ethanol/water system. The product was then added to a round bottom flask diluted with toluene and Lawesson's reagent (2.2 equiv) was added and the reaction was refluxed for 1-2 hours. The resulting product was purified by column chromatography (eluting with 25/75 ethylactetate/hexanes).

3.4.4 Characterization of Compounds 5a-b.

O-ethyl 4-(2,4-dichlorophenyl)-2,7,7-trimethyl-5-oxo-1,4,5,6,7,8-hexahydroquinoline-3-carbothioate (**5a**): ^{1}H δ ($CDCl_3$) 7.33-7.31 (1H, d), 7.24 (1H, s), 7.11-7.08 (1H, d), 6.53 (1H, s), 5.33 (1H,s), 4.07-3.99 (2H, m), 2.30 (3H, s), 2.29-2.21 (2H, dd), 2.18-2.09 (2H, dd), 1.19-1.16 (3H, t), 1.06 (3H, s), 0.94 (3H, s). [M+H] e: 424.08, o: 424.1. Yield 89-94%.

O-ethyl 2,7,7-trimethyl-5-oxo-4-phenyl-1,4,5,6,7,8-hexahydroquinoline-3-carbothioate (**5b**): ^{1}H δ ($CDCl_3$) 7.3-7.29 (2H, d), 7.21-7.17 (2H, t), 7.11-7.07 (1H, t),5.93 (1H, s), 5.05 (1H, s), 4.08-4.03 (2H, m), 2.37 (3H, s),2.34-2.2.22 (2H, dd), 2.21-2.13 (2H, dd), 1.21-1.17 (3H, t), 1.07 (3H, s), 0.93 (3H, s). [M+H] e: 356.16, o: 356.2. Yield 82-85%.

3.4.5 Synthesis of Compounds 7a-d (Scheme 3-5), 10a-d (Scheme 3-6), and 11a-k (Scheme 3-7).

The synthesis of compounds 7, 10, and 11 necessitated adding the amine (1 eq, 0.4 mmol) component to the beta-keto ester (1 eq, 0.4 mmol) in acetonitrile. The two

components were then stirred for 30 minutes. The catalyst $Yb(OTf)_3$ (10 mol %), the aldehyde (1 eq, 0.4 mmol), and 1,3-diketone (1.5 eq, 0.6 mmol) were then added to the reaction vessel and allowed to stir for the required amount of time. The reactions were added to brine and extracted with ethylacetate. Following concentration, these products were also recrystallized from ethanol.

3.4.6 Characterization of Compounds 7a-d, 10a-d, and 11a-k.

4-(4-(2,4-dichlorophenyl)-3-(ethoxycarbonyl)-2,7,7-trimethyl-5-oxo-5,6,7,8-tetrahydroquinolin-1(4H)-yl)butanoic acid (**7a**): ^{1}H δ ($CDCl_3$) 11.87, 7.39-7.09 (2H, dd), 7.06-6.95 (1H, d), 5.61-5.51 (1H, t), 4.84- 4.74 (1H, t), 3.21-3.11 (2H, t), 2.52-2.38 (6H, m), 2.35-2.29 (3H, t), 2.27-2.17 (2H, dd), 2.12-1.94 (2H, dd), 1.25-1.20 (4H, t), 1.15-0.99 (12H, d), 0.99-0.88 (3H), t). [M+H] e: 494.14, o: 494.1. Yield 71%.

Ethyl 4-(2,4-dichlorophenyl)-1-(4-hydroxybutyl)-2,7,7-trimethyl-5-oxo-1,4,5,6,7,8-hexahydroquinoline-3-carboxylate (**7b**): ^{1}H δ ($CDCl_3$) 7.32-7.25 (2H, m), 7.24-6.98 (1H, m), 4.91 (1H, bs), 4.15-3.97 (2H, m), 3.09-2.82 (2H, bd), 2.47 (3H, m), 2.42-2.15 (2H,m), 2.07-1.97 (1H, t), 1.58-1.46 (3H, t), 1.30-1.25 (2H, d), 1.24-0.83 (10H, m). [M+H] e: 480.16, o: 480.2. Yield 74%.

Ethyl 4-(2,4-dichlorophenyl)-1-(3-hydroxyphenyl)-2,7,7-trimethyl-5-oxo-1,4,5,6,7,8-hexahydroquinoline-3-carboxylate (**7c**): ^{1}H δ ($CDCl_3$) 7.60-7.58 (1H, d), 7.38-7.29 (1H, m), 7.25-7.04 (2H, m), 7.04-6.93 (2H, m), 6.78-6.53 (1H, dd), 6.44-6.34 (1H,dd), 5.63 (1H, s), 5.46 (1H, d), 4.15-4.05 (2H, m), 2.39-2.19 (2H, dd), 2.15-2.08 (2H, d), 2.08-2.05 (3H, s), 1.97-1.89 (1H, t), 1.28-1.24 (2H, t), 1.19-1.02 (3H, t), 0.98-0.84 (6H, d). [M+H] e: 500.13, o: 500.1. Yield 82%.

Ethyl 1-benzyl-4-(2,4-dichlorophenyl)-2,7,7-trimethyl-5-oxo-1,4,5,6,7,8-hexahydroquinoline-3-carboxylate (**7d**): ^{1}H δ ($CDCl_3$) 7.31-6.72 (9H), 5.31 (1H, s), 5.06-5.00 (2H, q), 2.32-2.25 (3H, s), 2.24-2.12 (3H, dd), 2.10-2.04 (2H, dd), 1.08 (3H, s), 0.96(3H, s). [M+H] e: 498.15, o: 498.2. Yield 77%.

Ethyl 4-(2,4-dichlorophenyl)-2-methyl-5-oxo-4,5-dihydro-1H-indeno[1,2-b]pyridine-3-carboxylate (**10a**): ^{1}H δ ($CDCl_3$) 7.93-7.10 (7H), 5.36 (1H, t), 4.09-3.98 (2H, m), 2.78-2.68 (3H, t), 2.39-2.24 (2H, dt), 1.34-1.28 (3H, m), 1.10-0.86 (3H, m). [M+H] e: 414.06, o: 414.1. Yield 71%.

Ethyl 5-acetyl-4-(2,4-dichlorophenyl)-2,6-dimethyl-1,4-dihydropyridine-3-carboxylate (**10b**): ^{1}H δ ($CDCl_3$) δ 7.31-7.09 (3H), 6.15 (1H, s), 5.43-5.33 (1H, t), 4.13-4.07 (2H, m), 2.32-2.28 (3H, t), 2.22-2.12 (6H, t),1.32-1.22 (3H, t). [M+H] e: 368.07, o: 368.1. Yield 75%.

Methyl 4-(2,4-dichlorophenyl)-2,7,7-trimethyl-5-oxo-1,4,5,6,7,8-hexahydroquinoline-3-carboxylate (**10c**): ^{1}H δ ($CDCl_3$) 7.35-7.16 (2H, m), 7.11-7.04 (1H, m), 6.44 (1H, bs), 5.38-5.28 (1H, t), 3.83-3.54 (3H, t), 2.37-2.27 (3H, t), 2.24-2.05 (4H, d), 1.24-1.02 (3H, t), 1.00-0.80 (3H, t). [M+H] e: 394.09, o: 394.1. Yield 82%.

Benzyl 4-(2,4-dichlorophenyl)-2,7,7-trimethyl-5-oxo-1,4,5,6,7,8-hexahydroquinoline-3-carboxylate (**10d**): ^{1}H δ ($CDCl_3$) 7.31-6.99 (7H, m), 6.98 (1H, d), 6.72 (1H, s), 5.31 (1H, s), 5.03- 5.00 (2H, q), 2.27 (3H, t), 2.25-2.16 (4H, d), 2.12-2.04 (2H,dd), 1.08-1.03 (3H, t), 0.98-0.91 (3H, t). [M+H] e: 470.12, o: 470.1. Yield 85%.

Benzyl 5-acetyl-4-(2,4-dichlorophenyl)-2,6-dimethyl-1,4-dihydropyridine-3-carboxylate (**11a**): ^{1}H δ ($CDCl_3$) 7.38-7.10 (8H), 6.28 (1H, t), 5.43 (1H, t), 5.21-5.11 (2H, t), 2.39-2.34 (3H, t), 2.33-2.21 (6H, t). [M+H] e: 430.09, o: 430.1. Yield 81%.

5-acetyl-N-(cyclohexylmethyl)-4-(2,4-dichlorophenyl)-2,6-dimethyl-1,4-dihydropyridine-3-carboxamide (**11b**): ^{1}H δ ($CDCl_3$) 8.20 (1H, s), 7.31-7.21 (3H), 6.90 (1H, m), 5.39 (1H, s), 3.77-3.60 (2H, dq), 3.18-2.96 (6H, m), 2.81 (3H, t), 2.37-2.30 (3H, dd), 1.99-1.58 (10H, m), 1.30-1.17 (3H, m). [M+H] e: 435.15, o: 435.2. Yield 82%.

5-acetyl-N-(4-(tert-butyl)benzyl)-4-(2,4-dichlorophenyl)-2,6-dimethyl-1,4-dihydropyridine-3-carboxamide (**11c**): ^{1}H δ ($CDCl_3$) 7.34-7.09 (7H, m), 5.37 (1H, t), 4.12-4.09 (2H, m), 3.08-2.66 (2H, dd), 2.54-2.28 (3H, m), 2.27-2.13 (6H, m), 1.41-1.15 (9H, m). [M+H] e: 485.17, o: 485.2. Yield 76%.

Ethyl 5-acetyl-4-(2,4-dichlorophenyl)-1-(4-hydroxybutyl)-2,6-dimethyl-1,4-dihydropyridine-3-carboxylate (**11d**): ^{1}H δ ($CDCl_3$) 7.41-7.09 (3H, m), 4.63- 4.55 (1H, m), 4.09 (2H, m), 2.56 (2H, m), 2.26-1.80 (4H, m), 1.76-1.59 (6H, t), 1.30-1.22 (6H, t), 1.18-1.03 (3H, m). [M+H] e: 440.13, o: 440.1. Yield 69%.

Ethyl 5-acetyl-1-benzyl-4-(2,4-dichlorophenyl)-2,6-dimethyl-1,4-dihydropyridine-3-carboxylate (**11e**) ^{1}H δ ($CDCl_3$) 7.36-7.19 (8H), 4.49 (1H, d), 4.44-4.40 (2H, m), 4.38 (2H, m), 3.47-3.37 (3H, t), 2.29 (6H, t), 1.99 (3H, t). [M+H] e: 458.12, o: 458.1. Yield 82%.

Ethyl 5-acetyl-2,6-dimethyl-4-(naphthalen-2-yl)-1,4-dihydropyridine-3-carboxylate (**11f**): ^{1}H δ ($CDCl_3$) 7.76-7.39 (7H), 6.23 (1H, t), 5.20 (1H, t), 4.19-4.14 (3H, m), 2.39-2.33 (3H, t), 2.28-2.19 (6H, t), 1.34-1.24 (3H, m). [M+H] e: 350.17, o: 350.2. Yield 71%.

Ethyl 5-acetyl-4-(4-bromophenyl)-2,6-dimethyl-1,4-dihydropyridine-3-carboxylate (**11g**): ^{1}H δ ($CDCl_3$) 7.35-7.24 (2H, m), 7.18-7.08 (2H, m), 6.19 (1H, t), 5.01-4.96 (1H, m), 4.17-4.08 (2H, m), 2.36-2.25 (6H, t), 2.23-2.18 (3H, t), 1.30-1.18 (3H, m). [M+H] e: 378.06, o: 378.1. Yield 84%.

Ethyl 5-acetyl-4-(3-fluorophenyl)-2,6-dimethyl-1,4-dihydropyridine-3-carboxylate (**11h**): ^{1}H δ ($CDCl_3$) 7.31-7.13 (, 7.01, 7.00, 6.99, 6.98, 6.72, 5.31, 5.06, 5.03, 5.03, 5.00, 4.12, 4.11, 2.32, 2.27, 2.25, 2.24, 2.22, 2.20, 2.17, 2.16, 2.12, 2.10, 2.08, 2.07, 2.07, 2.06, 2.04, 2.04, 1.27, 1.27, 1.26, 1.25, 1.24, 1.24, 1.08, 1.07, 1.03, 0.98, 0.96, 0.94, 0.93, 0.91. [M+H] e: 318.14, o: 318.1. Yield 82%.

Ethyl 5-acetyl-2,6-dimethyl-4-(4-(pyridin-2-yl)phenyl)-1,4-dihydropyridine-3-carboxylate (**11i**): ^{1}H δ ($CDCl_3$) 7.76-7.39 (7H), 6.23 (1H, t), 5.20 (1H, t), 4.19-4.14 (3H, m), 2.39-2.33 (3H, t), 2.28-2.19 (6H, t), 1.34-1.24 (3H, m). [M+H] e: 377.18, o: 377.2. Yield 79%.

Ethyl 5-acetyl-2,4,6-trimethyl-1,4-dihydropyridine-3-carboxylate (**11j**): ^{1}H δ ($CDCl_3$) 5.86 (1H, s), 4.24-4.15 (2H, m), 3.81 (1H, m), 2.32-2.14 (9H, t), 1.36-1.23 (3H, m), 1.01-0.90 (3H, t). [M+H] e: 238.14, o: 238.1. Yield 71%.

Ethyl 5-acetyl-4-(sec-butyl)-2,6-dimethyl-1,4-dihydropyridine-3-carboxylate (**11k**): ^{1}H NMR δ ($CDCl_3$) 5.72 (1H, t), 4.25-4.12 (2H, m), 3.93-3.89 (1H, m), 2.63-2.51 (1H, m), 2.37-2.18 (9H, t), 1.44-1.17 (6H, m), 1.01-0.77 (3H, m), 0.77-0.65 (2H, m). [M+H] e: 280.18, o: 280.2. Yield 74%.

3.4.7 Synthesis of Catalysts VI and VII

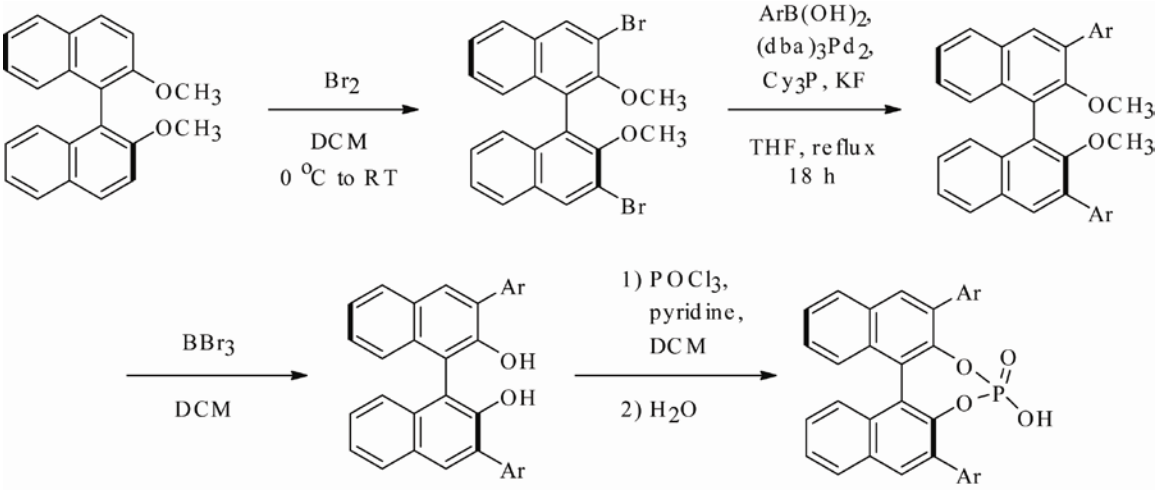

Scheme 3-8 . Synthesis of Catalyst VI and VII.

(S)-2,2'-dimethoxy-1,1'-binaphthyl (628.8mg, 2mmol) was added to 20mL of anhydrous dichloromethane. Once cooled down to 0°C, bromine (0.23mL, 4.5mmol) was added to the solution. After 1 hour, the solution was poured into 30 mL of saturated $NaHSO_3$. The mixture stirred for 1 hour. It was then extracted three times with dichloromethane. The organic layers were combined and dried over Na_2SO_4, filtered, and then concentrated. (S)-3,3'-dibromo-2,2'-dimethoxy-1,1'-binaphthyl (789.9mg, 1.7mmol), tris(dibenzylideneacetone) dipalladium (70mg, 0.077mmol), tricyclohexylphosphine (71.5mg, 0.255mmol), potassium fluoride (612.3mg, 10.54mmol), and an aryl boronic acid (5.1mmol) were added to a flame dried round bottom flask and 10mL of anhydrous tetrahydrofuran was added. For catalyst VI phenylboronic acid was employed while for catalyst VII 3,5-dimethylphenylboronic acid was employed. The reaction was allowed to reflux for 18 hours for both catalysts. Following cooling down to room temperature the reaction was diluted with ethylacetate and then filtered through a pad of celite. The organic was then concentrated and purified by a flash chromatography on silica. The product eluted with 1:1 benzene:hexanes giving a 90% yield for the catalyst VI precursor

and 82% yield for the catalyst VII precursor. Following the Suzuki coupling the methyl ether protecting group was removed by adding BBr_3 (for catalyst VI precursor 1.3415g, 5.36mmol and for catalyst VII 1.2188g, 4.865mmol) to the Suzuki product and stirring in 50mL dichloromethane at 0°C for 1 hour. It was allowed to warm to room temperature and then stirred for an additional 1 hour at room temperature. Water was then added to the reaction. The mixture was then diluted with dichloromethane. The organic layer was then dried over Na_2SO_4. The products were filtered and concentrated. Then they were purified by silica flash chromatography and eluted at 25:75 ethylacetate:hexanes. The yields obtained were 78% for the catalyst VI precursor and 81% for the catalyst VII precursor. Both unprotected catalyst precursors were dissolved in 3mL pyridine. To catalyst VI precursor 364.9mg (2.38mmol) of $POCl_3$ were added and stirred under nitrogen for 5 hours. To catalyst VII precursor 346.5mg (2.26mmol) of $POCl_3$ were added under nitrogen for 5 hours. After that time 3mL of water were added to each of the reactions. The reaction was stirred for 30 minutes. The reaction was then diluted with dichloromethane and was extracted with 1M HCl. The organic phases were dried over Na_2SO_4 and concentrated. The products were then purified by silica flash chromatography. The products eluted at 10:90 MeOH:CH_2Cl_2. The yield of catalyst VI was 75% yield (overall yield 0.89mmol, 44.5%) and for catalyst VII was 81% (overall yield 0.92, 46%).

3.4.8 Characterization of Catalysts VI and VII

All NMR collected and analyzed on Varian 400MHz system using VnmrJ™ version 2.2 revision C. Samples diluted in deuterated solvent immediately prior to data

collection. Mass spectrometry data collected on and Micromass LCT time-of-flight mass spectrometer in the ES+ mode.

Catalyst **VI**: ^{1}H δ (d-DMSO) 8.443 (2H, s), 8.276-8.253 (2H, d), 7.855-7.835 (4H, d), 7.793-7.771 (2H, d), 7.610-7.588 (2H, d), 7.546-7.489 (4H, m), 7.438-7.395 (4H, m). [M+H] e: 501.12, o: 501.1.

Catalyst **VII**: ^{1}H δ ($CDCl_3$) 8.12 (2H, s), 8.00-7.95 (3H, d), 7.58 (3H,s), 7.48-7.45 (4H, m), 7.33 (4H, s), 7.04 (2H, s), 2.41 (12H, s). [M+H] e: 557.18, o: 557.2.

Notes

This work has been published as "Enantioselective Organocatalytic Hantzsch Synthesis of Polyhydroquinolones," Evans, C.G. and Gestwicki, J.E., Org Lett, 2009, 11(14), 2957-9 and "Identification of Dihydropyridines That Reduce Cellular Tau Levels," Evans, C.G., Jinwal, U.K., Dickey, C.A., and Gestwicki, J.E., Chem Comm, submitted.

Author Contributions

Christopher G. Evans, Dr. Umesh K. Jinwal, Dr. Chad A. Dickey, and Dr. Jason E. Gestwicki designed the experiments;
Christopher G. Evans synthesized the dihydropyridine library and the phosphoric acid BINOL catalysts, chiral HPLC analysis, polarimetry, and quantification Western blot data;
Dr. Umesh K. Jinwal performed the tau stability experiments and performed the Western blots;
Dr. Gladis Walter performed the yeast polyQ assay and the microscopy.

3.5 Appendix of Selected ^{1}H NMR Spectra and HPLC Chromatograms

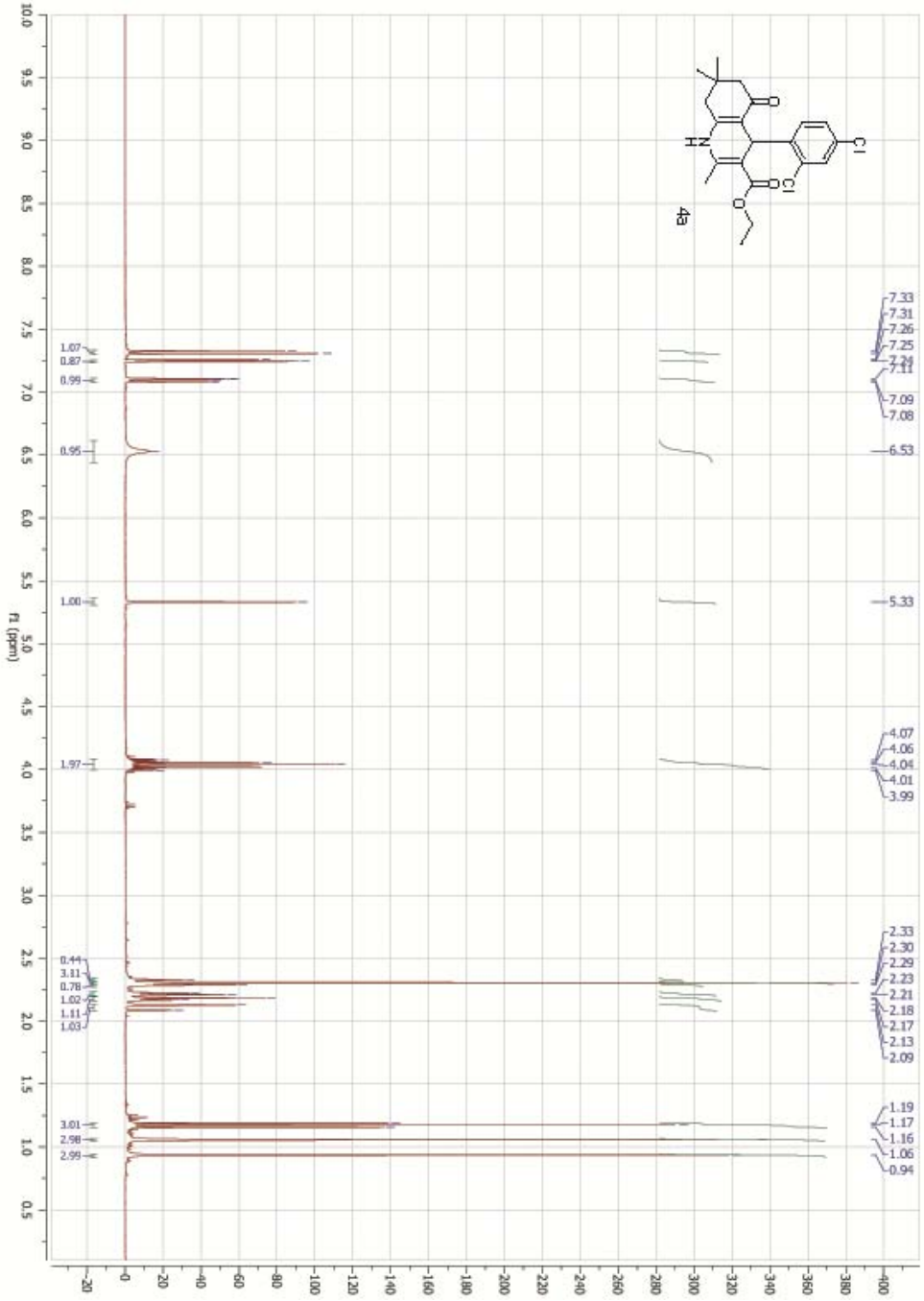

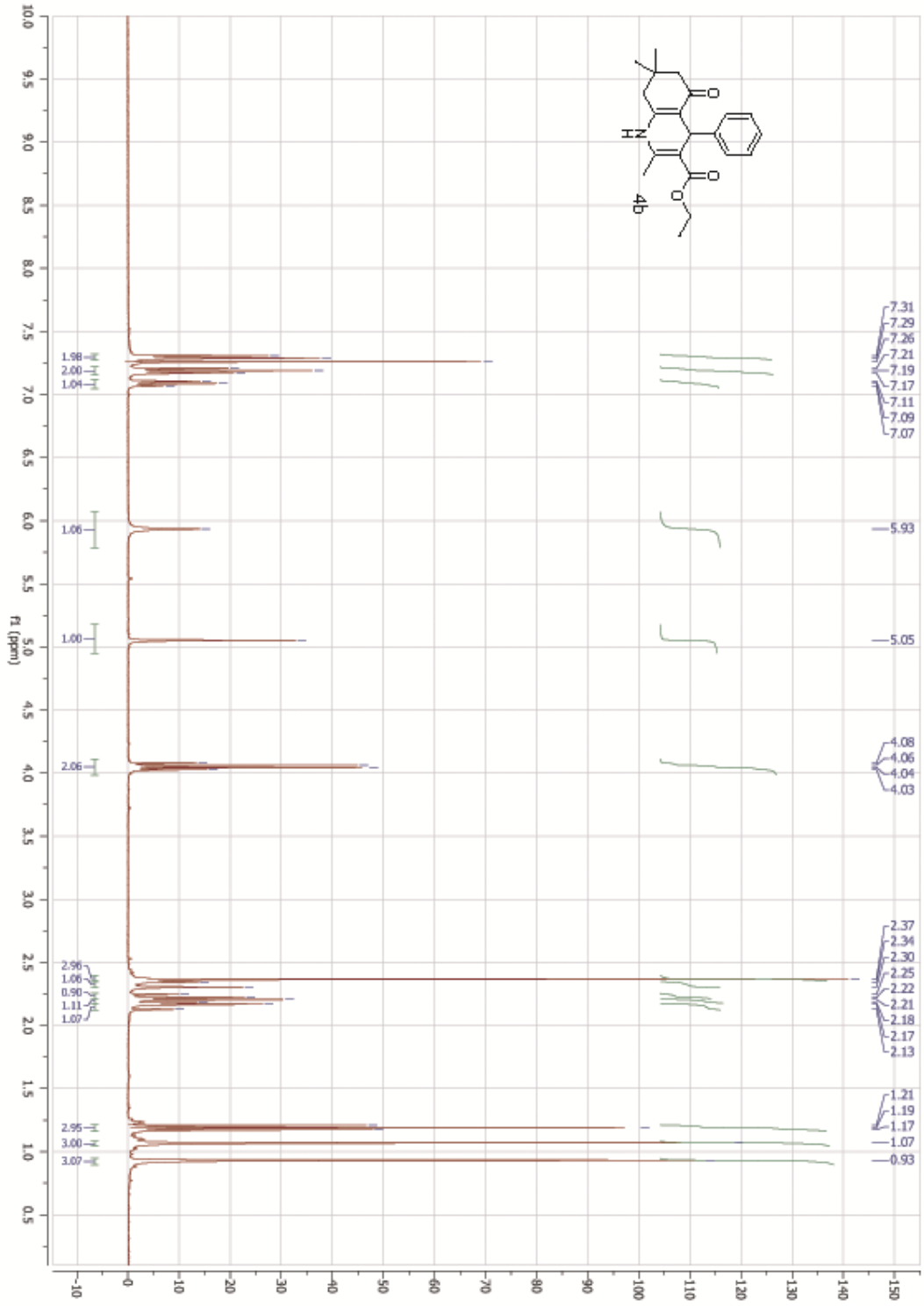
4b
f1 (ppm)
7.31
7.29
7.26
7.21
7.19
7.17
7.11
7.09
7.07
5.93
5.05
4.08
4.06
4.04
4.03
2.37
2.34
2.30
2.25
2.22
2.21
2.18
2.17
2.13
1.21
1.19
1.17
1.07
0.93
1.98
2.00
1.04
1.06
1.00
2.06
2.96
1.06
0.90
1.11
1.07
2.95
3.00
3.07

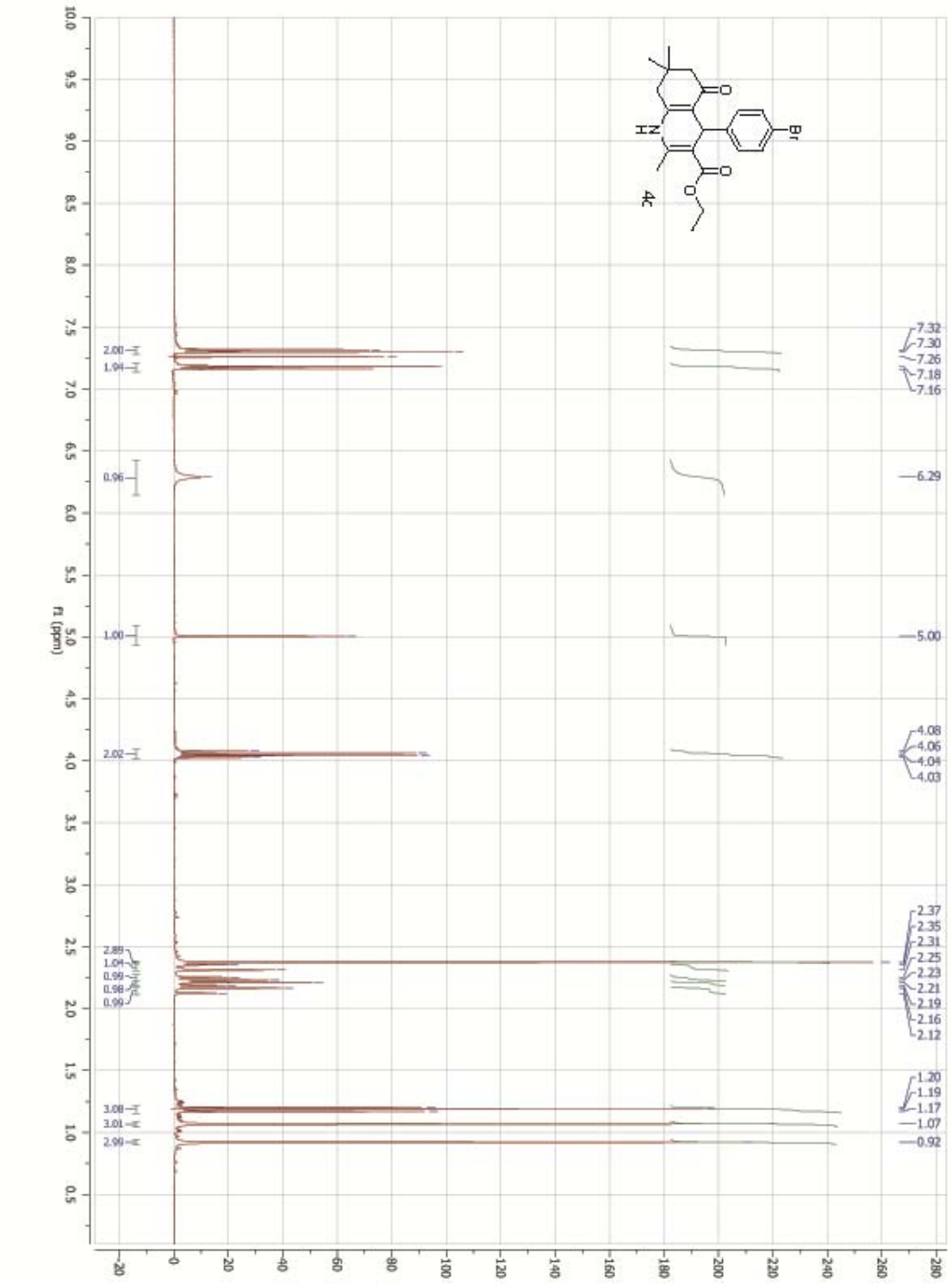
4c
f1 (ppm)
7.32
7.30
7.26
7.18
7.16
6.29
5.00
4.08
4.06
4.04
4.03
2.37
2.35
2.31
2.25
2.23
2.21
2.19
2.16
2.12
1.20
1.19
1.17
1.07
0.92

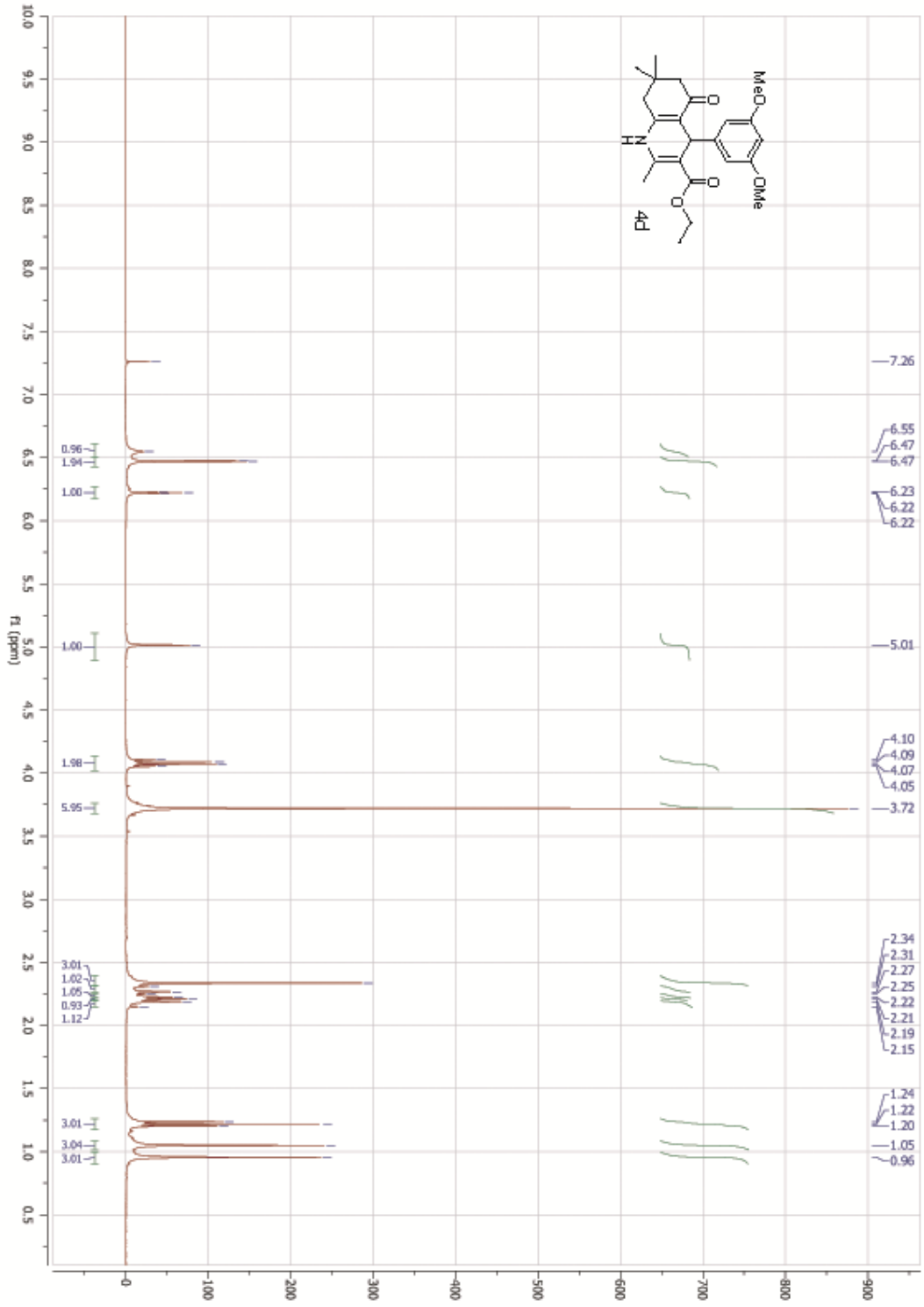
4d
MeO
OMe
O
O
O
H
N
f1 (ppm)
7.26
6.55
6.47
6.47
6.23
6.22
6.22
5.01
4.10
4.09
4.07
4.05
3.72
2.34
2.31
2.27
2.25
2.22
2.21
2.19
2.15
1.24
1.22
1.20
1.05
0.96
0.96
1.94
1.00
1.00
1.98
5.95
3.01
1.02
1.05
0.93
1.12
3.01
3.04
3.01

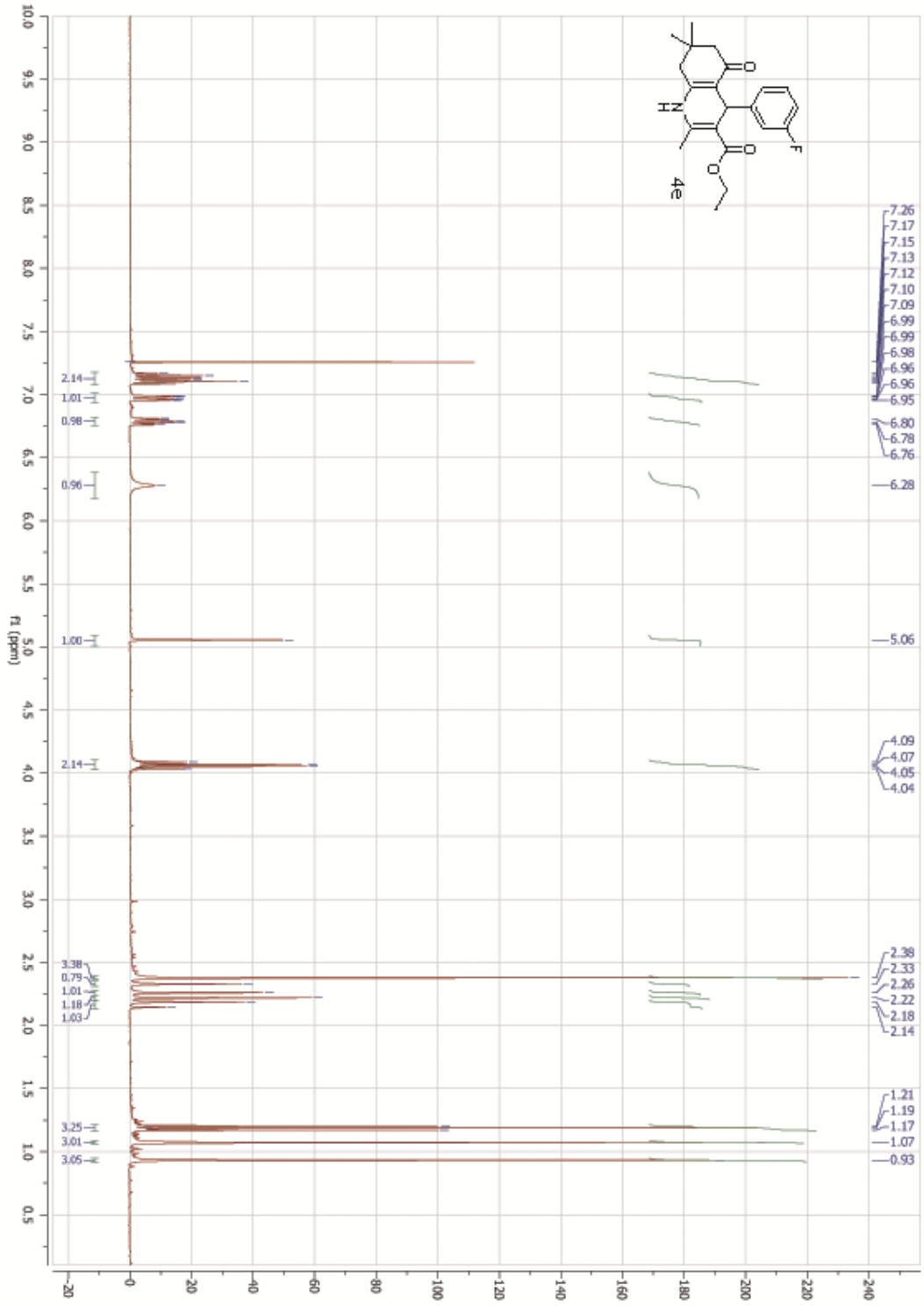
4e
f1 (ppm)
7.26
7.17
7.15
7.13
7.12
7.10
7.09
6.99
6.99
6.98
6.96
6.96
6.95
6.80
6.78
6.76
6.28
5.06
4.09
4.07
4.05
4.04
2.38
2.33
2.26
2.22
2.18
2.14
1.21
1.19
1.17
1.07
0.93
2.14
1.01
0.98
0.96
1.00
2.14
3.38
0.79
1.01
1.18
1.03
3.25
3.01
3.05

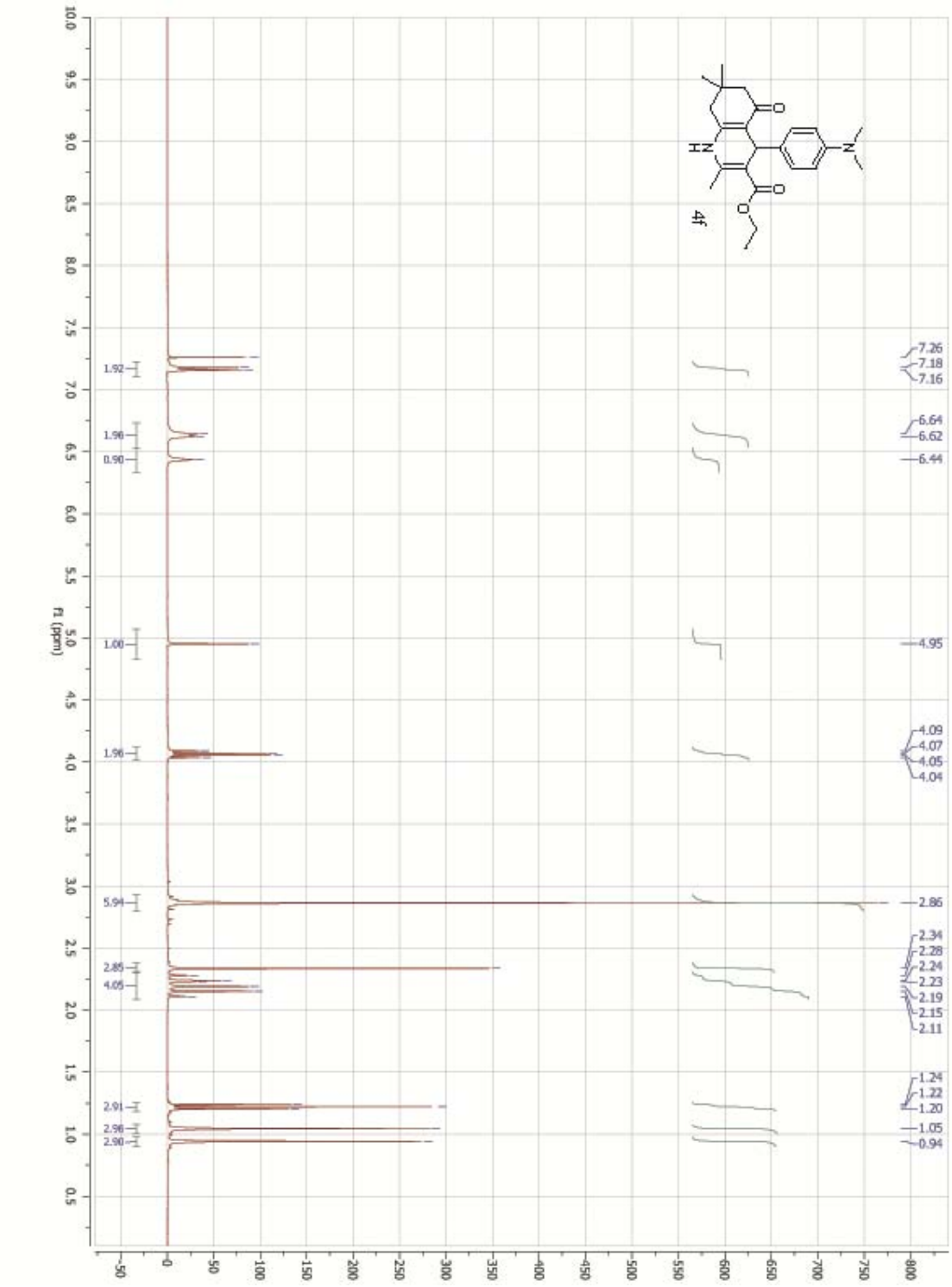
4f
f1 (ppm)
1.92
1.96
0.90
1.00
1.96
5.94
2.85
4.05
2.91
2.96
2.90
7.26
7.18
7.16
6.64
6.62
6.44
4.95
4.09
4.07
4.05
4.04
2.86
2.34
2.28
2.24
2.23
2.19
2.15
2.11
1.24
1.22
1.20
1.05
0.94

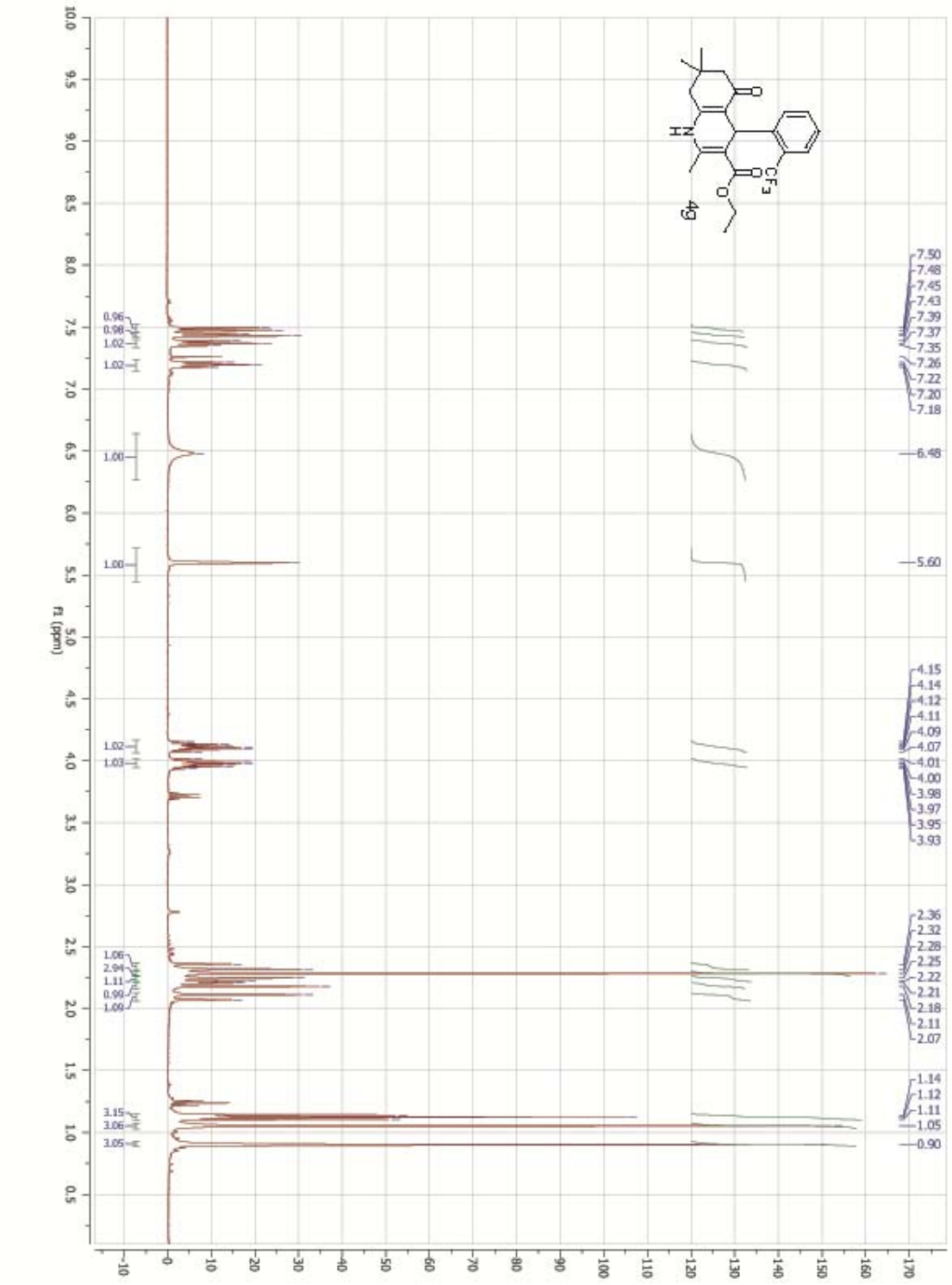
4g
f1 (ppm)

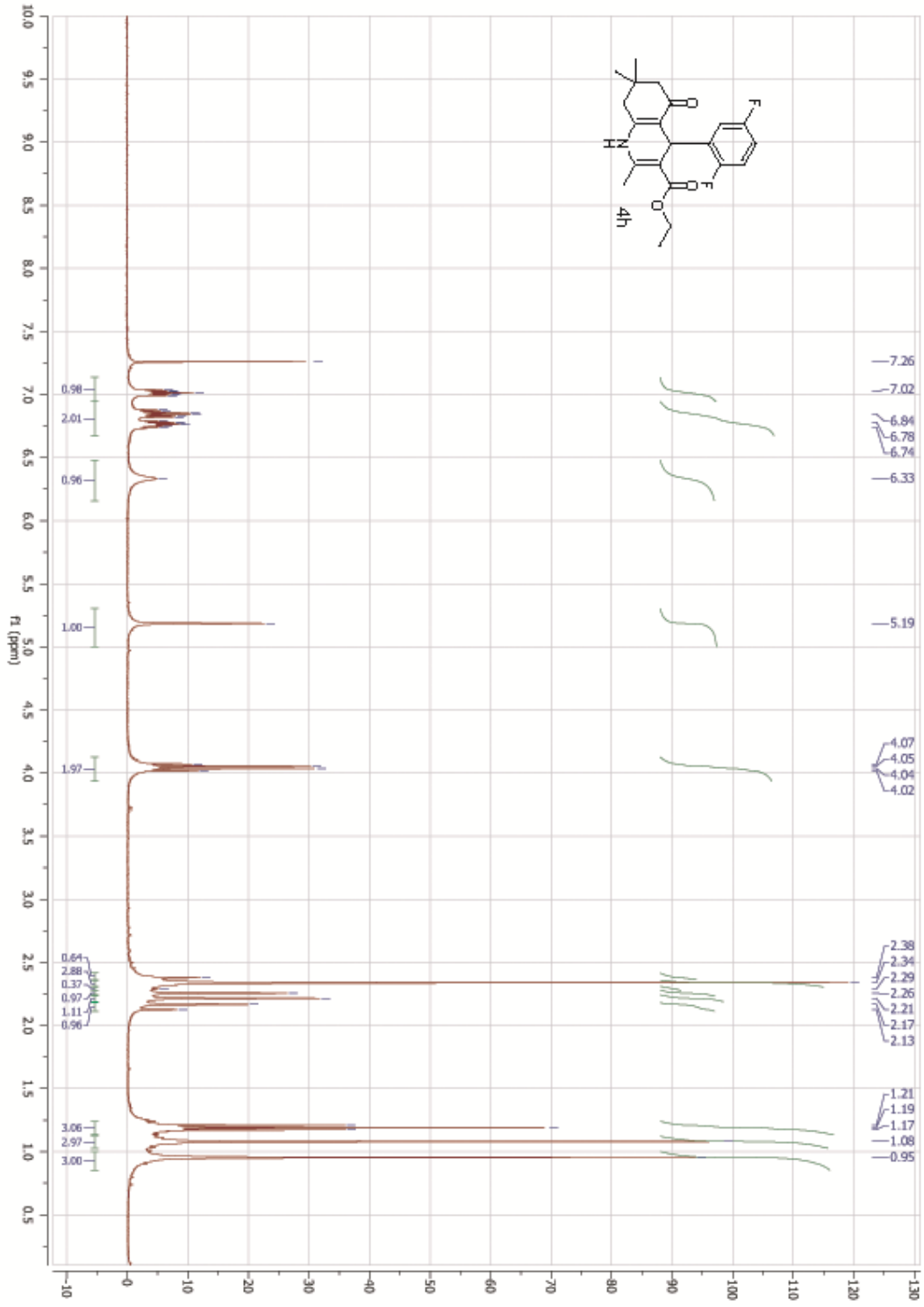
4h
f1 (ppm)
7.26
7.02
6.84
6.78
6.74
6.33
5.19
4.07
4.05
4.04
4.02
2.38
2.34
2.29
2.26
2.21
2.17
2.13
1.21
1.19
1.17
1.08
0.95
0.98
2.01
0.96
1.00
1.97
0.64
2.88
0.37
0.97
1.11
0.96
3.06
2.97
3.00

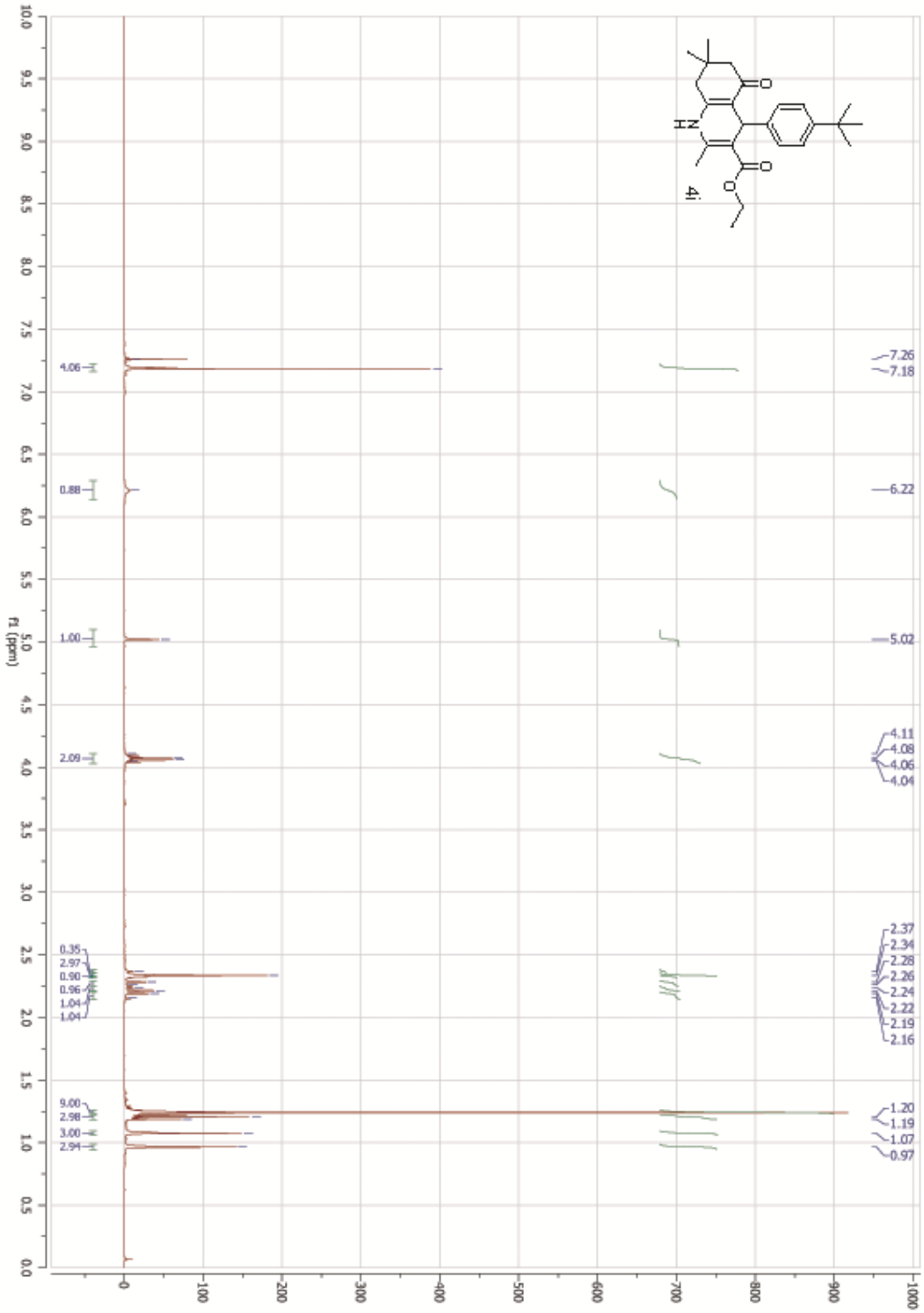
4i
f1 (ppm)
4.06
0.88
1.00
2.09
0.35
2.97
0.90
0.96
1.04
1.04
9.00
2.98
3.00
2.94
7.26
7.18
6.22
5.02
4.11
4.08
4.06
4.04
2.37
2.34
2.28
2.26
2.24
2.22
2.19
2.16
1.20
1.19
1.07
0.97

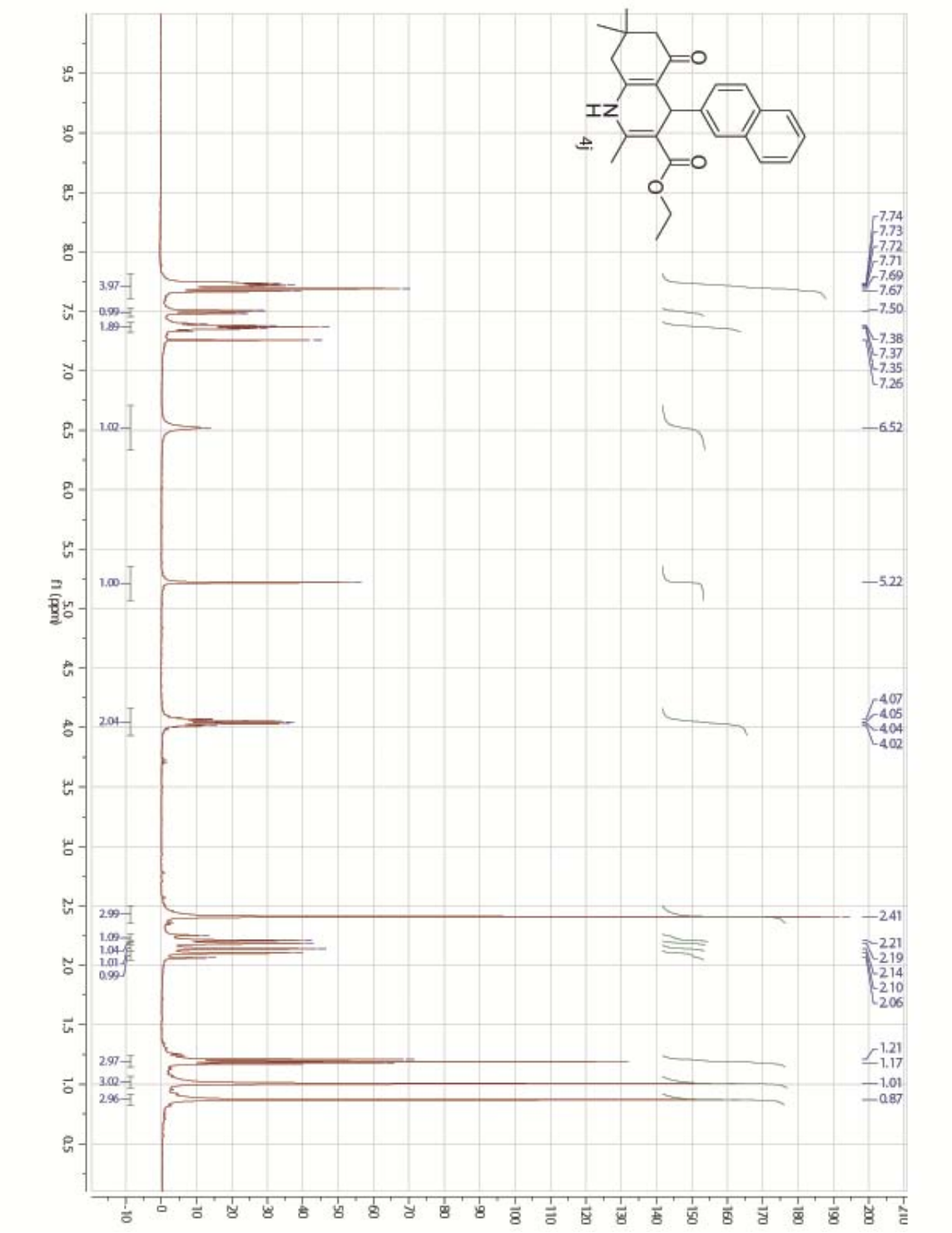
4j
f1 (ppm)
7.74
7.73
7.72
7.71
7.69
7.67
7.50
7.38
7.37
7.35
7.26
6.52
5.22
4.07
4.05
4.04
4.02
2.41
2.21
2.19
2.14
2.10
2.06
1.21
1.17
1.01
0.87
3.97
0.99
1.89
1.02
1.00
2.04
2.99
1.09
1.04
1.01
0.99
2.97
3.02
2.96

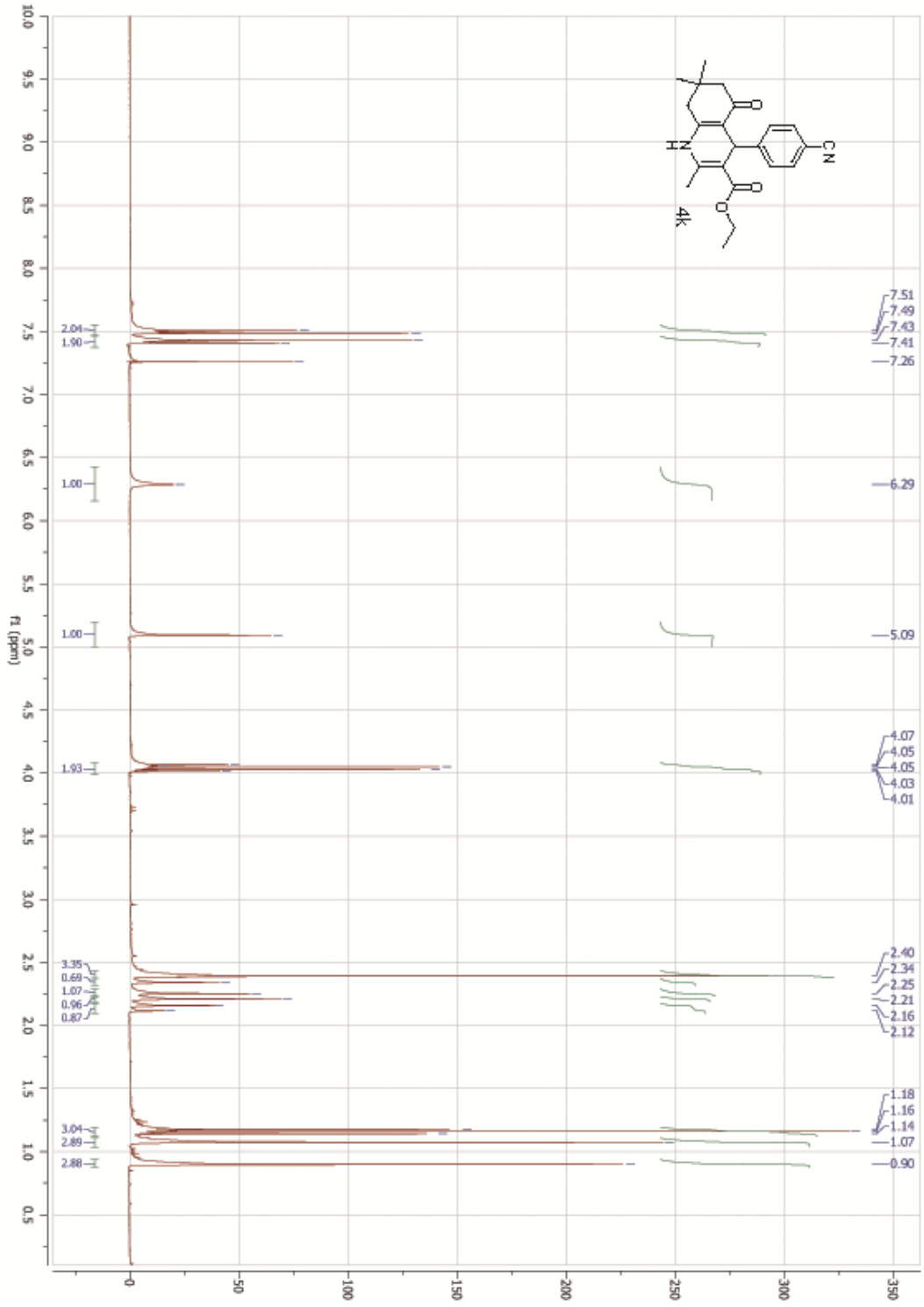
4k
f1 (ppm)
2.04
1.90
1.00
1.00
1.93
3.35
0.69
1.07
0.96
0.87
3.04
2.89
2.88
7.51
7.49
7.43
7.41
7.26
6.29
5.09
4.07
4.05
4.05
4.03
4.01
2.40
2.34
2.25
2.21
2.16
2.12
1.18
1.16
1.14
1.07
0.90

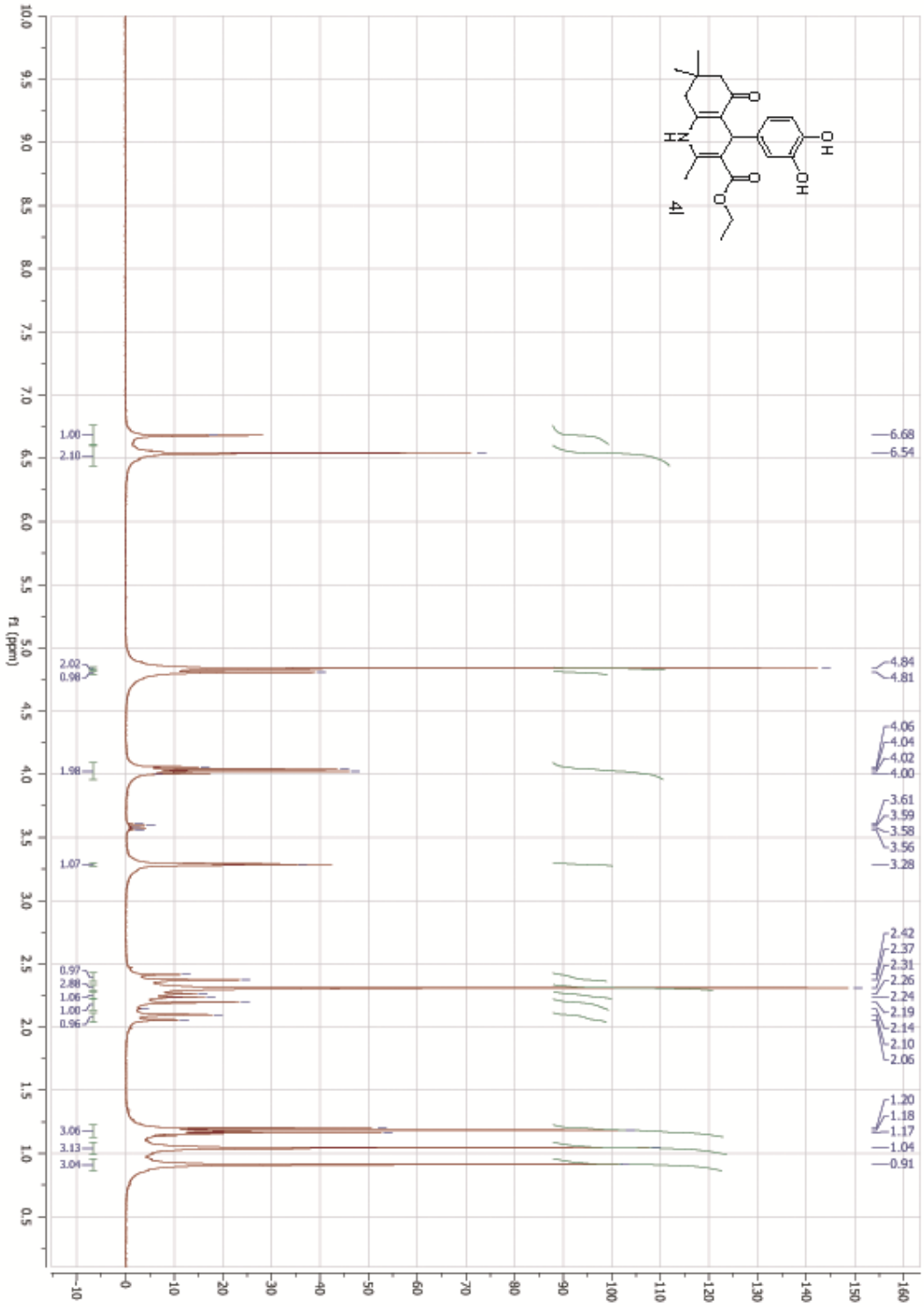
4l
f1 (ppm)
1.00
2.10
2.02
0.98
1.98
1.07
0.97
2.88
1.06
1.00
0.96
3.06
3.13
3.04
6.68
6.54
4.84
4.81
4.06
4.04
4.02
4.00
3.61
3.59
3.58
3.56
3.28
2.42
2.37
2.31
2.26
2.24
2.19
2.14
2.10
2.06
1.20
1.18
1.17
1.04
0.91

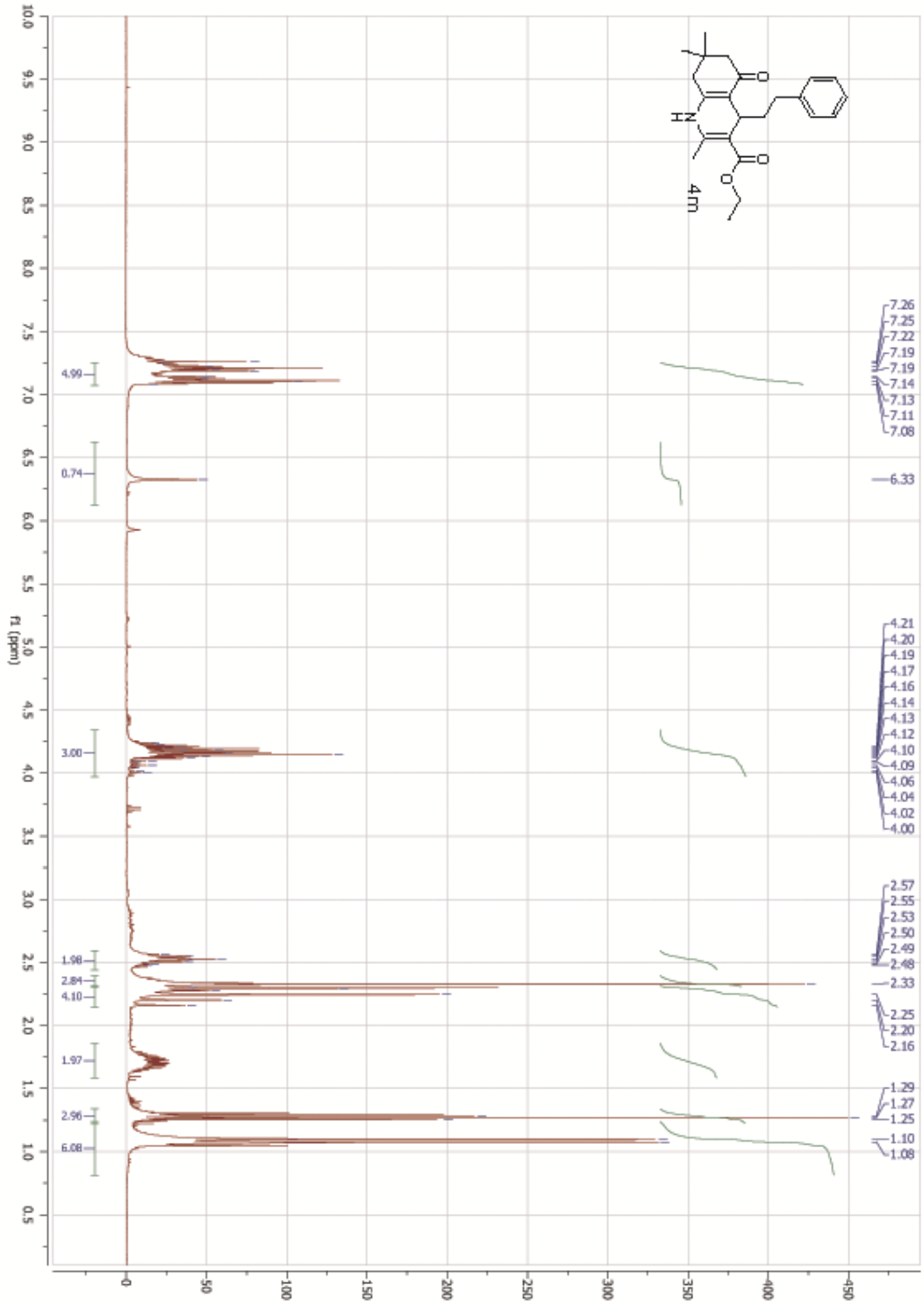
4m
f1 (ppm)
4.99
0.74
3.00
1.98
2.84
4.10
1.97
2.96
6.08
7.26
7.25
7.22
7.19
7.19
7.14
7.13
7.11
7.08
6.33
4.21
4.20
4.19
4.17
4.16
4.14
4.13
4.12
4.10
4.09
4.06
4.04
4.02
4.00
2.57
2.55
2.53
2.50
2.49
2.48
2.33
2.25
2.20
2.16
1.29
1.27
1.25
1.10
1.08

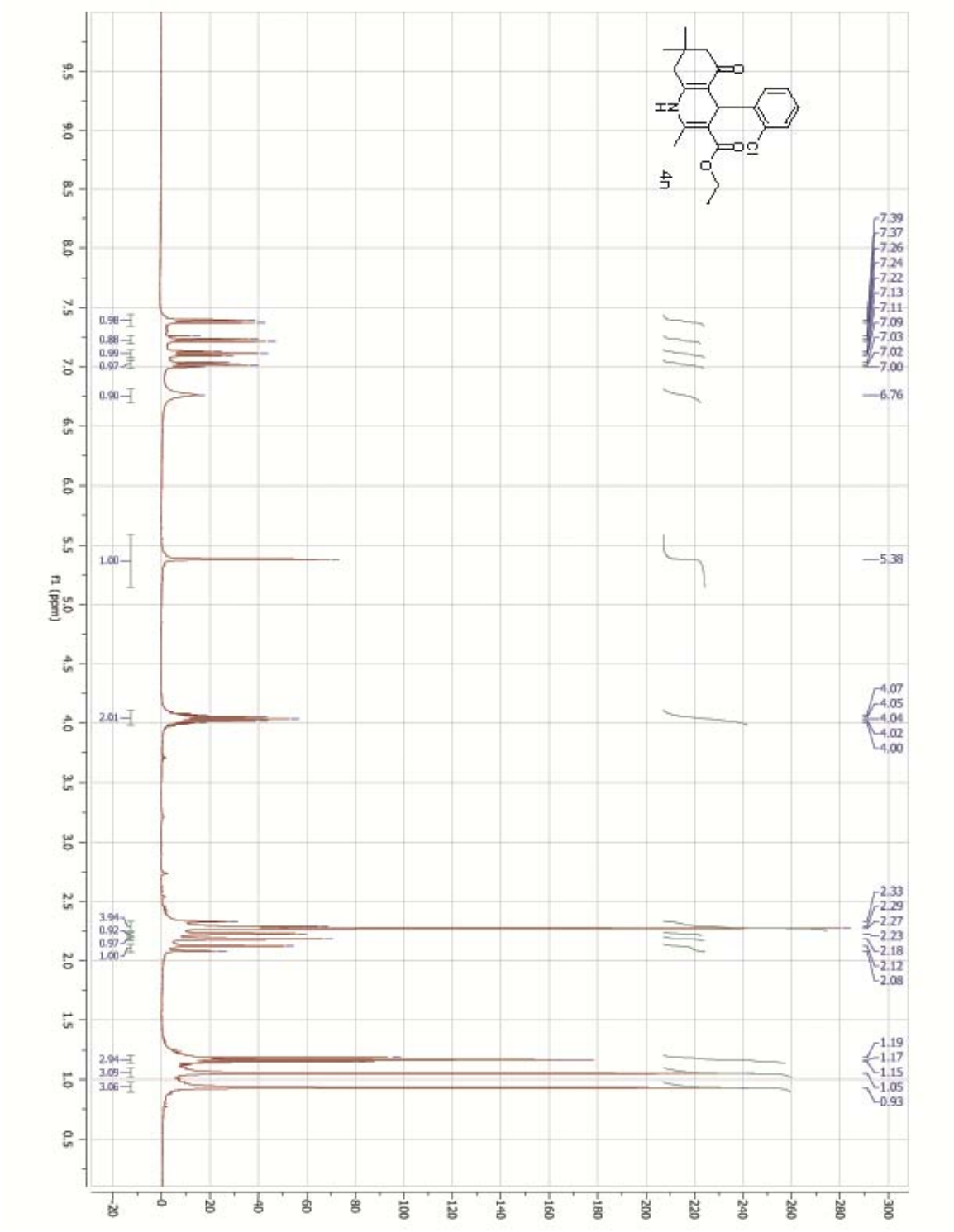
4n
7.39
7.37
7.26
7.24
7.22
7.13
7.11
7.09
7.03
7.02
7.00
6.76
5.38
4.07
4.05
4.04
4.02
4.00
2.33
2.29
2.27
2.23
2.18
2.12
2.08
1.19
1.17
1.15
1.05
0.93
0.98
0.88
0.99
0.97
0.90
1.00
2.01
3.94
0.92
0.97
1.00
2.94
3.09
3.06
f1 (ppm)

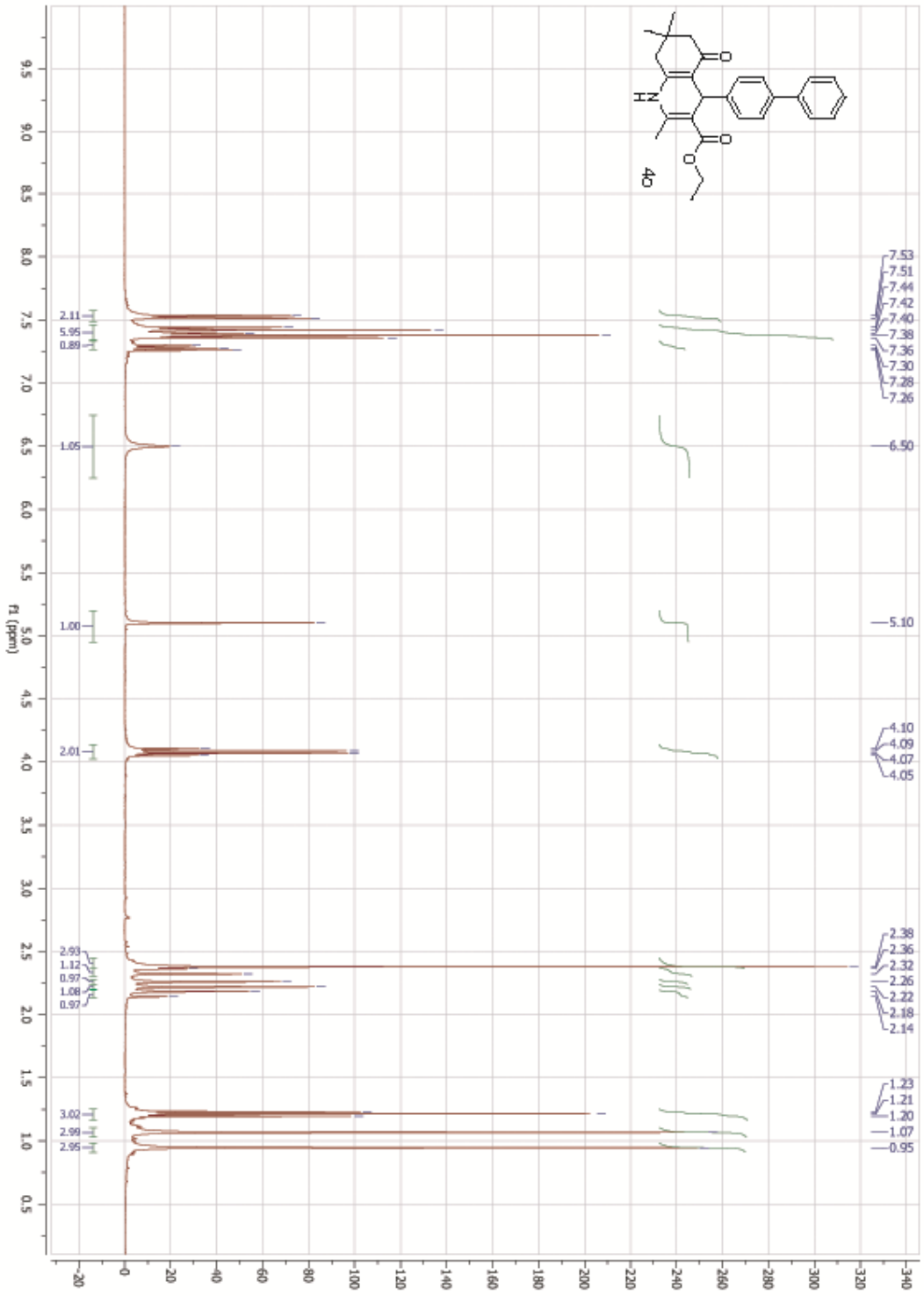
4o
f1 (ppm)
7.53
7.51
7.44
7.42
7.40
7.38
7.36
7.30
7.28
7.26
6.50
5.10
4.10
4.09
4.07
4.05
2.38
2.36
2.32
2.26
2.22
2.18
2.14
1.23
1.21
1.20
1.07
0.95
2.11
5.95
0.89
1.05
1.00
2.01
2.93
1.12
0.97
1.08
0.97
3.02
2.99
2.95

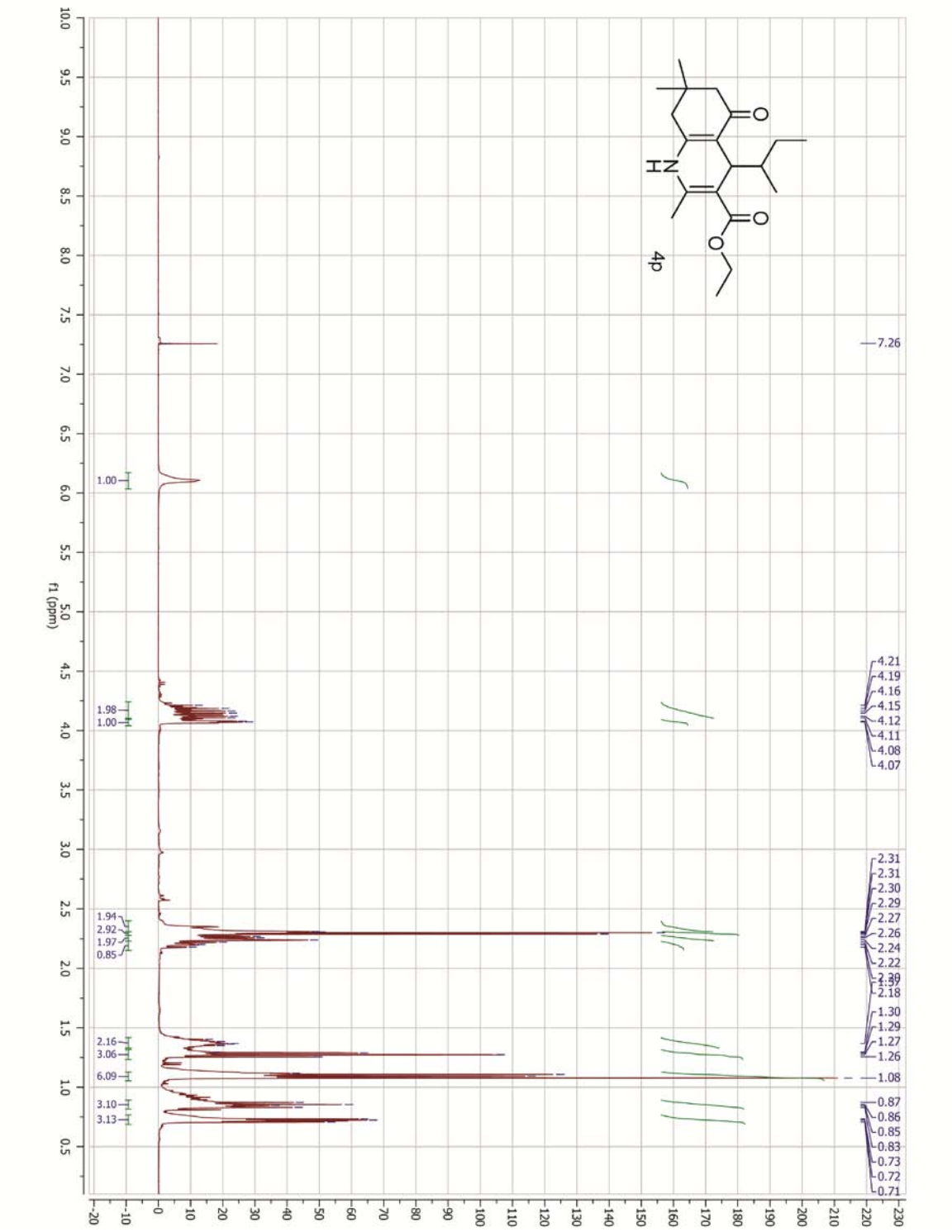
4p
f1 (ppm)
7.26
1.00
1.98
1.00
1.94
2.92
1.97
0.85
2.16
3.06
6.09
3.10
3.13
4.21
4.19
4.16
4.15
4.12
4.11
4.08
4.07
2.31
2.31
2.30
2.29
2.27
2.26
2.24
2.22
2.18
1.30
1.29
1.27
1.26
1.08
0.87
0.86
0.85
0.83
0.73
0.72
0.71

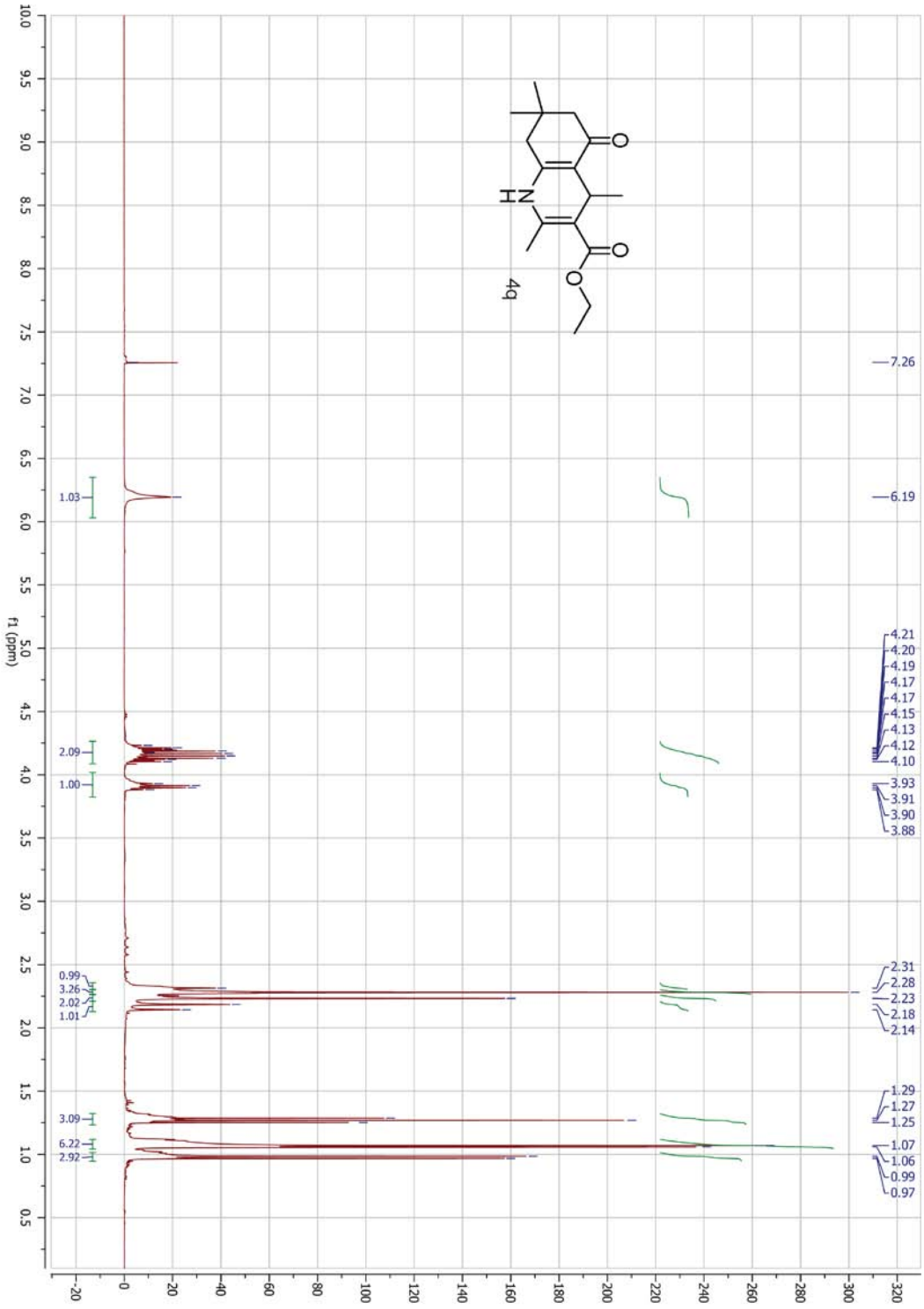
4q
7.26
6.19
4.21
4.20
4.19
4.17
4.17
4.15
4.13
4.12
4.10
3.93
3.91
3.90
3.88
2.31
2.28
2.23
2.18
2.14
1.29
1.27
1.25
1.07
1.06
0.99
0.97
1.03
2.09
1.00
0.99
3.26
2.02
1.01
3.09
6.22
2.92
f1 (ppm)

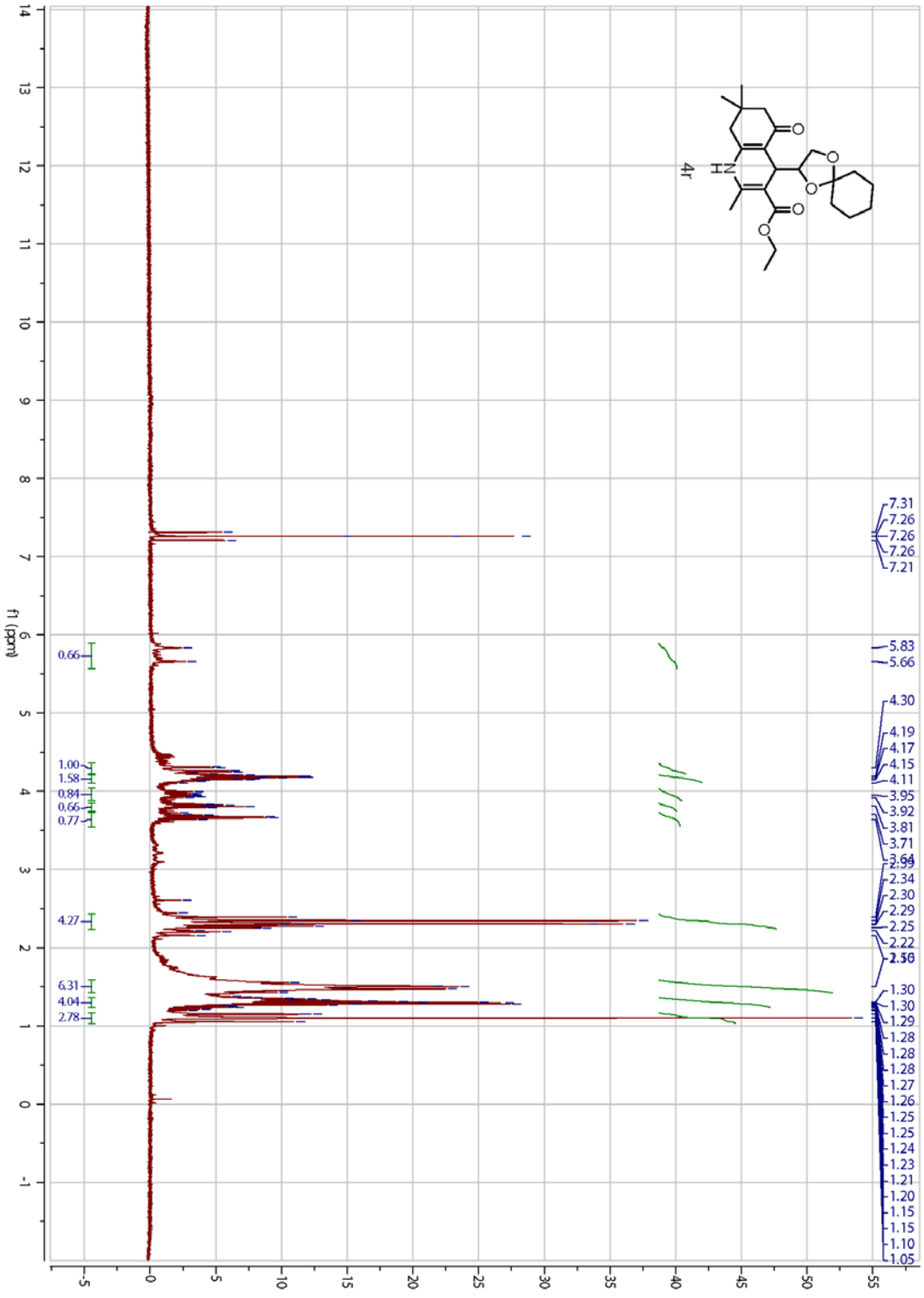
4r
f1 (ppm)
7.31
7.26
7.26
7.26
7.21
5.83
5.66
4.30
4.19
4.17
4.15
4.11
3.95
3.92
3.81
3.71
2.34
2.30
2.29
2.25
2.22
1.30
1.30
1.29
1.28
1.28
1.28
1.27
1.26
1.25
1.25
1.24
1.23
1.21
1.20
1.15
1.15
1.10
1.05
0.66
1.00
1.58
0.84
0.66
0.77
4.27
6.31
4.04
2.78

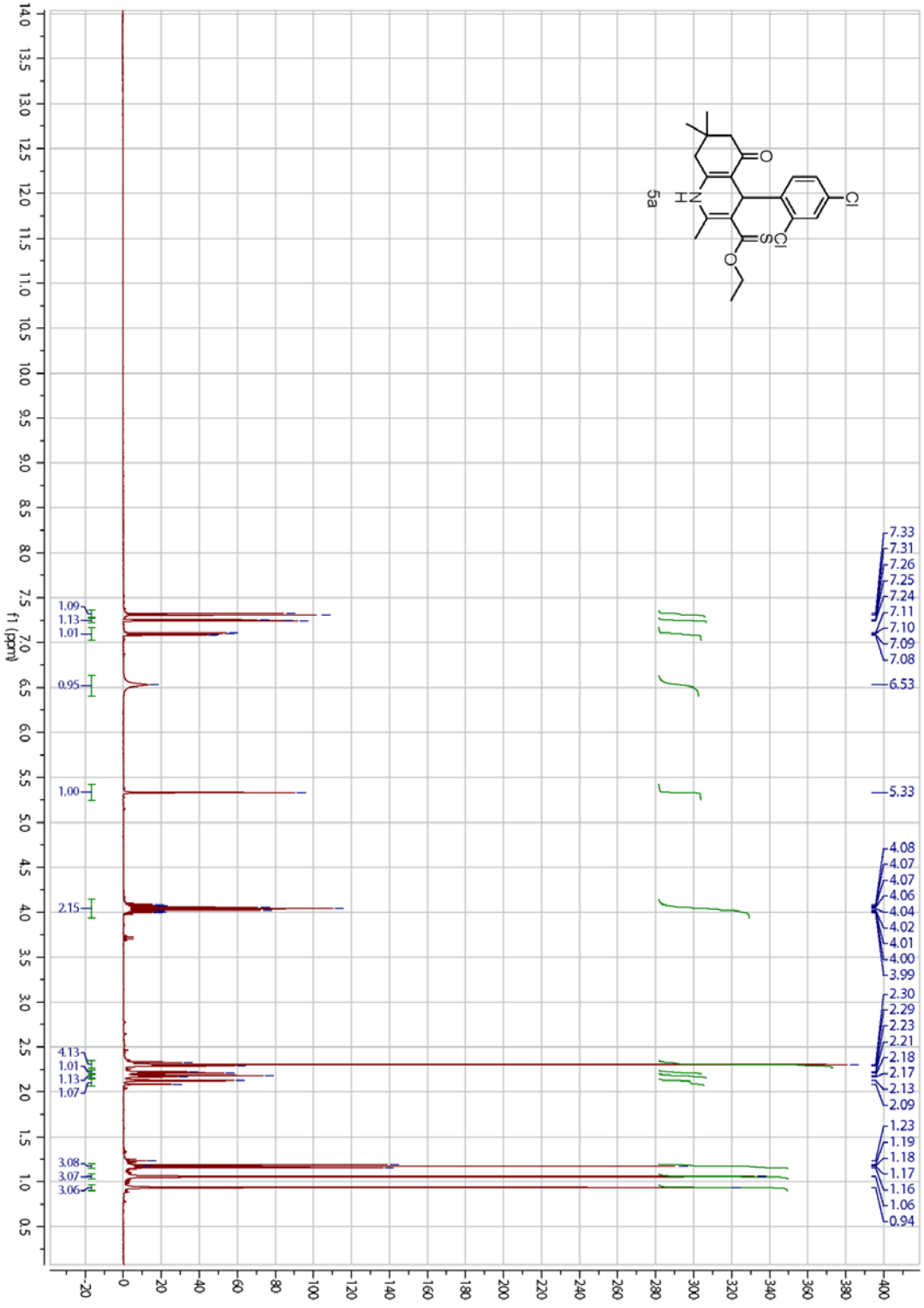
5a
f1 (ppm)
1.09
1.13
1.01
0.95
1.00
2.15
4.13
1.01
1.13
1.07
3.08
3.07
3.06
7.33
7.31
7.26
7.25
7.24
7.11
7.10
7.09
7.08
6.53
5.33
4.08
4.07
4.07
4.06
4.04
4.02
4.01
4.00
3.99
2.30
2.29
2.23
2.21
2.18
2.17
2.13
2.09
1.23
1.19
1.18
1.17
1.16
1.06
0.94

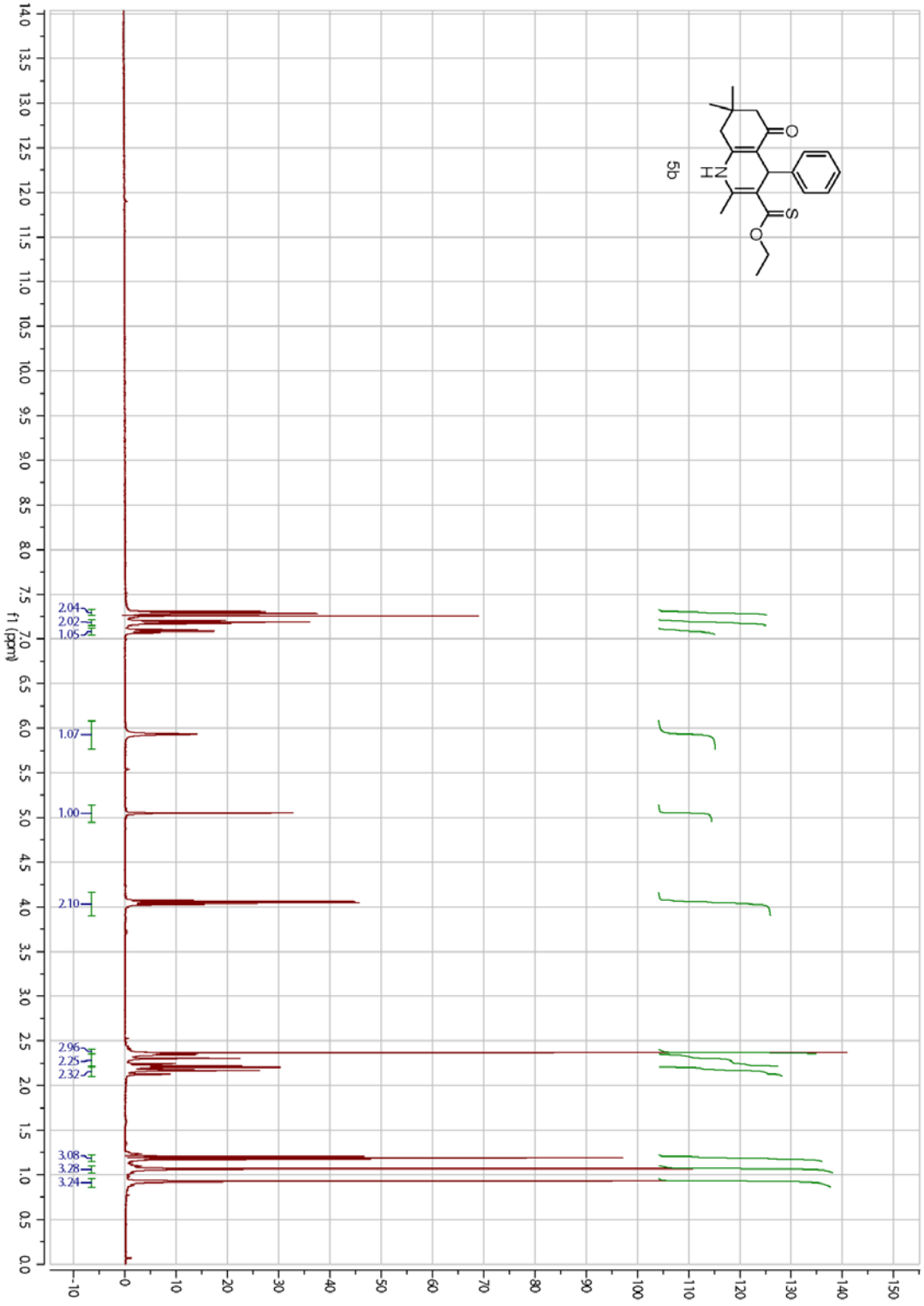
5b
f1 (ppm)
2.04
2.02
1.05
1.07
1.00
2.10
2.96
2.25
2.32
3.08
3.28
3.24

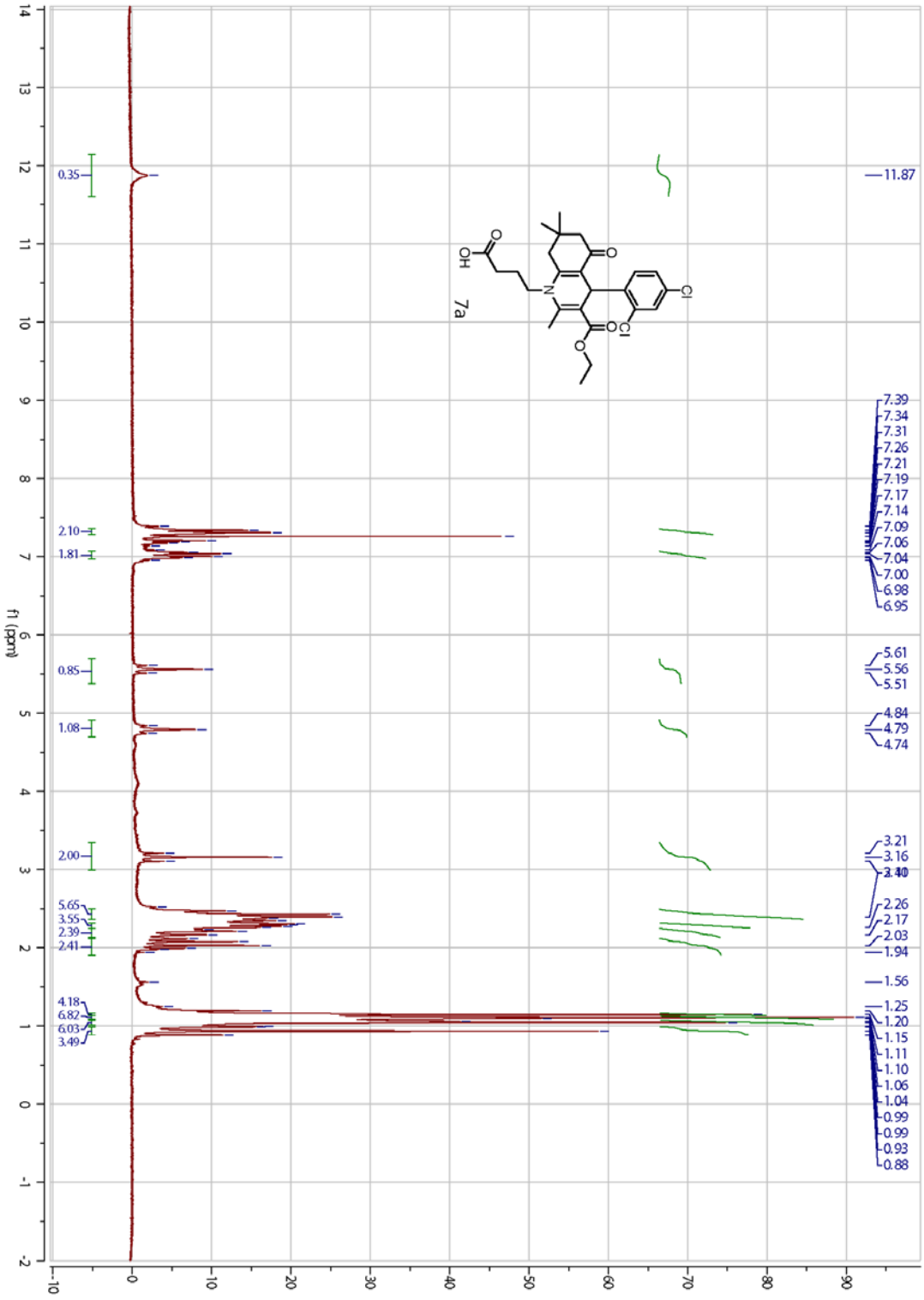
7a
f1 (ppm)
11.87
7.39
7.34
7.31
7.26
7.21
7.19
7.17
7.14
7.09
7.06
7.04
7.00
6.98
6.95
5.61
5.56
5.51
4.84
4.79
4.74
3.21
3.16
2.26
2.17
2.03
1.94
1.56
1.25
1.20
1.15
1.11
1.10
1.06
1.04
0.99
0.99
0.93
0.88
0.35
2.10
1.81
0.85
1.08
2.00
5.65
3.55
2.39
2.41
4.18
6.82
6.03
3.49

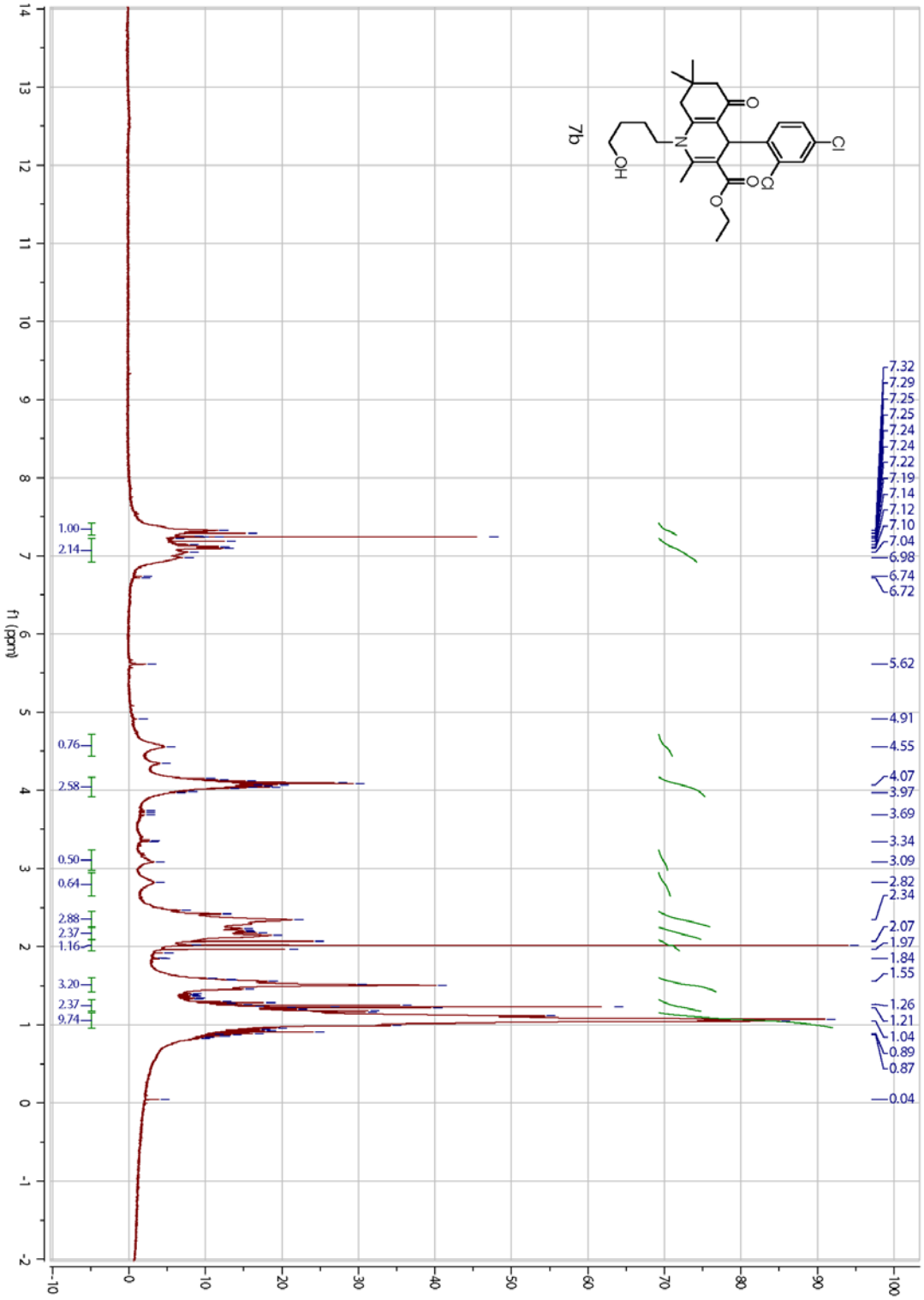
7b
f1 (ppm)
1.00
2.14
0.76
2.58
0.50
0.64
2.88
2.37
1.16
3.20
2.37
9.74
7.32
7.29
7.25
7.25
7.24
7.24
7.22
7.19
7.14
7.12
7.10
7.04
6.98
6.74
6.72
5.62
4.91
4.55
4.07
3.97
3.69
3.34
3.09
2.82
2.34
2.07
1.97
1.84
1.55
1.26
1.21
1.04
0.89
0.87
0.04

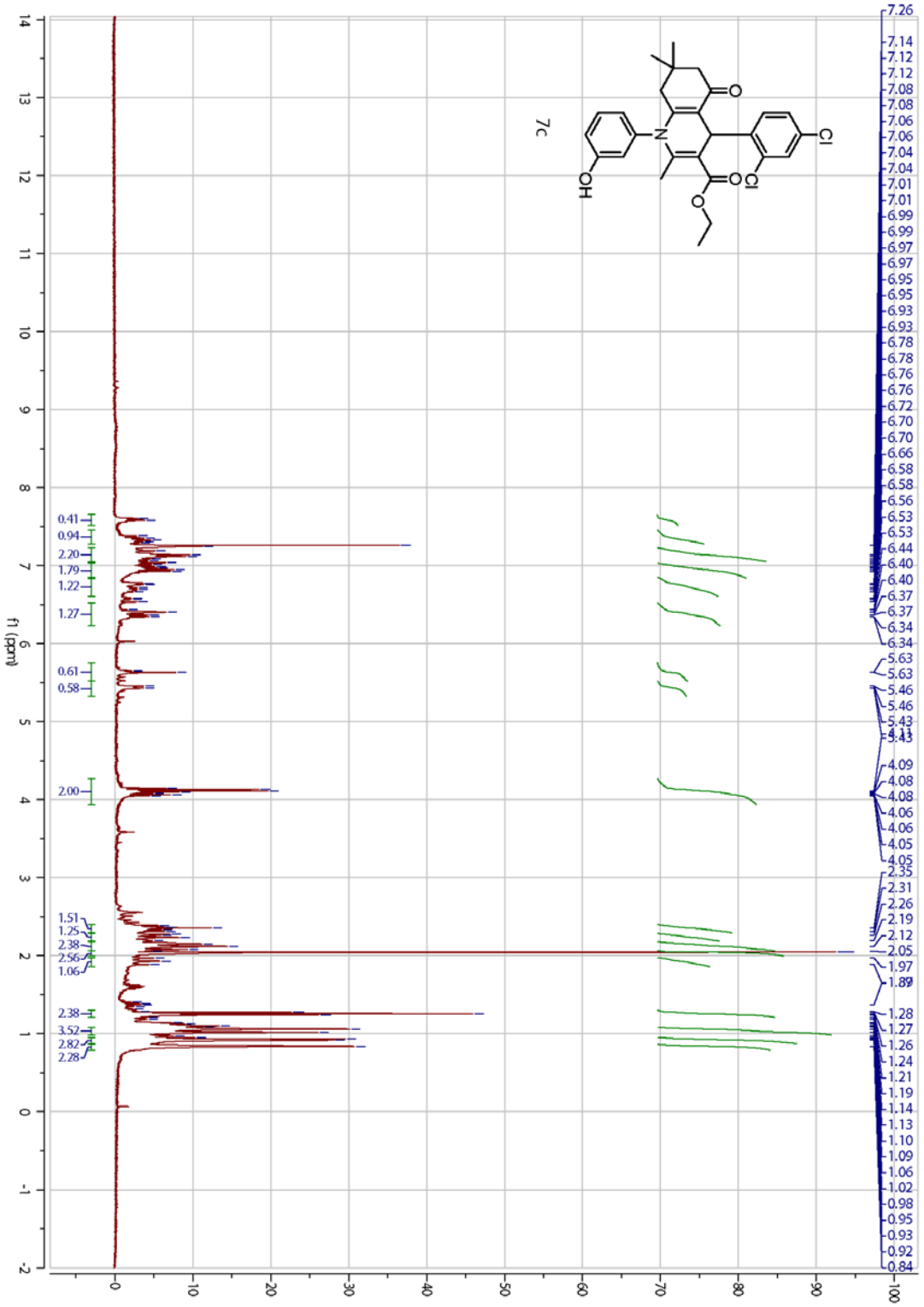
7c
f1 (ppm)

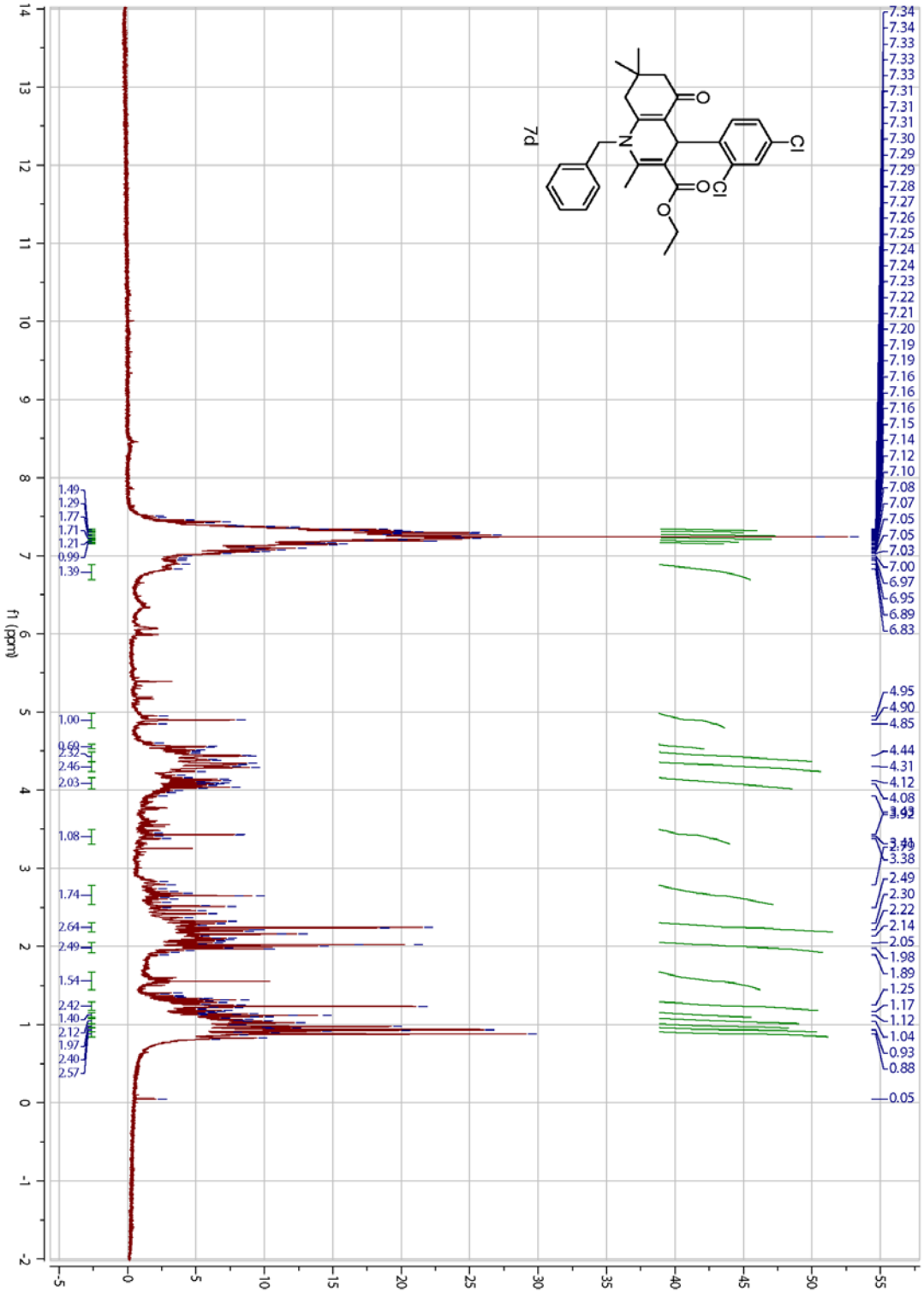
7d
f1 (ppm)

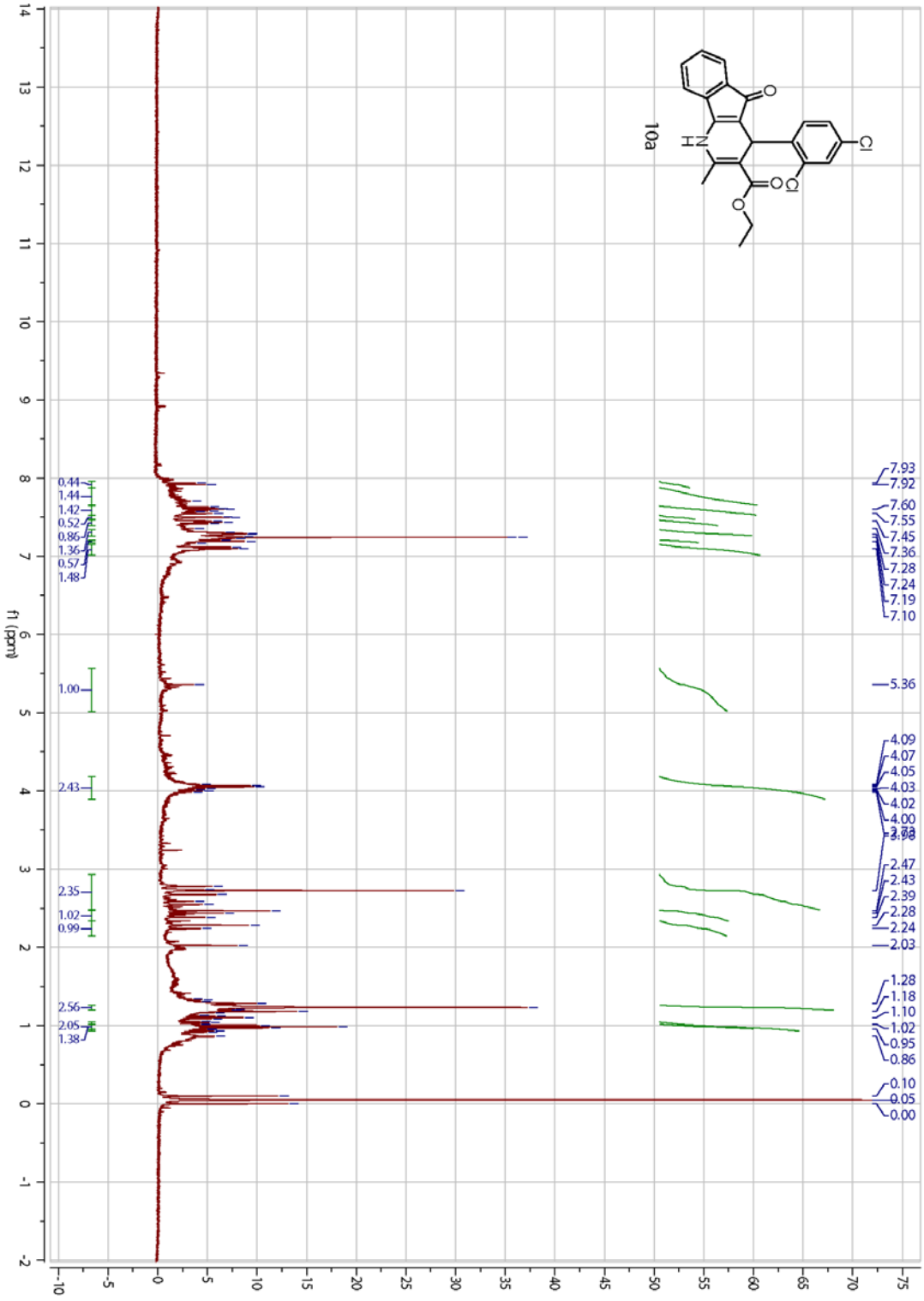
10a
f1 (ppm)
0.44
1.44
1.42
0.52
0.86
1.36
0.57
1.48
1.00
2.43
2.35
1.02
0.99
2.56
2.05
1.38
7.93
7.92
7.60
7.55
7.45
7.36
7.28
7.24
7.19
7.10
5.36
4.09
4.07
4.05
4.03
4.02
4.00
2.47
2.43
2.39
2.28
2.24
2.03
1.28
1.18
1.10
1.02
0.95
0.86
0.10
0.05
0.00

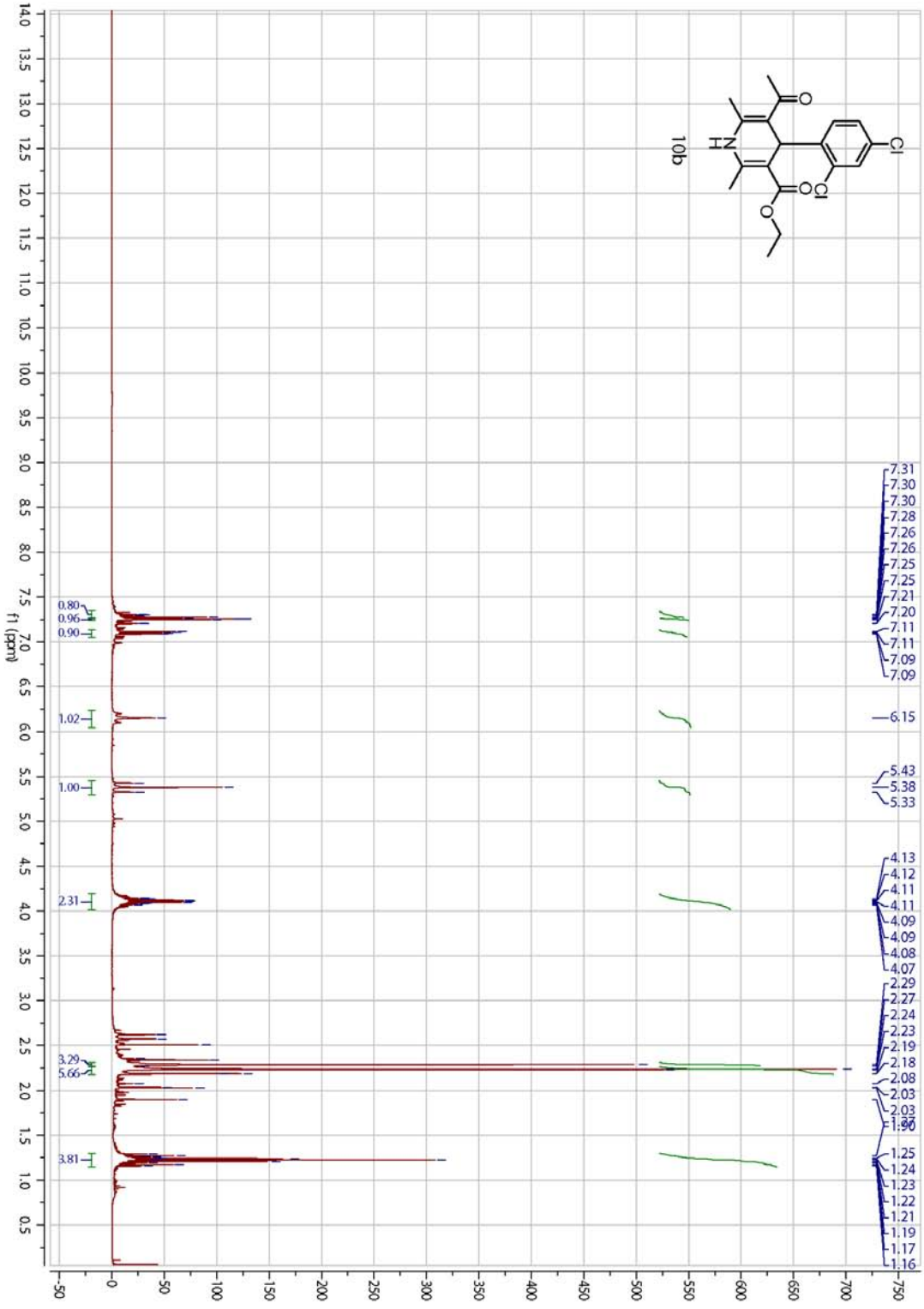
10b
f1 (ppm)
0.80
0.96
0.90
1.02
1.00
2.31
3.29
5.66
3.81
7.31
7.30
7.30
7.28
7.26
7.26
7.25
7.25
7.21
7.20
7.11
7.11
7.09
7.09
6.15
5.43
5.38
5.33
4.13
4.12
4.11
4.11
4.09
4.09
4.08
4.07
2.29
2.27
2.24
2.23
2.19
2.18
2.08
2.03
2.03
1.90
1.25
1.24
1.23
1.22
1.21
1.19
1.17
1.16

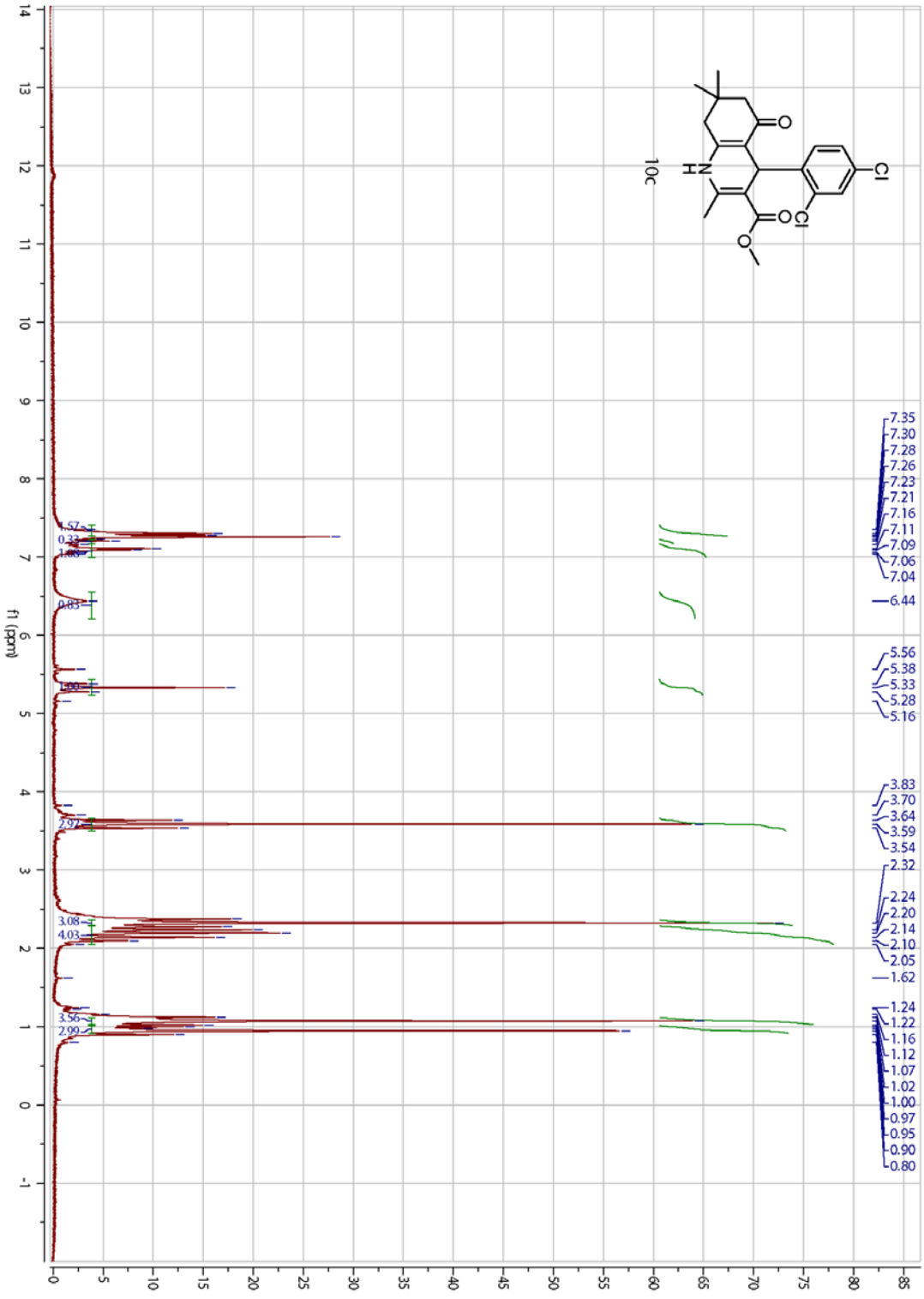
10c
f1 (ppm)
7.35
7.30
7.28
7.26
7.23
7.21
7.16
7.11
7.09
7.06
7.04
6.44
5.56
5.38
5.33
5.28
5.16
3.83
3.70
3.64
3.59
3.54
2.32
2.24
2.20
2.14
2.10
2.05
1.62
1.24
1.22
1.16
1.12
1.07
1.02
1.00
0.97
0.95
0.90
0.80

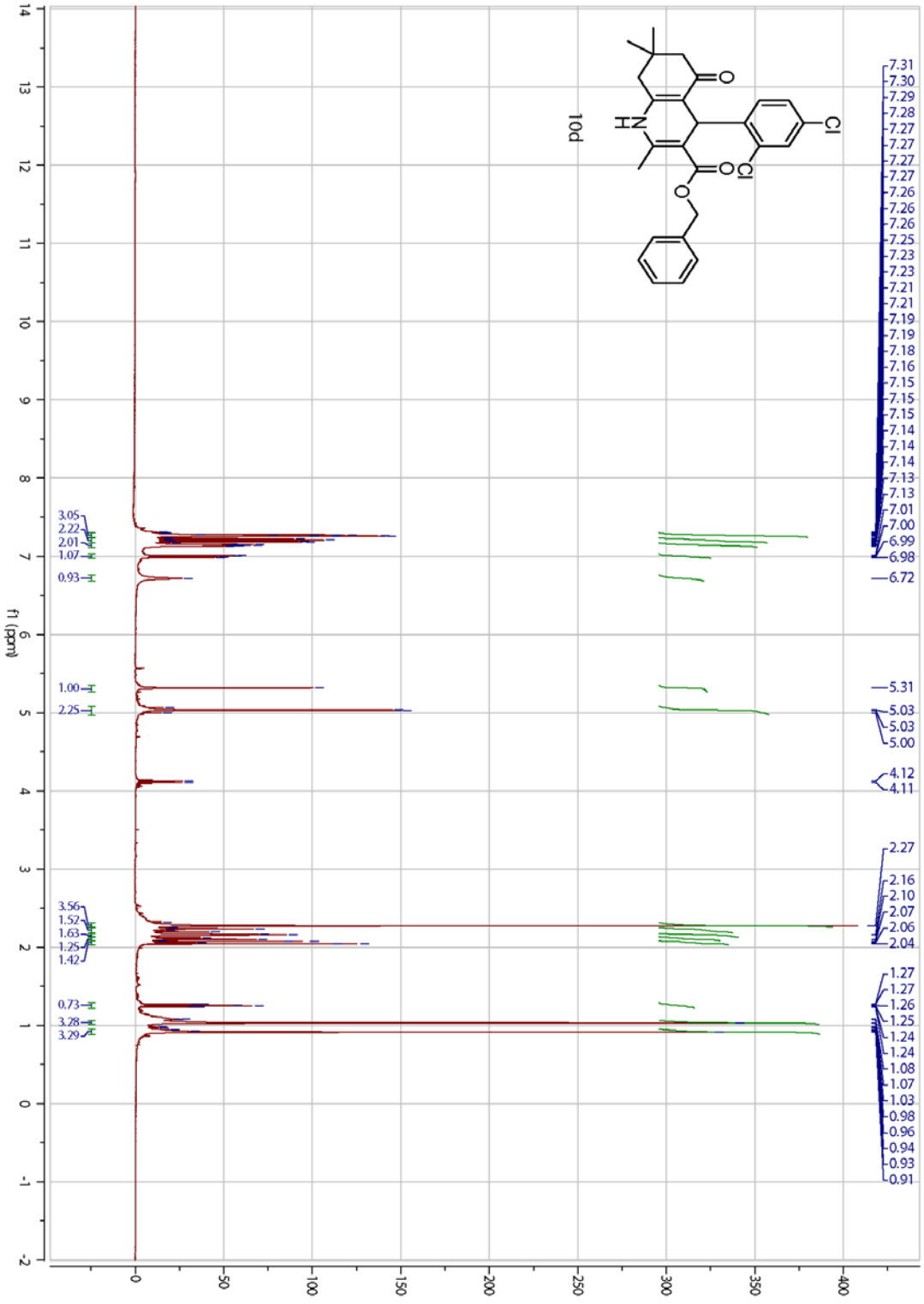
10d
f1 (ppm)

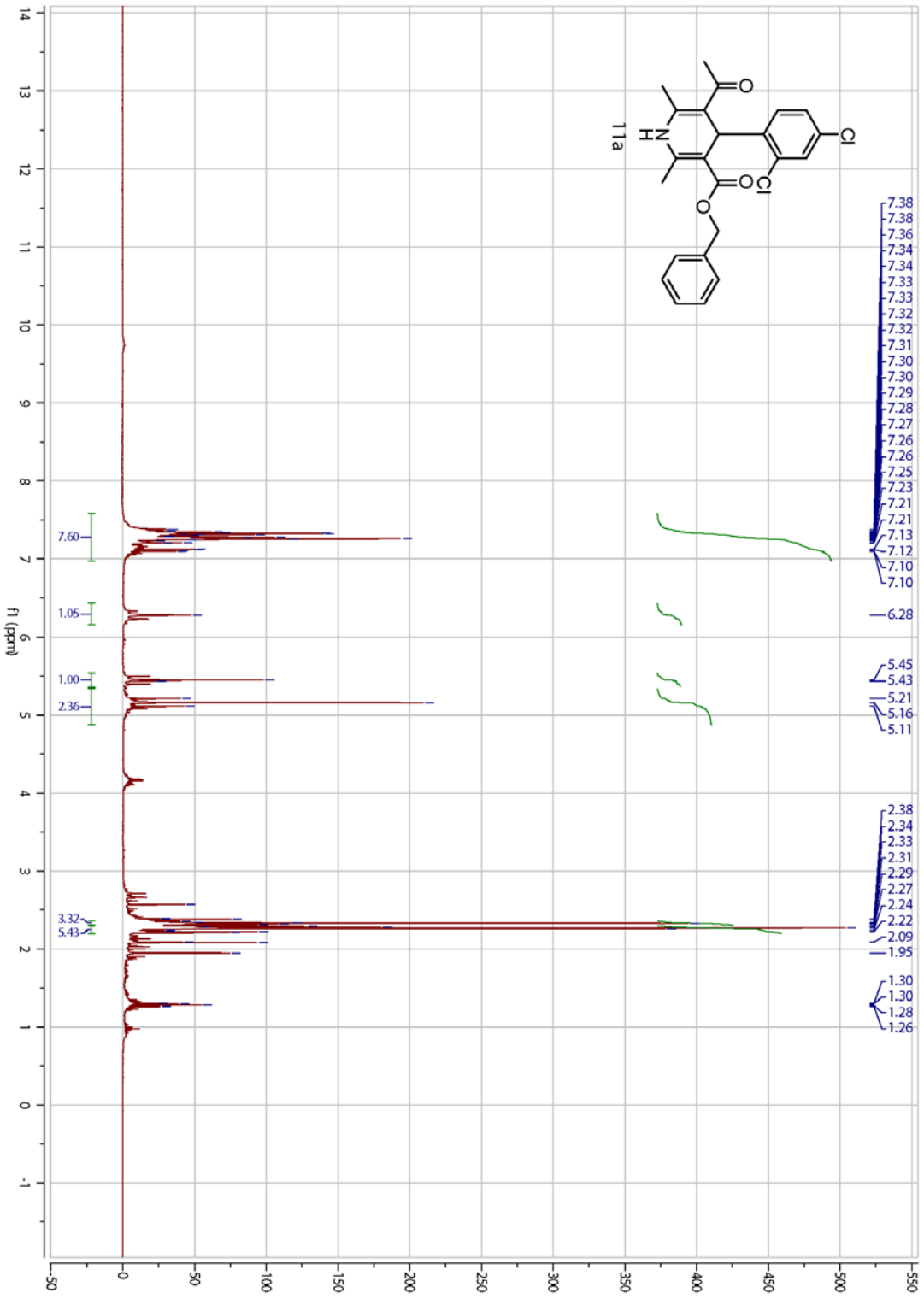
11a
f1 (ppm)
7.60
1.05
1.00
2.36
3.32
5.43
7.38
7.38
7.36
7.34
7.34
7.33
7.33
7.32
7.32
7.31
7.30
7.30
7.29
7.28
7.27
7.26
7.26
7.25
7.23
7.21
7.21
7.13
7.12
7.10
7.10
6.28
5.45
5.43
5.21
5.16
5.11
2.38
2.34
2.33
2.31
2.29
2.27
2.24
2.22
2.09
1.95
1.30
1.30
1.28
1.26

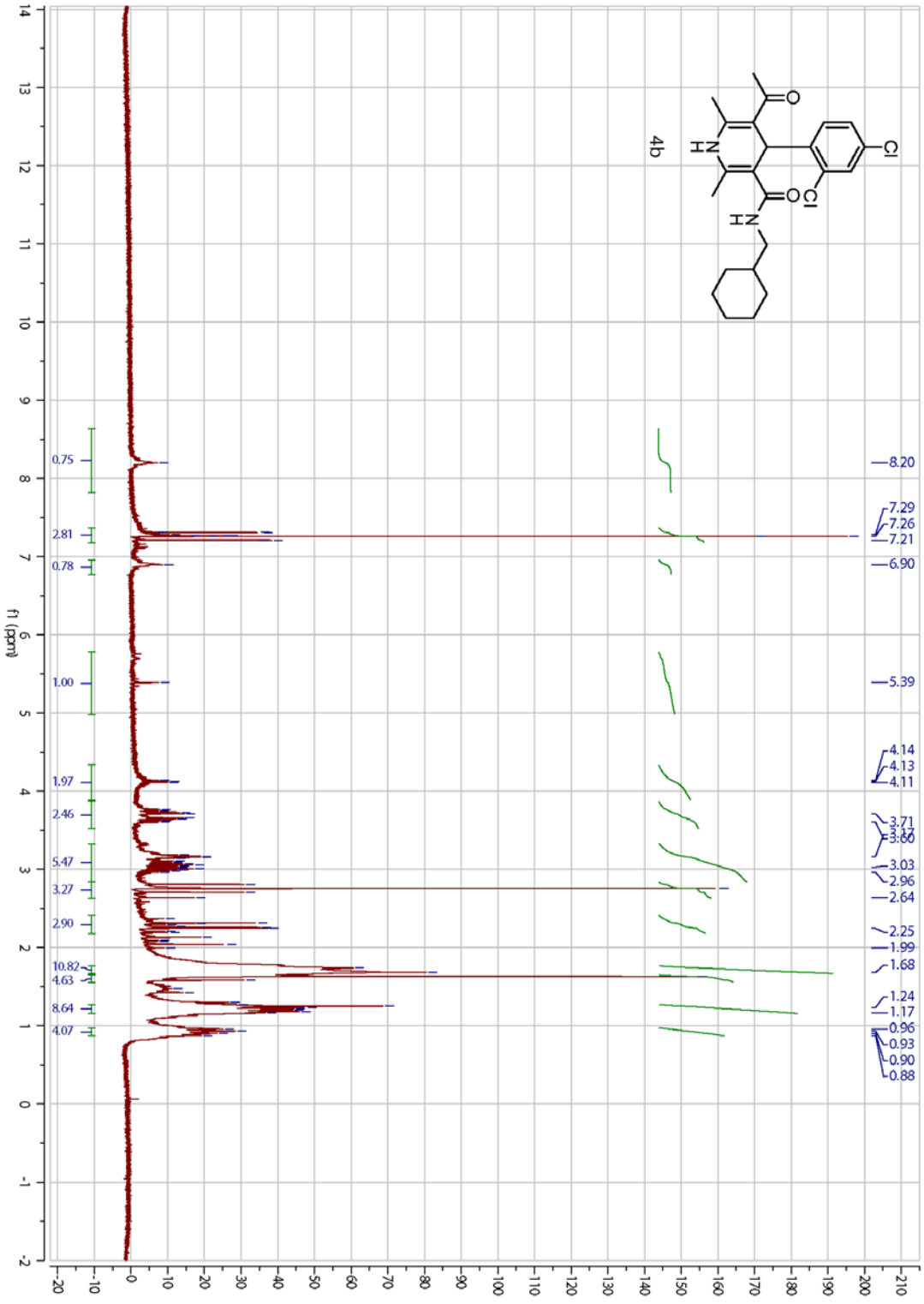
4b
f1 (ppm)
0.75
2.81
0.78
1.00
1.97
2.46
5.47
3.27
2.90
10.82
4.63
8.64
4.07
8.20
7.29
7.26
7.21
6.90
5.39
4.14
4.13
4.11
3.71
3.60
3.03
2.96
2.64
2.25
1.99
1.68
1.24
1.17
0.96
0.93
0.90
0.88

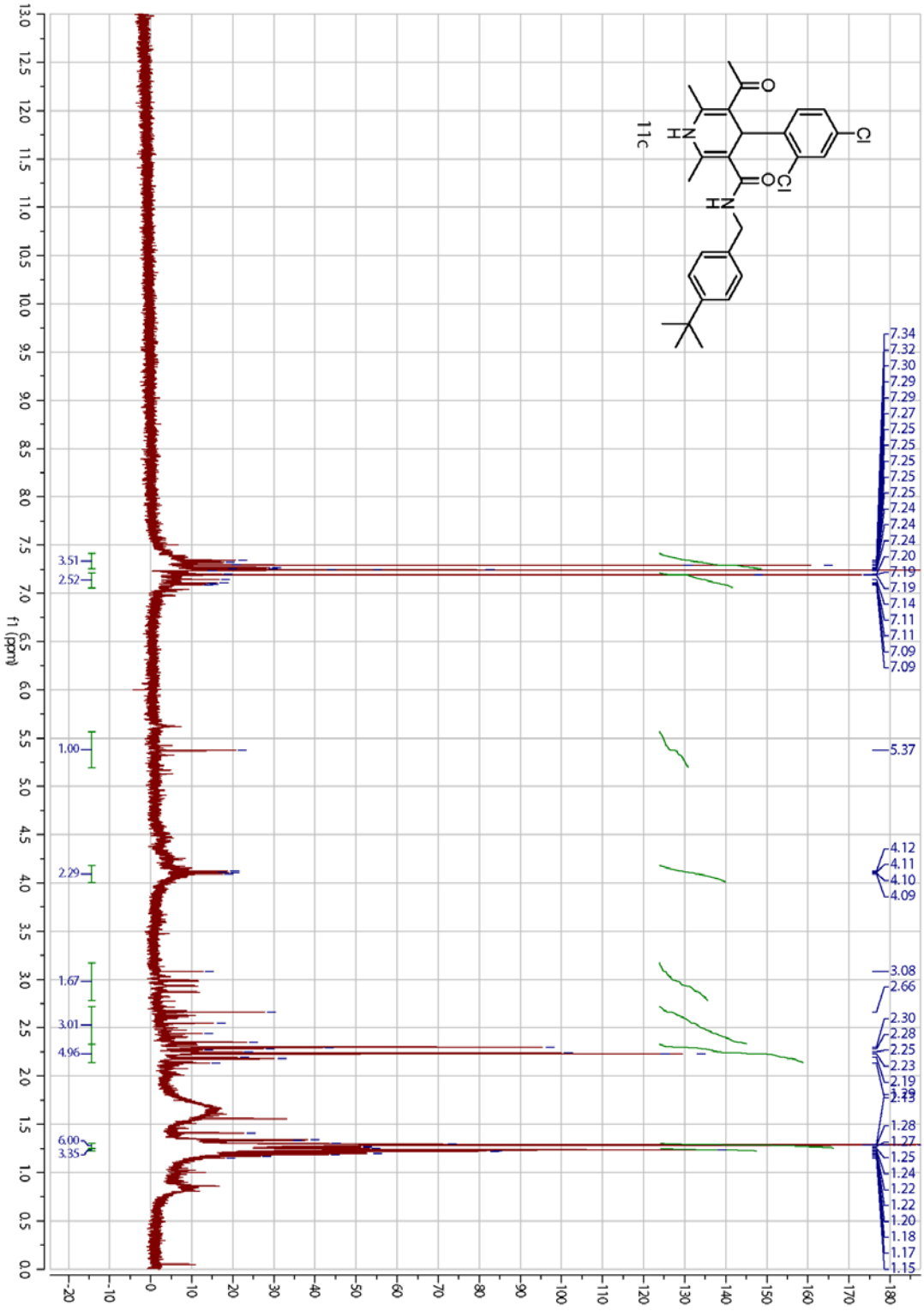
11c
f1 (ppm)
7.34
7.32
7.30
7.29
7.29
7.27
7.25
7.25
7.25
7.25
7.25
7.25
7.24
7.24
7.24
7.20
7.19
7.19
7.14
7.11
7.11
7.09
7.09
5.37
4.12
4.11
4.10
4.09
3.08
2.66
2.30
2.28
2.25
2.23
2.19
1.28
1.27
1.25
1.24
1.22
1.22
1.20
1.18
1.17
1.15
3.51
2.52
1.00
2.29
1.67
3.01
4.96
6.00
3.35

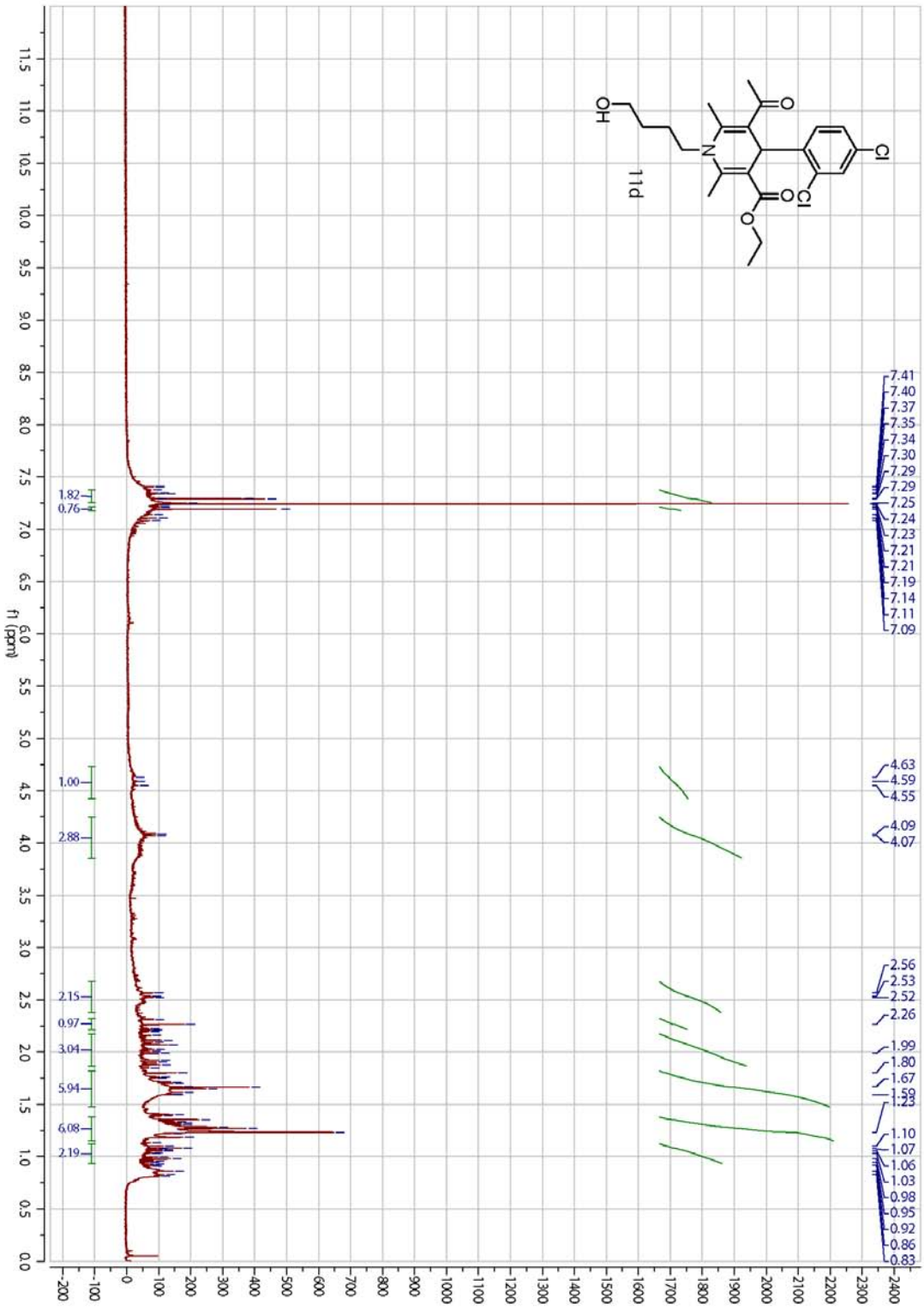
11d
OH
N
O
O
O
Cl
Cl
f1 (ppm)
1.82
0.76
1.00
2.88
2.15
0.97
3.04
5.94
6.08
2.19
7.41
7.40
7.37
7.35
7.34
7.30
7.29
7.29
7.25
7.24
7.23
7.21
7.21
7.19
7.14
7.11
7.09
4.63
4.59
4.55
4.09
4.07
2.56
2.53
2.52
2.26
1.99
1.80
1.67
1.59
1.23
1.10
1.07
1.06
1.03
0.98
0.95
0.92
0.86
0.83

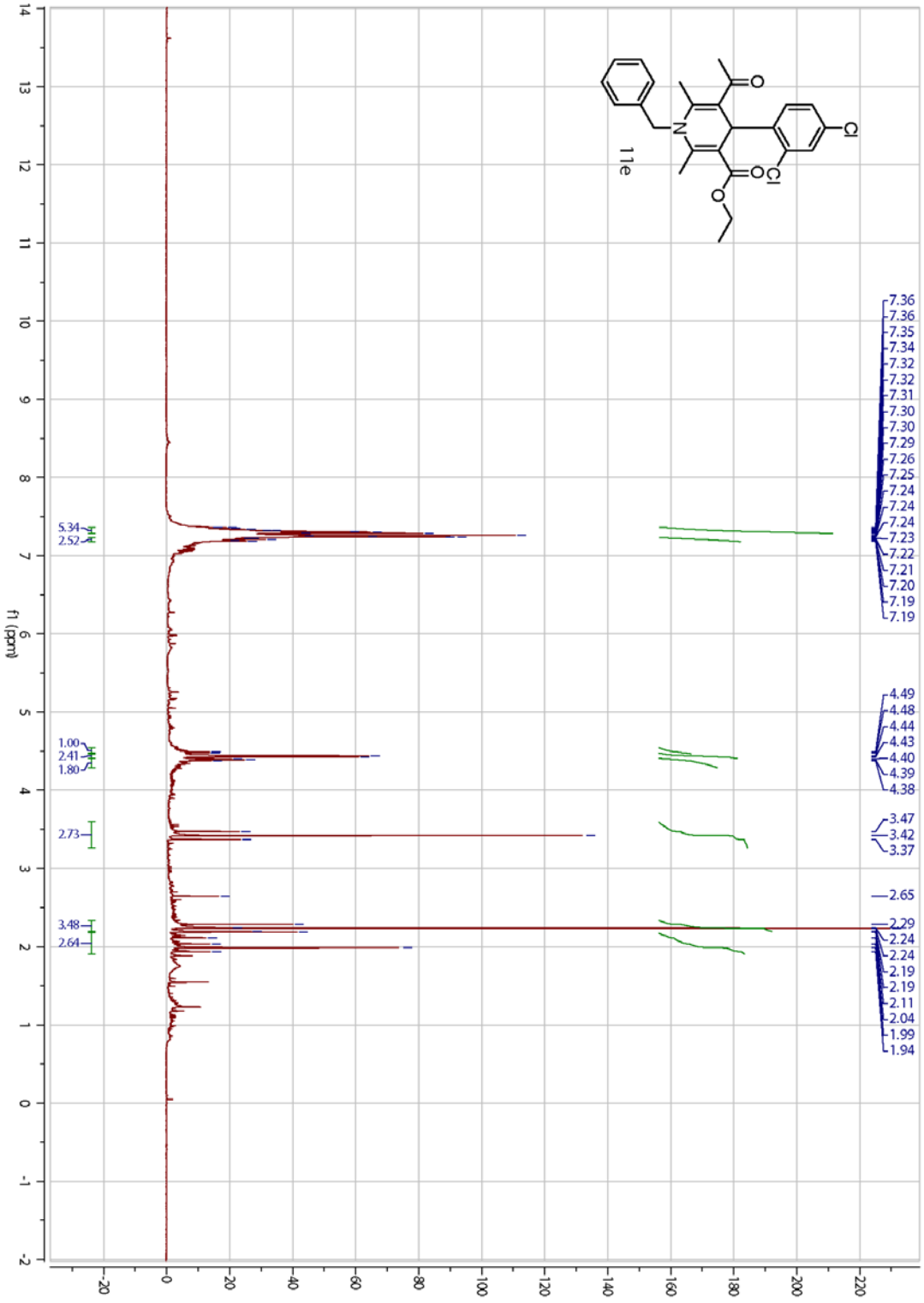
11e
f1 (ppm)
5.34
2.52
1.00
2.41
1.80
2.73
3.48
2.64
7.36
7.36
7.35
7.34
7.32
7.32
7.31
7.30
7.30
7.29
7.26
7.25
7.24
7.24
7.24
7.23
7.22
7.21
7.20
7.19
7.19
4.49
4.48
4.44
4.43
4.40
4.39
4.38
3.47
3.42
3.37
2.65
2.29
2.24
2.24
2.19
2.19
2.11
2.04
1.99
1.94

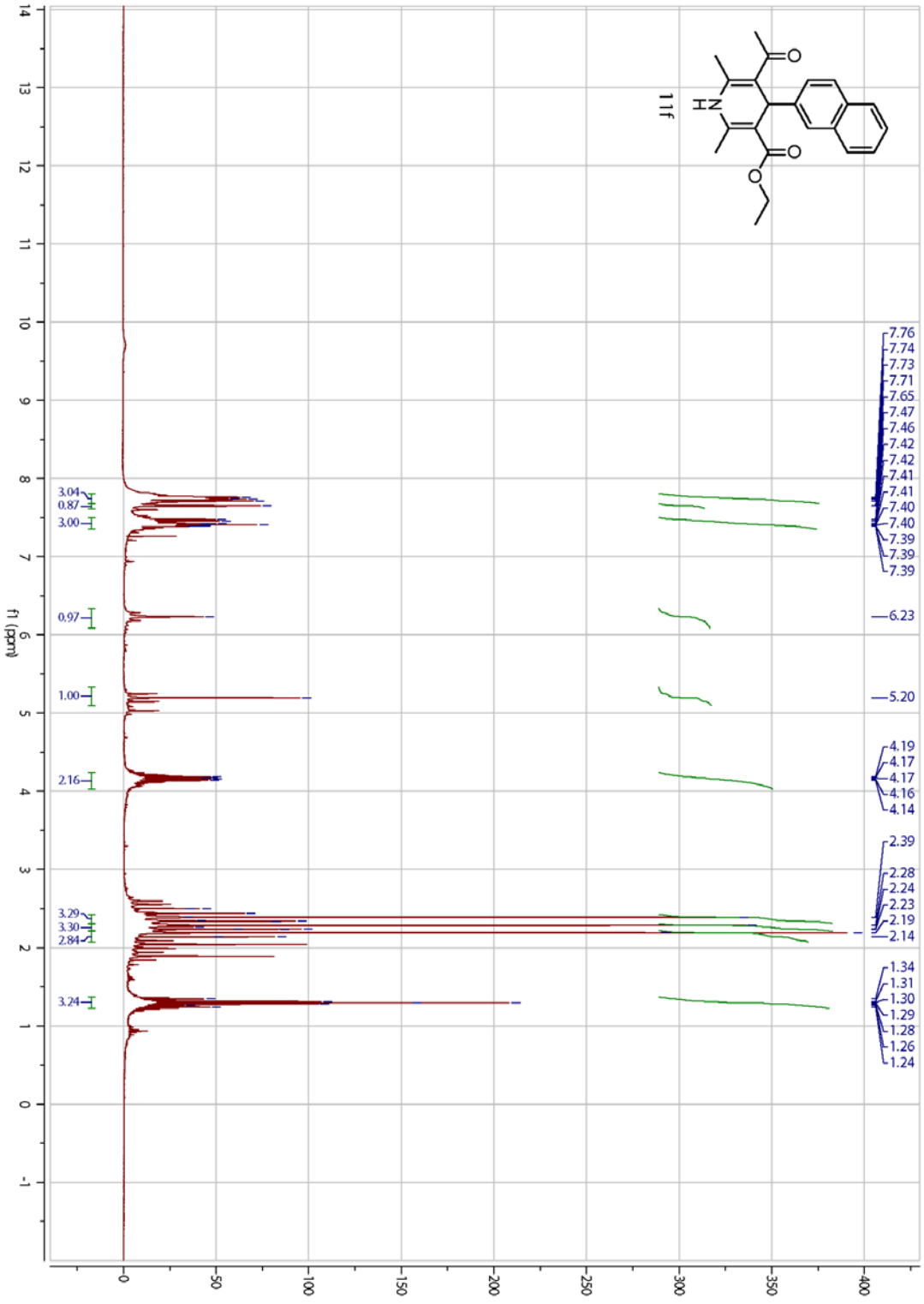
11f
f1 (ppm)
3.04
0.87
3.00
0.97
1.00
2.16
3.29
3.30
2.84
3.24
7.76
7.74
7.73
7.71
7.65
7.47
7.46
7.42
7.42
7.41
7.41
7.40
7.40
7.39
7.39
7.39
6.23
5.20
4.19
4.17
4.17
4.16
4.14
2.39
2.28
2.24
2.23
2.19
2.14
1.34
1.31
1.30
1.29
1.28
1.26
1.24

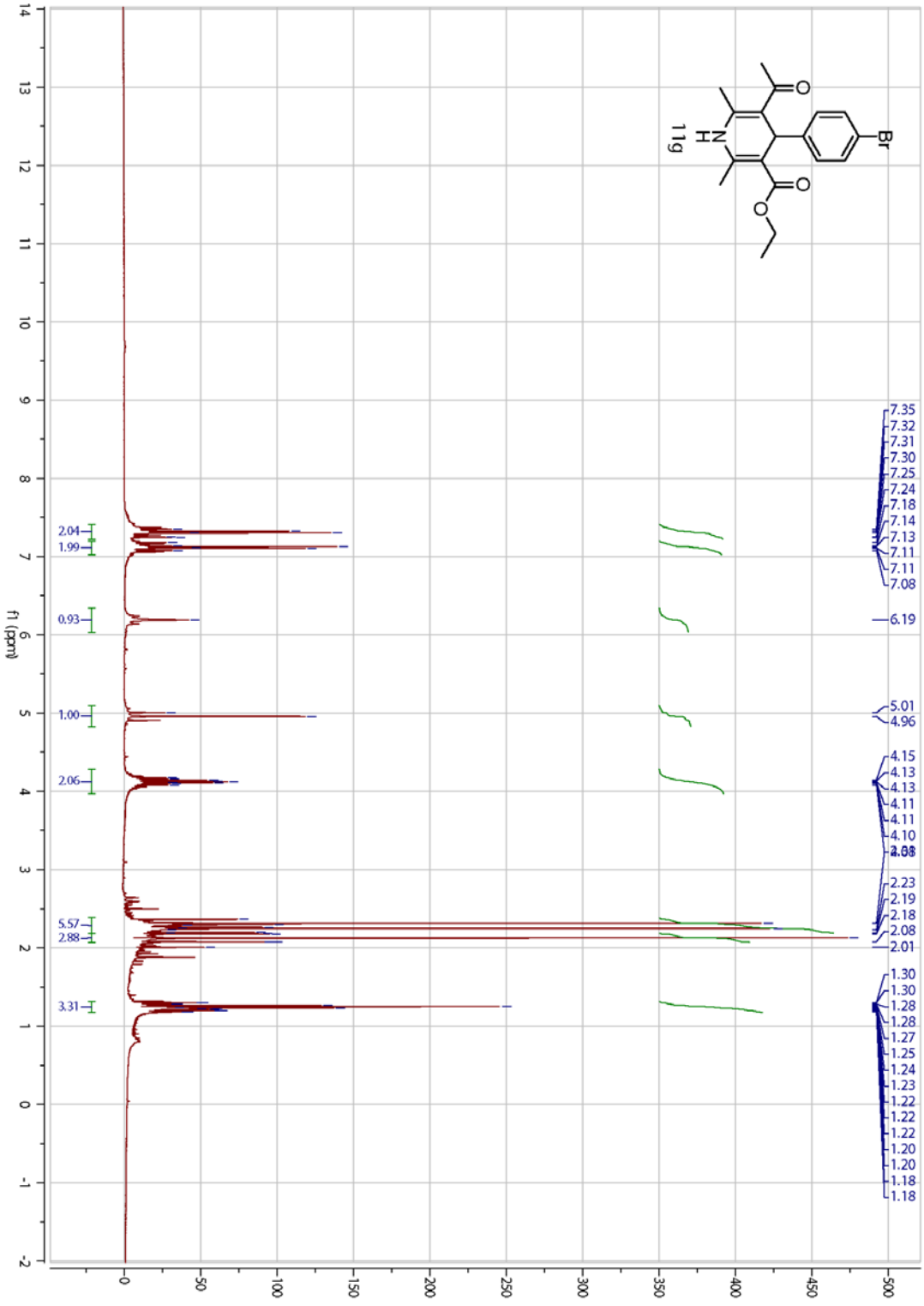
11g
Br
O
O
O
N
H
f1 (ppm)
2.04
1.99
0.93
1.00
2.06
5.57
2.88
3.31
7.35
7.32
7.31
7.30
7.25
7.24
7.18
7.14
7.13
7.11
7.11
7.08
6.19
5.01
4.96
4.15
4.13
4.13
4.11
4.11
4.10
2.23
2.19
2.18
2.08
2.01
1.30
1.30
1.28
1.28
1.27
1.25
1.24
1.23
1.22
1.22
1.22
1.20
1.20
1.18
1.18

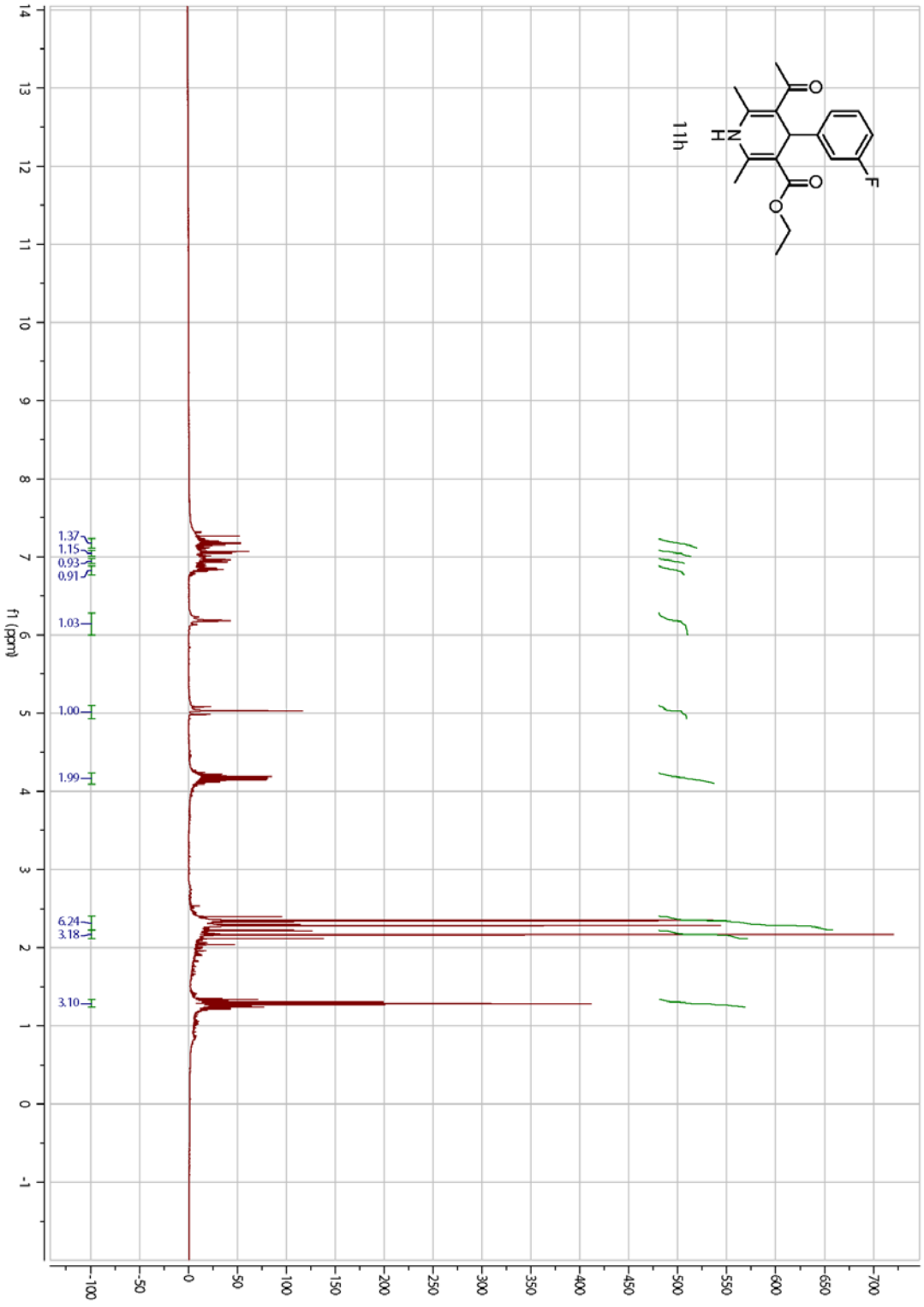
11h
1.37
1.15
0.93
0.91
1.03
1.00
1.99
6.24
3.18
3.10
f1 (ppm)

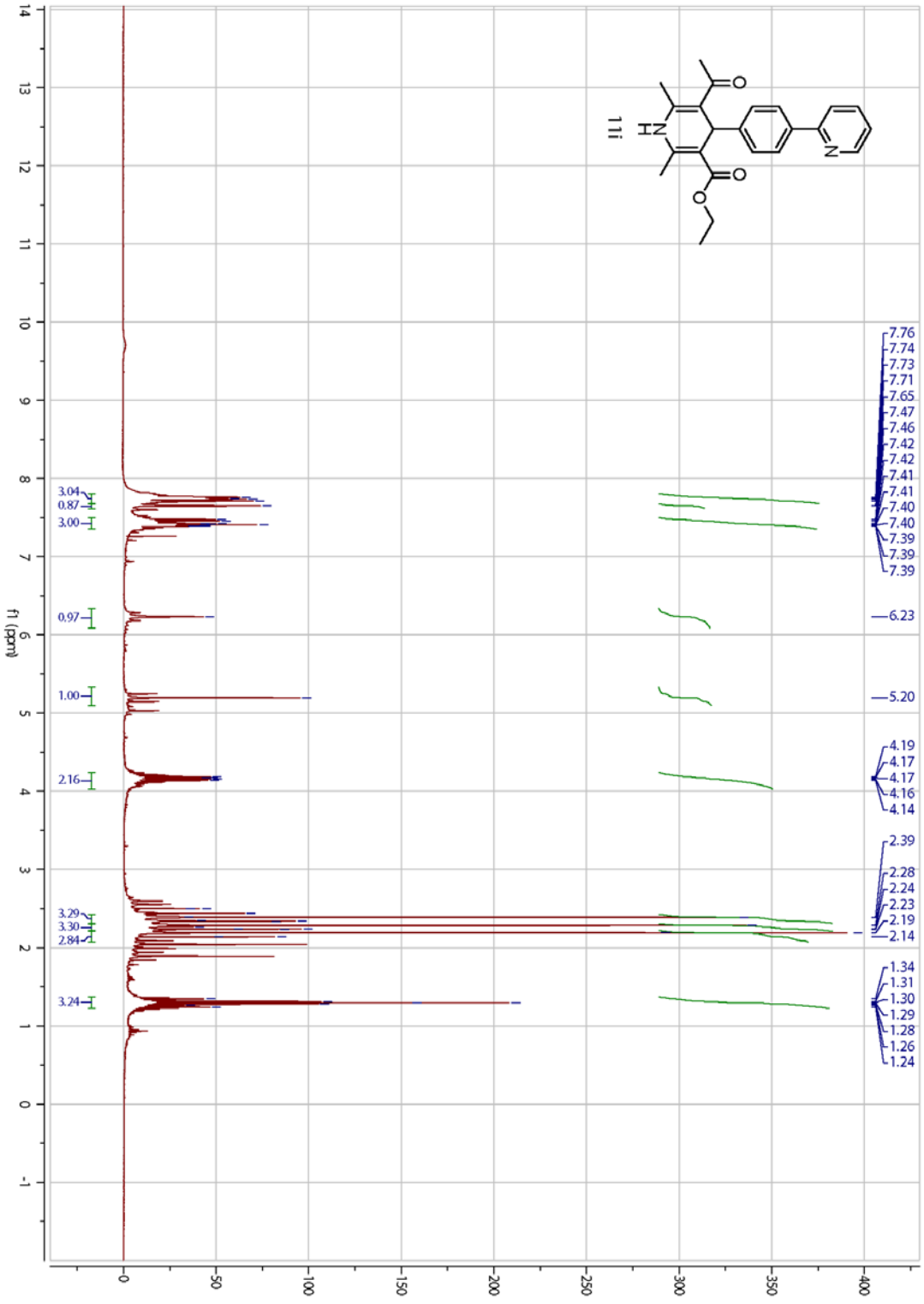
11i
f1 (ppm)
3.04
0.87
3.00
0.97
1.00
2.16
3.29
3.30
2.84
3.24
7.76
7.74
7.73
7.71
7.65
7.47
7.46
7.42
7.42
7.41
7.41
7.40
7.40
7.39
7.39
7.39
6.23
5.20
4.19
4.17
4.17
4.16
4.14
2.39
2.28
2.24
2.23
2.19
2.14
1.34
1.31
1.30
1.29
1.28
1.26
1.24

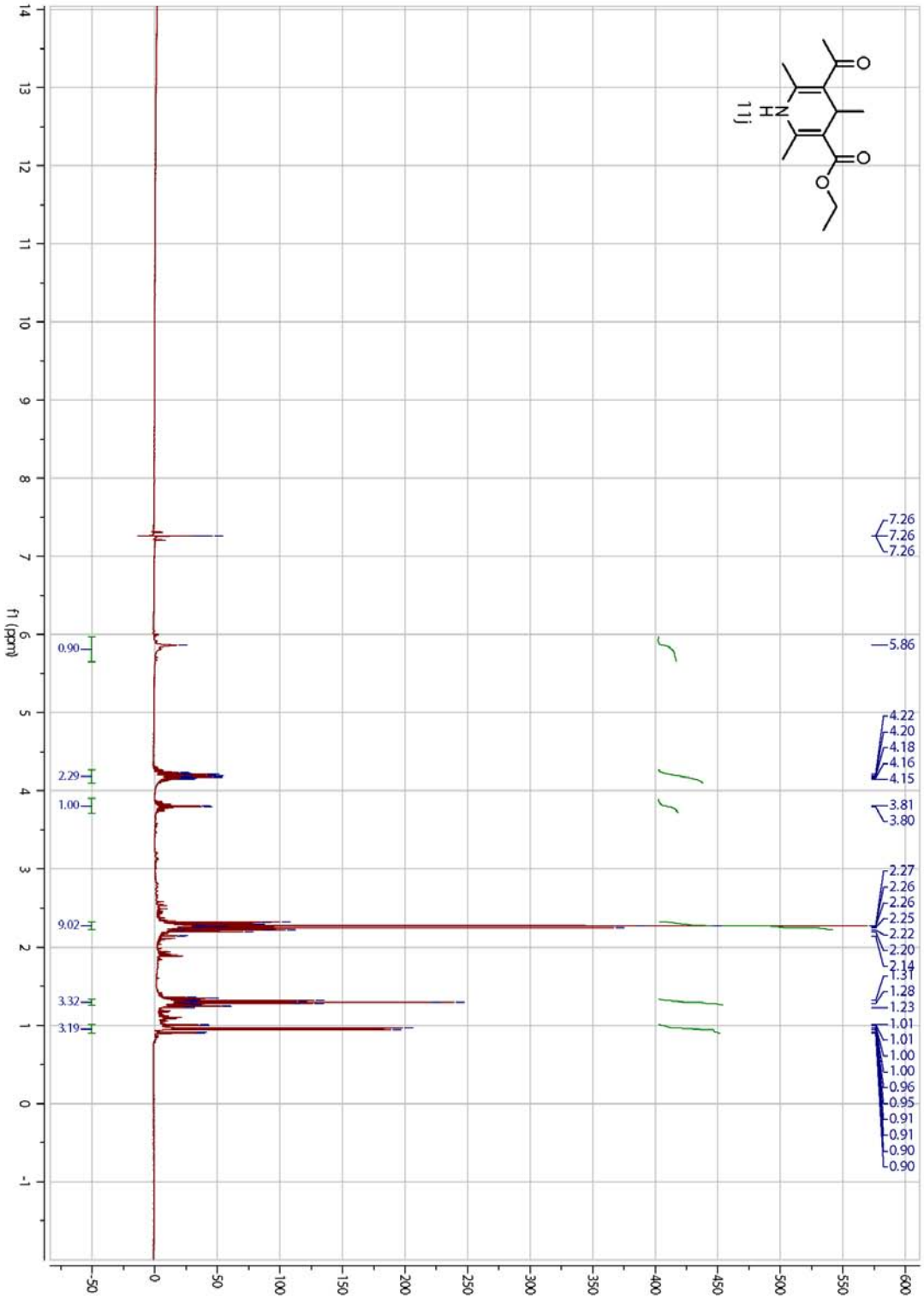
11j
f1 (ppm)
0.90
2.29
1.00
9.02
3.32
3.19
7.26
7.26
7.26
5.86
4.22
4.20
4.18
4.16
4.15
3.81
3.80
2.27
2.26
2.26
2.25
2.22
2.20
2.14
1.31
1.28
1.23
1.01
1.01
1.00
1.00
0.96
0.95
0.91
0.91
0.90
0.90

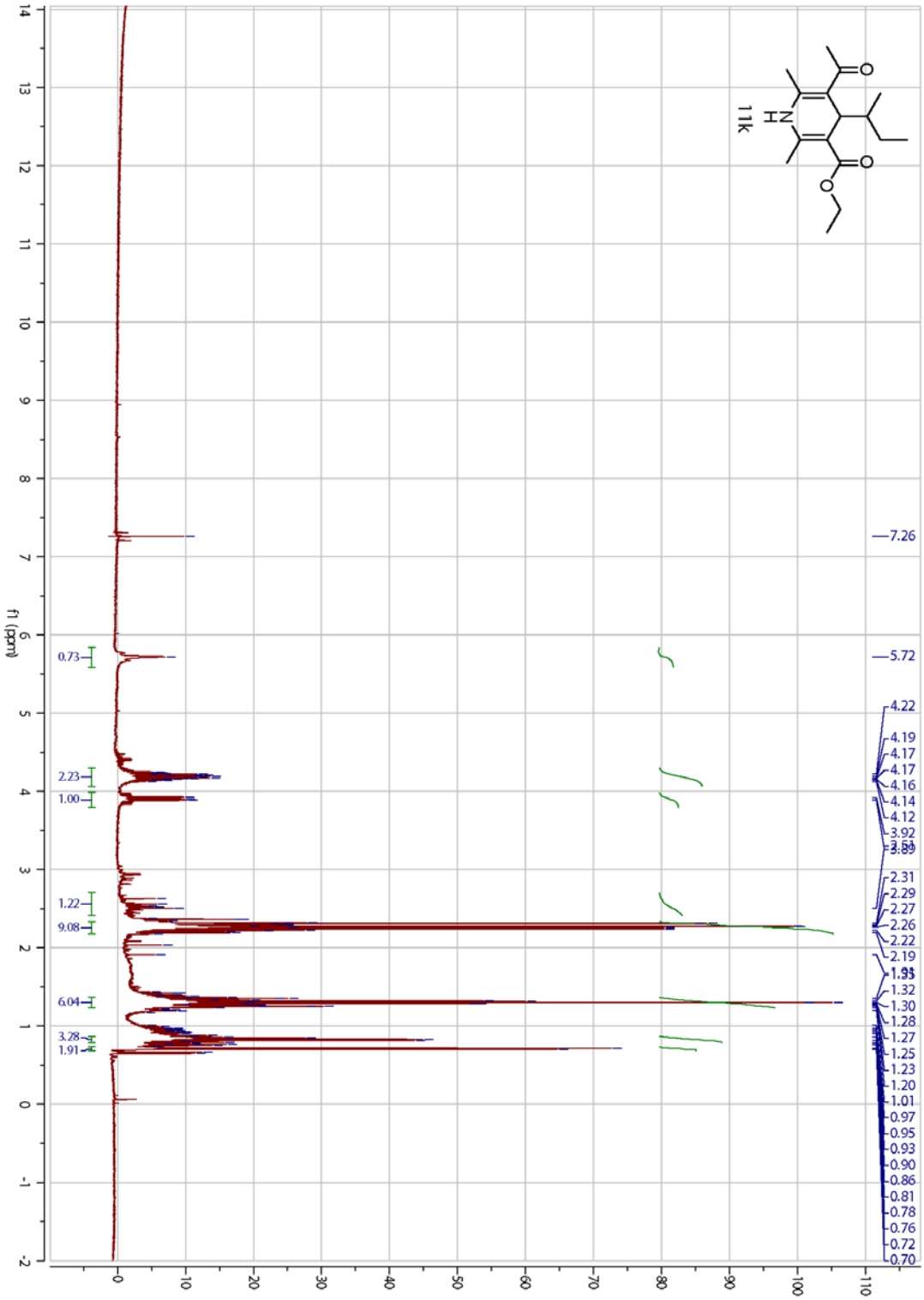
11k
f1 (ppm)
0.73
2.23
1.00
1.22
9.08
6.04
3.28
1.91
7.26
5.72
4.22
4.19
4.17
4.17
4.16
4.14
4.12
3.92
2.31
2.29
2.27
2.26
2.22
2.19
1.32
1.30
1.28
1.27
1.25
1.23
1.20
1.01
0.97
0.95
0.93
0.90
0.86
0.81
0.78
0.76
0.72
0.70

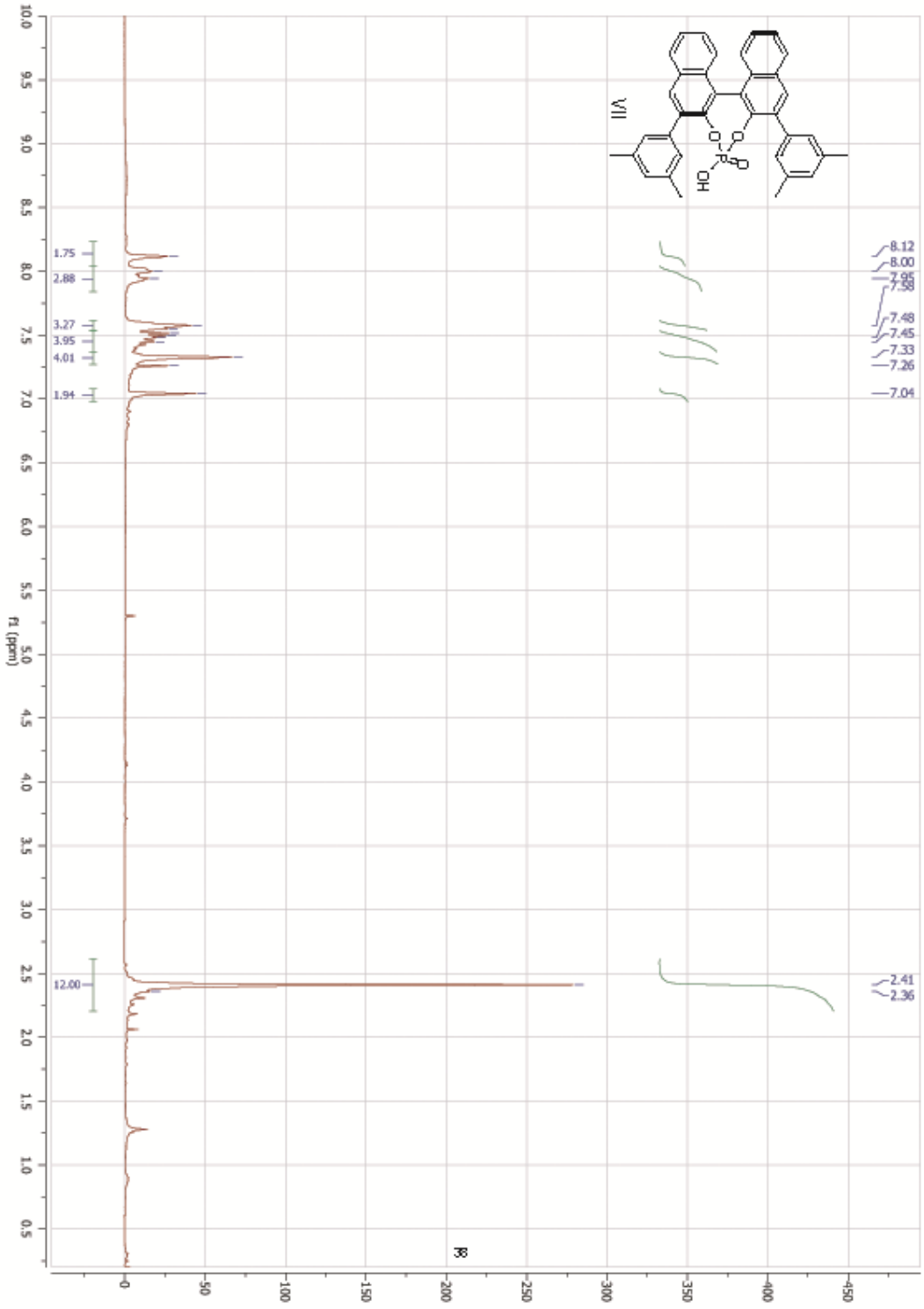
VII
OH
1.75
2.88
3.27
3.95
4.01
1.94
12.00
8.12
8.00
7.95
7.58
7.48
7.45
7.33
7.26
7.04
2.41
2.36
f1 (ppm)

Table 3-4. HPLC Data from Chirobiotic™ V2 Column

Compound	Catalyst	Aldehyde	Solvent (Iso: Hex)	Flow Rate	RT_1	RT_2	A_1	A_2	er	%ee
4a	VII	2,4-Cl-Ph	25: 75	1.0	8.300		5497421			>99%
4b	VII	Ph	20: 80	1.5	7.950	9.600	6481	625675	99:1	98%
4b	VI	Ph	20: 80	1.5	7.750	9.517	20041	2800205	99:1	98%
4c	VII	4-Br-Ph	15:85	1.2	10.367	11.867	1407053	28688	98:2	96%
4d	VII	3,5-MeO-Ph	20:80	1.5	4.700	6.933	10234	6970822	99.8:0.2	>99%
4e	VII	3-F-Ph	20: 80	1.5	4.717	6.900	4100313	290877	93:7	86%
4f	VII	4-$(CH_3)_2$-N-Ph	20: 80	1.5	5.883	8.717	472179	18343	96:4	92%
4g	VII	4-(CF_3)-Ph	20: 80	1.5	8.033		11687834			>99%
4h	VII	2,5-F-Ph	20: 80	1.5	6.100	9.550	24673010	108580	99.6: 0.4	>99%
4i	VII	4-tBu-Ph	20: 80	1.5	3.267	5.100	81453	4822759	98:2	96%
4j	VII	2-Naphth	20: 80	1.5	4.967	7.500	1582	4829329	99.9: 0.1	>99%
4k	VII	4-CN-Ph	35: 65	1.2	5.633	13.483	8022403	54360	99:1	98%
4l	VII	3,4-OH-Ph	40: 60	1.0	8.183	10.267	62685	2718748	98:2	96%
4m	VII	Ph-CH_2-CH_2-	40: 60	1.0	3.950	4.967	197757	6444488	97:3	94%
4n	VII	2-Cl-Ph	20: 80	1.5	4.250	6.867	15169	3937516	99.6: 0.4	>99%
4o	VII	4-Ph-Ph	20: 80	1.5	6.650		2972254			>99%

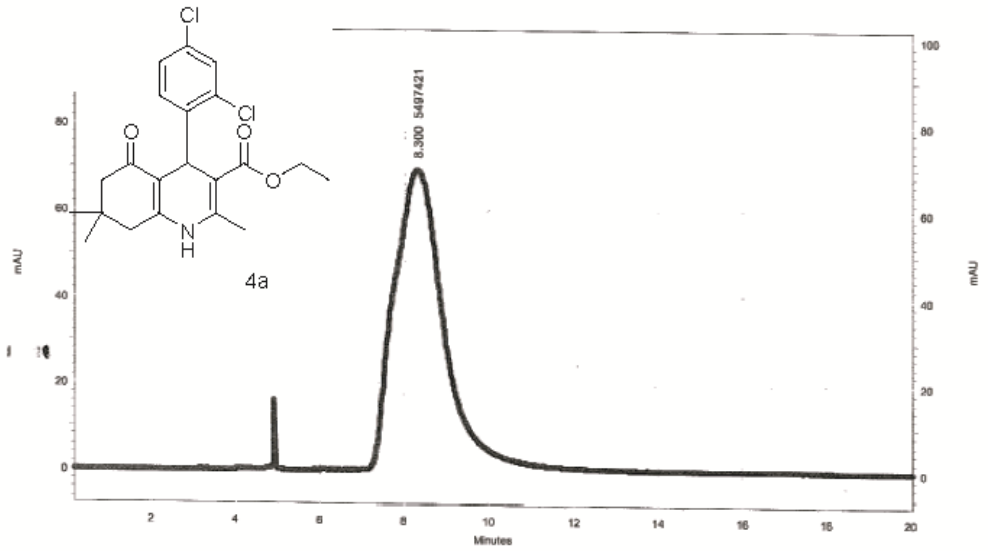
Cl
Cl
O
O
O
N
H
4a
8.300 5497421
mAU
Minutes

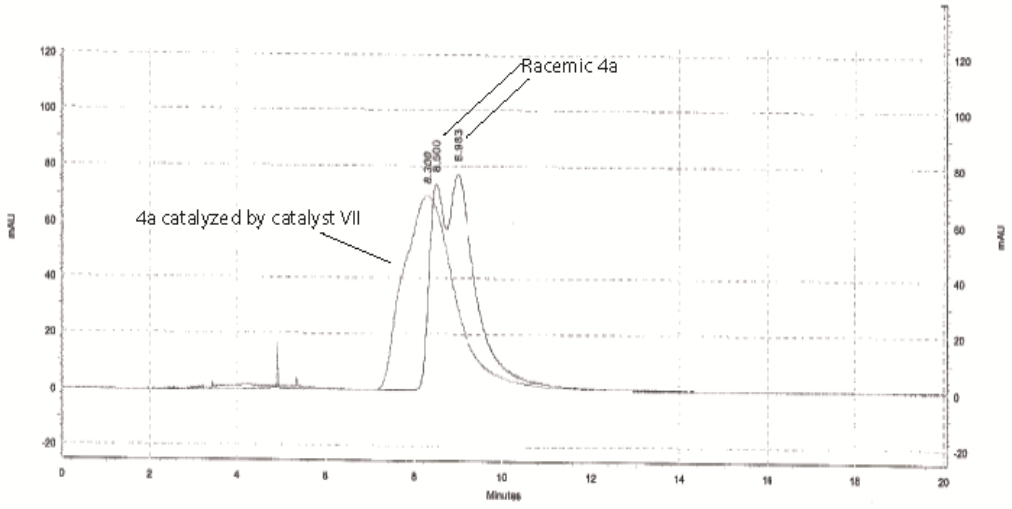
Racemic 4a
4a catalyzed by catalyst VII
8.300
8.500
8.983
mAU
Minutes

40

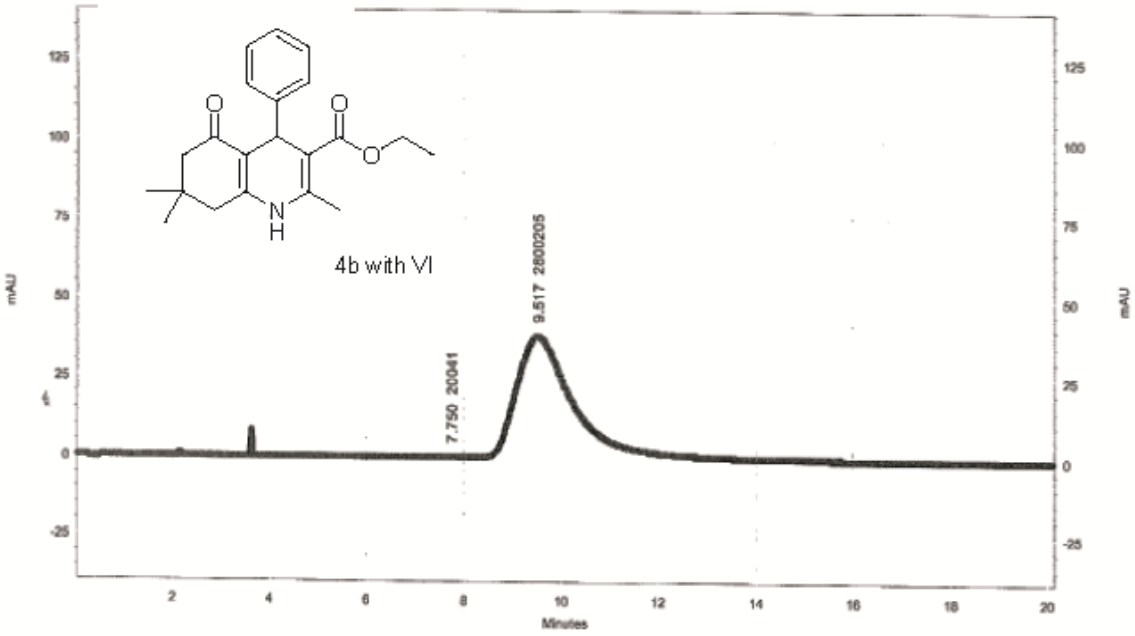
4b with VI
7.750 20041
9.517 2800205
mAU
Minutes

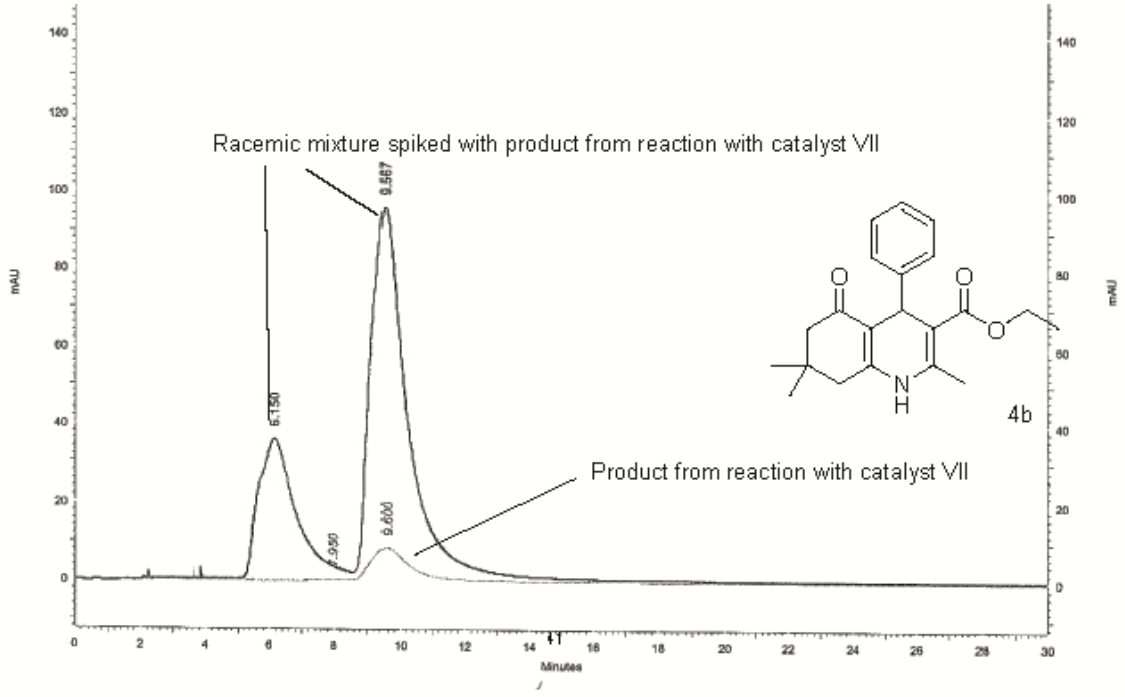
Racemic mixture spiked with product from reaction with catalyst VII
6.150
8.567
8.950
9.600
4b
Product from reaction with catalyst VII
mAU
Minutes

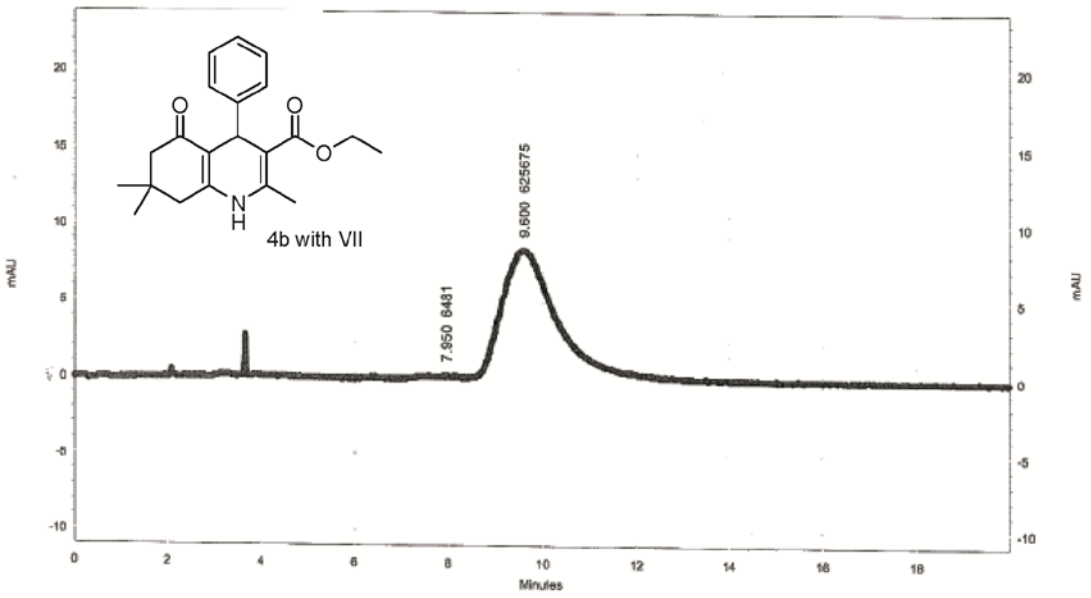
4b with VII
7.950 6481
9.600 625675
mAU
Minutes

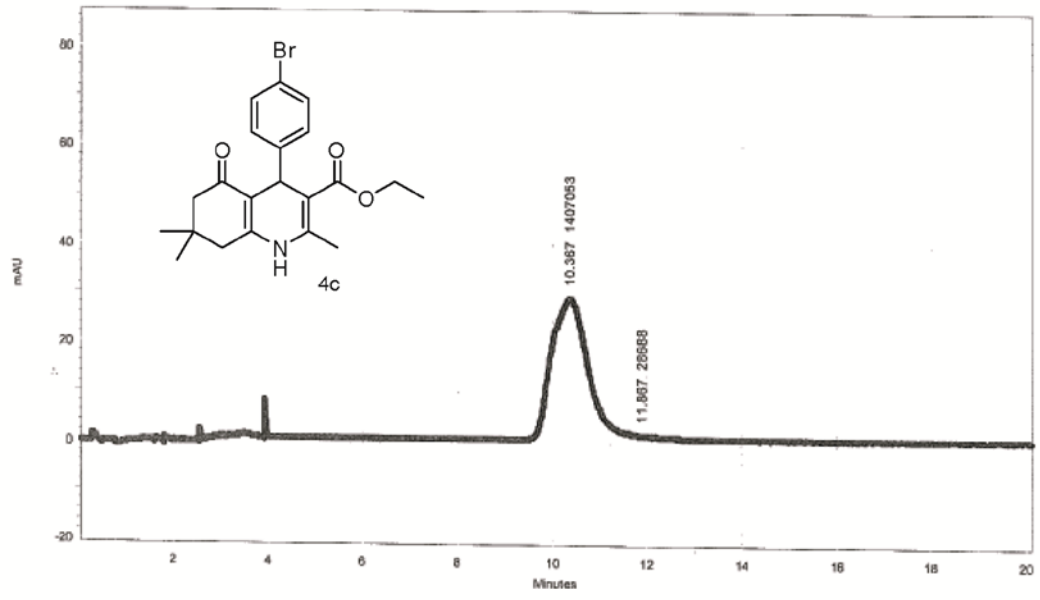
Br
4c
10.367 1407053
11.867 26688
mAU
Minutes

42

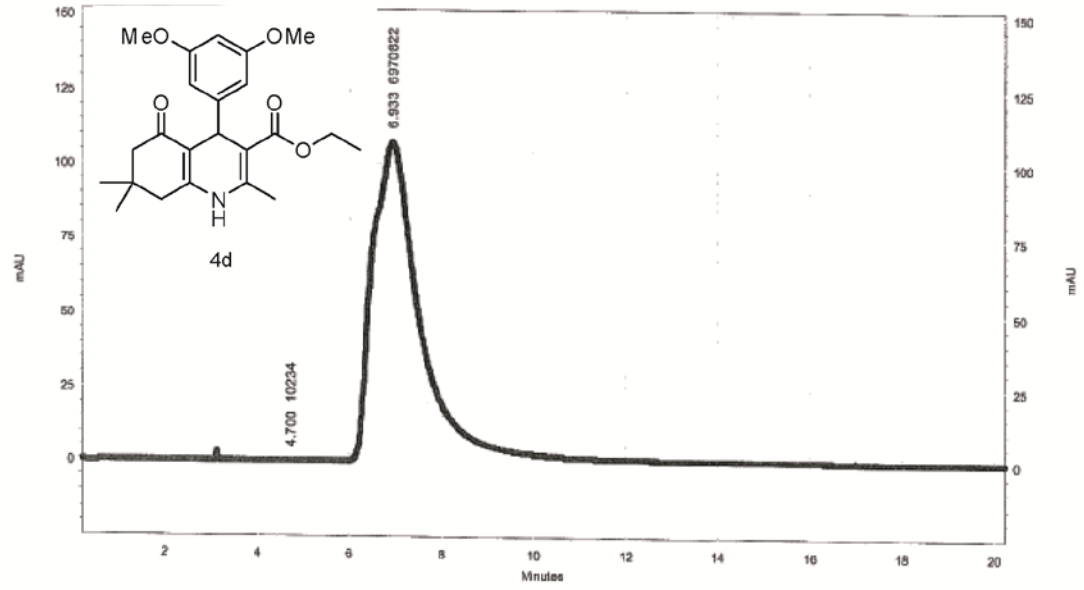
MeO
OMe
O
O
O
N
H
4d
6.933 6970622
4.700 10234
mAU
Minutes

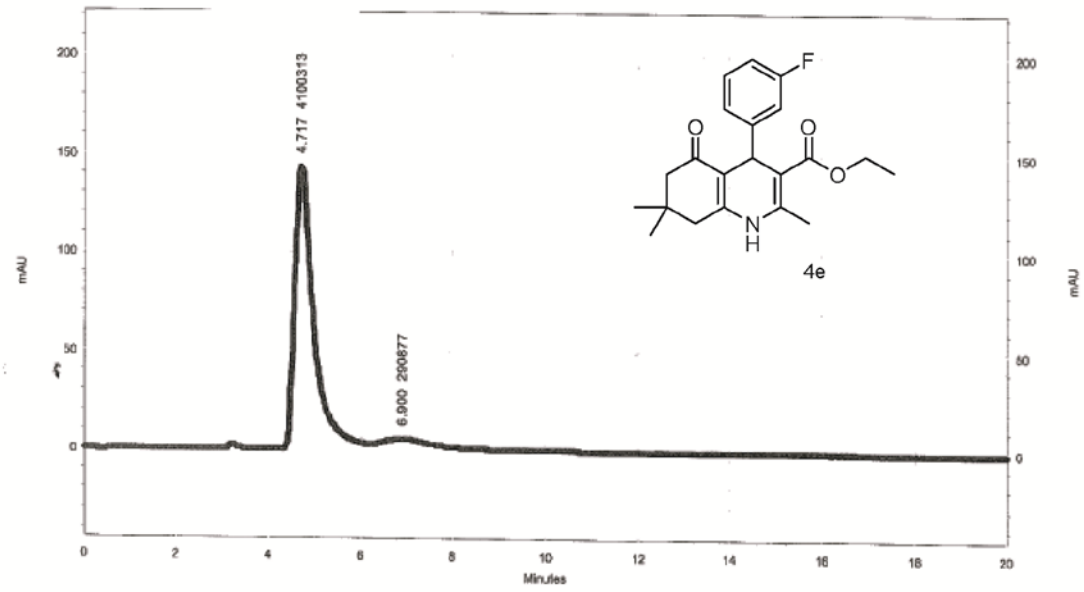
F
O
O
O
N
H
4e
4.717 4100313
6.900 290877
mAU
Minutes

43

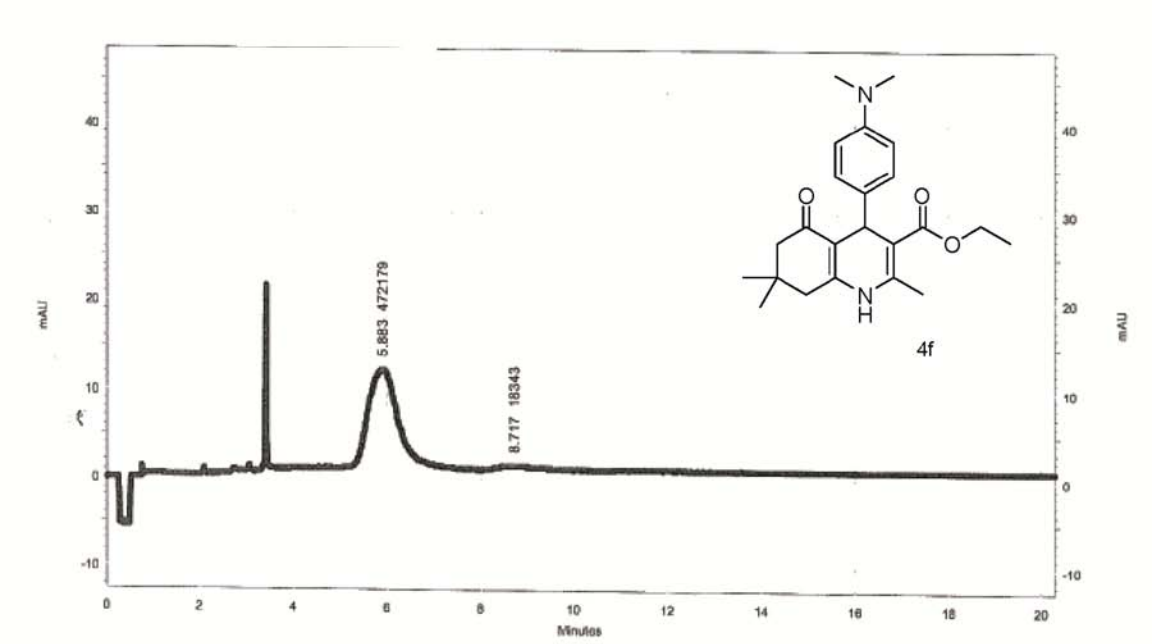
5.883 472179
8.717 18343
mAU
Minutes
4f

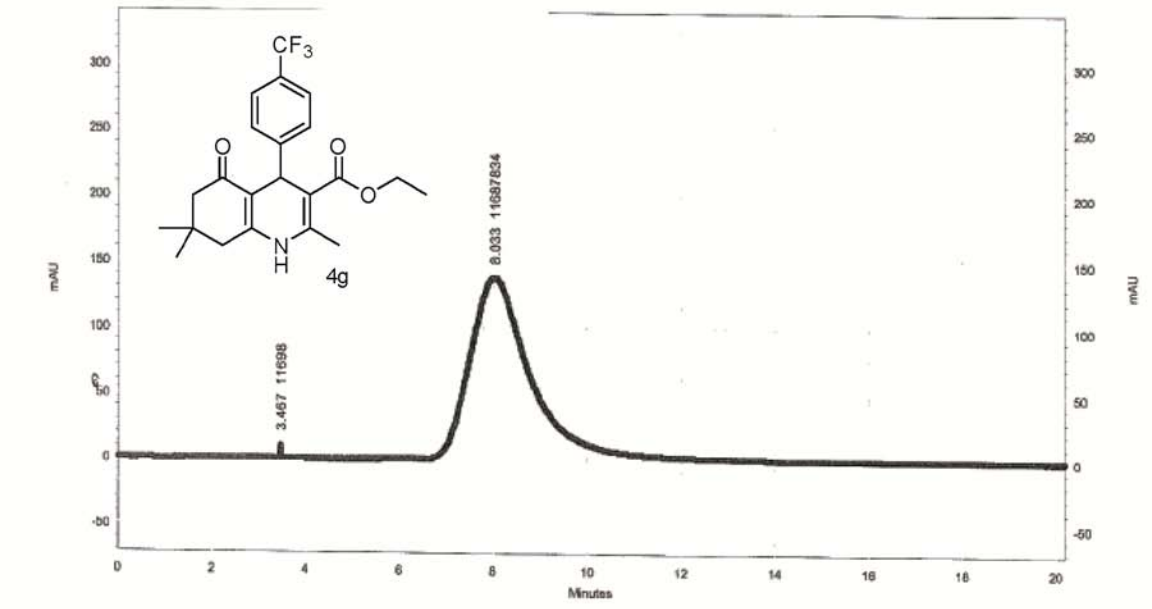
3.467 11698
8.033 11687834
mAU
Minutes
4g

44

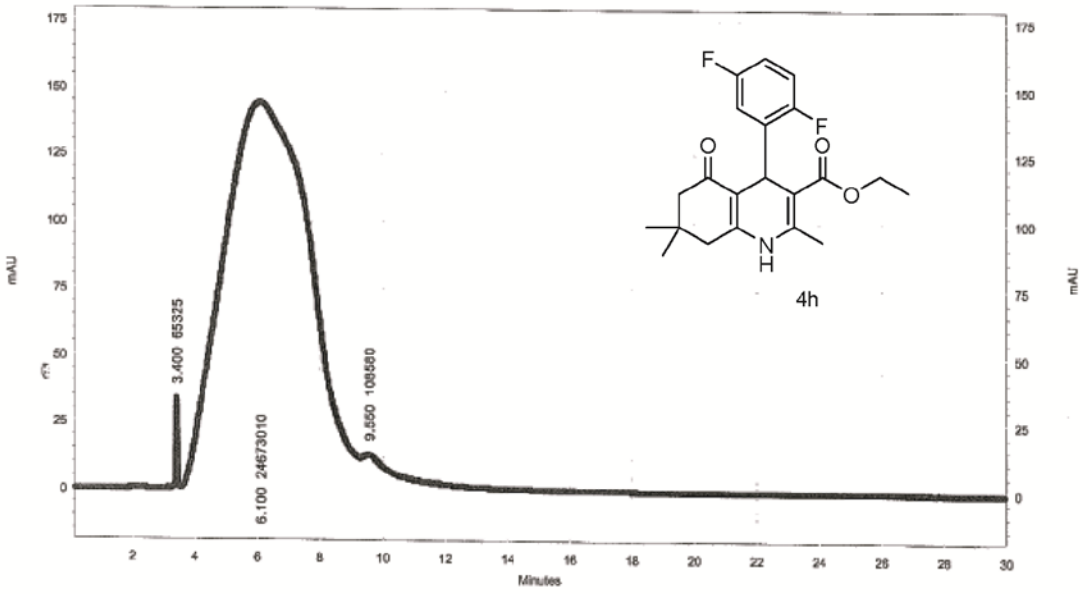
3.400 65325
6.100 24673010
9.550 108580
mAU
Minutes
4h

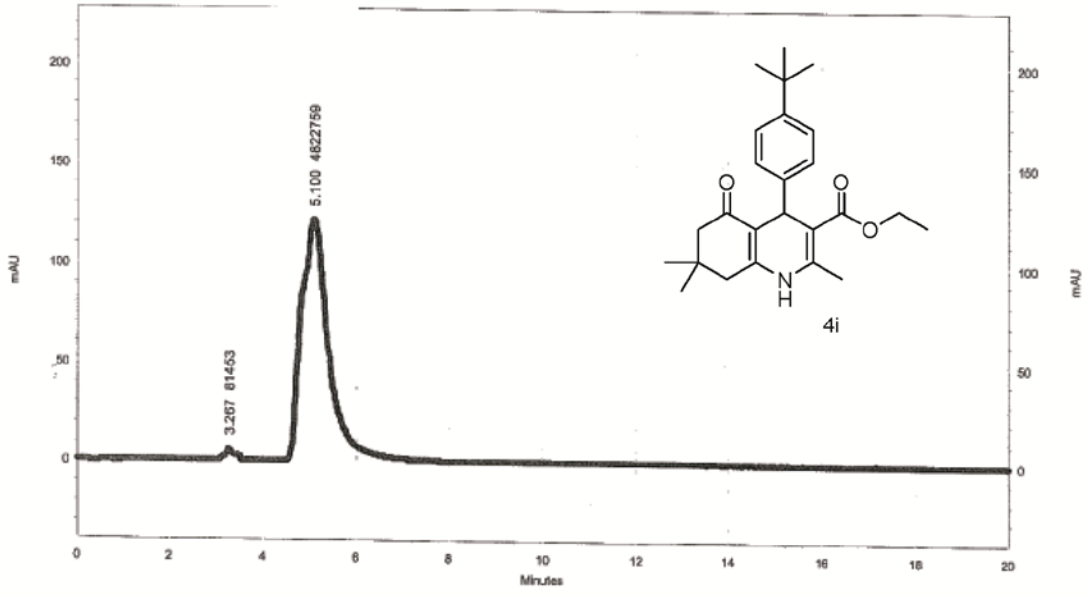
3.267 81453
5.100 4622759
mAU
Minutes
4i

45

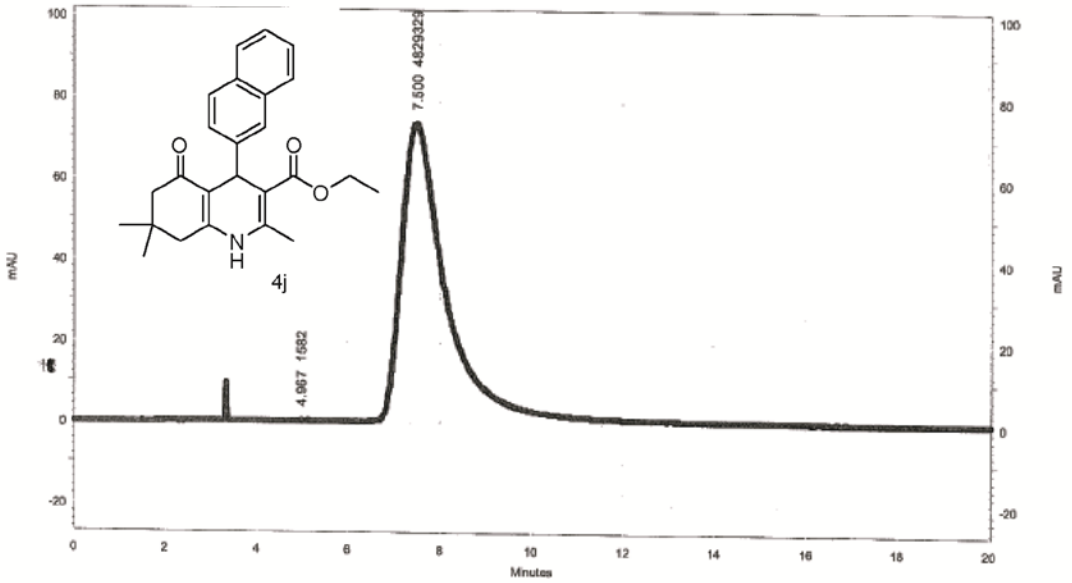
4j
7.500 4829329
4.967 1582
mAU
Minutes

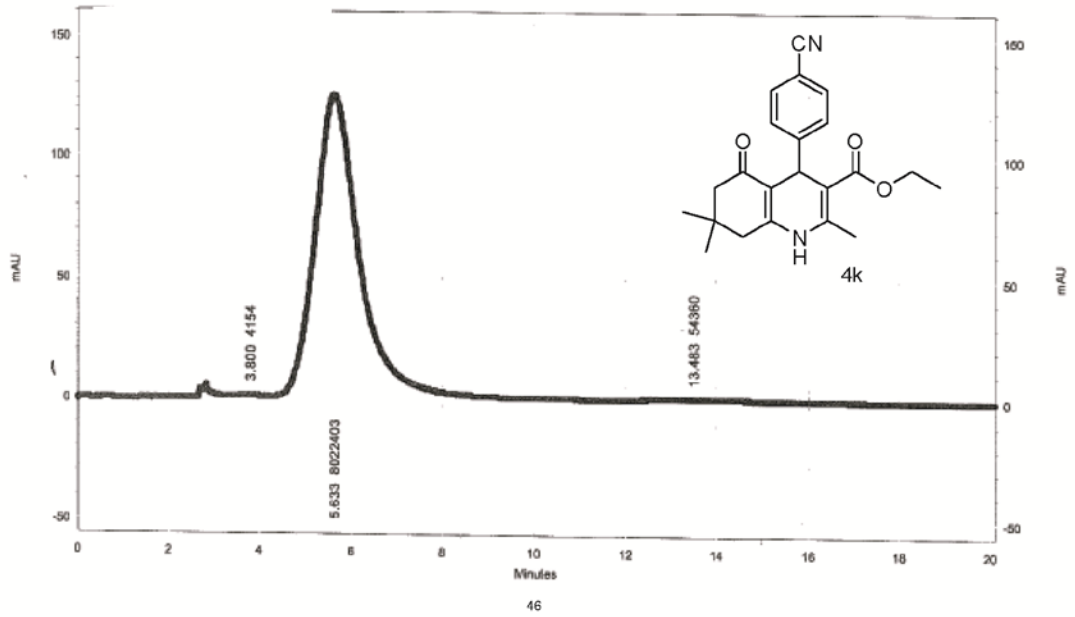
CN
4k
3.800 4154
5.633 8022403
13.483 54360
mAU
Minutes

46

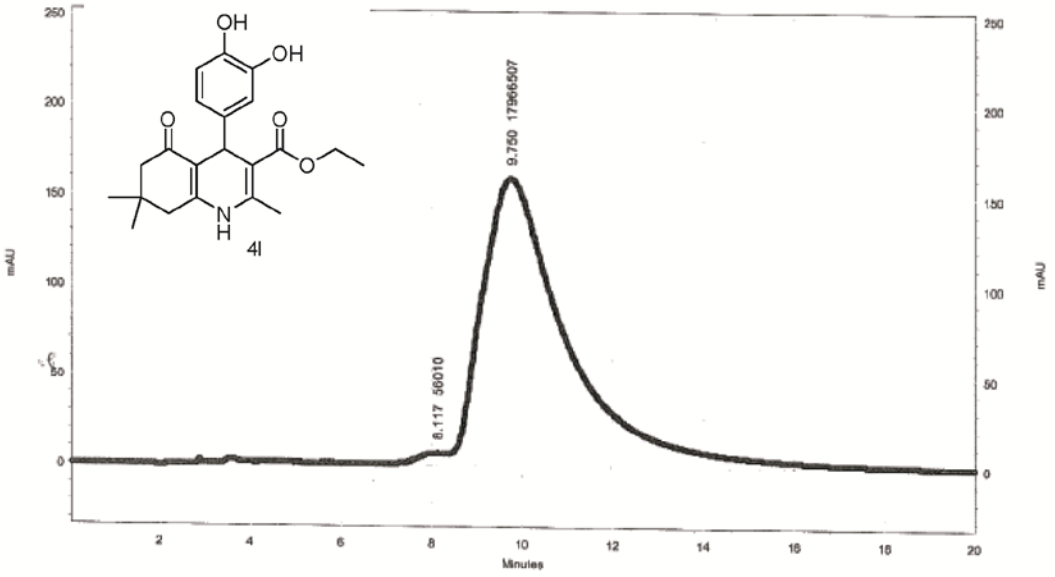
OH
OH
O
O
O
N
H
4l
mAU
9.750 17966507
8.117 56010
Minutes

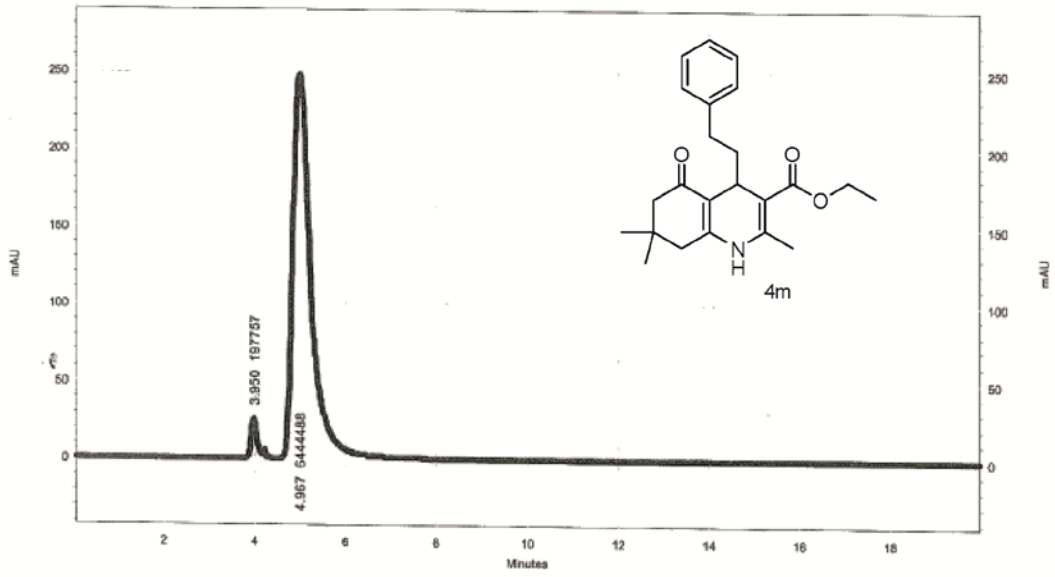
O
O
O
N
H
4m
mAU
3.950 197757
4.967 644488
Minutes

47

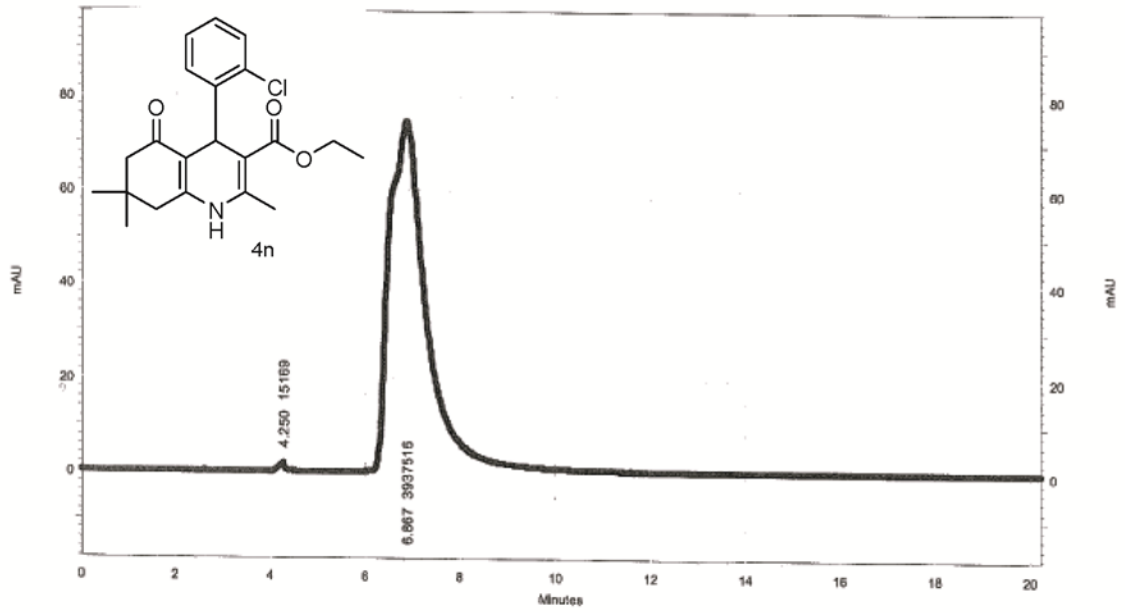
Cl
O
O
O
N
H
4n
mAU
80
60
40
20
0
4.250 15169
6.867 3937516
0
2
4
6
8
10
12
14
16
18
20
Minutes

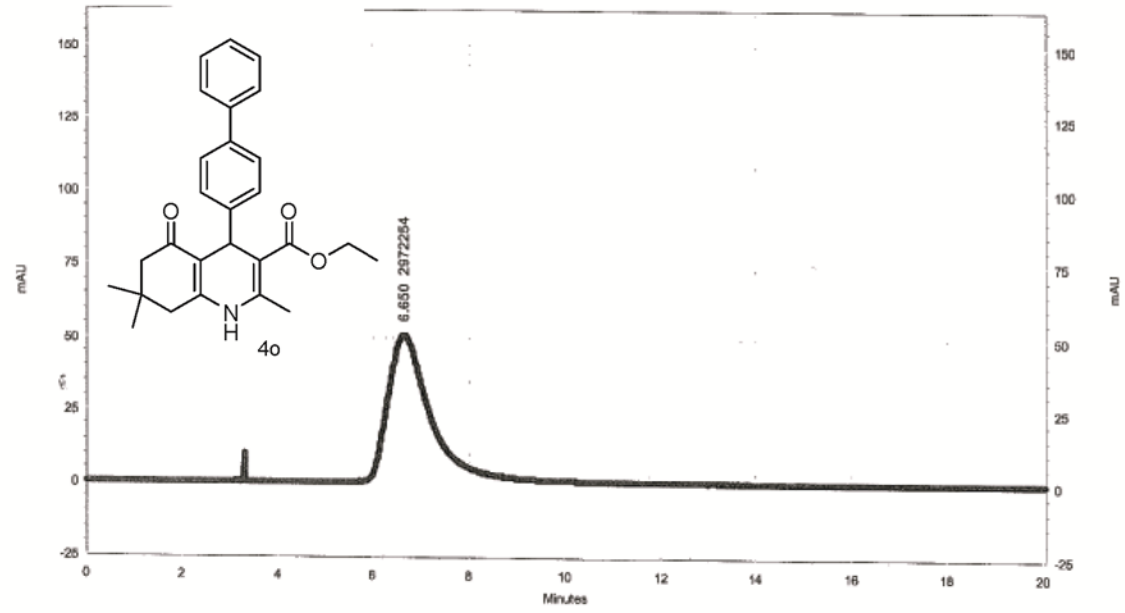
O
O
O
N
H
4o
mAU
150
125
100
75
50
25
0
-25
6.650 2972254
0
2
4
6
8
10
12
14
16
18
20
Minutes

48

3.6 References

1. Spires-Jones, T. L.; Stoothoff, W. H.; de Calignon, A.; Jones, P. B.; Hyman, B. T., Tau pathophysiology in neurodegeneration: a tangled issue. *Trends Neurosci* **2009,** *32* (3), 150-9.

2. Jeganathan, S.; von Bergen, M.; Mandelkow, E. M.; Mandelkow, E., The natively unfolded character of tau and its aggregation to Alzheimer-like paired helical filaments. *Biochemistry* **2008,** *47* (40), 10526-39.

3. Wolfe, M. S., Tau mutations in neurodegenerative diseases. *J Biol Chem* **2009,** *284* (10), 6021-5.

4. Braak, H.; Braak, E., Neuropathological stageing of Alzheimer-related changes. *Acta Neuropathol* **1991,** *82* (4), 239-59.

5. Taniguchi, S.; Suzuki, N.; Masuda, M.; Hisanaga, S.; Iwatsubo, T.; Goedert, M.; Hasegawa, M., Inhibition of heparin-induced tau filament formation by phenothiazines, polyphenols, and porphyrins. *J Biol Chem* **2005,** *280* (9), 7614-23.

6. Wischik, C. M.; Edwards, P. C.; Lai, R. Y.; Roth, M.; Harrington, C. R., Selective inhibition of Alzheimer disease-like tau aggregation by phenothiazines. *Proc Natl Acad Sci U S A* **1996,** *93* (20), 11213-8.

7. Mazanetz, M. P.; Fischer, P. M., Untangling tau hyperphosphorylation in drug design for neurodegenerative diseases. *Nat Rev Drug Discov* **2007,** *6* (6), 464-79.

8. Koren, J., 3rd; Jinwal, U. K.; Lee, D. C.; Jones, J. R.; Shults, C. L.; Johnson, A. G.; Anderson, L. J.; Dickey, C. A., Chaperone signalling complexes in Alzheimer's disease. *J Cell Mol Med* **2009,** *13* (4), 619-30.

9. Jinwal, U. K.; Miyata, Y.; Koren, J., 3rd; Jones, J. R.; Trotter, J. H.; Chang, L.; O'Leary, J.; Morgan, D.; Lee, D. C.; Shults, C. L.; Rousaki, A.; Weeber, E. J.; Zuiderweg, E. R.; Gestwicki, J. E.; Dickey, C. A., Chemical manipulation of hsp70 ATPase activity regulates tau stability. *J Neurosci* **2009,** *29* (39), 12079-88.

10. Oddo, S.; Caccamo, A.; Tseng, B.; Cheng, D.; Vasilevko, V.; Cribbs, D. H.; LaFerla, F. M., Blocking Abeta42 accumulation delays the onset and progression of tau pathology via the C terminus of heat shock protein70-interacting protein: a mechanistic link between Abeta and tau pathology. *J Neurosci* **2008,** *28* (47), 12163-75.

11. Dickey, C. A.; Kamal, A.; Lundgren, K.; Klosak, N.; Bailey, R. M.; Dunmore, J.; Ash, P.; Shoraka, S.; Zlatkovic, J.; Eckman, C. B.; Patterson, C.; Dickson, D. W.; Nahman, N. S., Jr.; Hutton, M.; Burrows, F.; Petrucelli, L., The high-affinity HSP90-CHIP complex recognizes and selectively degrades phosphorylated tau client proteins. *J Clin Invest* **2007,** *117* (3), 648-58.

12. Chebanov, V. A.; Muravyova, E. A.; Desenko, S. M.; Musatov, V. I.; Knyazeva, I. V.; Shishkina, S. V.; Shishkin, O. V.; Kappe, C. O., Microwave-assisted three-component synthesis of 7-aryl-2-alkylthio-4,7-dihydro-1,2,4-triazolo[1,5-a]-pyrimidine-6-carboxam ides and their selective reduction. *J Comb Chem* **2006,** *8* (3), 427-34.

13. Dallinger, D.; Kappe, C. O., Automated generation of a dihydropyrimidine compound library using microwave-assisted processing. *Nat Protoc* **2007,** *2* (7), 1713-21.

14. Dondoni, A.; Massi, A.; Sabbatini, S.; Bertolasi, V., Three-component Biginelli cyclocondensation reaction using C-glycosylated substrates. Preparation of a collection of

dihydropyrimidinone glycoconjugates and the synthesis of C-glycosylated monastrol analogues. *J Org Chem* **2002,** *67* (20), 6979-94.

15. Kappe, C. O., Biologically active dihydropyrimidones of the Biginelli-type--a literature survey. *Eur J Med Chem* **2000,** *35* (12), 1043-52.

16. Ma, Y.; Qian, C.; Wang, L.; Yang, M., Lanthanide triflate catalyzed Biginelli reaction. one-pot synthesis of dihydropyrimidinones under solvent-free conditions. *J Org Chem* **2000,** *65* (12), 3864-8.

17. Nilsson, B. L.; Overman, L. E., Concise synthesis of guanidine-containing heterocycles using the Biginelli reaction. *J Org Chem* **2006,** *71* (20), 7706-14.

18. Pisani, L.; Prokopcova, H.; Kremsner, J. M.; Kappe, C. O., 5-aroyl-3,4-dihydropyrimidin-2-one library generation via automated sequential and parallel microwave-assisted synthesis techniques. *J Comb Chem* **2007,** *9* (3), 415-21.

19. Vugts, D. J.; Jansen, H.; Schmitz, R. F.; de Kanter, F. J.; Orru, R. V., A novel four-component reaction for the synthesis of functionalised dihydropyrimidines. *Chem Commun (Camb)* **2003,** (20), 2594-5.

20. Vugts, D. J.; Koningstein, M. M.; Schmitz, R. F.; de Kanter, F. J.; Groen, M. B.; Orru, R. V., Multicomponent synthesis of dihydropyrimidines and thiazines. *Chemistry* **2006,** *12* (27), 7178-89.

21. Xu, L. W.; Xia, C. G.; Li, L., Transition metal salt-catalyzed direct three-component mannich reactions of aldehydes, ketones, and carbamates: efficient synthesis of N-protected beta-aryl-beta-amino ketone compounds. *J Org Chem* **2004,** *69* (24), 8482-4.

22. Fewell, S. W.; Smith, C. M.; Lyon, M. A.; Dumitrescu, T. P.; Wipf, P.; Day, B. W.; Brodsky, J. L., Small molecule modulators of endogenous and co-chaperone-stimulated Hsp70 ATPase activity. *J Biol Chem* **2004,** *279* (49), 51131-40.

23. Chebanov, V. A.; Saraev, V. E.; Desenko, S. M.; Chernenko, V. N.; Shishkina, S. V.; Shishkin, O. V.; Kobzar, K. M.; Kappe, C. O., One-pot, multicomponent route to pyrazoloquinolizinones. *Org Lett* **2007,** *9* (9), 1691-4.

24. De Silva, R. A.; Santra, S.; Andreana, P. R., A tandem one-pot, microwave-assisted synthesis of regiochemically differentiated 1,2,4,5-tetrahydro-1,4-benzodiazepin-3-ones. *Org Lett* **2008,** *10* (20), 4541-4.

25. Glasnov, T. N.; Stadlbauer, W.; Kappe, C. O., Microwave-assisted multistep synthesis of functionalized 4-arylquinolin-2(1H)-ones using palladium-catalyzed cross-coupling chemistry. *J Org Chem* **2005,** *70* (10), 3864-70.

26. Groenendaal, B.; Ruijter, E.; Orru, R. V., 1-Azadienes in cycloaddition and multicomponent reactions towards N-heterocycles. *Chem Commun (Camb)* **2008,** (43), 5474-89.

27. Ng, P. Y.; Masse, C. E.; Shaw, J. T., Cycloaddition reactions of imines with 3-thiosuccinic anhydrides: synthesis of the tricyclic core of martinellic acid. *Org Lett* **2006,** *8* (18), 3999-4002.

28. Ramon, D. J.; Yus, M., Asymmetric multicomponent reactions (AMCRs): the new frontier. *Angew Chem Int Ed Engl* **2005,** *44* (11), 1602-34.

29. Rivera, D. G.; Vercillo, O. E.; Wessjohann, L. A., Rapid generation of macrocycles with natural-product-like side chains by multiple multicomponent macrocyclizations (MiBs). *Org Biomol Chem* **2008,** *6* (10), 1787-95.

30. Santra, S.; Andreana, P. R., A one-pot, microwave-influenced synthesis of diverse small molecules by multicomponent reaction cascades. *Org Lett* **2007,** *9* (24), 5035-8.

31. Wei, J.; Shaw, J. T., Diastereoselective synthesis of gamma-lactams by a one-pot, four-component reaction. *Org Lett* **2007,** *9* (20), 4077-80.

32. Wipf, P.; Stephenson, C. R., Three-component synthesis of alpha,beta-cyclopropyl-gamma-amino acids. *Org Lett* **2005,** *7* (6), 1137-40.

33. Wisen, S.; Androsavich, J.; Evans, C. G.; Chang, L.; Gestwicki, J. E., Chemical modulators of heat shock protein 70 (Hsp70) by sequential, microwave-accelerated reactions on solid phase. *Bioorg Med Chem Lett* **2008,** *18* (1), 60-5.

34. Cherkupally, S. R.; Mekala, R., P-TSA catalyzed facile and efficient synthesis of polyhydroquinoline derivatives through hantzsch multi-component condensation. *Chem Pharm Bull (Tokyo)* **2008,** *56* (7), 1002-4.

35. Das, B.; Ravikanth, B.; Ramu, R.; Vittal Rao, B., An efficient one-pot synthesis of polyhydroquinolines at room temperature using HY-zeolite. *Chem Pharm Bull (Tokyo)* **2006,** *54* (7), 1044-5.

36. Dondoni, A.; Massi, A.; Aldhoun, M., Hantzsch-type three-component approach to a new family of carbon-linked glycosyl amino acids. Synthesis of C-glycosylmethyl pyridylalanines. *J Org Chem* **2007,** *72* (20), 7677-87.

37. Miri, R.; Mehdipour, A., Dihydropyridines and atypical MDR: a novel perspective of designing general reversal agents for both typical and atypical MDR. *Bioorg Med Chem* **2008,** *16* (18), 8329-34.

38. Tu, S.; Zhu, X.; Zhang, J.; Xu, J.; Zhang, Y.; Wang, Q.; Jia, R.; Jiang, B.; Yao, C., New potential biologically active compounds: design and an efficient synthesis of N-substituted 4-aryl-4,6,7,8-tetrahydroquinoline-2,5(1H,3H)-diones under microwave irradiation. *Bioorg Med Chem Lett* **2006,** *16* (11), 2925-8.

39. Tu, S. J.; Jiang, B.; Jia, R. H.; Zhang, J. Y.; Zhang, Y.; Yao, C. S.; Shi, F., An efficient one-pot, three-component synthesis of indeno[1,2-b]quinoline-9,11(6H,10H)-dione, acridine-1,8(2H,5H)-dione and quinoline-3-carbonitrile derivatives from enaminones. *Org Biomol Chem* **2006,** *4* (19), 3664-8.

40. Tu, S. J.; Jiang, B.; Zhang, J. Y.; Jia, R. H.; Zhang, Y.; Yao, C. S., Efficient and direct synthesis of poly-substituted indeno[1,2-b]quinolines assisted by p-toluene sulfonic acid using high-temperature water and microwave heating via one-pot, three-component reaction. *Org Biomol Chem* **2006,** *4* (21), 3980-5.

41. Kang, Q.; Zhao, Z. A.; You, S. L., Asymmetric transfer hydrogenation of beta,gamma-alkynyl alpha-imino esters by a Bronsted acid. *Org Lett* **2008,** *10* (10), 2031-4.

42. Ouellet, S. G.; Walji, A. M.; MacMillan, D. W., Enantioselective organocatalytic transfer hydrogenation reactions using Hantzsch esters. *Acc Chem Res* **2007,** *40* (12), 1327-39.

43. Storer, R. I.; Carrera, D. E.; Ni, Y.; MacMillan, D. W., Enantioselective organocatalytic reductive amination. *J Am Chem Soc* **2006,** *128* (1), 84-6.

44. Tuttle, J. B.; Ouellet, S. G.; MacMillan, D. W., Organocatalytic transfer hydrogenation of cyclic enones. *J Am Chem Soc* **2006,** *128* (39), 12662-3.

45. Gong, L. Z.; Chen, X. H.; Xu, X. Y., Asymmetric organocatalytic Biginelli reactions: a new approach to quickly access optically active 3,4-dihydropyrimidin-2-(1H)-ones. *Chemistry* **2007,** *13* (32), 8920-6.

46. Huang, Y.; Yang, F.; Zhu, C., Highly enantioselective Biginelli reaction using a new chiral ytterbium catalyst: asymmetric synthesis of dihydropyrimidines. *J Am Chem Soc* **2005,** *127* (47), 16386-7.

47. Lou, S.; Taoka, B. M.; Ting, A.; Schaus, S. E., Asymmetric Mannich reactions of beta-keto esters with acyl imines catalyzed by cinchona alkaloids. *J Am Chem Soc* **2005,** *127* (32), 11256-7.

48. Lou, S.; Dai, P.; Schaus, S. E., Asymmetric Mannich reaction of dicarbonyl compounds with alpha-amido sulfones catalyzed by cinchona alkaloids and synthesis of chiral dihydropyrimidones. *J Org Chem* **2007,** *72* (26), 9998-10008.

49. Andreana, P. R.; Liu, C. C.; Schreiber, S. L., Stereochemical control of the Passerini reaction. *Org Lett* **2004,** *6* (23), 4231-3.

50. Dondoni, A.; Massi, A., Decoration of dihydropyrimidine and dihydropyridine scaffolds with sugars via Biginelli and Hantzsch multicomponent reactions: an efficient entry to a collection of artificial nucleosides. *Mol Divers* **2003,** *6* (3-4), 261-70.

51. Franke, P. T.; Johansen, R. L.; Bertelsen, S.; Jorgensen, K. A., Organocatalytic enantioselective one-pot synthesis and application of substituted 1,4-dihydropyridines--Hhantzsch ester analogues. *Chem Asian J* **2008,** *3* (2), 216-24.

52. Enders, D., Muller, S., and Demir, A.S., Enantioselective hantzsch dihydropyridine synthesis via metalated chiral alkyl acetoacetate hydrazones. *Tetrahderon Letters* **1988,** *29* (49), 6437-440.

53. Vigante, B. A., Ozols, Y.Y., Chekavichus, B.S., and Dubur, G.Y., *Khimiya Geterotsiklicheskikh Soednenii* **1988,** *9*, 1232.

54. el-Sabbagh, O. I.; Rady, H. M., Synthesis of new acridines and hydrazones derived from cyclic beta-diketone for cytotoxic and antiviral evaluation. *Eur J Med Chem* **2009,** *44* (9), 3680-6.

55. Tu, S. J., Zhang, Y., Jia, R.H., Jiang, B., Zahang, Y.J., and Ji, S.J., A multi-component reaction for the synthesis of N-substituted furo[3,4-b]quinoline derivatives under microwave irradiation. *Tetrahedron Letters* **2006,** *47* (37), 6521-25.

56. Kumar, A. a. M., R.A., Synthesis of polyhydroquinoline derivatives through unsymmetric Hantzsch reaction using organocatalysts. *Tetrahedron* **2007,** *63* (9), 1946-52.

57. Legeay, J. C.; Goujon, J. Y.; Vanden Eynde, J. J.; Toupet, L.; Bazureau, J. P., Liquid-phase synthesis of polyhydroquinoline using task-specific ionic liquid technology. *J Comb Chem* **2006,** *8* (6), 829-33.

58. Vohra, R. K., Bruneau, C., and Renaud, J.-L., Lewis Acid-Catalyzed Sequential Transformations: Straightforward Preparation of Functional Dihydropyridines. *Adv Synth Catal* **2006,** *348* (18), 2571-2574.

59. Wang, L.-M., Sheng, J., Zhang, L., Han, J.-W., Fan, Z.-Y., Tian, H., and Qian, C.-T., Facile $Yb(OTf)_3$ promoted one-pot synthesis of polyhydroquinoline derivatives through Hantzsch reaction. *Tetrahedron* **2005,** *61* (6), 1539-43.

60. Chen, X. H.; Xu, X. Y.; Liu, H.; Cun, L. F.; Gong, L. Z., Highly enantioselective organocatalytic Biginelli reaction. *J Am Chem Soc* **2006,** *128* (46), 14802-3.

61. McDougal, N. T.; Schaus, S. E., Asymmetric Morita-Baylis-Hillman reactions catalyzed by chiral Bronsted acids. *J Am Chem Soc* **2003,** *125* (40), 12094-5.

62. Schrock, R. R., Jamieson, J.Y., Dolman, S.J., Miller, S.A., Bonitatebus, P.J., and Hoveyda, A.H., New Chiral Molybdenum Catalysts for Asymmetric Olefin Metathesis that Contain 3,3‘-Disubstituted Octahydrobinaphtholate or 2,6-Dichlorophenylimido Ligands. *Organometallics* **2002,** *21* (2), 409-17.

63. Jinwal, U. K.; O'Leary, J. C., 3rd; Borysov, S. I.; Jones, J. R.; Li, Q.; Koren, J., 3rd; Abisambra, J. F.; Vestal, G. D.; Lawson, L. Y.; Johnson, A. G.; Blair, L. J.; Jin, Y.; Miyata, Y.; Gestwicki, J. E.; Dickey, C. A., Hsc70 rapidly engages tau after microtubule destabilization. *J Biol Chem* **2010,** *285* (22), 16798-805.

Chapter 4

Improved Synthesis of 15-Deoxyspergualin and Its Analogs: Targeting the C-Terminus of Hsp70 and Hsp90

4.1 Abstract

Derivatives of the immunosuppressive, natural product, spergualin,[1, 2] are used in the clinic to treat acute allograft rejection, either as a stand-alone agents or in combination with other immunosuppressives.[3-11] Biochemical evidence suggests that these compounds bind the C-terminus that is common to both Hsp70 and Hsp90. However, the molecular consequences of this interaction are not clear and the mechanisms of spergualin-mediated immunosuppression remain unknown.[12-15] Progress towards these goals is complicated by the cumbersome synthesis of spergualin analogs, its limited availability for research use and the poor chemical stability of the products. To overcome these challenges, we have re-investigated the synthesis of spergualin and designed a route that reduces the number of synthetic steps and improves the overall yield by at least 6-fold. This route employs the Ugi multi-component reaction to generate the peptoid-like core of spergualin. This approach facilitates rapid and modular generation of derivatives, including the clinically important derivatives, 15-deoxyspergualin (15-DSG) and 15-methoxyspergualin (MeDSG). When compared to spergualin, products of this reaction have dramatically improved stability in both basic and acidic conditions. Moreover, access to these derivatives has allowed initial exploration of the molecular

mechanisms of this class, including the discovery that spergualin-like compounds inhibit interactions between Hsp70 and the important E3 ligase, CHIP, likely by shielding contacts at the chaperone's C-terminus. Thus, this improved synthetic route allows for the improved creation of spergualin derivatives. This advancement should permit new studies of their mechanism of action.

4.1.1 Introduction to Spergualin and Its Analogs

As discussed briefly in Chapter 1, Umezawa and colleagues first identified spergualin in 1982 and characterized its antibiotic activity (Figure 4-1A).[16, 17,18-21] This polyamine natural product was isolated from a soil sample and found to originated from a species similar to *Bacillus lateroporus*. Later work established that spergualin was a potent immunosuppressive, prolonging the survival of mice undergoing allograft rejection.

Figure 4-1. Structure of relavent polyamines. (A) spergaulin, (B) 15-deoxyspergualin, and (C) tresperimus. 15-Deoxyspergualin is a synthetic derivative of spergualin that has improved antitumor activity. Tresperimus is a synthetic derivative of 15-deoxyspregualin that vastly improves upon its stability problems.

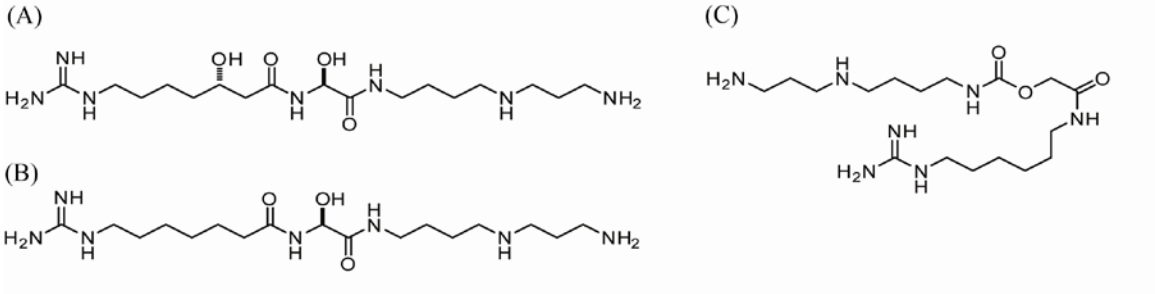

Based on these promising biological activities, the total synthesis of spergualin was conducted by Kondo et al. using L-lysine and 3-amino-1-propanol as the starting materials in a convergent synthesis (Scheme 4-1A). Briefly, L-lysine was converted to (S)-7-guanidino-3-hydroxyheptamide over nine steps, while 11-amino-1,1-dihydroxy-3,8-diazaundecan-2-one was produced from 3-amino-1-propanol over four steps. These

two intermediates were then condensed under acidic conditions for a 14% overall yield.[22] Using this approach, a series of derivatives were produced, which revealed initial structure-activity relationships (SAR). Specifically, the 7-guanidino-3-hydroxyacyl and spermidine groups were found to be essential for activity.[18-20] However, the hydroxyl group at carbon 15 was found to be dispensable and, moreover, removing this group to create 15-deoxyspergualin (15-DSG) appeared to significantly improved stability in basic buffer (Figure 4-1B). Despite this improvement, 15-DSG was first synthesized in a poor 0.3% yield.[20] Later synthetic efforts, also employing a convergent route, mildly improved the yield to around 7% (Scheme 4-1B).[23, 24]

Scheme 4-1. Retrosynthetic analysis of early polyamines. (A) The retrosynthetic analysis of spergualin. (B) The retrosynthetic analysis of 15-deoxyspergualin.

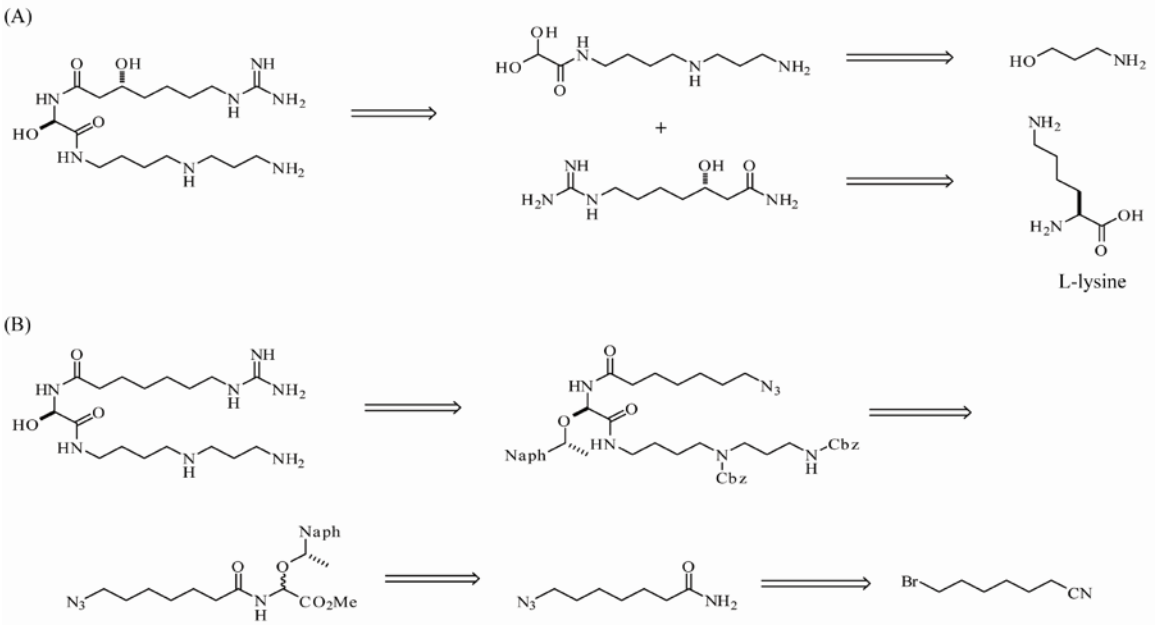

4.1.2 Analogs of 15-Deoxyspergualin

Given the promising activity of spergualin and 15-DSG, more recent attempts were made by Umeda *et al.* and Lebreton *et al.* to enhance the synthetic route, identify

derivatives with better potency and produce compounds with less susceptibility to degradation (Scheme 4-2A).[25, 26] Early studies of 15-DSG metabolism had suggested that it hydrolyzed to glyoxylspermidine and 7-guanadinoheptamide, especially in basic, aqueous buffer.[17, 1825] Thus, Umeda *et al*. focused on replacing the unstable

Scheme 4-2. Retrosynthetic ananlysis of routes to 15-deoxyspergualin analogs. (A) Convergent synthesis of 15-DSG analogs following multiple linear steps. (B) Retrosynthetic analysis of the Ugi strategy to 15-DSG analogs.

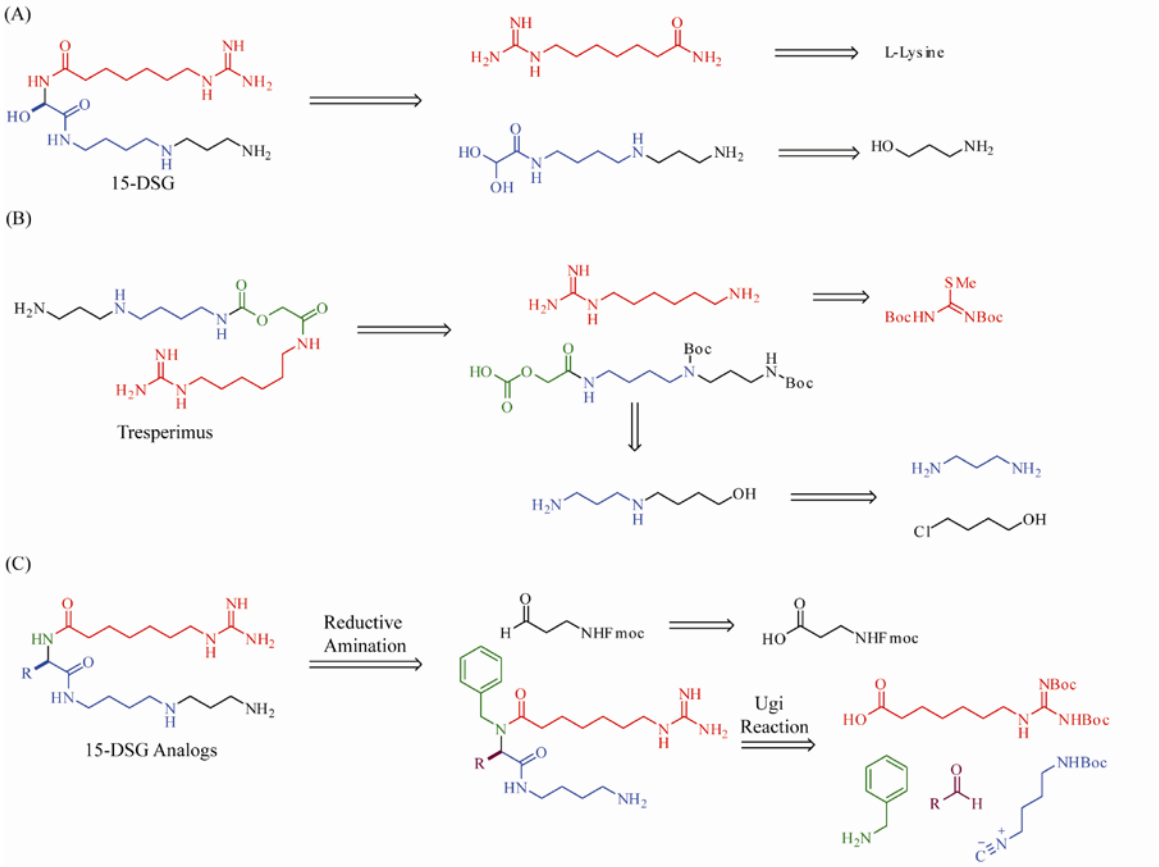

hydroxyglycine as carbon 11 with variety of amino acids while Lebreton et al. focused on switching this group to a carbamate (Scheme 4-2B).[25, 28] These studies revealed that substitutions with serine, alanine, or glycine retained activity, while the larger phenylalanine was not tolerated.[18, 27] Together, these efforts led to the identification of tresperimus (Figure 4-1C), which has improved stability compared to 15-DSG, while retaining immunosuppressant activity.[28, 29] However, these compounds were still

produced through a 14-step, complicated synthetic route, which resulted in poor yield (7%) and loss of the chiral center at position 11. We envisioned that an alternative would be to use the Ugi multi-component reaction, followed by a subsequent reductive amination, to produce the spermidine core, thus yielding a 15-DSG analog in fewer synthetic transformations and with retention of the chiral center (Scheme 4-2C).[30]

4.1.3 The Hsp70-15-Deoxyspergualin Interaction

When potential use of 15-DSG analogs would be in the exploration of its mechanism of action. Although these compounds are potent immunosuppressants and they are used in the clinic, their mechanisms are still unknown. Current models suggest that Hsp70 and Hsp90 are among the cellular targets of 15-DSG.[31, 32] Sugawara *et al.* proposed that 15-DSG inhibits the activation of dendritic cells by interacting with Hsp70.[33] This activity is thought to be mediated by interactions between spergualin derivatives and the EEVD motif found at the C-terminus of both Hsp70 and Hsp90. Removing this motif from Hsp70 ablated the effect of 15-DSG. Further, Nadler *et al.* identified Hsc70, a mammalian constitutively expressed member of the Hsp70 family, as the cellular target of 15-DSG in pull-down assays and the EEVD motif was found to be required.[34, 3536] The K_d for the interaction between Hsc70 or Hsp90 and 15-DSG has been determined to be approximately 5 μM.[37, 38]

4.2 Results and Discussion

4.2.1 Application of the Ugi Reaction to Create Spergualin Analogs

The Ugi reaction allows synthesis of a peptoid backbone from four components, a carboxylic acid, amine, isocyanide, and aldehyde or ketone.[17, 40-44] This reaction is used to produce several pharmaceuticals and has provided a powerful way to create libraries

Scheme 4-3. Mechanism of the Ugi reaction. The frist step of the reactioninvolves the condensaation of an amine with an aldehyde. Next there is a proton transfer, leading to an iminium ion. Following this, the nucelophilic carbon of the isocyanide addsto the iminium ion. The caboxylic acid then adds to the carbon of the isocyanide. The linear compound then undergoes a cyclic transition that upon ring opening gives the peptoid backbone.

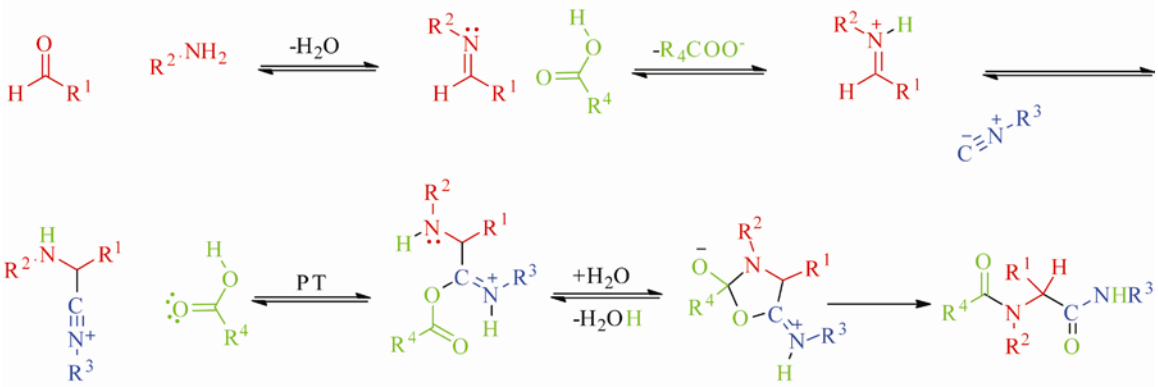

for high throughput screening.[45-47] The first step is thought to be the formation of the imine by the condensation of the amine and the aldehyde or ketone, followed by proton transfer from the carboxylic acid to form the iminium ion and attack by the isocyanide. To complete the reaction, the carboxylic acid then adds to the isocyanide and the peptoid is obtained through a five-membered ring intermediate (Scheme 4-3).

As envisioned, our Ugi-based synthesis of spergualin analogs would proceed through the synthesis of two key components: guanidinylated amines and a series of isocynanides. The first component was generated using the method reported by Feischtingnder *et al*., who used N,N'-di-Boc-N''-triflylguanidine as the guanidinylating reagent.[49] To achieve the final 7-guanidinoheptanoic acid or its derivatives, the published

Scheme 4-4. Synthesis of guanidinylated amino acids. Once guanidinylated these amino acids serve as the acid component of the Ugi reaction.

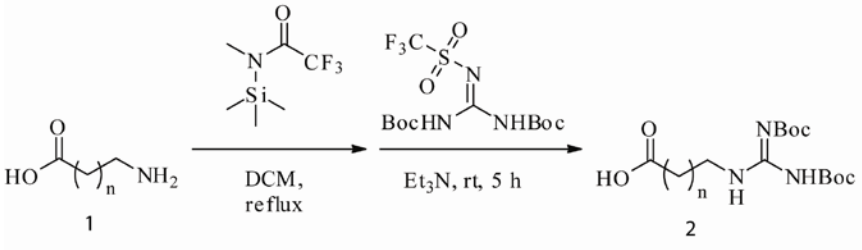

n	yield (%)
2	64
4	72-75
5	69

procedure was slightly modified (Scheme 4-4). Briefly, a flame-dried round bottom flask containing 1 mmol of the amino acid was diluted with 8 mL of anhydrous dichloromethane (DCM). Then, N-methyl-N-trimethylsilyl-trifluoroacetamide (2.2 mmol) was added, and the reaction was heated to a reflux under an argon atmosphere. Upon clarification of the solution, it was cooled and triethylamine (1.1 mmol) and N,N'-di-Boc-N''-triflylguanidine (1.1 mmol) were added. The reaction was then stirred at room temperature for 4-5 hours, diluted with DCM and washed with brine and water. Following drying with sodium sulfate, the mixture was concentrated and purified by flash column chromatography (eluted 50:50 ethylacetate:hexanes). Using this procedure, a series of intermediates was developed, varying in the length of their alkane chains. The yields for the guanidinylation of aminoheptanoic acid, aminohexanoic acid, and γ-aminobutyric acid ranged from 64-75% (**2**, Scheme 4-4).

To create the isocynamide-based intermediate for the Ugi reaction and satisfy the known SAR findings, we pursued 1, 4-diaminobutane (1, 4-DAB). Because DAB has two equivalent amines, we first mono-protected one of these using literature precedent.[51] Briefly, 1, 4-DAB (7.5 g, 85.08 mmol) was diluted in 30 mL of dioxane. A solution of di-tert-butyldicarbonate (2.4 g, 11 mmol) in 30 mL of dioxane was then added to the stirring 1, 4-DAB drop-wise over 1.5 hours.[51] This reaction was stirred for 24 hours and the solvent removed under vacuum. To this mixture, 50 mL of water was added and the resulting insoluble material was removed by filtration. The filtrate was extracted three times with 45 mL of DCM. The organic layers were dried with sodium sulfate and concentrated to give a 56-61% yield (Scheme 4-5A).

Scheme 4-5. Synthesis of isocyanides for later use in the Ugi reaction. (A) The synthesis of tert-butyl (4-isocyanobutyl)carbamate. (B) The synthesis of tert-butyl (4-isocyanophenyl)carbamate.

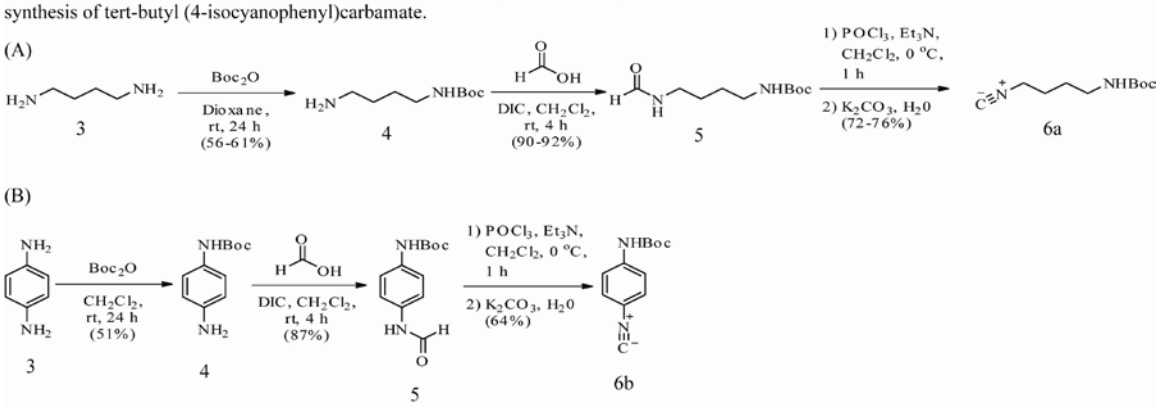

The next step in the generation of tert-butyl (4-isocyanobutyl)carbamate is the addition of formic acid to the remaining free amine group (Scheme 4-5A). Towards that goal, tert-butyl (4-aminobutyl)carbamate (2 mmol) was diluted in 5 mL DCM and formic acid (2 mmol) was added to the stirring reaction. The reaction was then placed into an ice-bath. Once cooled, DIC (2 mmol) was added to the solution and the mixture stirred for 4 hours at room temperature. The reaction was filtered and the filtrate was washed with saturated sodium bicarbonate solution.[52] The organic layer was then dried with sodium sulfate and concentrated. The resulting product, tert-butyl (4-aminobutyl)-carbamate, was synthesized in 90-92% yield. Tert-butyl (4-aminobutyl)carbamate (8.7 mmol) was diluted with 13 mL of DCM. Triethylamine (26.2 mmol) was then added and the solution was cooled in an ice-bath. $POCl_3$ (8.7 mmol) was then added dropwise. The reaction was stirred for 30 minutes and then potassium carbonate (8.7 mmol) was added (Scheme 4-5A). The reaction was then stirred for another 30 minutes. The aqueous layer was extracted five times with DCM 5 times. The DCM layers were combined, then washed with water, dried with sodium sulfate, and concentrated.[52] The product was then purified by flash column chromatography (eluting at 50:50 ethylacetate: hexanes) giving a 72-76% yield. The same procedure was used to synthesize tert-butyl (4-isocyano-

phenyl)carbamate from mono-Boc- 1, 4-phenylenediamine as a way of adding rigidity to the four carbon linker of the spermidine tail (Scheme 4-5B).

4.2.2 Developing the Methodology for the 15-Deoxyspergualin Core with the Ugi Reaction

Using these key intermediates, we next wanted to develop optimized conditions for the Ugi reaction. Many conditions for this reaction have been reported and recent studies have focused on using microwave irradiation to improve yield and reaction times.[53, 54] To explore the best conditions for 15-DSG derivatives, we first used the commercially available isocyanide 1-isocyanopentane as a model reactant. Briefly, the solution of benyzlamine (0.1mmol), benzaldehyde (0.1 mmol), 6-guanidinohexanoic acid (1.1 mmol), and 1-isocyanopentane (0.1 mmol) was heated in 0.5 mL methanol (MeOH) using a Biotage Initiator microwave at 120 °C for 20 minutes (Scheme 4-6). This process yielded the product in 70% yield following column purification using silica gel (eluting 75:25 ethylacetate:hexanes). However, when tert-butyl (4-isocyanobutyl)carbamate was substituted in the reaction, the yield decreased to a less desirable 11%. Therefore, we screened conditions to boost the yield while employing the target, tert-butyl (4-isocyanobutyl)carbamate.

Scheme 4-6. Testing Feasibiilty of Reaction Using Commercially Available Isocyanide.

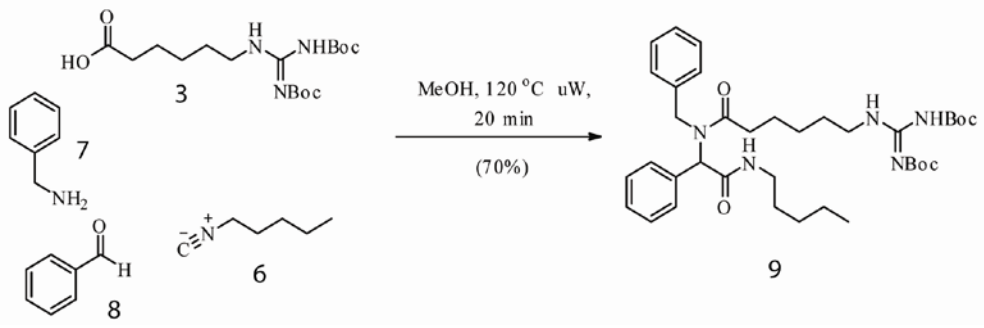

In this effort, we focused on three variables, reaction time, temperature, and solvent. Using the common microwave-compatible solvents, methanol, DMF and ethanol, we screened at temperatures from 90 to 120 °C for 10 to 20 minutes. This search identified DMF, 100 °C for 20 minutes as the best conditions, yielding 46% yield (Table 4-1).

Table 4-1. Optimization of the Ugi reaction for the synthesis of 15-DSG analogs.

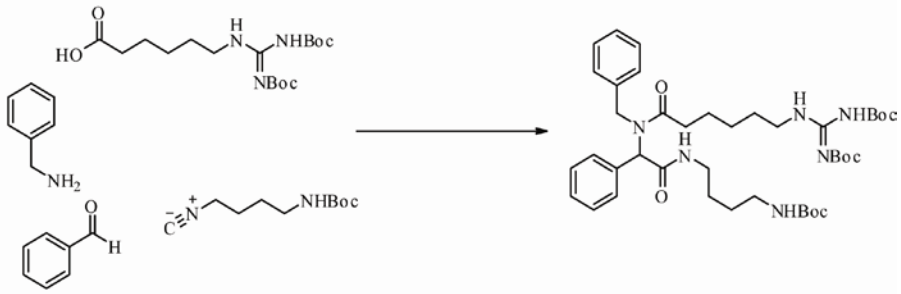

Entry	Solvent	Temp (°C)	Time (min)	Yield (%)
1	MeOH	100	20	2-10
2	MeOH	100	30	<2
3	MeOH	90	20	36
4	MeOH	90	30	22
5	MeOH	110	20	<2
6	MeOH	120	10	12
7	MeOH	130	10	ND
8	MeOH	RT	240	35
9	EtOH	90	20	27
10	EtOH	90	40	17
11	DMF	100	20	46
12	DMF	120	20	32
13	DMF	RT	240	43

Following this optimized protocol, the library of 15-DSG analogs was synthesized. To build diversity in the series while also maintaining the previous SAR features, the aldehyde component was systematically varied while the 7-guanidinohepatnoic acid, benzylamine, and tert-butyl (4-isocyanobutyl)carbamate were

held constant (entries 21-24, Table 4-2). Another set of derivatives was synthesized by varying the aldehyde component while 6-guanidinoheptanoic acid, benzylamine, and tert-butyl (4-isocyanobutyl)carbamate were held constant (entries 1-12, Table 4-2). Finally, three derivatives were synthesized using tert-butyl (4-isocyanophenyl)carbamate as the isocyanide (entries 3-4, Table 4-2). Given that earlier publications had suggested the spermidine tail was important for 15-DSG's activity, several truncated versions were synthesized (entries 1-2, Table 4-2) by deprotecting the Ugi reaction product with 85% phosphoric acid to remove the Boc groups.[55] The benzyl group was then removed under oxidative conditions by CAN (2.1 equiv) in a water/acetonitrile (1/5 ratio) over 2 hours.[56] Following purification on basic alumina oxide and eluting with 10:90 methanol:chloroform, the truncated product was isolated in 50-56% yield. All products were deprotected using 85% phosphoric acid to prepare the free amine for the subsequent reductive amination to produce the full spermidine tail.[55]

4.2.3 Producing the Spermidine Tail Employing a Reductive Amination Strategy

To complete the 15-DSG analogs, we envisioned reductive amination with Fmoc-3-amino-1-propanal. This compound is readily available from Fmoc-β-alanine (Scheme 4-7). Briefly, Fmoc-β-alanine (3 mmol, 1 equiv) was added to a flame dried round bottom flask, followed by dilution with 20 mL anhydrous DCM. Then triphenylphosphine (6 mmol, 2 equiv) and trichloroacetonitrile (6 mmol, 3 equiv) were added. After the Fmoc-

Scheme 4-7. The synthesis of Fmoc-3-amino-1-propanal.

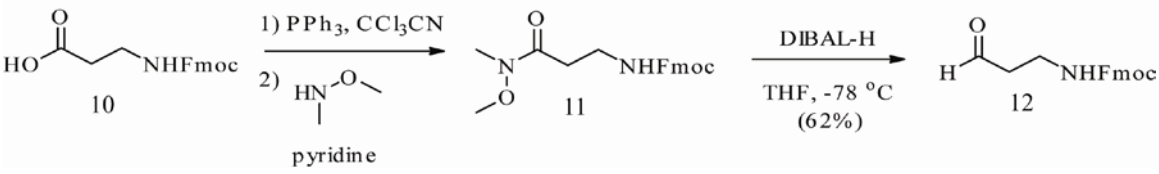

β-alanine appeared to be consumed, N-O-dimethylhydroxylamine hydrochloride (6.3 mmol, 2.1 equiv) and pyridine (15 mmol, 5 equiv) were added at 0 °C. After 1 hour, the reaction was washed with brine and dried over sodium sulfate. After concentration, the product, N-methoxy-N-methyl-3-(Fmoc-amino)-propionamide, was purified by flash column chromatography (eluting at 50:50 ethylacetate:hexanes) to give a 97% yield.[58] N-methoxy-N-methyl-3-(Fmoc-amino)-propionamide (1.15 mmol, 1 eq) was dissolved in 10 mL anhydrous THF. The reaction was cooled to -78 °C under an argon atmosphere. 3.45 mL of a 1.0 M solution of diisobutylaluminum hydride in THF was added dropwise over 10 minutes. After 5 minutes the reaction was quenched with 5% HCl in EtOH and it was allowed to warm to room temperature. The solution was diluted into DCM and washed with brine, the organic layers were treated with sodium sulfate and then concentrated under vacuum. The product was then purified by flash column chromatography (eluting with 50:50 ethaylacetate:hexanes) to afford Fmoc-3-amino-1-propanal in 62% yield.

To conduct the reductive amination (Scheme 4-8) the phosphoric acid[55] deprotected Ugi products was employed as the amine (0.05 mmol, 1 equiv) and was diluted in 2 mL THF or DCE. Then Fmoc-3-amino-1-propanal (0.05mmol, 1 equiv) was added to the reaction, followed $NaBH(OAc)_3$ (0.07 mmol, 1.4 equiv). $NaBH(OAc)_3$ was chosen for this study because it doesn't require low pH's like $NaBH_3CN$ and the chemical stability of 15-DSG analogs has proven to be a hurdle in the past.[57] Moreover, $NaBH(OAc)_3$ appears to provide a broader scope to the reaction, while generating less side product.[57] The reaction containing $NaBH(OAc)_3$ was allowed to stir for 1.5 hours under a nitrogen atmosphere, quenched with a saturated sodium bicarbonate solution and

Scheme 4-8. A reductive amination of the primary amine on the 15-DSG analog yields the spermidine tail following two deprtotection steps.

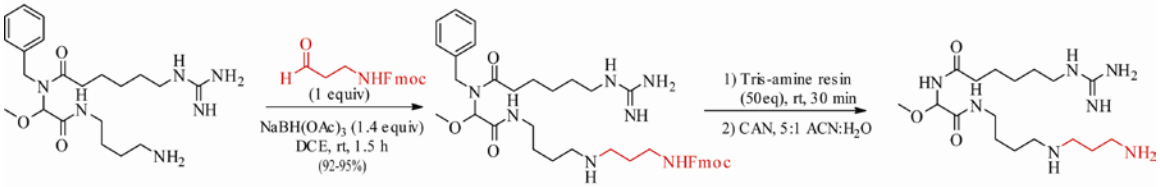

the product extracted with ethylacetate, dried over sodium sulfate, and concentrated by vacuum. The crude product was column purified on basic alumina oxide, eluting with 10:90 methanol:ethylacetate. The yield for this step generally ranged from 80-94% (entries 3-12, Table 4-2).

4.2.4 Deprotection Strategy

Following reductive amination, the Fmoc group needed to be removed to produce the 15-DSG derivatives. One common way to remove Fmoc groups is with base, such as 20% piperidine in DMF. However, we found that the stability of the products under these conditions was not optimal and, moreover, the cleaved Fmoc adduct needed to be removed by column chromatography. To circumvent similar issues, Tris(2-aminoethyl)amine has been reported to remove Fmoc groups.[59] Guided by those efforts, we stirred Tris-amine resin (50 equiv) with the 15-DSG analog in $CHCl_3$ for 20 minutes. This time was required to allow for complete scavenging of the 9-methylene-9H-fluorene byproduct of Fmoc cleavage.

Table 4-2. Library of 15-DSG analogs synthesized using the Ugi reaction/reductive amination strategy.

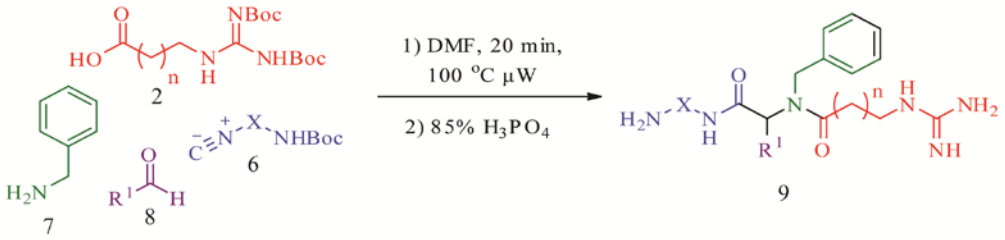

Entry	Compound	n	R^1	X	Yield
1	9a	4	CH_3O	$(CH_2)_4$	52%
2	9b	4	4-Br-Ph	$(CH_2)_4$	57%
3	13a	5	CH_3O	$(CH_2)_4$	41%
4	13b	5	4-Br-Ph	$(CH_2)_4$	33%
5	13c	4	CH_3	$(CH_2)_4$	38%
6	13d	4	$C_2H_5CH(CH_3)$	$(CH_2)_4$	44%
7	13e	4	4-Br-Ph	$(CH_2)_4$	42%
8	13f	4	3-OH-Ph	$(CH_2)_4$	36%
9	13g	4	3,5-OMe-Ph	$(CH_2)_4$	46%
10	13h	2	CH_3O	$(CH_2)_4$	33%
11	13i	2	4-Br-Ph	$(CH_2)_4$	31%
12	13j	4	CH_3O	C_6H_4	49%

Finally, removal of the benzyl group was carried out using mild conditions and CAN.[56] In this method, CAN (2.1 equiv) is added to the 15-DSG analog in a solution of 1:5 water:acetonitrile (2 mL). After stirring for 2 hours, the reaction is quenched with saturated sodium bicarbonate, stirred for 10 minutes and extracted with ethylacetate. The organic layers were combined, dried over sodium sulfate and concentrated under vacuum. The product is then purified on a basic alumina oxide column (eluting at 10:90 methanol:ethylacetate) to afford the final product (Table 4-2).

4.2.5 Biological Activity of Methoxy-15-Deoxyspergualin

One of our major goals in this study was to produce sufficient quantities of spergualin derivatives to permit more detailed studies into its mechanism of action. Preliminary findings support the feasibility of this idea. For example, a fellow graduate student, Matt Smith, found that treatment of yeast cells with MeDSG (compound **13a**), significantly decreased the aggregation of a polyglutamine construct (Fig 4-2). This result suggests that the spergualin derivatives will be useful, membrane-permeable probes of Hsp70 and Hsp90 function in cells.

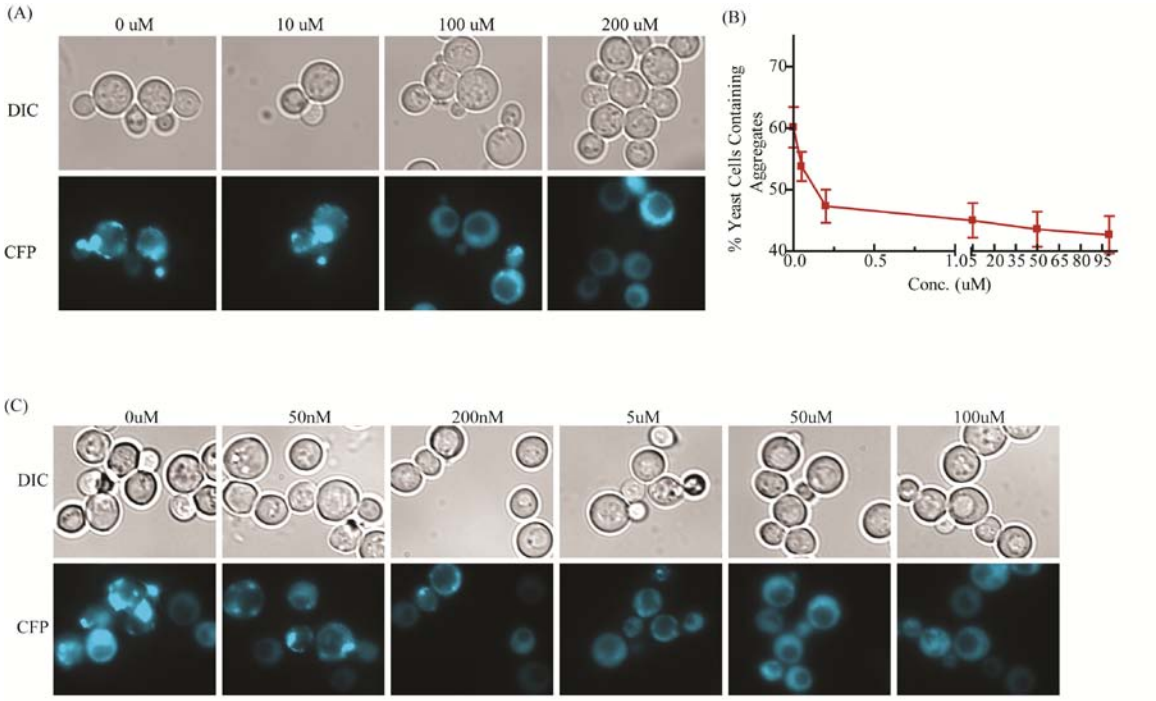

Figure 4-2 Polyamines affect the aggregation of proteins in a yeast model of neurodegeneration. (A) Spergualin caused a dose dependent decrease in the number of yeast cells with aggregates following treatment with the small molecule in these microscopy images. (B) Quantitation of data from yeast cells treated with methoxy-15-DSG. Methoxy-15-DSG causes a dose dependent decrease in the percentage of cells with polyQ aggregates. (C) Microscopy images of methoxy-15-DSG showing fewer aggregates of fluorescently labeled polyQ proteins.

4.2.6 Stability of MeDSG

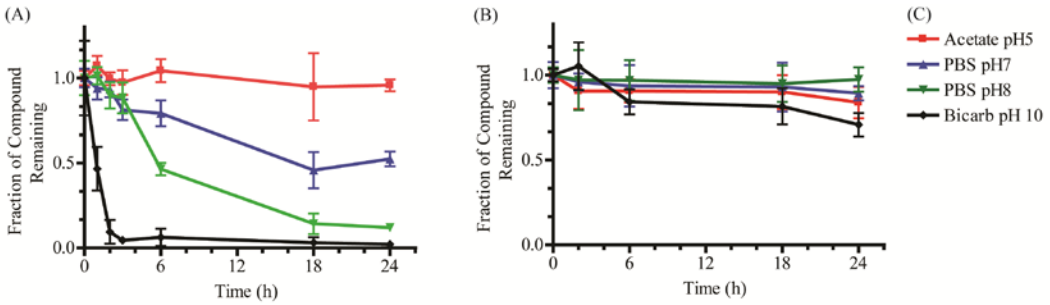

Figure 4-3 Stability testing of polyamines revealed that methoxy-15-DSG is more stable than spregualin under several buffer conditions. (A) Spergualin and (B) methoxy-15-DSG were tested for stability under four different buffer conditions (C). A sample was taken from a tube containing the polyamine under each condition at a prescribed time. The sample was then run on TLC at 3:2:2:0.5 butanol:water:acetic acid:pyridine. The developed TLC was then stained with ninhydrin.

Another problem of the spergualin scaffold that we had hoped to address was its poor intrinsic, chemical stability. Previous studies had shown that 15-DSG had a half-life of a few hours in basic buffers. It has hoped that by changing the hydroxyl at position 11, a more stable derivative could be synthesized. Towards that goal, methoxy-15-DSG (**13a**) was synthesized where the hydroxyl at position 11 was now a methoxy group. We found that this subtle change greatly improved the stability of this compound (Figure 4-3). Thus it appears that the Ugi reaction/reductive amination strategy has provided small molecules that address our concerns about both potency and stability. Hopefully with these contributions it will be able to use these small molecules to parse out Hsp70's and Hsp90's roles in neurodegeneration.

4. 3 Summary

In this work, a rapid method for producing 15-DSG analogs was developed. The overall yields ranged from 29-56%, which is a significant improvement over the previous 7% yields. The key transformation in the new route is the Ugi reaction to generate the core peptoid in a single step. Unlike the previous, liner routes, this multi-component approach is amenable to combinatorial chemistry and diversity can be quickly installed. Finally, initial experiments suggest that these compounds may affect the aggregation of

proteins in cellular models of neurodegeneration. This is an important step, which could improve our knowledge of the biology that occurs at the C-terminus of Hsp70 and Hsp90.

4.4 Experimental Methods

4.4.1 Synthesis of Guanidinylated Amino Acids (2)

A flame-dried round bottom flask containing 1 mmol of the amino acid was diluted with 8 mL of anhydrous dichloromethane (DCM). Then, N-Methyl-N-trimethylsilyl-trifluoroacetamide (2.2 mmol) was added, and the reaction was heated to a reflux under an argon atmosphere. Once the solution became clear, the reaction was cooled and triethylamine (1.1 mmol) and N,N'-di-Boc-N''-triflylguanidine (1.1 mmol) were added to the stirring reaction. The reaction stirred at room temperature for 4-5 hours. After the reaction reached completion, it is diluted with DCM and washed with brine and water. Following drying with sodium sulfate the mixture was concentrated and purified by flash column chromatography (eluted 50:50 ethylacetate:hexanes). The yields for the guanidinylation of aminoheptanoic acid, aminohexanoic acid, and γ-aminobutyric acid ranged from 64-75%.

4.4.2 Characterization of Guanidinylated Amino Acids

4-(2,3-bis(tert-butoxycarbonyl)guanidino)butanoic acid (**2a**, n=2): ^{1}H NMR ($CDCl_3$) δ 11.4 (1H, bs), 8.56 (1H, s), 2.93 (2H, s), 2.41 (2H ,s), 1.89 (2H, s), 1.41 (18H, s). ^{13}C NMR ($CDCl_3$) δ 176.61, 162.70, 156.76, 153.10, 83.63, 79.95, 39.74, 31.71, 28.40, 25.30. [M+H] e: 346.19, o: 346.2.

6-(2,3-bis(tert-butoxycarbonyl)guanidino)hexanoic acid (**2b**, n=4): ^{1}H NMR ($CDCl_3$) δ 11.4 (1H,bs), 8.34 (1H, s), 3.39 (2H, s), 2.94 (1H, s), 2.35 (2H, s), 1.64-1.58 (4H, d), 1.48 (18H, s). ^{13}C NMR ($CDCl_3$) δ 178.92, 163.31, 156.08, 153.23, 83.14, 79.39, 40.67, 33.76, 28.62, 28.20, 26.21, 24.24. [M+H] e: 375.22, o: 375.2.

7-(2,3-bis(tert-butoxycarbonyl)guanidino)heptanoic acid (**2c**, n=5): ^{1}H NMR ($CDCl_3$) 11.4 (1H, bs), 8.32 (1H, s), 3.38 (2H, s), 2.94 (1H, s), 2.32 (2H, s), 2.62 (4H, d), 1.55 (18H, s), 1.35 (4H, s). ^{13}C NMR ($CDCl_3$) δ 178.80, 156.02, 153.25, 83.15, 79.70, 40.87, 33.79, 28.71, 28.58, 26.40, 24.45. [M+H] e: 388.24, o: 388.2.

4.4.3 Synthesis of Isocyanides (6)

To mono-protect 1, 4-DAB, 1, 4-DAB (7.5 g, 85.08 mmol) was diluted in 30 mL of dioxane. A solution of di-tert-butyldicarbonate (2.4 g, 11 mmol) that was diluted in 30 mL of dioxane was added to the stirring 1, 4-DAB dropwise over 1.5 hours. The reaction was allowed to stir for 24 hours. The solvent was then removed under vacuum and 50 mL of water was added. Any insoluble material was filtered off and the filtrate was extracted with 45 mL of DCM three times. The organic layers were dried with sodium sulfate and concentrated to give a 56-61% yield.

The next step in the generation of tert-butyl (4-isocyanobutyl)carbamate is the addition of formic acid to the remaining free amine group (Scheme 4-). Tert-butyl (4-aminobutyl)carbamate (2 mmol) was diluted in 5 mL DCM and formic acid (2 mmol) was added to the stirring reaction. The reaction was then placed into an ice-bath. Once cooled, DIC (2 mmol) was added to the solution and the mixture stirred for 4 hours at room temperature. The reaction was filtered and the filtrate was washed with saturated sodium bicarbonate solution. The organic layer was then dried with sodium sulfate and concentrated. The resulting product, tert-butyl (4-aminobutyl)carbamate, was synthesized in 90-92% yield. Tert-butyl (4-aminobutyl)carbamate (8.7 mmol) was diluted with 13 mL of DCM. Triethylamine (26.2 mmol) was then added and the solution was cooled in an ice-bath. $POCl_3$ (8.7 mmol) was then added dropwise. The

reaction stirred for 30 minutes at which time potassium carbonate (8.7 mmol) was added to the stirring reaction. The reaction was then stirred for another 30 minutes. The aqueous layer was extracted with DCM 5 times. The DCM layers were then washed with water, dried with sodium sulfate, and concentrated. The product was then purified by flash column chromatography (eluting at 50:50 ethylacetate: hexanes) giving a 72-76% yield. The same procedure was used to synthesize tert-butyl (4-isocyanophenyl)-carbamate from mono-Boc- 1, 4-phenylenediamine as a way of adding rigidity to the four carbon linker of the spermidine tail.

4.4.4 Characterization of Isocyanides

tert-butyl (4-isocyanobutyl)carbamate (**6a**): ^{1}H NMR ($CDCl_3$) δ 8.48 (1H, s), 3.40 (2H, s), 3.13 (2H, s), 2.22-2.01 (2H, d), 1.35 (9H, s), 1.17-1.10 (2H, d). ^{13}C NMR ($CDCl_3$) δ 164.35, 155.95, 79.50, 41.19, 39.40, 28.34, 22.89. [M+H] e: 199.14, o: 199.1.

tert-butyl (4-isocyanophenyl)carbamate (**6b**): ^{1}H NMR ($CDCl_3$) δ 7.39-8.38 (2H, d), 7.29-7.26 (2H, d), 6.70 (1H, s), 1.50 (9H, s). 13C NMR (CDCl3) δ 163.02, 152.22, 139.35, 127.14, 118.55, 81.31, 28.33. [M+H] e: 219.11, o: 219.1.

4.4.5 Synthesis of Fmoc-aminopropanal (12)

The first step is to add Fmoc-β-alanine (3 mmol, 1 equiv) to a flame dried round bottom flask then diluting the amino acid with 20 mL anhydrous DCM. Then triphenylphosphine (6 mmol, 2 equiv) and trichloroacetonitrile (6 mmol, 3 equiv) were added. After the Fmoc-β-alanine appeared to be consumed , N-O-dimethyl-hydroxylamine hydrochloride (6.3 mmol, 2.1 equiv) and pyridine (15 mmol, 5 equiv) were added at 0 °C. After 1 hour, the reaction was washed with brine and dried over sodium sulfate. After concentration, the product, N-methoxy-N-methyl-3-(Fmoc-amino)-

propionamide, was purified by flash column chromatography (eluting at 50:50 ethylacetate:hexanes) to give a 97% yield. N-methoxy-N-methyl-3-(Fmoc-amino)-propionamide (1.15 mmol, 1 eq) was dissolved in 10 mL anhydrous THF. The reaction was cooled to -78 °C under an argon atmosphere. 3.45 mL of a 1.0 M solution of diisobutylaluminum hydride (3 equiv) in THF was added dropwise over 10 minutes. After 5 minutes the reaction was complete and 5% HCl in EtOH was added to quench the reaction, and the reaction was then allowed to warm to room temperature. The solution was diluted into DCM and washed with brine. The organic layers were sodium sulfate and then concentrated under vacuum. The product was then purified by flash column chromatography (eluting with 50:50 ethaylacetate:hexanes) to afford Fmoc-3-amino-1-propanal in 62% yield.

4.4.6 Characterization of Fmoc-3-amino-1-propanal (12)

^{1}H NMR ($CDCl_3$): δ 9.83 (1H, s), 7.78 (2H, d), 7.60 (2H, d), 7.33 (4H, m), 5.3 (1H, bs), 4.40 (2H, d), 4.20 (1H, t), 3.52 (2H, t), 2.76 (2H, t). ^{13}C NMR ($CDCl_3$) δ 190.55, 155.40, 143.73, 141.26, 127.66, 127.00, 125.00, 119.95, 60.40, 47.17, 20.92, 14.17. [M+H] e: 296.12, o: 296.1.

4.4.7 Synthesis of 15-Deoxyspergualin Analogs (9 and 13)

The optimized conditions for the Ugi reaction consisted of the mixing of benyzlamine (0.1mmol), benzaldehyde (0.1 mmol), 6-guanidinoamino acid (1.1 mmol), and tert-butyl (4-isocyanobutyl)carbamate (0.1 mmol) in 0.5 mL of MeOH and then heating the reaction using a Biotage Initiator microwave at 120 °C for 20 minutes.

Tris(2-aminoethyl)amine has been published to remove Fmoc groups. Using previous accounts as a guide, Tris-amine resin (50 equiv) was stirred with the 15-DSG

analog in $CHCl_3$ for 20 minutes. This time was required to allow for complete scavenging of the 9-methylene-9H-fluorene byproduct of Fmoc cleavage.

The removal of the final protecting group involves the removal of the benzyl group from the nitrogen of the amide backbone of the 15-DSG core structure. One method that seemed less harsh and would remove the benzyl group rather quickly was through the oxidative capabilities of CAN. In this method CAN (2.1 equiv) is added to the 15-DSG analog that is in a solution of 1:5 water:acetonitrile (2 mL). After stirring for 2 hours, the reaction is quenched by the addition of saturated sodium bicarbonate and stirred for 10 minutes. The solution is then extracted with ethylacetate. The organic layers were then dried over sodium sulfate and concentrated under vacuum. The product is then purified on a basic alumina oxide column (eluting at 10:90 methanol:ethylacetate) to afford the final product.

4.4.8 Characterization of 15-Deoxyspergualin Analogs

N-(2-((4-aminobutyl)amino)-1-methoxy-2-oxoethyl)-6-guanidinohexanamide (**9a**): ^{1}H NMR ($CDCl_3$) δ 8.09 (2H, s), 5.88 (1H, s), 4.32 (3H, d), 3.41-3.06 (6H, d), 2.26 (2H, s), 1.41 (6H, m), 1.19-1.06 (4H, m). Overall yield 52%.

N-(2-((4-aminobutyl)amino)-1-(4-bromophenyl)-2-oxoethyl)-6-guanidinohexanamide (**9b**): ^{1}H NMR ($CDCl_3$) δ 8.03 (2H, s), 7.81-7.69 (2H, d), 7.63-7.57 (2H, d), 5.82 (1H, s), 4.42 (2H, s), 4.04 (2H, s), 3.41-2.98 (4H, m), 2.25-2.17 (2H, m), 1.97 (2H, s), 1.42 (4H ,m), 1.20 (4H, m), 0.86 (2H, d). Overall yield 57%.

N-(2-((4-((3-aminopropyl)amino)butyl)amino)-1-methoxy-2-oxoethyl)-7-guanidinoheptanamide **(13a):** ^{1}H NMR ($CDCl_3$) δ 8.16 (2H, s), 5.84 (1H, s), 4.61-4.38

(2H, d), 4.10-3.75 (2H ,d), 3.31 (3H, d), 3.13 (2H, s), 2.70 (6H ,s), 2.32-2.03 (8H, m), 1.64-1.51 (10H, m) 1.25-1.14 (4H ,m). Overall yield 41%.

N-(2-((4-((3-aminopropyl)amino)butyl)amino)-1-(4-bromophenyl)-2-oxoethyl)-7-guanidinoheptanamide (**13b**): ^{1}H NMR ($CDCl_3$) δ 8.16 (2H, s), 7.79 (2H, d), 7.51 (2H, d), 5.82 (1H, s), 4.56-4.18 (4H, m), 4.15 (2H, s), 3.20 (2H, s), 3.05 (2H, s), 1.54-1.49 (6H, m), 1.19 (6H, s), 0.86 (2H, s). Overall yield 33%.

N-(1-((4-((3-aminopropyl)amino)butyl)amino)-1-oxopropan-2-yl)-6-guanidinohexanamide **(13c):** ^{1}H NMR ($CDCl_3$) δ 8.16 (2H, s), 5.82 (1H ,s), 4.60 (2H, s), 4.38 (2H, s), 3.31 (4H, d), 3.13 (6H, s), 1.65-1.53 (6H, m), 1.14 (h$, d), 0.83 (5H, d). Overall yield 38%.

N-(1-((4-((3-aminopropyl)amino)butyl)amino)-3-methyl-1-oxopentan-2-yl)-6-guanidinohexanamide (**13d**): ^{1}H NMR ($CDCl_3$) δ 8.16 (2H, s), 5.83 (1H, s), (3.48 (4H, d), 3.13 (4H, s), 1.27 (6H, s), 1.53 (8H, s), 1.48 (16H, s), 1.25 (3H, s). Overall yield 44%.

N-(2-((4-((3-aminopropyl)amino)butyl)amino)-1-(4-bromophenyl)-2-oxoethyl)-6-guanidinohexanamide (**13e**): ^{1}H NMR ($CDCl_3$) δ 8.16 (2H, s), 7.34-6.98 (4H, m), 5.67 (1H, s), 4.68-4.52 (2H, m), 4.49 (2H, s), 3.31-3.06 (4H, dd), 2.43 (2H, m), 2.03 (2H, s), 1.70 (4H, s), 1.48-1.41 (10H, m), 1.13 (4H, d). Overall yield 42%.

N-(2-((4-((3-aminopropyl)amino)butyl)amino)-1-(3-hydroxyphenyl)-2-oxoethyl)-6-guanidinohexanamide **(13f):** ^{1}H NMR ($CDCl_3$) δ 8.03 (2H, s), 7.71 (1H, s), 7.36-7.26 (2H, m), 6.83 (1H, s), 5.82 (1H, s), 4.31-4.22 (2H, d), 3.30 (2H, m), 3.09-2.92 (4H, d), 2.55 (10H, s), 1.41 (14H, s), 1.27 (2H, s). Overall yield 36%.

N-(2-((4-((3-aminopropyl)amino)butyl)amino)-1-(3,5-dimethoxyphenyl)-2-oxoethyl)-6-guanidinohexanamide (**13g**): ^{1}H NMR ($CDCl_3$) δ 8.16 (2H, s), 7.53-7.06 (3H, s), 5.88

(1H, s), 4.15-3.91 (3H, m), 3.82 (3H, m), 2.91 (4H, m), 1.84 (2H, d), 1.81 (6H, m), 1.49 (4H, d), 1.05 (6H, t), 0.63 (4H, s). Overall yield 46%.

N-(2-((4-((3-aminopropyl)amino)butyl)amino)-1-methoxy-2-oxoethyl)-4-guanidinobutanamide **(13h):** ^{1}H NMR ($CDCl_3$) δ 8.16 (2H, s), 5.87 (1H, s), 3.32 (3H, s), 3.13 (2H, s), 1.54 (8H, m), 1.49 (10H, s). Overall yield 33%.

N-(2-((4-((3-aminopropyl)amino)butyl)amino)-1-(4-bromophenyl)-2-oxoethyl)-4-guanidinobutanamide **(13i):** ^{1}H NMR ($CDCl_3$) δ 8.17 (2H, s), 7.77-7.58 (2H, d), 7.40-7.31 (2H, d), 5.87 (1H, s), 4.63 (2H, s), 3.33 (2H, s), 3.14 (2H, s), 1.55 (4H, s), 1.44 (10H, s), 1.15 (2H, d). Overall yield 31%.

N-(2-((4-((3-aminopropyl)amino)phenyl)amino)-1-methoxy-2-oxoethyl)-6-guanidinohexanamide (**13j**): ^{1}H NMR ($CDCl_3$) δ 8.28 (2H, s), 7.47 (2H, d), 7.34-7.30 (2H, d), 5.82 (1H, s), 4.50 (2H, d), 3.49 (2H, m), 2.04 (1H, s), 1.74 (4H, m), 1.51 (4H, d), 1.26 (4H, s), 0.84 (2H, d). Overall yield 49%.

Author contributions

Christopher G. Evans, Matthew Smith, and Dr. Jason E. Gestwicki designed the experiments;
Christopher G. Evans synthesized the isocyanides, guanidinylated amino acids, and 15-DSG analogs;
Christopher G. Evans and Matthew Smith worked out TLC conditions for the spergualin stability testing.
Matthew Smith conducted the stability test and yeast polyQ assay.

4.5 Appendix of Selected ^{1}H NMR Spectra

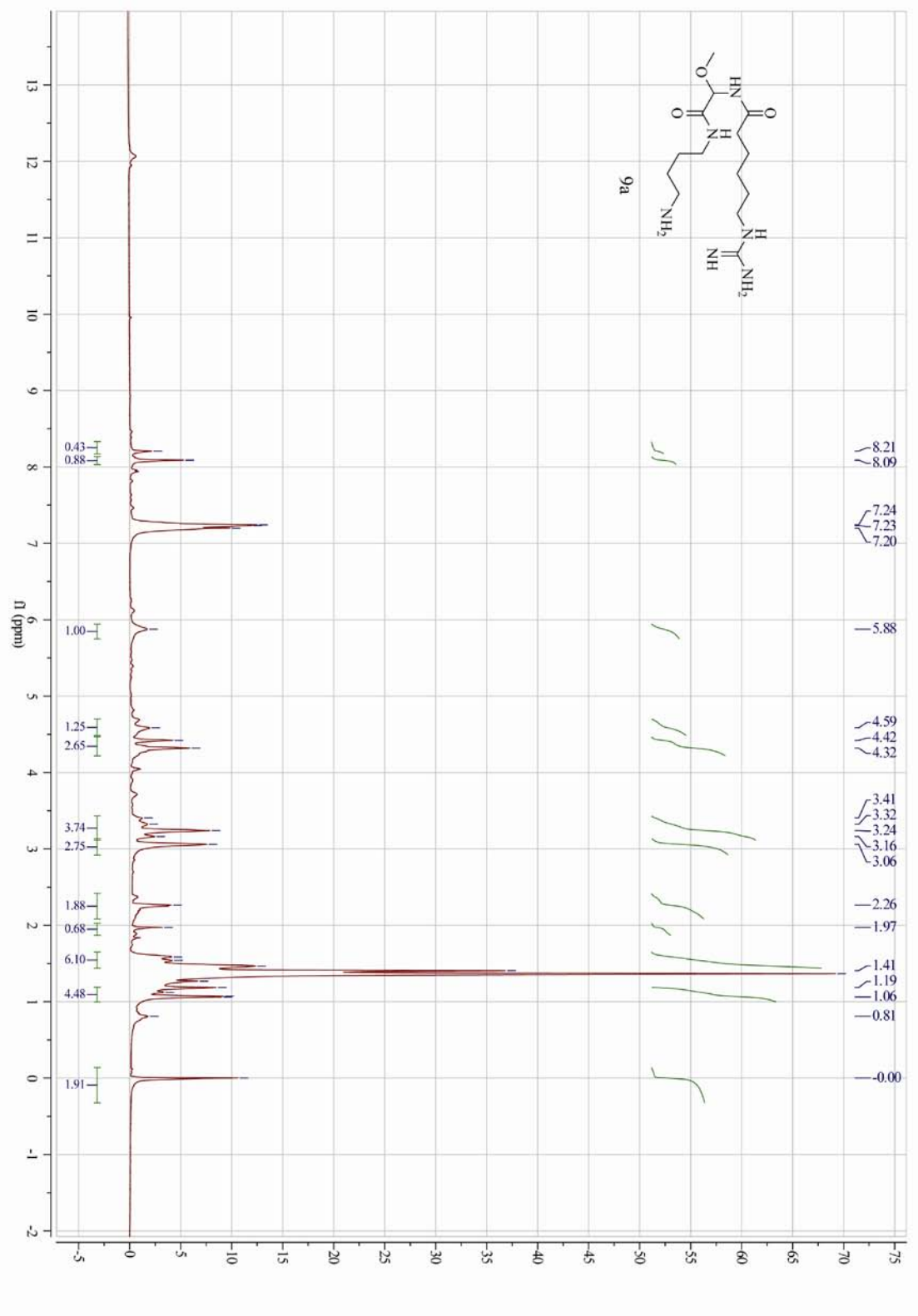

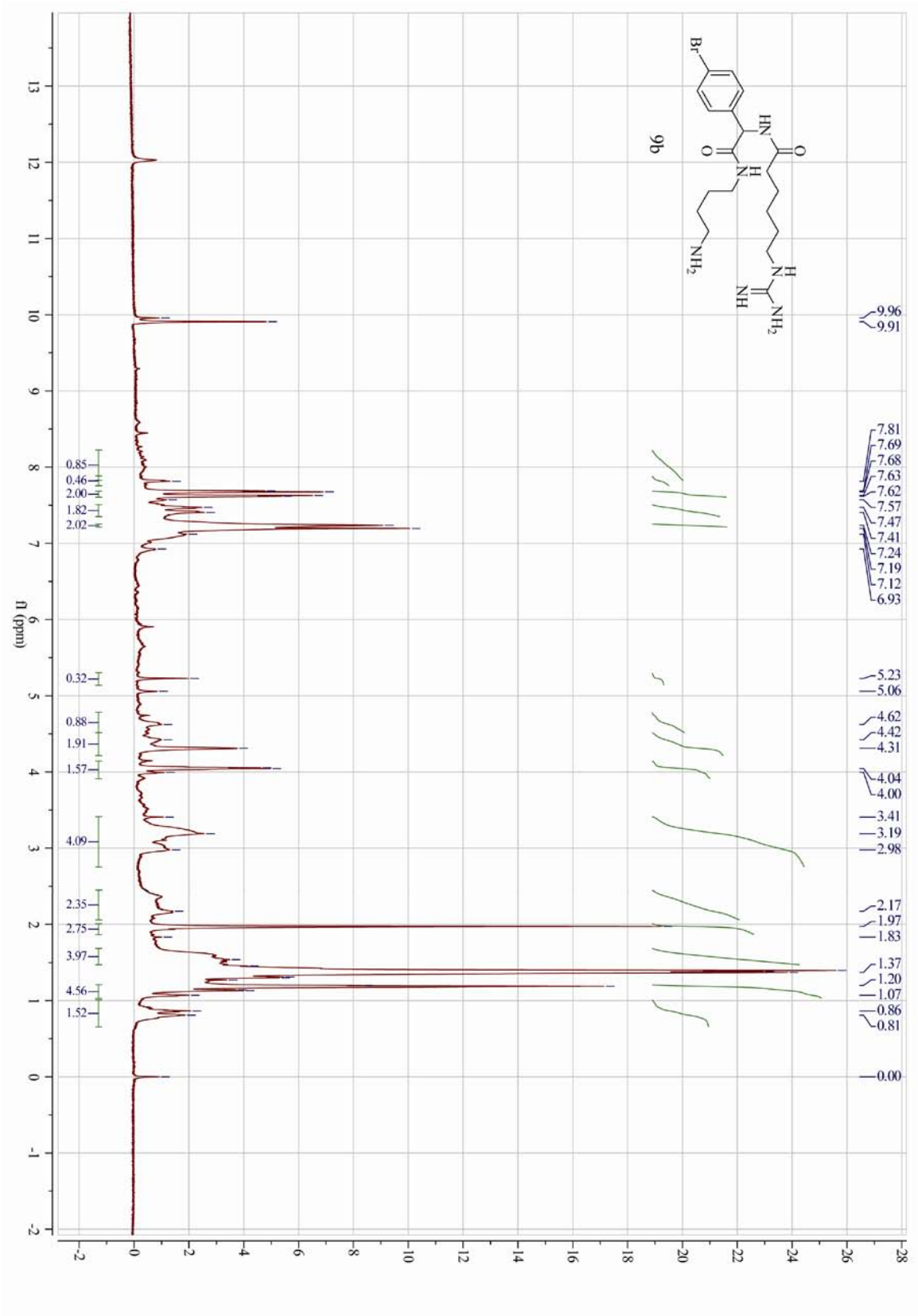
9b
f1 (ppm)
9.96
9.91
7.81
7.69
7.68
7.63
7.62
7.57
7.47
7.41
7.24
7.19
7.12
6.93
5.23
5.06
4.62
4.42
4.31
4.04
4.00
3.41
3.19
2.98
2.17
1.97
1.83
1.37
1.20
1.07
0.86
0.81
0.00
0.85
0.46
2.00
1.82
2.02
0.32
0.88
1.91
1.57
4.09
2.35
2.75
3.97
4.56
1.52

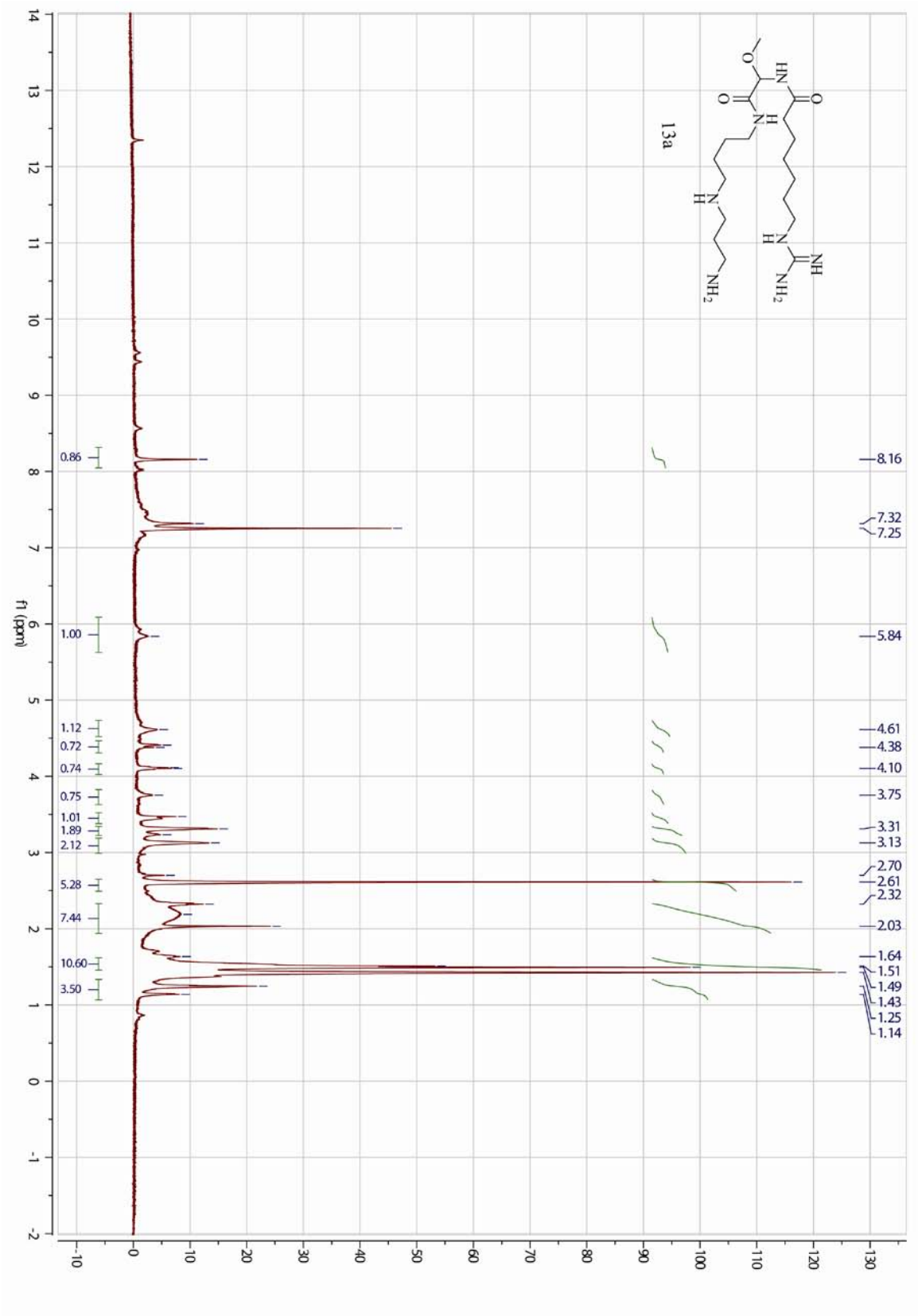
13a
f1 (ppm)
0.86
1.00
1.12
0.72
0.74
0.75
1.01
1.89
2.12
5.28
7.44
10.60
3.50
8.16
7.32
7.25
5.84
4.61
4.38
4.10
3.75
3.31
3.13
2.70
2.61
2.32
2.03
1.64
1.51
1.49
1.43
1.25
1.14

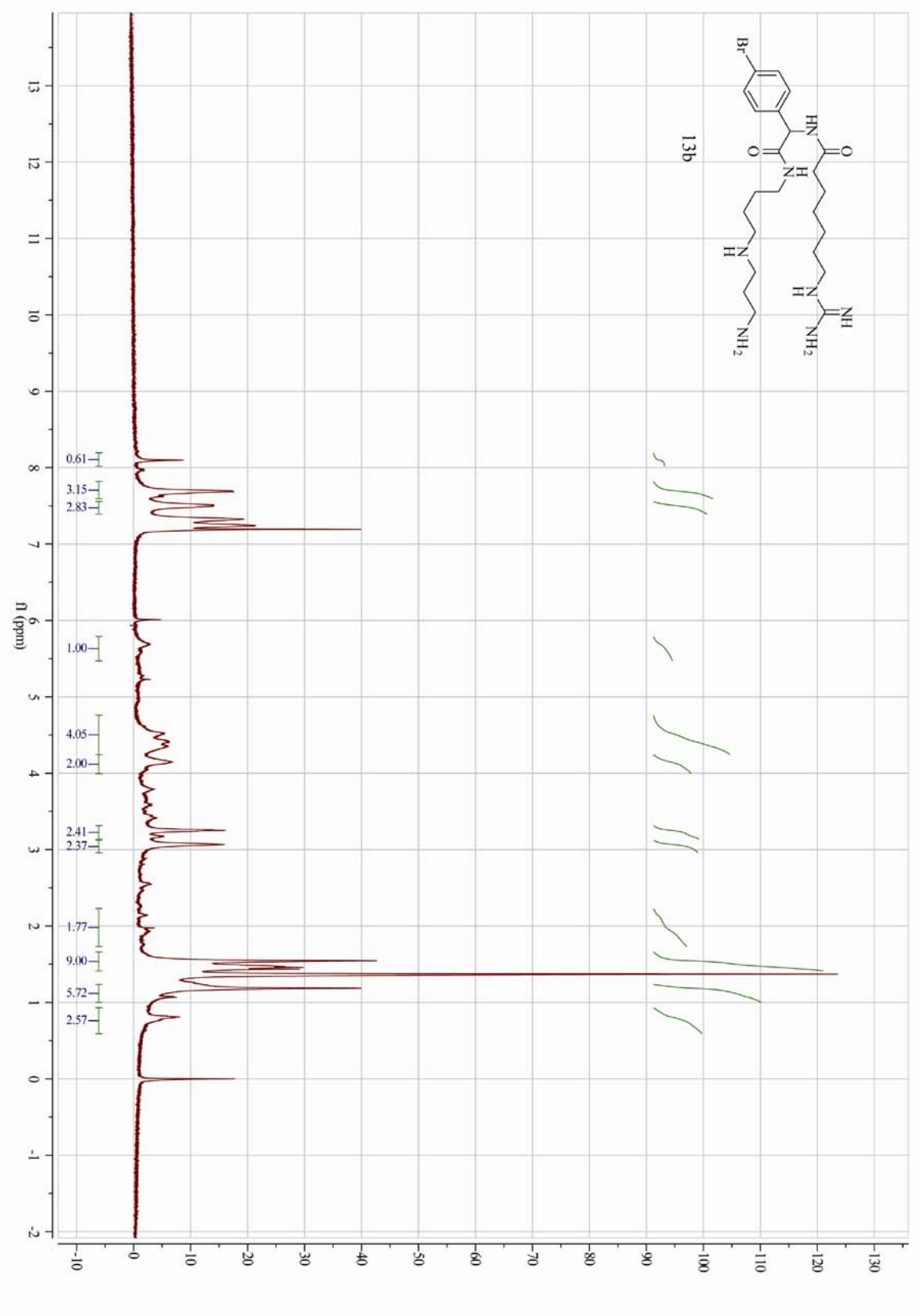
13b
f1 (ppm)
0.61
3.15
2.83
1.00
4.05
2.00
2.41
2.37
1.77
9.00
5.72
2.57

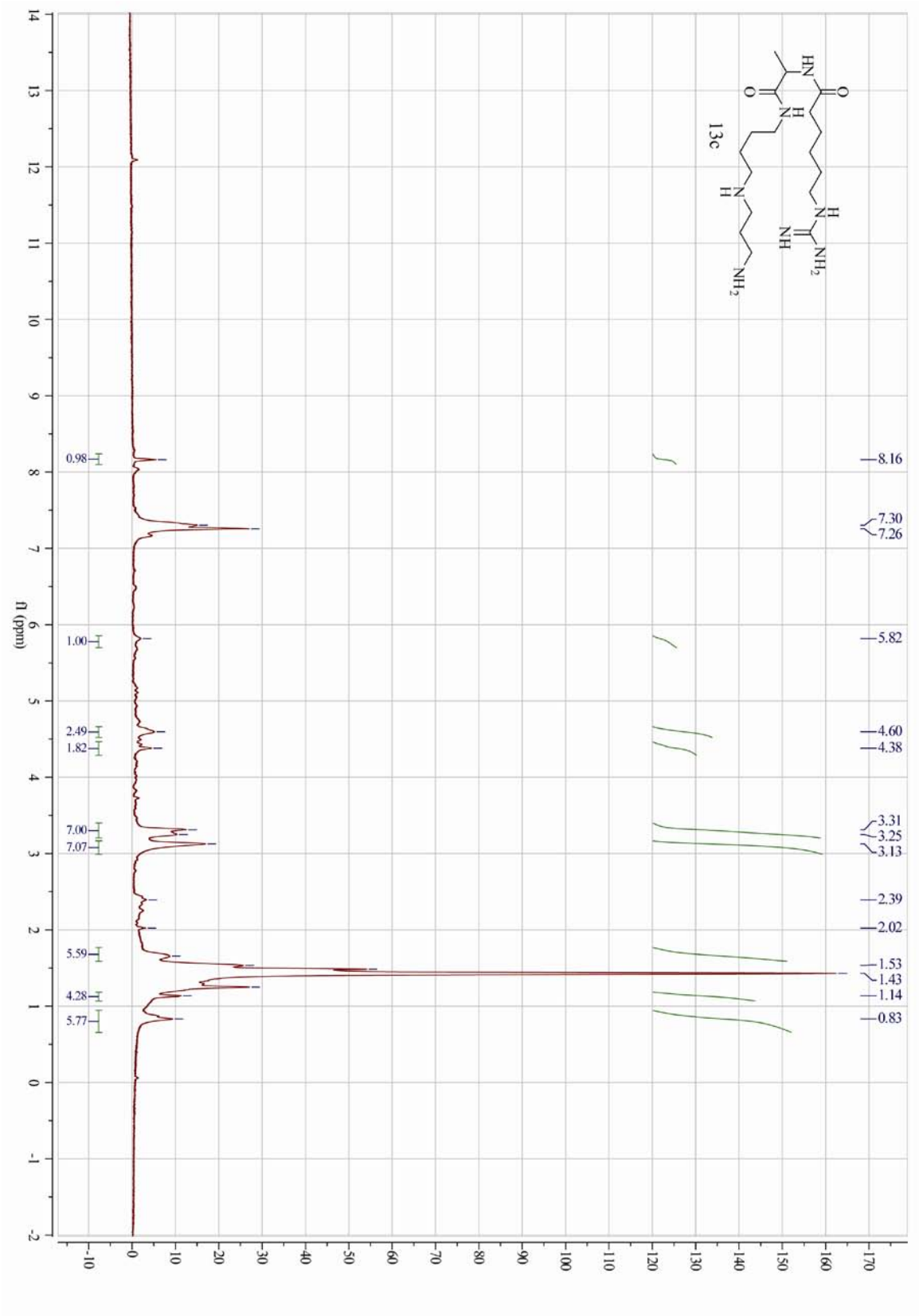
13c
f1 (ppm)
0.98
1.00
2.49
1.82
7.00
7.07
5.59
4.28
5.77
8.16
7.30
7.26
5.82
4.60
4.38
3.31
3.25
3.13
2.39
2.02
1.53
1.43
1.14
0.83

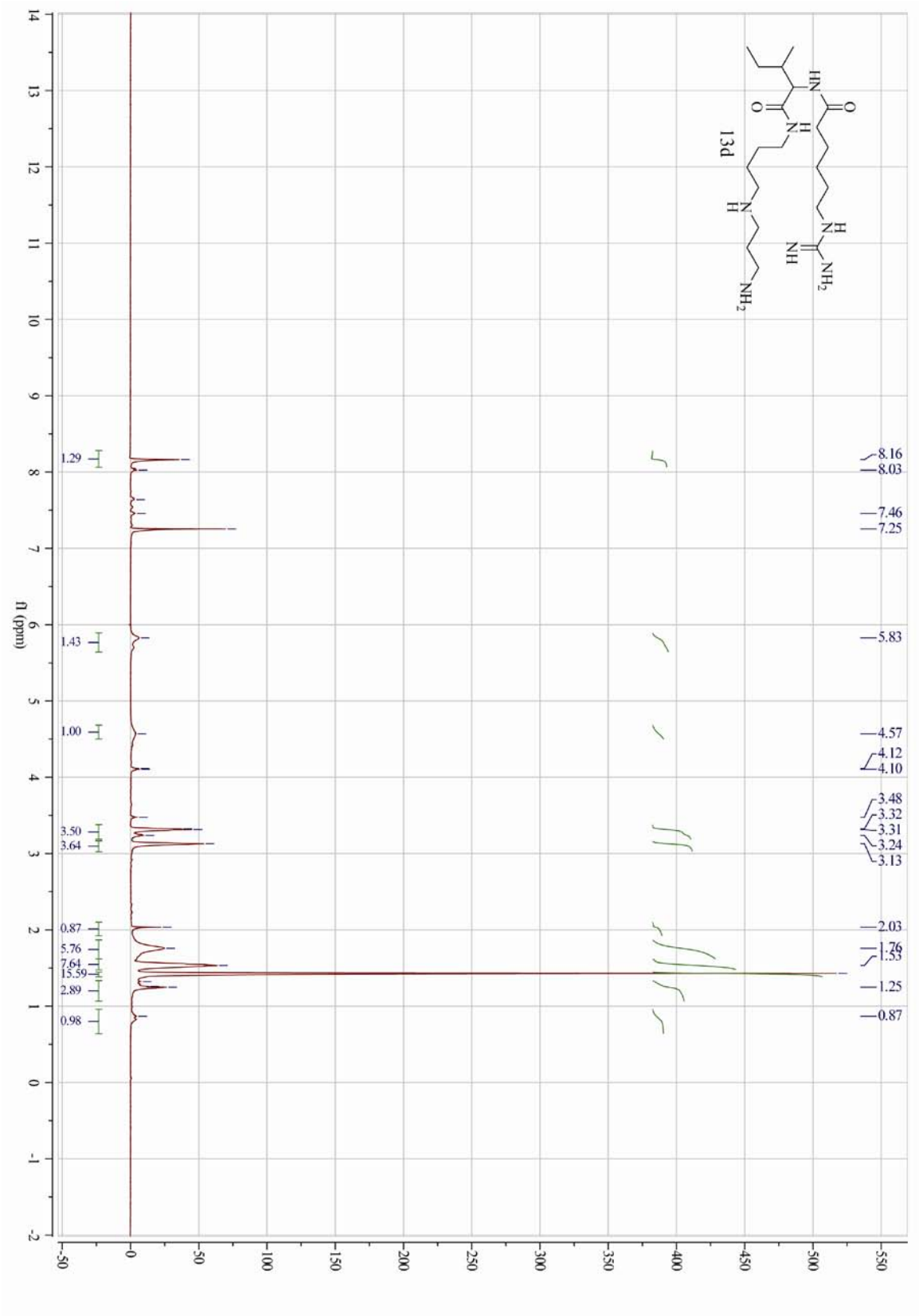
13d
f1 (ppm)
1.29
1.43
1.00
3.50
3.64
0.87
5.76
7.64
15.59
2.89
0.98
8.16
8.03
7.46
7.25
5.83
4.57
4.12
4.10
3.48
3.32
3.31
3.24
3.13
2.03
1.76
1.53
1.25
0.87

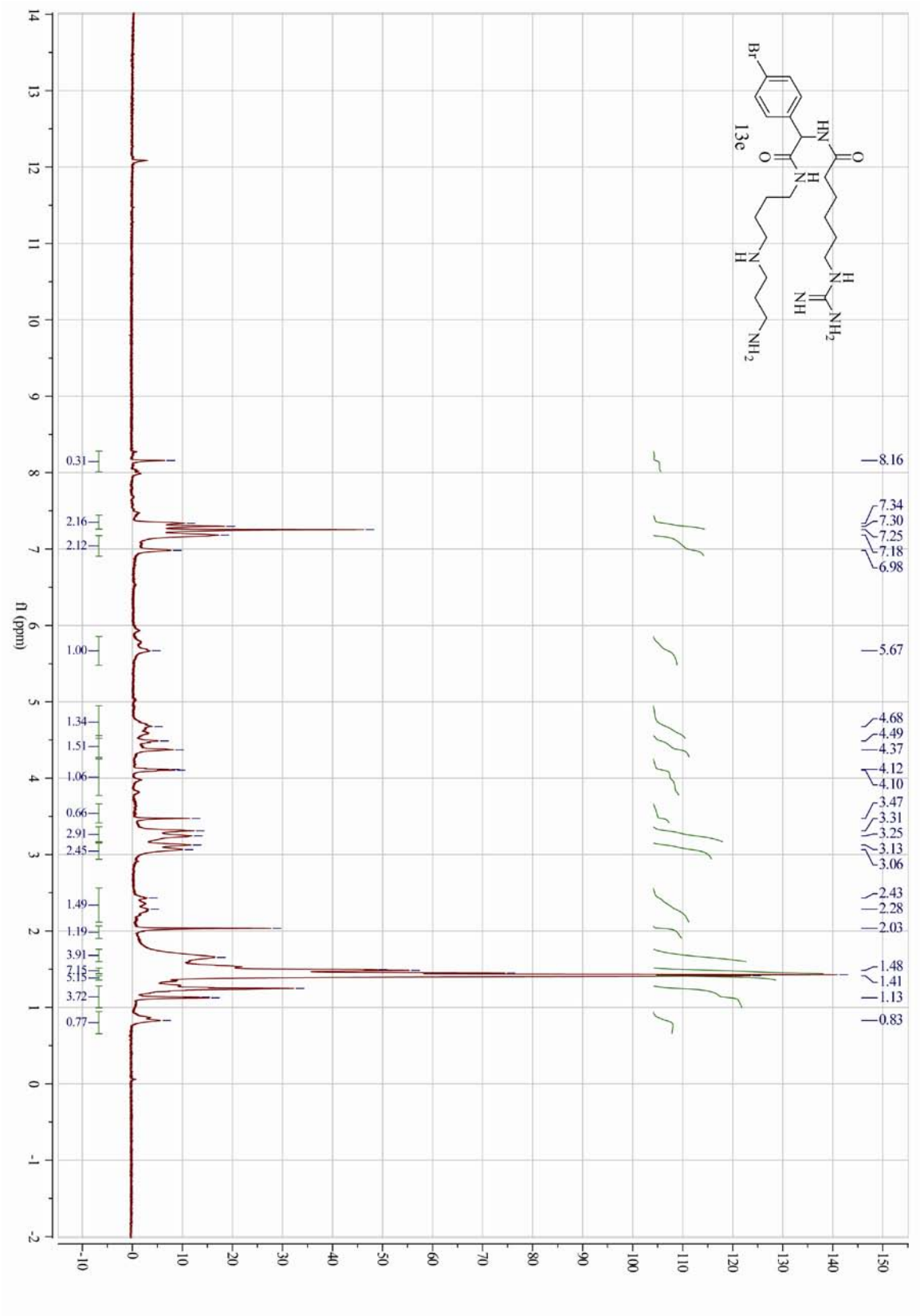
13e
f1 (ppm)
0.31
2.16
2.12
1.00
1.34
1.51
1.06
0.66
2.91
2.45
1.49
1.19
3.91
7.15
5.15
3.72
0.77
8.16
7.34
7.30
7.25
7.18
6.98
5.67
4.68
4.49
4.37
4.12
4.10
3.47
3.31
3.25
3.13
3.06
2.43
2.28
2.03
1.48
1.41
1.13
0.83

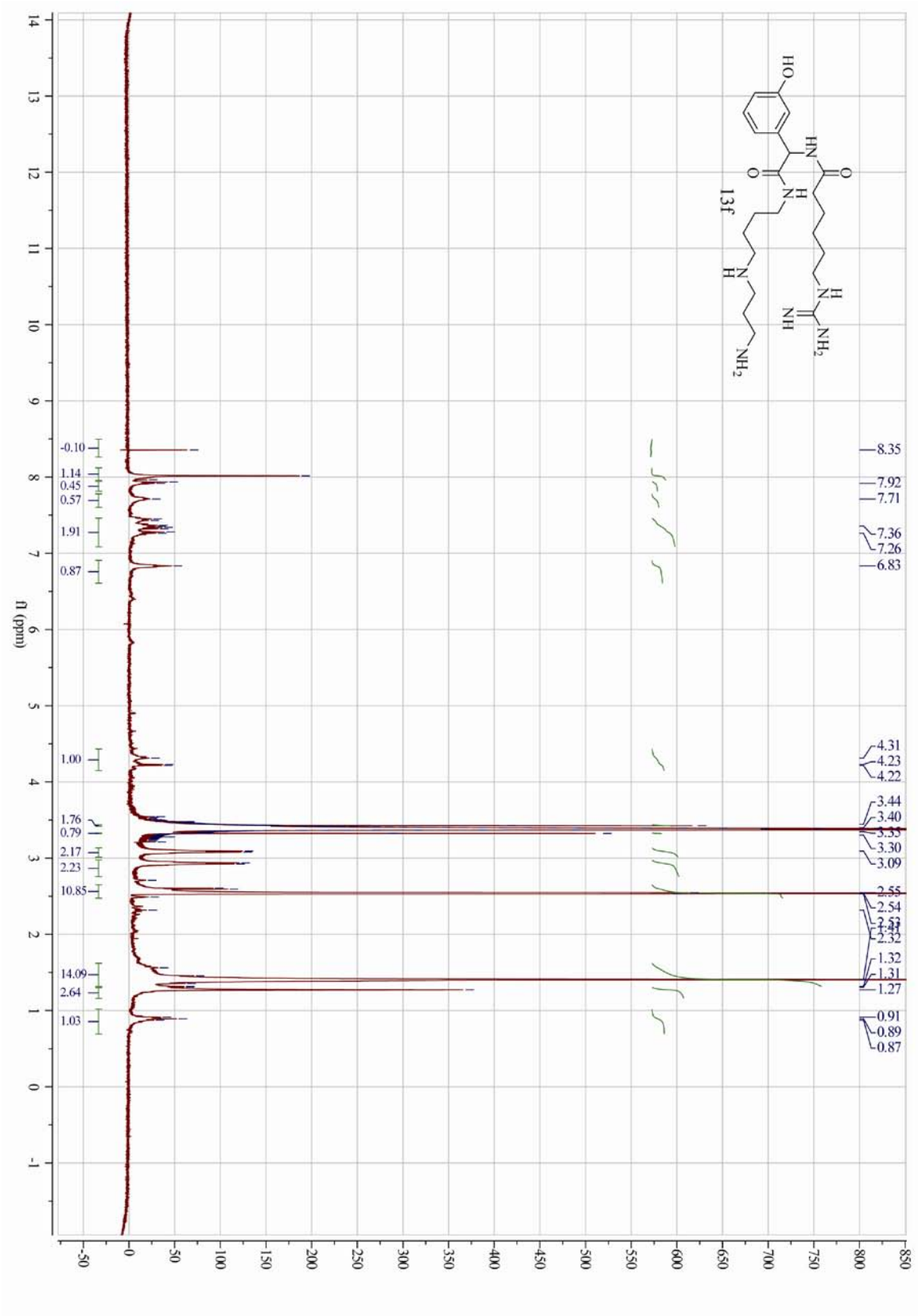
13f
f1 (ppm)
-0.10
1.14
0.45
0.57
1.91
0.87
1.00
1.76
0.79
2.17
2.23
10.85
14.09
2.64
1.03
8.35
7.92
7.71
7.36
7.26
6.83
4.31
4.23
4.22
3.44
3.40
3.30
3.09
2.55
2.54
2.32
1.32
1.31
1.27
0.91
0.89
0.87

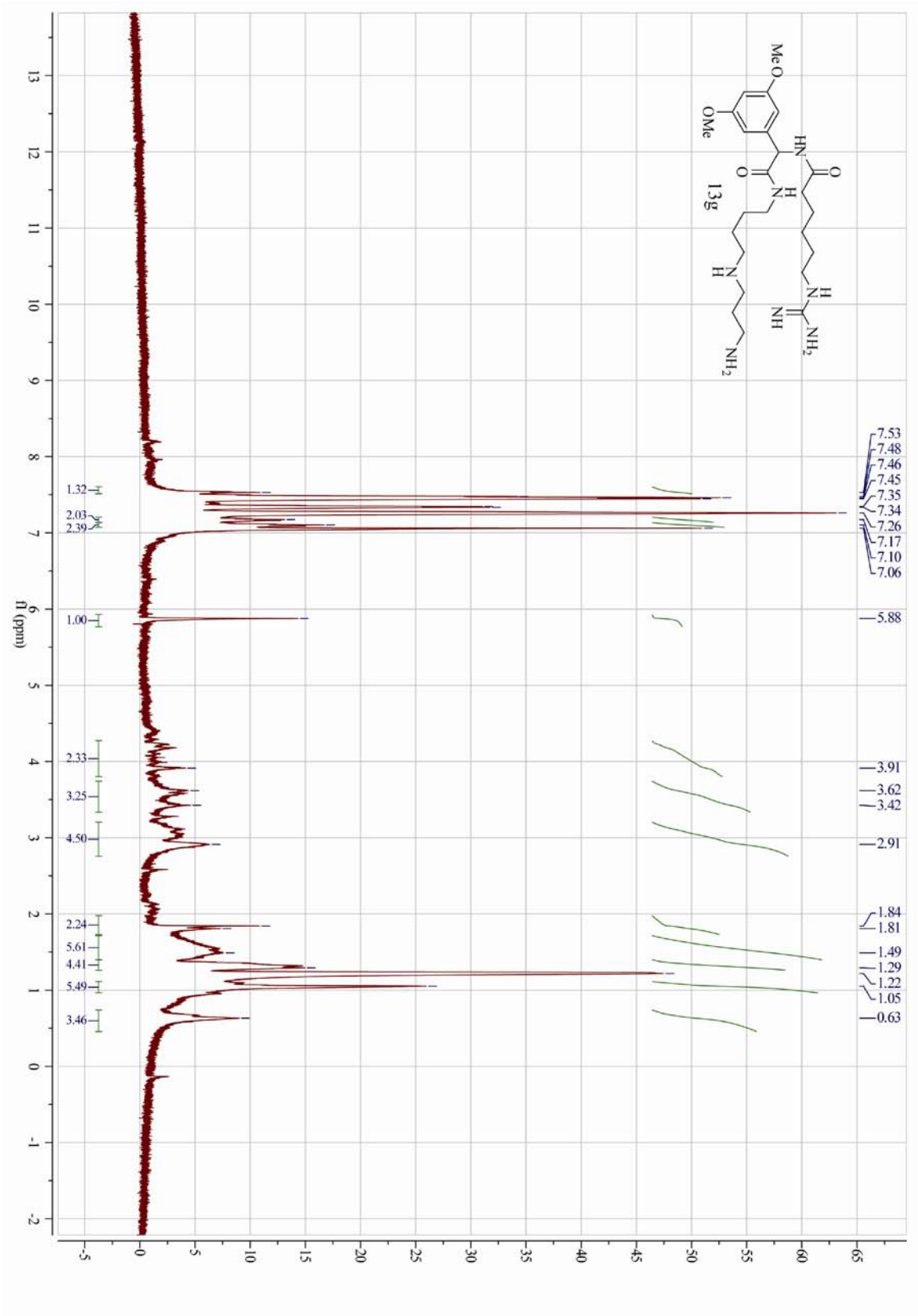
13g
f1 (ppm)
1.32
2.03
2.39
1.00
2.33
3.25
4.50
2.24
5.61
4.41
5.49
3.46
7.53
7.48
7.46
7.45
7.35
7.34
7.26
7.17
7.10
7.06
5.88
3.91
3.62
3.42
2.91
1.84
1.81
1.49
1.29
1.22
1.05
0.63

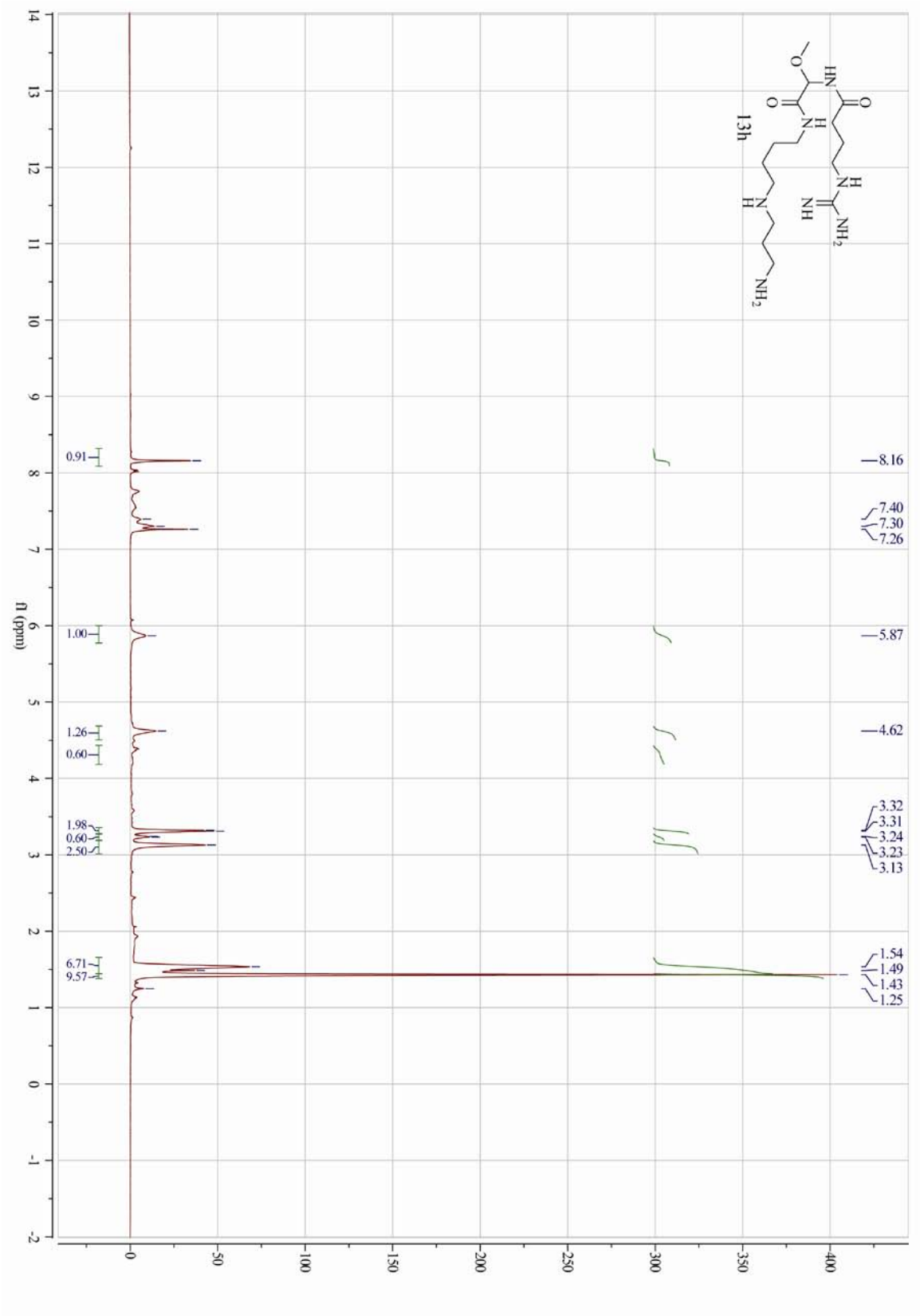
13h
f1 (ppm)
0.91
1.00
1.26
0.60
1.98
0.60
2.50
6.71
9.57
8.16
7.40
7.30
7.26
5.87
4.62
3.32
3.31
3.24
3.23
3.13
1.54
1.49
1.43
1.25

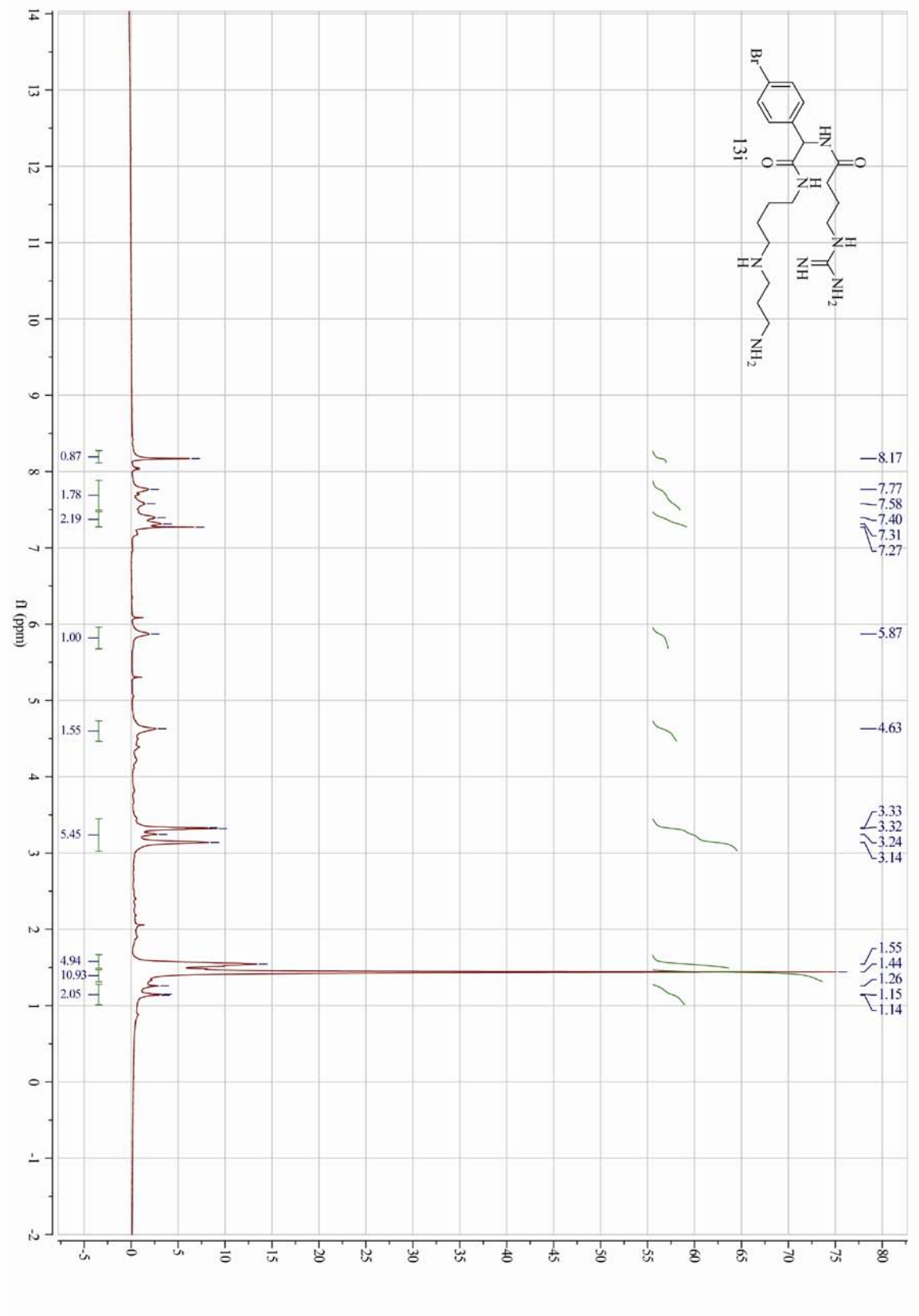
131i
f1 (ppm)
0.87
1.78
2.19
1.00
1.55
5.45
4.94
10.93
2.05
8.17
7.77
7.58
7.40
7.31
7.27
5.87
4.63
3.33
3.32
3.24
3.14
1.55
1.44
1.26
1.15
1.14

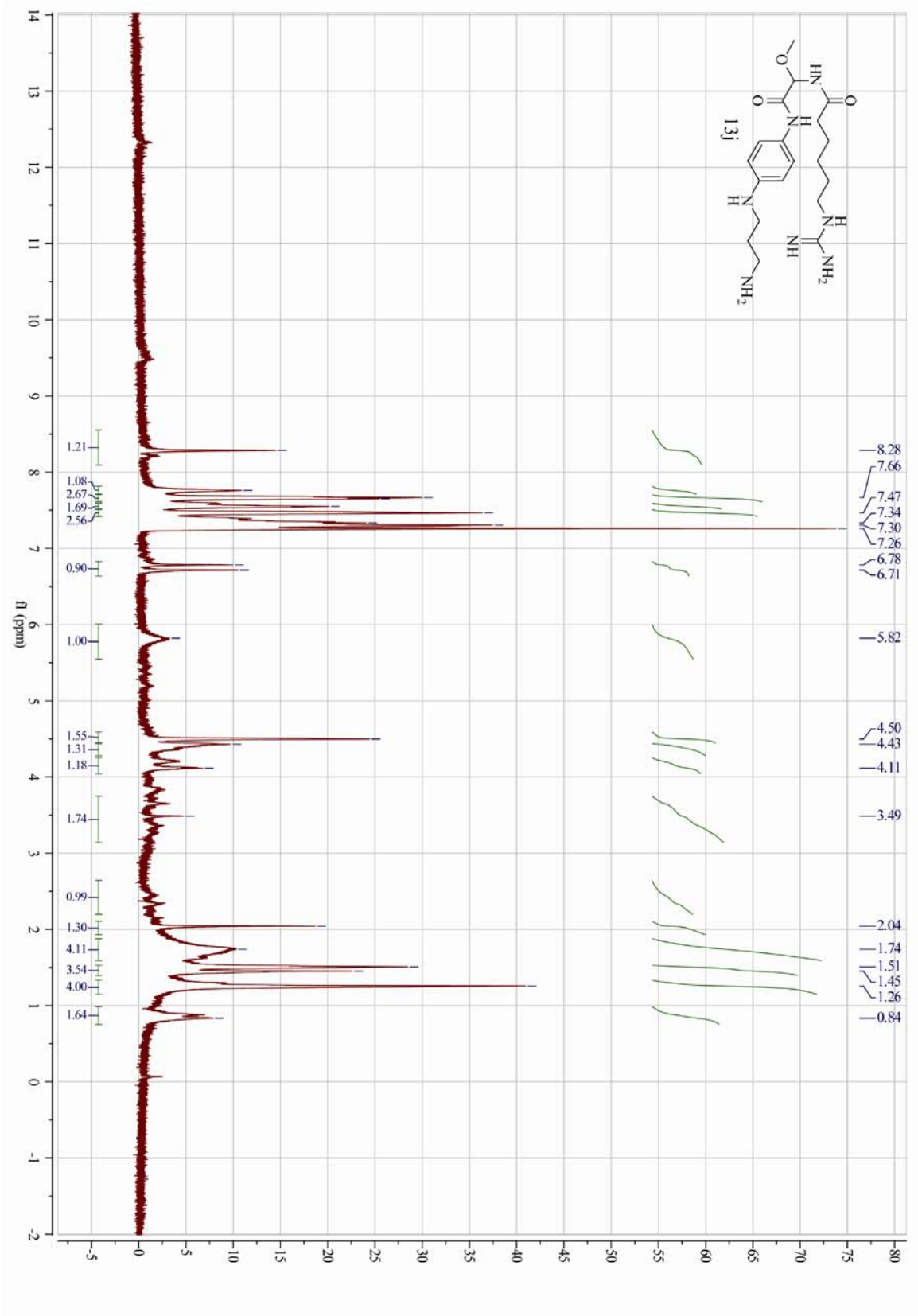
13j
f1 (ppm)
1.21
1.08
2.67
1.69
2.56
0.90
1.00
1.55
1.31
1.18
1.74
0.99
1.30
4.11
3.54
4.00
1.64
8.28
7.66
7.47
7.34
7.30
7.26
6.78
6.71
5.82
4.50
4.43
4.11
3.49
2.04
1.74
1.51
1.45
1.26
0.84

4.6 References

1. Dhingra, K.; Valero, V.; Gutierrez, L.; Theriault, R.; Booser, D.; Holmes, F.; Buzdar, A.; Fraschini, G.; Hortobagyi, G., Phase II study of deoxyspergualin in metastatic breast cancer. *Invest New Drugs* **1994,** 12, (3), 235-41.

2. Thomas, F. T.; Tepper, M. A.; Thomas, J. M.; Haisch, C. E., 15-Deoxyspergualin: a novel immunosuppressive drug with clinical potential. *Ann N Y Acad Sci* **1993,** 685, 175-92.

3. Amada, N.; Okazaki, H.; Sato, T.; Ohashi, Y.; Kikuchi, H., Deoxyspergualin prophylaxis with tacrolimus further improves long-term graft survival in living-related renal-transplant recipients transfused with donor-specific blood. *Transplant Proc* **2005,** 37, (2), 927-9.

4. Birck, R.; Warnatz, K.; Lorenz, H. M.; Choi, M.; Haubitz, M.; Grunke, M.; Peter, H. H.; Kalden, J. R.; Gobel, U.; Drexler, J. M.; Hotta, O.; Nowack, R.; Van Der Woude, F. J., 15-Deoxyspergualin in patients with refractory ANCA-associated systemic vasculitis: a six-month open-label trial to evaluate safety and efficacy. *J Am Soc Nephrol* **2003,** 14, (2), 440-7.

5. Kalsch, A. I.; Schmitt, W. H.; Breedijk, A.; Marinaki, S.; Weigerding, S.; Nebe, T. C.; Nemoto, K.; van der Woude, F. J.; Yard, B. A.; Birck, R., In vivo effects of cyclic administration of 15-deoxyspergualin on leucocyte function in patients with Wegener's granulomatosis. *Clin Exp Immunol* **2006,** 146, (3), 455-62.

6. Kaufman, D. B., 15-Deoxyspergualin in experimental transplant models: a review. *Transplant Proc* **1996,** 28, (2), 868-70.

7. Kaufman, D. B.; Field, M. J.; Gruber, S. A.; Farney, A. C.; Stephanian, E.; Gores, P. F.; Sutherland, D. E., Extended functional survival of murine islet allografts with 15-deoxyspergualin. *Transplant Proc* **1992,** 24, (3), 1045-7.

8. Kaufman, D. B.; Gores, P. F.; Field, M. J.; Farney, A. C.; Gruber, S. A.; Stephanian, E.; Sutherland, D. E., Effect of 15-deoxyspergualin on immediate function and long-term survival of transplanted islets in murine recipients of a marginal islet mass. *Diabetes* **1994,** 43, (6), 778-83.

9. Ohlman, S.; Gannedahl, G.; Tyden, G.; Tufveson, G.; Groth, C. G., Treatment of renal transplant rejection with 15-deoxyspergualin--a dose-finding study in man. *Transplant Proc* **1992,** 24, (1), 318-20.

10. Okubo, M.; Tamura, K.; Kamata, K.; Tsukamoto, Y.; Nakayama, Y.; Osakabe, T.; Sato, K.; Go, M.; Kumano, K.; Endo, T., 15-Deoxyspergualin "rescue therapy" for methylprednisolone-resistant rejection of renal transplants as compared with anti-T cell monoclonal antibody (OKT3). *Transplantation* **1993,** 55, (3), 505-8.

11. Yang, H.; Chen, G.; Kanai, N.; Shum, J.; Garcia, B.; Huang, X.; Min, W.; Luo, Y.; Dutartre, P.; Zhong, R., Monotherapy with LF 15-0195, an analogue of 15-deoxyspergualin, significantly prolongs renal allograft survival in monkeys. *Transplantation* **2003,** 75, (8), 1166-71.

12. Tepper, M. A.; Nadler, S. G.; Esselstyn, J. M.; Sterbenz, K. G., Deoxyspergualin inhibits kappa light chain expression in 70Z/3 pre-B cells by blocking lipopolysaccharide-induced NF-kappa B activation. *J Immunol* **1995,** 155, (5), 2427-36.

13. Hoeger, P. H.; Tepper, M. A.; Faith, A.; Higgins, J. A.; Lamb, J. R.; Geha, R. S., Immunosuppressant deoxyspergualin inhibits antigen processing in monocytes. *J Immunol* **1994,** 153, (9), 3908-16.

14. Lee, J.; Kim, M. S.; Kim, E. Y.; Park, H. J.; Chang, C. Y.; Jung, D. Y.; Kwon, C. H.; Joh, J. W.; Kim, S. J., 15-deoxyspergualin prevents mucosal injury by inhibiting production of TNF-alpha and down-regulating expression of MD-1 in a murine model of TNBS-induced colitis. *Int Immunopharmacol* **2007,** 7, (8), 1003-12.
15. Ducoroy, P.; Micheau, O.; Perruche, S.; Dubrez-Daloz, L.; de Fornel, D.; Dutartre, P.; Saas, P.; Solary, E., LF 15-0195 immunosuppressive agent enhances activation-induced T-cell death by facilitating caspase-8 and caspase-10 activation at the DISC level. *Blood* **2003,** 101, (1), 194-201.

16. Takeuchi, T.; Iinuma, H.; Kunimoto, S.; Masuda, T.; Ishizuka, M.; Takeuchi, M.; Hamada, M.; Naganawa, H.; Kondo, S.; Umezawa, H., A new antitumor antibiotic, spergualin: isolation and antitumor activity. *J Antibiot (Tokyo)* **1981,** 34, (12), 1619-21.

17. Umezawa, H.; Kondo, S.; Iinuma, H.; Kunimoto, S.; Ikeda, Y.; Iwasawa, H.; Ikeda, D.; Takeuchi, T., Structure of an antitumor antibiotic, spergualin. *J Antibiot (Tokyo)* **1981,** 34, (12), 1622-4.

18. Umeda, Y.; Moriguchi, M.; Kuroda, H.; Nakamura, T.; Iinuma, H.; Takeuchi, T.; Umezawa, H., Synthesis and antitumor activity of spergualin analogues. I. Chemical modification of 7-guanidino-3-hydroxyacyl moiety. *J Antibiot (Tokyo)* **1985,** 38, (7), 886-98.

19. Umeda, Y.; Moriguchi, M.; Kuroda, H.; Nakamura, T.; Fujii, A.; Iinuma, H.; Takeuchi, T.; Umezawa, H., Synthesis and antitumor activity of spergualin analogues. II. Chemical modification of the spermidine moiety. *J Antibiot (Tokyo)* **1987,** 40, (9), 1303-15.

20. Umeda, Y.; Moriguchi, M.; Ikai, K.; Kuroda, H.; Nakamura, T.; Fujii, A.; Takeuchi, T.; Umezawa, H., Synthesis and antitumor activity of spergualin analogues. III. Novel method for synthesis of optically active 15-deoxyspergualin and 15-deoxy-11-O-methylspergualin. *J Antibiot (Tokyo)* **1987,** 40, (9), 1316-24.

21. Plowman, J.; Harrison, S. D., Jr.; Trader, M. W.; Griswold, D. P., Jr.; Chadwick, M.; McComish, M. F.; Silveira, D. M.; Zaharko, D., Preclinical antitumor activity and pharmacological properties of deoxyspergualin. *Cancer Res* **1987,** 47, (3), 685-9.

22. Kondo, S.; Iwasawa, H.; Ikeda, D.; Umeda, Y.; Ikeda, Y.; Iinuma, H.; Umezawa, H., The total synthesis of spergualin, an antitumor antibiotic. *J Antibiot (Tokyo)* **1981,** 34, (12), 1625-7.

23. Bergeron, R. J. a. M., J.S., Total Synthesis of 15-Deoxyspergualin. *J Org Chem* **1987,** 52, (9), 1700-03.

24. Durand, P., Richard, P., and Renaut, P., (-)-15-Deoxyspergualin: A New and Efficient Enantioselective Synthesis Which Allows the Definitive Assignment of the Absolute Configuration. *J Org Chem* **1998,** 63, (26), 9723-27.

25. Lebreton, L.; Annat, J.; Derrepas, P.; Dutartre, P.; Renaut, P., Structure-immunosuppressive activity relationships of new analogues of 15-deoxyspergualin. 1. Structural modifications of the hydroxyglycine moiety. *J Med Chem* **1999,** 42, (2), 277-90.

26. Ohlman, S.; Zilg, H.; Schindel, F.; Lindholm, A., Pharmacokinetics of 15-deoxyspergualin studied in renal transplant patients receiving the drug during graft rejection. *Transpl Int* **1994,** 7, (1), 5-10.

27. Nishizawa, R.; Takei, Y.; Yoshida, M.; Tomiyoshi, T.; Saino, T.; Nishikawa, K.; Nemoto, K.; Takahashi, K.; Fujii, A.; Nakamura, T.; et al., Synthesis and biological activity of spergualin analogues. I. *J Antibiot (Tokyo)* **1988,** 41, (11), 1629-43.

28. Lebreton, L.; Jost, E.; Carboni, B.; Annat, J.; Vaultier, M.; Dutartre, P.; Renaut, P., Structure-immunosuppressive activity relationships of new analogues of 15-deoxyspergualin. 2. Structural modifications of the spermidine moiety. *J Med Chem* **1999,** 42, (23), 4749-63.

29. Komesli, S.; Dumas, C.; Dutartre, P., Analysis of in vivo immunosuppressive and in vitro interaction with constitutive heat shock protein 70 activity of LF08-0299 (Tresperimus) and analogues. *Int J Immunopharmacol* **1999,** 21, (5), 349-58.

30. Gulevich, A. V.; Balenkova, E. S.; Nenajdenko, V. G., The first example of a diastereoselective thio-Ugi reaction: a new synthetic approach to chiral imidazole derivatives. *J Org Chem* **2007,** 72, (21), 7878-85.

31. Brodsky, J. L., Selectivity of the molecular chaperone-specific immunosuppressive agent 15-deoxyspergualin: modulation of Hsc70 ATPase activity without compromising DnaJ chaperone interactions. *Biochem Pharmacol* **1999,** 57, (8), 877-80.

32. Fewell, S. W.; Day, B. W.; Brodsky, J. L., Identification of an inhibitor of hsc70-mediated protein translocation and ATP hydrolysis. *J Biol Chem* **2001,** 276, (2), 910-4.

33. Sugawara, A.; Torigoe, T.; Tamura, Y.; Kamiguchi, K.; Nemoto, K.; Oguro, H.; Sato, N., Polyamine compound deoxyspergualin inhibits heat shock protein-induced activation of immature dendritic cells. *Cell Stress Chaperones* **2009,** 14, (2), 133-9.

34. Nadler, S. G.; Tepper, M. A.; Schacter, B.; Mazzucco, C. E., Interaction of the immunosuppressant deoxyspergualin with a member of the Hsp70 family of heat shock proteins. *Science* **1992,** 258, (5081), 484-6.

35. Mazzucco, C. E.; Nadler, S. G., A member of the Hsp70 family of heat-shock proteins is a putative target for the immunosuppressant 15-deoxyspergualin. *Ann N Y Acad Sci* **1993,** 685, 202-4.

36. Nadler, S. G.; Dischino, D. D.; Malacko, A. R.; Cleaveland, J. S.; Fujihara, S. M.; Marquardt, H., Identification of a binding site on Hsc70 for the immunosuppressant 15-deoxyspergualin. *Biochem Biophys Res Commun* **1998,** 253, (1), 176-80.

37. Nadler, S. G.; Eversole, A. C.; Tepper, M. A.; Cleaveland, J. S., Elucidating the mechanism of action of the immunosuppressant 15-deoxyspergualin. *Ther Drug Monit* **1995,** 17, (6), 700-3.

38. Nadeau, K.; Nadler, S. G.; Saulnier, M.; Tepper, M. A.; Walsh, C. T., Quantitation of the interaction of the immunosuppressant deoxyspergualin and analogs with Hsc70 and Hsp90. *Biochemistry* **1994,** 33, (9), 2561-7.

39. Ugi, I.; Offermann, K.; Herlinger, H.; Marquarding, D., [The reaction of (S)-alpha-phenylethylamine and isobuteraldehyde with benzoic acid and tert-butyl-isocyanide as model reactions for stereoselective peptide-synthesis intermediate. Four component condensations]. *Justus Liebigs Ann Chem* **1967,** 709, 1-10.

40. De Silva, R. A.; Santra, S.; Andreana, P. R., A tandem one-pot, microwave-assisted synthesis of regiochemically differentiated 1,2,4,5-tetrahydro-1,4-benzodiazepin-3-ones. *Org Lett* **2008,** 10, (20), 4541-4.

41. Isaacson, J.; Kobayashi, Y., An Ugi reaction in the total synthesis of (-)-dysibetaine. *Angew Chem Int Ed Engl* **2009,** 48, (10), 1845-8.

42. Kazmaier, U.; Ackermann, S., A straightforward approach towards thiazoles and endothiopeptides via Ugi reaction. *Org Biomol Chem* **2005,** 3, (17), 3184-7.

43. Marcaccini, S.; Torroba, T., The use of the Ugi four-component condensation. *Nat Protoc* **2007,** 2, (3), 632-9.

44. Wang, W.; Domling, A., Efficient synthesis of arrays of amino acid derived Ugi products with subsequent amidation. *J Comb Chem* **2009,** 11, (3), 403-9.

45. Ugi, I.; Heck, S., The multicomponent reactions and their libraries for natural and preparative chemistry. *Comb Chem High Throughput Screen* **2001,** 4, (1), 1-34.

46. Ilyin, A.; Kysil, V.; Krasavin, M.; Kurashvili, I.; Ivachtchenko, A. V., Complexity-enhancing acid-promoted rearrangement of tricyclic products of tandem Ugi 4CC/intramolecular Diels-Alder reaction. *J Org Chem* **2006,** 71, (25), 9544-7.

47. Ramazani, A.; Rezaei, A., Novel one-pot, four-component condensation reaction: an efficient approach for the synthesis of 2,5-disubstituted 1,3,4-oxadiazole derivatives by a Ugi-4CR/aza-Wittig sequence. *Org Lett* 12, (12), 2852-5.

48. Simila, S. T.; Martin, S. F., Applications of the Ugi reaction with ketones. *Tetrahedron Lett* **2008,** 49, (29-30), 4501-4504.

49. Feichtinger, K., Zapf, C., Sings, H.L., and Goodman, M., Diprotected Triflylguanidines: A New Class of Guanidinylation Reagents. *J Org Chem* **1998,** 63, (12), 3804-05.

50. Domling, A.; Ugi, I. I., Multicomponent Reactions with Isocyanides. *Angew Chem Int Ed Engl* **2000,** 39, (18), 3168-3210.

51. Kalayda, G. V.; Zhang, G.; Abraham, T.; Tanke, H. J.; Reedijk, J., Application of fluorescence microscopy for investigation of cellular distribution of dinuclear platinum anticancer drugs. *J Med Chem* **2005,** 48, (16), 5191-202.

52. Xu, P. Z., Ting; Wang, Wenhao; Zou, Xiaomin; Zhang, Xin; Fu, Yiqiu, Synthesis of PNA Monomers and Dimers by Ugi Four-Component Reaction. *Synthesis* **2003,** 2003, (8), 1171-76.

53. Lew, A.; Krutzik, P. O.; Hart, M. E.; Chamberlin, A. R., Increasing rates of reaction: microwave-assisted organic synthesis for combinatorial chemistry. *J Comb Chem* **2002,** 4, (2), 95-105.

54. Tei, L.; Gugliotta, G.; Avedano, S.; Giovenzana, G. B.; Botta, M., Application of the Ugi four-component reaction to the synthesis of ditopic bifunctional chelating agents. *Org Biomol Chem* **2009,** 7, (21), 4406-14.

55. Li, B., Bemish, R., Buzon, R.A., Chiu, C.K.-F., Colgan, S.T., Kissel, W., Le, T., Leeman, K.R., Newell, L., and Roth, J., Aqueous phosphoric acid as a mild reagent for deprotection of the t-butoxycarbonyl group. *Tetrahedron Lett* **2003,** 44, (44), 8113-8115.

56. Bull, S. D., Davies, S.G., Fenton, G., Mulvaney, A.W., Prasad, R.S., and Smith, A.D., Chemoselective debenzylation of N-benzyl tertiary amines with ceric ammonium nitrate. *J Chem Soc, Perkin Trans I* **2000,** 2000, (22), 3765-3774.

57. Abdel-Magid, A. F.; Carson, K. G.; Harris, B. D.; Maryanoff, C. A.; Shah, R. D., Reductive Amination of Aldehydes and Ketones with Sodium Triacetoxyborohydride. Studies on Direct and Indirect Reductive Amination Procedures(1). *J Org Chem* **1996,** 61, (11), 3849-3862.

58. Nahm, S. a. W., S.M., N-methoxy-n-methylamides as effective acylating agents. *Tetrahedron Lett* **1981,** 41, (39), 3815-18.

59. Carpino, L. A., Sadat-Aalaee, D., and Beyermann, M., Tris(2-aminoethyl)amine as a Substitute for 4-(Aminomethyl)piperidine in the FMOC/Polyamine Approach to Rapid Peptide Synthesis. *J Org Chem* **1990,** 55, (5), 1673-1675.

Chapter 5

Conclusions and Future Directions

5.1 Conclusions

Over the last five years, there has been increasing interest in developing inhibitors of Hsp70 family members because these chaperones seem to have a role in multiple diseases. This dissertation has focused on advancing our understanding of chaperones and their involvement in neurodegenerative diseases by applying multicomponent reactions to the synthesis of new chemical probes.

When I started in 2005, there were few inhibitors that had been identified for Hsp70s.[1] Taking inspiration from literature accounts, which suggested that dihydropyrimidines may modulate Hsc70 activity, I employed the Biginelli reaction to generate a library of compounds in hopes of developing a structure-activity relationship (**1**, Figure 5-1).[2] From this work, one interesting observation was that some of these compounds modulated tau levels in cell lines. While there appeared to be no discernable SAR within the series, these studies led us to screen other scaffolds that might have the same phenotype (but with increased potency and a discernable SAR profile). The resulting dihydropyridine compound 4a (**2**, Figure 5-1) increased tau levels in this cellular model, so a library of analogs was synthesized. Dihydropyridines were synthesized by employing the Hantzsch reaction and then screened for their ability to alter tau levels. From this effort, a rough structure-activity relationship was

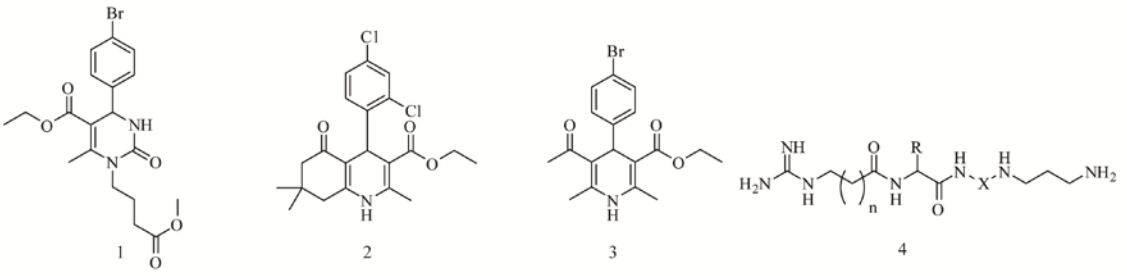

Figure 5-1. Ligands affecting protein-protein interactions in neurdegenerative diseases. (1) SW02 is a dihydropyrimidine that enables members of the Hsp70 fa mily to prevent Aβ aggregation and increase tau stability. (2) Compound 4a was the first dihydropyridine that was found to affect tau satbility. It decreased tau stability. (3) Compound 11g demonstrated a dose-dependent activity and a 7 μM IC_{50}. (4) 15-DSG analogs were created my varying n for chain length, R, and X.

developed. Importantly, compound 11g (**3**, Figure 5-1) was further tested to see if there was any dose-dependency to its decrease in tau levels. It did appear to affect tau levels in a dose-dependent manner and appeared to have an IC_{50} of about ~7 μM, which is a ~10-fold improvement over the dihydropyrimidines. This work also produced the first enantio-selective, four-component Hantszch reaction. Finally, I employed the Ugi reaction to synthesize a library of 15-DSG analogs. Using the Ugi reaction I was able to dramatically improve the synthetic route to these types of polyamines (**4**, Figure 5-1). Rather than taking 14 steps to get a 7% yield using methods published in the literature, I was able to shorten the number of steps to 7 and improve the yield to the 30-50% range for 15-DSG analogs. Also owing to the fact that the four-component Ugi reaction was used, a variety of substitution patterns were created or are anticipated. I expect that this work will allow for the eventual development of a structure-activity relationship.

While most of my projects have revolved around creating libraries of compounds explore structure-activity relationships, the development of an enantioselective Hantzsch reaction was a foray into synthetic methodology. Until the organocatalytic version of this reaction was developed, the only way to achieve enantioselection was through the use of chiral auxillaries or through chiral resolution. The identification of chiral BINOL-

phosphoric acid catalysts that achieved high enantioselectivity in moderate to high yield allowed me to develop an elegant way to synthesize chiral dihydropyridines with aromatic substitutions at the C4 position of the heterocycle.

I have learned a great deal over the last five years. In 2005, there were only a handful of weak Hsp70 inhibitors and little known about "druggable" sites on this family of proteins. The interceding years have provided great opportunities to expand my knowledge in synthesis (e.g. by applying a multitude of reactions and even performing new methodology studies) - but they have also allowed me to expand my understanding of the biology of Hsp70 proteins and molecular chaperones. It has been rewarding to see examples of my Hsp70 inhibitors being applied (by the Gestwicki laboratory, our collaborators and others in the field) to help us gain a greater understanding of the complicated biology of the Hsp70 family of proteins.

5.2 Future Directions

5.2.1 Target Identification for the Dihydropyridine Scaffold

While changing the scaffold to a dihydropyridine from a dihydropyrimidine allowed for the identification of a new scaffold with more potent activity and a preliminary SAR, the binding site for these compounds remains unknown. Since compound 11g (**3**, Figure 5-1) was the most potent thus far, it might serve as a starting point for the generation of biotin-labeled derivatives that could then be used in pull-down assays to determine the binding partners of dihydropyridines. Depending on the target protein identified, more rational design of compounds that alter tau stability could be done and other scaffolds might be identified through screening. For this strategy to be possible the synthesis of N-(2aminoehtyl)biotinamide was necessary. The strategy had

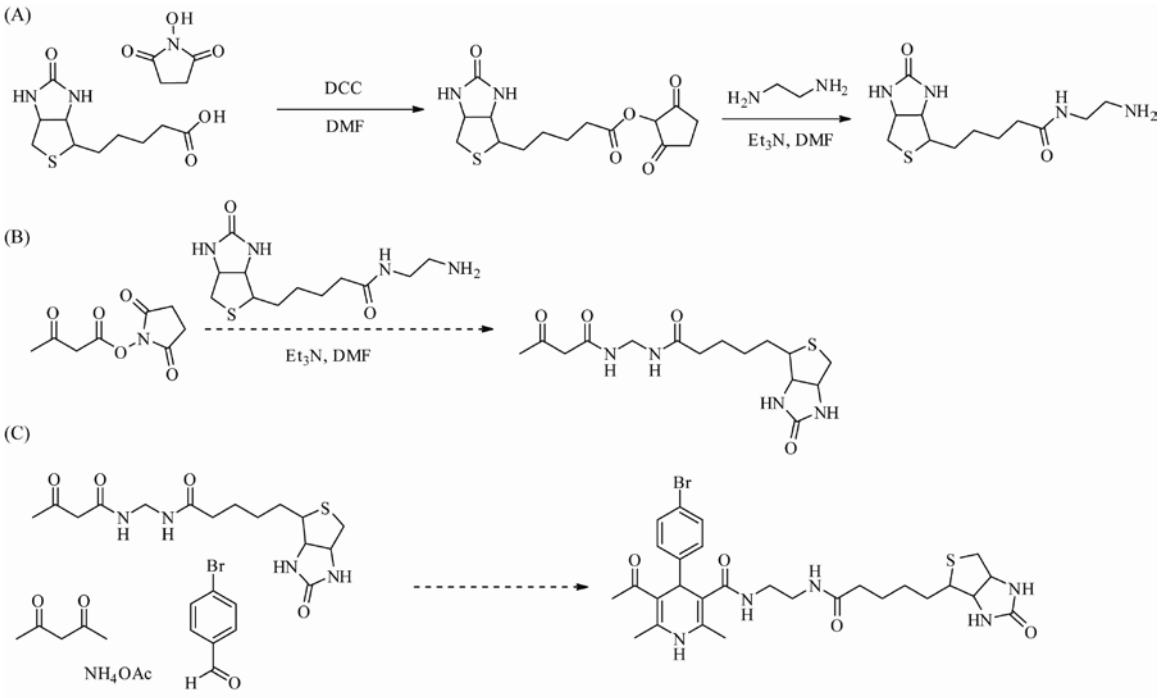

Scheme 5-1. Synthesis of biotinylated dihydropyridines. (A) Synthesis of amine-labled biotin. (B) Synthesis of b-ketoaminde of biotin. (C) Synthesis of biotinylated 11g.

been published previously.[3] The NHS-ester of biotin was synthesized and then ethylenediamine was coupled (Scheme 5-1 A). Once ethylenediamine is coupled to biotin it can then be reacted with NHS-acetoacetate under basic conditions (Scheme 5-1 B). This β-keto amide can then be used in the Hantzsch reaction to synthesize a biotinylated dihydropyridine (Scheme 5-1 C). This route is currently being pursued by another graduate student.

5.2.2 Scaffold Hopping to Identify Other Scaffolds

The dihydropyrimidine scaffold has become a starting point in the identification of small molecules that bind to members of the Hsp70 protein family. The binding site on DnaK for one of these compound 115-7c was identified in collaboration with Prof. Erik Zuiderweg's laboratory using NMR experiments to identify the putative binding pocket.[4] However, making substitutions to the dihydropyrimidine scaffold did not

provide any compounds that were potent than ~75 μM. I approached this limitation by generating dihydropyridines with a related structure. In the future, these scaffold-hopping efforts might be combined with *in silico* screens. Ideally, one would retain the interesting binding site of the dihydropyrimidines, but achieve improved potency. In addition, it is also possible that scaffolds that bind to other binding sites could still be identified during on-going screening in the Center for Chemical Genomics at the University of Michigan's Life Sciences Institute. Several members of the laboratory have continued to develop new assays and new compound collections continue to become available. From my work on the dihydropyrimidines and dihydropyridines (and in collaboration with Sussi Wisen, Lyra Chang, Yoshi Miyata and others in the group), a "flow chart" of assays and criteria are developing, which should aid these efforts. Specifically, we have learned a great deal about how different co-chaperones can be employed to modulate the available protein-protein interactions.

5.2.3 SAR of 15-DSG Analogs

The logical next step in the spergualin synthetic project is that more derivatives need to be made. From my reading of the literature, I will make a few suggestions: While substitutions at the 11 position were not tolerated well in the early SAR studies, using the Ugi multicomponent reaction provides new opportunities for substitution (**4**, Figure 5-1). Further, new derivatives of the starting materials could permit greater diversity, such as substitutions to the spermidine tail. Also only the length of the guanidinylated amino acid chain has been probed, while its rigidity and polarity could be interesting modifications.

In addition to new syntheses, more biochemical tests are needed. Right now, surface plasmon resonance appears most promising. In this experiment, Hsc70 is bound to a chip and the co-chaperone CHIP is flowed over this surface, with the 15-DSG analogs competing for the protein-protein interaction. However, it would be useful to have an alternative biochemical assay to measure the affect of the 15-DSG analogs. Some [possibilities include: ubiquitin transfer assays and radioactive ATPase assays.[5] These methods would not be ideal for high throughput screening, but they might be useful for screening a focused library. This project is obviously at its initial phases.

5.2.4 The Preparation of Cyclic 15-DSG Derivatives

While early indications are that the linear 15-DSG analogs that I have synthesized are more stable than spergualin, there are several other ways that would be interesting to further increase the stability of these compounds. One potential way is by forming cyclic products. The first method that I could envision to cyclize the 15-DSG core is to take deprotected products and heating them in the microwave with Lawesson's reagent in toluene. This should produce a five-membered 1,3-thiazole ring (Scheme 5-2).[6] The

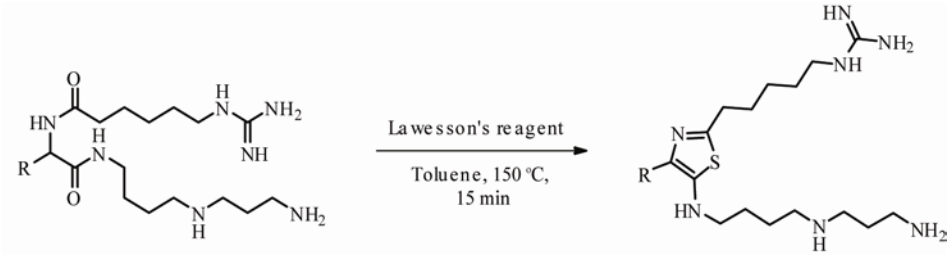

Scheme 5-2. Synthesis of thiazole 15-DSG analog.

alternative method to form a macrocylic ring is to perform the Ugi reaction with propargylamine. The rest of the route remains the same. After the reductive amination, the secondary amine in the spermidine tail undergoes coupling to azido-acetic acid[7] using

recently published conditions.[8] The product is then subjected to an intramolecular 1,3-cycloaddition using conditions that had been worked out for intramolecular peptide cyclization using 1,3-cycloaddition (Scheme 5-3).[9, 10] Following deprotection a large macrocyclic ring with appendages for the guanidinylated tail, spermidine, and the R group replacing the 11 position OH will be present.

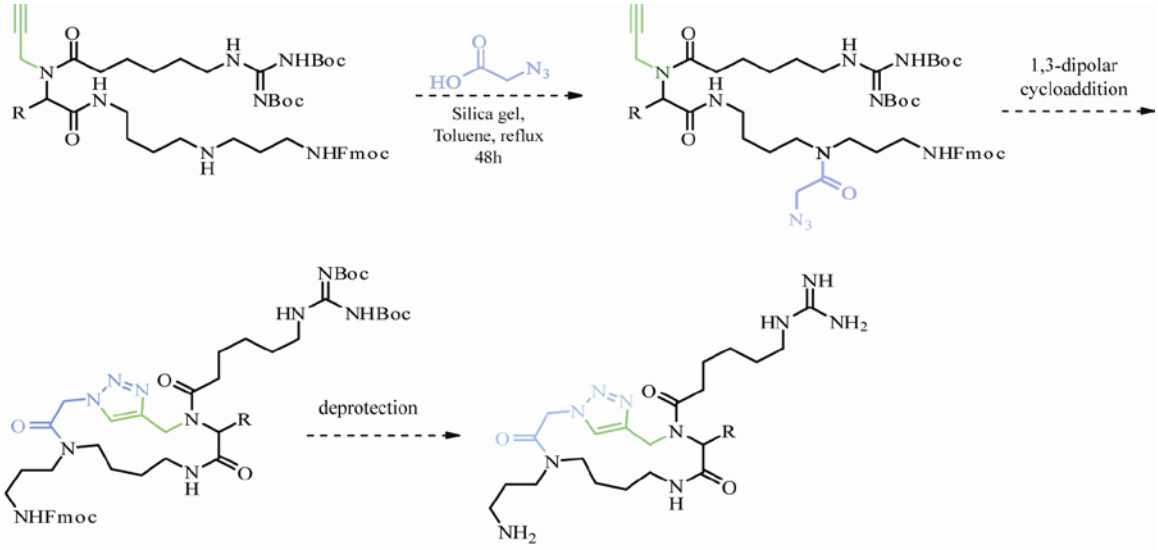

Scheme 5-3. Synthesis of macrocyclic 15-DSG analog.

5.2.5 Probe vs. Therapeutic

The current state of small molecule modulators of Hsp70 proteins are more likely to lead to the development of probes than therapeutic agents. Specifically, the current compounds have modest affinities and lack extensive SAR or toxicology studies. However, these compounds may be able to answer important questions about Hsp70 family members and their roles in biology. While the ultimate goal might be to develop a therapeutic agent, more immediate questions might include: What is the optimal affinity for the small molecule? How much modulation of activity is ideal? What are the best

targets for each disease and how do co-chaperones affect them? What is the role of protein aggregation in diseases?

5.3 References

1. Evans, C. G.; Chang, L.; Gestwicki, J. E., Heat shock protein 70 (hsp70) as an emerging drug target. *J Med Chem* 53, (12), 4585-602.

2. Fewell, S. W.; Smith, C. M.; Lyon, M. A.; Dumitrescu, T. P.; Wipf, P.; Day, B. W.; Brodsky, J. L., Small molecule modulators of endogenous and co-chaperone-stimulated Hsp70 ATPase activity. *J Biol Chem* 2004, 279, (49), 51131-40.

3. Jiang, X.; Ahmed, M.; Deng, Z.; Narain, R., Biotinylated glyco-functionalized quantum dots: synthesis, characterization, and cytotoxicity studies. *Bioconjug Chem* 2009, 20, (5), 994-1001.

4. Wisen, S.; Bertelsen, E. B.; Thompson, A. D.; Patury, S.; Ung, P.; Chang, L.; Evans, C. G.; Walter, G. M.; Wipf, P.; Carlson, H. A.; Brodsky, J. L.; Zuiderweg, E. R.; Gestwicki, J. E., Binding of a small molecule at a protein-protein interface regulates the chaperone activity of hsp70-hsp40. *ACS Chem Biol* 5, (6), 611-22.

5. Brodsky, J. L., Selectivity of the molecular chaperone-specific immunosuppressive agent 15-deoxyspergualin: modulation of Hsc70 ATPase activity without compromising DnaJ chaperone interactions. *Biochem Pharmacol* 1999, 57, (8), 877-80.

6. Ozturk, T.; Ertas, E.; Mert, O., Use of Lawesson's reagent in organic syntheses. *Chem Rev* 2007, 107, (11), 5210-78.

7. Ju, Y.; Kumar, D.; Varma, R. S., Revisiting nucleophilic substitution reactions: microwave-assisted synthesis of azides, thiocyanates, and sulfones in an aqueous medium. *J Org Chem* 2006, 71, (17), 6697-700.

8. Yang, X. D.; Zeng, X. H.; Zhao, Y. H.; Wang, X. Q.; Pan, Z. Q.; Li, L.; Zhang, H. B., Silica gel-mediated amide bond formation: an environmentally benign method for liquid-phase synthesis and cytotoxic activities of amides. *J Comb Chem* 12, (3), 307-10.

9. Cantel, S.; Isaad Ale, C.; Scrima, M.; Levy, J. J.; DiMarchi, R. D.; Rovero, P.; Halperin, J. A.; D'Ursi, A. M.; Papini, A. M.; Chorev, M., Synthesis and conformational analysis of a cyclic peptide obtained via i to i+4 intramolecular side-chain to side-chain azide-alkyne 1,3-dipolar cycloaddition. *J Org Chem* 2008, 73, (15), 5663-74.

10. Amblard, F.; Cho, J. H.; Schinazi, R. F., Cu(I)-catalyzed Huisgen azide-alkyne 1,3-dipolar cycloaddition reaction in nucleoside, nucleotide, and oligonucleotide chemistry. *Chem Rev* 2009, 109, (9), 4207-20.